

**ANALYSIS OF VEGETATION CHANGE IMPACT ON
LAND USE/LAND COVER OF AOI**

Thesis Submitted for the Award of the Degree of

DOCTOR OF PHILOSOPHY

in

Electronics and Communication Engineering

By

V Kiranmai A Somayajula

Registration Number: 41800634

Supervised By

Dr. Deepika Ghai (21507)

Associate Professor,

School of Electronics and Electrical

Engineering (SEEE),

Lovely Professional University,

Phagwara, Punjab, India.

Co-Supervised by

Dr. Sandeep Kumar,

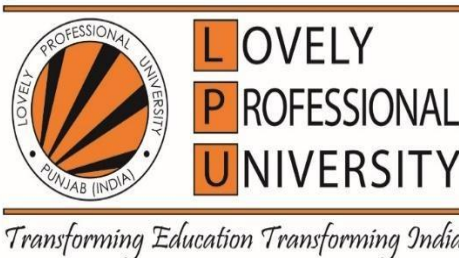
Deputy Director & Professor,

Department of Computer Science and

Engineering,

Symbiosis Institute of Technology,

Nagpur, India.



**LOVELY PROFESSIONAL UNIVERSITY, PUNJAB
2025**

DECLARATION

I, hereby declared that the presented work in the thesis entitled “ANALYSIS OF VEGETATION CHANGE IMPACT ON LAND USE/LAND COVER OF AOI” in fulfilment of degree of **Doctor of Philosophy (Ph. D.)** is outcome of research work carried out by me under the supervision of Dr. Deepika Ghai, working as Associate Professor, in the School of Electronics and Electrical Engineering of Lovely Professional University, Punjab, India. In keeping with the general practice of reporting scientific observations, due acknowledgements have been made whenever work described here has been based on findings of other investigator. This work has not been submitted in part or full to any other University or Institute for the award of any degree.

(Signature of Scholar)

Name of the scholar: V Kiranmai A Somayajula

Registration No.: 41800634

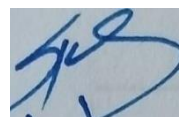
Department/school: Electronics and Electrical Engineering

Lovely Professional University,

Punjab, India

CERTIFICATE

This is to certify that the work reported in the Ph. D. thesis entitled “ANALYSIS OF VEGETATION CHANGE IMPACT ON LAND USE/LAND COVER OF AOI” submitted in fulfillment of the requirement for the award of degree of **Doctor of Philosophy (Ph.D.)** in the School of Electronics and Electrical Engineering, is a research work carried out by V Kiranmai A Somayajula, 41800634, is bonafide record of her original work carried out under my supervision and that no part of thesis has been submitted for any other degree, diploma or equivalent course.



(Signature of Supervisor)

Dr. Deepika Ghai,
Associate Professor,
School of Electronics and Electrical Engineering,
Lovely Professional University,
India.

(Signature of Co-Supervisor)

Dr. Sandeep Kumar,
Deputy Director & Professor,
Computer Science and Engineering,
Symbiosis Institute of Technology,
Nagpur, India.

ABSTRACT

The transformation of land due to natural processes and evolution, and its impact on the local environment, is a substantial problem for empathy in the association amongst civilization and the environment. Land use and land cover are decisive factors in determining the implementation of administrative methods to meet basic human desires. It is significant to assess changes in land use and land cover and recognize factors driving these changes. This is pertinent for identifying areas susceptible to risk and devising strategies for sustainable ecosystem services. Innovative approaches must be developed to formulate suitable policies and practices for managing land. As a result, ongoing agricultural land monitoring and mapping are critical to long-term survival and prosperity. Most farm monitoring solutions rely on standard techniques or traditional tactics, which are expensive and require considerable time. Remote sensing, on the other hand, provides a low-cost method for obtaining information regarding wholesome or unhealthy vegetation on farmland by employing a variety of advanced geospatial techniques such as categorization, change detection, and pan-sharpening. A low-cost, successful method for surveying and ongoing agricultural land monitoring is remote sensing. Previously, numerous categorization algorithms were devised and applied for vegetation change analysis. Conventional techniques are typically based on machine learning algorithms, which are simple to deploy but require human interaction in decision-making. Change detection is one of the most important methods for analyzing multitemporal variations over time with remote sensing data. In recent years, several remote sensing researchers have chosen DL algorithms to handle change detection problems that would otherwise be implemented using traditional machine learning approaches. Deep learning methods are gaining popularity due to their ability to extract object-level information from trained models. However, the Deep Learning (DL) model demands a significant amount of computing time and must be evaluated in multiple locations for various applications. This study intends to examine how changes in vegetation affect LULC dynamics within a specific Area of Interest (AoI) via conventional classification techniques and deep learning algorithms. To validate the output classified maps, they are compared to reference datasets gathered from field observations at certain sites. In this study, we employed Temporal Landsat satellite data to assess the LULC classification, Land

Surface Temperature (LST), and inverse correlation between LST and NDVI with a focus on regions like VSP, BZA, TPTY, A.P., India, spanning from 2000 to 2020 with a 5-year interval. The classification was carried out by utilizing a pixel-based classifier, a period of LANDSAT satellite imagery, and a vast LULC field database. There have been five primary land use and cover types recognized. Dense Vegetation, Vegetation, Built-up, Barren Land, and Water. There were considerable increases in the area enclosed under vegetation, dense vegetation, and built-up land over the specified time frame, while there was a noticeable diminution in waterbodies and barren land. We assessed the assorted effects of land conversion on the natural environment using LST and NDVI. The technique used accomplished high accuracy values (90%-97%) and a kappa coefficient of (0.89- 0.96) with minimal commission and omission issues. The Mono-window technique was used to evaluate variations in land surface temperature. Change detection along with the alteration from natural land cover against synthetic land use was quantitatively estimated for the subject of study, demonstrating significant changes in ground cover and utilization for the specified intervals. Conventional techniques are typically based on machine learning algorithms, which are simple to deploy but require human interaction in decision-making. There is a substantial requirement for sustainable development in decision-making processes related to agriculture and urban planning, which can benefit from Deep Learning (DL) techniques. Land cover mapping has been shown to benefit from applying deep learning techniques in recent times by classifying remote sensing imagery. This research uses transfer learning techniques, including ResNet50 and ResNet50+LSTM, for fine-tuning previously trained networks. These proposed methodologies successfully handled the difficulty of limited data, yielding exceptional accuracy. The research conducted in Vijayawada City, Andhra Pradesh, India, observed the deviations in LULC for six years. The research was conducted using remote sensing and GIS methods and involved gathering information from the local community regarding their knowledge and views on LULC patterns and factors that influence them. Seven major LULC types (i.e., hilly area, dense vegetation, vegetation, built-up, shrubs, barren area, and water). The analysis of land cover and land use change was conducted by examining Landsat images from three different years - 2016, 2019, and 2022. The analysis indicated that built-up land covered the most significant portion of the region surveyed, which increased by 11.97%. The

proposed results suggest that the ResNet50+LSTM-based strategy surpassed ResNet50 in terms of both computing efficiency and Correctness an inefficiency of 98.1%, a Kappa coefficient of 0.96, an average precision of 88%, a recall of 90%, and an F1-Score of 89% on UCM dataset. Recent research has shown that there has been a notable increase in areas covered by vegetation in the past six years. On the other hand, there has been a significant decrease in environmentally essential land areas, such as hilly regions, associated with the development of built-up areas and vegetation. In 2016, hilly regions accounted for 2.7% of the total study area, but by 2022, they only accounted for 1.77%. In contrast, vegetation increased from 32.25% in 2016 to 35.73% in 2022, while built-up areas increased from 21.75% to 33.72% in the same period. However, dense vegetation decreased from 34.25% to 20.44%. The prime reasons for the variations in land use and cover in this region include population growth, uncertainty in land ownership, communal property rights, enduring poverty, ecosystem, fluctuations, and deficiency of widespread awareness. As a result, it is critical to manage the sources that cause LULC variations and prioritize sustainable resource utilization. Through the integration of RS and GIS, the work detects and analyzes LULC change dynamics in agricultural lands, leveraging high-resolution images to extract LULC information from the AOI. Moreover, this research aims to find out the correlation between the lines LULC dynamics and demographic, economic, and environmental factors within the study area. This analysis enables complete knowledge of the factors influencing LULC changes, providing policymakers with valuable insights for effective land use planning and ways to achieve equitable growth. The utilization of deep learning algorithms alongside conventional techniques enhances the accuracy and efficiency of LULC pattern analysis in the AOI. The outcomes of this investigation offered illumination on the dynamics of LULC changes and their environmental and social implications, enabling policymakers to develop effective land use planning and management strategies.

LIST OF FIGURES

Figure No.	Figure Name	Page No.
Chapter-1		
1.1	Remote Sensing process	2
1.2	Types of Remote Sensing Sensors	4
1.3	Electromagnetic Spectrum	6
1.4	Geographic Information System	9
1.5	Types of Land use	14
1.6	Types of Land Cover	15
1.7	Urban planning using GIS	17
1.8	Environmental impact	17
1.9	Need for LULC changes	18
1.10	Disaster Management	18
1.11	Factors affecting LULC	20
1.12	Land Use/Land Cover area	21
1.13	Vegetation change	23
1.14	Vegetation change analysis	26
Chapter-2		
2.1	Impacts of vegetation change	32
2.2	Factors driving land use and land cover change process	36
Chapter-3		
3.1	Geographical representation of Andhra Pradesh	75
3.2	Geographical location of Vijayawada city	76
3.3	Geographical location of Visakhapatnam district	77
3.4	Geographical location of Tirupati	78

3.5	Landsat datasets represent NDVI and False color of Vijayawada, Visakhapatnam and Tirupati	80
3.6	Sentinel-2 dataset bands	80
3.7	Sentinel-2 datasets of years 2015 (9 May), 2020 (28 April), and 2022 (09 April) -NDVI representation and False color composition representation	81
3.8	Environment for visualizing images (ENVI) software	83
3.9	Earth Resources Data Analysis System (ERDAS) software	84
3.10	Advanced geographic information system	85
3.11	Advanced geographic information system (ArcGIS Pro) software	86
3.12	QGIS software	87
3.13	Sentinel application platform (SNAP) software	88
3.14	MATLAB (Matrix Laboratory) software	88
3.15	Google Earth Pro software	89

Chapter-4

4.1	Flow Chart of LULC maps of the survey region	91
4.2	Flowchart for Computation of LST	98
4.3	Flowchart of the proposed work	101
4.4	Architecture of ResNet50	104
4.5	Graphical representation of (a) ReLu function and (b) softmax	105
4.6	LSTM Internal Architecture	106
4.7	Sample input images fed into the preprocessing	108

Chapter-5

5.1	Classified images of the Tirupati area of the years 2000, 2005, 2010, 2015 and 2020	113
5.2	Classified images of the Vijayawada area of the years 2000, 2005, 2010, 2015 and 2020	114
5.3	Classified images of Visakhapatnam area of the years 2000, 2005, 2010, 2015, and 2020	115

5.4	Graphical representation of LULC changes in Tirupati, Visakhapatnam, and Vijayawada regions	121
5.5	LST map of Tirupati region of years 2000, 2005, 2010, 2015, 2020	122
5.6	LST map of Visakhapatnam region of years 2000, 2005, 2010, 2015, 2020	123
5.7	LST map of Vijayawada region of years 2000, 2005, 2010, 2015, 2020	124
5.8	LST acquired for different classes of Tirupati, Visakhapatnam, and Vijayawada area	127
5.9	Accuracy and Loss of training vs. validation data for ResNet50 +LSTM	129
5.10	Accuracy and Loss of training vs. validation data for ResNet50	129
5.11	LULC maps of Vijayawada in 2015, 2020, and 2022 using ResNet50 and ResNet50 +LSTM	130
5.12	Precision, Recall, and F1-Score for ResNet50	134-135
5.13	Precision, Recall, and F1-Score for ResNet50+LSTM	135-136
5.14	Overall Accuracy of ResNet50 and ResNet50+LSTM	137
5.15	Kappa Coefficient of ResNet50 and ResNet50+LSTM	137

LIST OF TABLES

Table No.	Table Name	Page No.
Chapter-1		
1.1	Earth observation remote sensing satellites [Source: ISRO, NASA]	7
Chapter-2		
2.1	Literature Survey	65
Chapter-3		
3.1	Spatial information of the study area	79
3.2	Spatial information of the study area for the year 2015	81
3.3	Spatial information of the study area for the year 2020	82
3.4	Spatial information of the study area for the year 2022	82
Chapter-4		
4.1	Thermal conversion constants	96
4.2	Categorization system implemented for land cover mapping actions	103
4.3	Hyperparameters setting for training data	109
Chapter-5		
5.1	LULC consequences of the study area (Tirupati)	112
5.2	LULC consequences of the study area (Visakhapatnam)	112
5.3	LULC consequences of the study area (Vijayawada)	116
5.4	Transition matrix of Vijayawada for the period 2020	117
5.5	Overall Accuracy and Kappa Coefficient for the period 2000, 2005, 2010, 2015, and 2020 of Region of Interest	118
5.6	User's Accuracy (%) for the period 2000, 2005, 2010, 2015, and 2020 of Region of Interest	118

5.7	Producer's Accuracy (%) for the period 2000, 2005, 2010, 2015, and 2020 of Region of Interest	119
5.8	Error of Commission for the period 2000, 2005, 2010, 2015, and 2020 of Region of Interest	119
5.9	Error of Omission for the period 2000, 2005, 2010, 2015, and 2020 of Region of Interest	119
5.10	Specificity for the period 2000, 2005, 2010, 2015, and 2020 of Region of Interest	120
5.11	F-Score (%) for the period 2000, 2005, 2010, 2015, and 2020 of Region of Interest	120
5.12	False Positive Rate for the period 2000, 2005, 2010, 2015, and 2020 of Region of Interest	120
5.13	LST acquired over different classes in Tirupati, Visakhapatnam, and Vijayawada regions	125
5.14	Spatial coverage of LULC types in Vijayawada at different periods in 2016, 2019, and 2022	133
5.15	Overall Accuracy and Kappa coefficient for ResNet50, ResNet50+LSTM model for the years 2016, 2019 and 2022	133
5.16	ResNet50 model for class performances in precision, recall, and F1-score for the years 2016, 2019, and 2022	133
5.17	ResNet50+LSTM model for class performances in precision, recall, and F1-score for the years 2016, 2019, and 2022	134

LIST OF ABBREVIATIONS

Abbreviations	Descriptions
LULC	Land Use Land Cover
RS	Remote Sensing
GIS	Geographical Information System
USGS	United States Geological Services
AoI	Area of Interest
MLC	Maximum Likelihood Classifier
SVM	Support Vector Machine
CNN	Convolutional Neural Network
ResNet	Residual Network
NDVI	Normalized Difference Vegetation Index
PCA	Principal Component Analysis
LST	Land Surface Temperature
LSE	Land Surface Emissivity
DL	Deep Learning
TL	Transfer Learning
LSTM	Long Short-Term Memory
OA	Overall Accuracy
KC	Kappa Coefficient
GCP	Ground Control Points

CHAPTER-I

INTRODUCTION

Key points:

- Overview of remote sensing technology and parameters.
 - Earth observation satellite imaging sensors and their technical specifications.
 - The significance of remote sensing in LULC classification.
-

This chapter delves into the fundamental concepts of land, land use, land cover, and land use types, and focuses specifically on changes in agricultural land use. The analysis explores the intricacies of land use and vegetation transformation, examining essential components of land, its utilization, and the alterations in land use patterns.

1.1 BACKGROUND

Land transformation from one usage type to another is generally irreversible and leads to permanent ecological changes in the affected region. Nevertheless, ongoing development activities, such as industrialization, urbanization, and the expansion of settlements, contribute to the gradual reduction of agricultural land. Agriculture, one of humanity's oldest and most fundamental endeavors, has traditionally served as a crucial source of sustenance. Despite the global trends of increasing industrialization and urbanization, almost half of the global workforce is still involved in agriculture. In many developing nations, the agricultural sector plays a significant role in providing employment opportunities and contributes substantially to the national economy. Agriculture serves as the backbone of India's economy, with over fifty percent of its population depending on this sector for their livelihoods. Despite advancements in technology and the ability to harness natural resources, agricultural activities worldwide are still heavily influenced by environmental factors. Developing countries, in particular, grapple with two primary challenges related to agriculture. The first

challenge involves meeting the growing demand for food and supplying agricultural products to support the ever-expanding population. The second challenge pertains to the unequal development of agriculture and the shifting patterns of land use for agricultural purposes. Land is a critical component of agriculture from a geographical perspective, and the rapid pace of development has had a detrimental impact on agriculture because of urbanization, industrialization, and infrastructure expansion. Consequently, land previously well-suited for agriculture has been converted to various other uses, resulting in a decline in available agricultural land.

1.2 REMOTE SENSING

The science and expertise of collecting information concerning an object has been referred to as remote sensing., area, or process by analyzing data collected by a device, not in direct contact with the object, area, or process (Richards et al., 2006; Yangchen et al., 2015). Remote sensing (RS) involves gathering and representing information about a physical object or area without making physical contact (M. Dharani et al., 2019). It allows for the assessment of the Earth's condition over a large area and monitoring changes in the environment (Adedeji et al., 2009). Remote sensing is gathering information about an object, area, or phenomenon without physical contact with it. It involves using various sensors and instruments, usually installed to collect data on satellites, planes, or unmanned aircraft from a distance. This technology is widely used in environmental monitoring, natural resource management, agriculture, urban planning, disaster management, and scientific research (Adi et al., 2021).

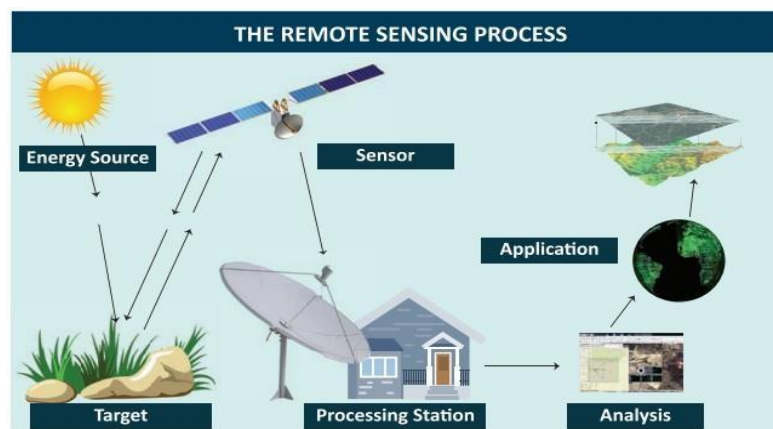


Figure 1.1. Remote Sensing process

A Remote Sensing (RS) system serves the purpose of examining and making sense of the physical reality observed from a distance, and this process can be divided into several distinct phases involving the interaction between incident radiation and the collection of information shown in **Figure 1.1**.

i) Energy Source or Illumination: The primary necessity for remote sensing is an energy source that emits electromagnetic radiation tailored to the target of interest.

ii) Radiation and the Atmosphere: As the energy travels from the source to the target, it encounters and interacts with the Earth's atmosphere. This interaction takes place both during its journey to the target and its return journey to the sensor.

iii) Interaction with the Target: Upon reaching the target through the atmosphere, the energy engages with the target, affected by the distinctive qualities of both the target and the electromagnetic radiation.

iv) Recording of Energy by the Sensor: A remote sensor, which doesn't physically touch the target, captures the energy that is either scattered or emitted from the target. This captured electromagnetic radiation is then recorded.

v) Transmission, Reception, and Processing: The recorded energy is transmitted and received by the processing station on Earth. The data is received in electronic form and subsequently processed.

vi) Interpretation and Analysis: The processing station is where the data undergoes scrutiny using a variety of visualization and interpretation tools, often involving computer-based analysis of digital data.

vii) Application: The information derived from the processed data is compiled into the form of maps or computer files.

This information is then presented to end-users who apply specific techniques to address issues or problems. This systematic approach deploys remote sensing for assistance to diverse fields by offering valuable insights and data for informed decision-making.

1.3 TYPES OF REMOTE SENSING SENSORS

Various satellite datasets have been used for agricultural applications in recent decades, including optical and microwave data such as Landsat-8 with a spatial resolution of 30m (V kiranmai et al., 2020) (Phiri and Morgenroth, 2017); Sentinel with

a spatial resolution of 10m (Shendryk et al., 2019), Synthetic Aperture Radar (SAR) microwave data (Zhou et al., 2018), and ESA's Sentinel-2 satellite, which is available on the United States Geological Survey (USGS) website. The spatial resolution of Sentinel-2 data varies from 10m to 60m for its 13 spectral bands (ranging from 0.443 μm to 2.190 μm), while MODIS has the degree of spatial accuracy of 500m (P. Feng et al., 2019) and offers global monitoring every 1-2 days within its 36 spectral bands. Satellite sensors can be passive or active, depending on the method of light or radiation used represented in **Figure 1.2**.

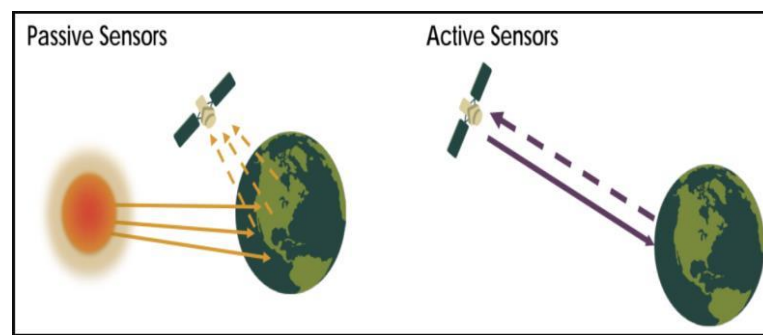


Figure 1.2. Types of Remote Sensing Sensors

Remote sensing works by detecting and measuring the electromagnetic radiation that is reflected or transmitted, including microwaves, infrared, and visible light from the Earth's surface. Different features reflect on the surface of the Earth or emit radiation in distinctive ways, allowing remote sensing systems to capture valuable information about the land, oceans, and atmosphere. There are two main types of remote sensing: **Passive Remote Sensing:** Passive sensors detect natural radiation discharged or reflected by the surface of the Earth. They rely on external sources of radiation, such as the Sun, to illuminate the target area. These sensors measure the radiation threshold coming from the outer layer of Earth and provide valuable data about land cover, vegetation, water bodies, and other surface features. **Active Remote Sensing:** Active sensors, on the other hand, emit their radiation and measure the response. For example, radar is commonly used in remote sensing in activity. Radar systems send out microwave signals and measure the signals that bounce back after hitting the Earth's surface. Active sensors are useful for capturing data in adverse weather conditions or at night because they do not rely on sunlight. Remote sensing data is examined and processed using specialized software to make thorough maps and

track modifications in the environment, detect natural disasters, assess crop health, and much more. It plays a crucial role in modern Earth observation and is essential for informed decision-making in various fields.

1.4 MULTISPECTRAL IMAGING

Satellite imaging systems developed for Earth observation and natural resource management purposes now utilize multispectral scanners. These scanners allow data acquisition from various spectral bands, spanning from visible to thermal wavelengths, all at once through the Multispectral Scanner (MSS). Multispectral imaging is a method used in remote sensing to store images in multiple discrete bands across the electromagnetic spectrum. Unlike traditional RGB (Red, Green, Blue) imaging, multispectral imaging involves capturing data in several specific wavelengths beyond the visible spectrum, such as infrared and ultraviolet, represented in **Figure 1.3**. Each band represents a different range of wavelengths and provides unique information about the target object or area. In comparison to single-spectral band images, multispectral imagery provides additional information by capturing signals in multiple bands. Advancements in remote sensing technology have led to measurements with broader spectral coverage and higher spatial resolution, as well as increased temporal frequency. Modern systems can capture Very High-Resolution (VHR) multispectral images with excellent geometric and spectral resolution. Multispectral (MS) sensors can detect narrow spectral bands across a continuous spectral range. These sensors capture hundreds of bands associated with specific spatial channels, enabling dense sampling of the spectral features of dissimilar land covers. Notably, there is a significant difference in band coverage between hyperspectral and multispectral sensors. Multispectral sensing provides continuous spectral signatures across various wavelengths, unlike hyperspectral sensors, which offer only a few bands lumped over a range of wavelengths.

1.5 EARTH OBSERVATION SATELLITES

The expansion of agriculture and urbanization, along with natural phenomena like flooding, are causing manmade activities like these to alter the global land cover quickly. These changes have a significant impact on human life.

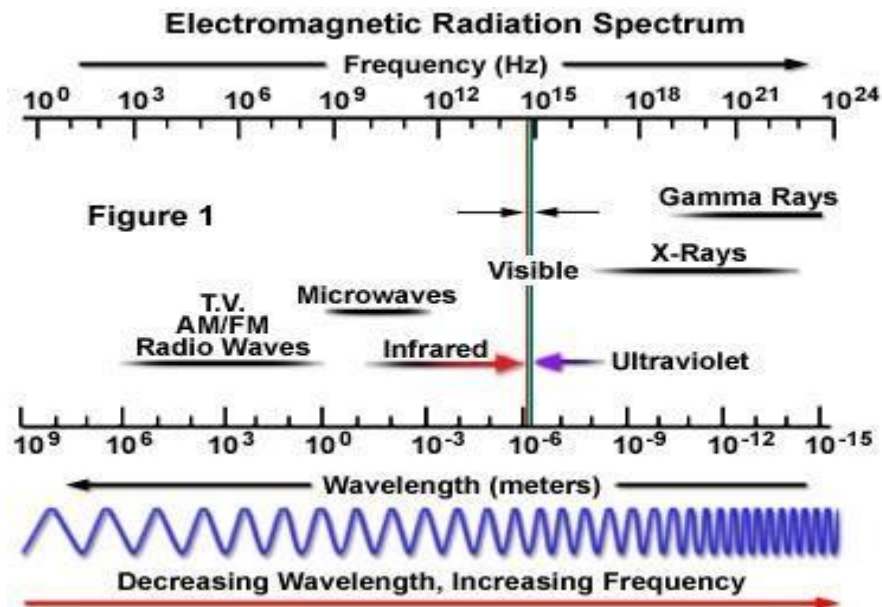


Figure 1.3. Electromagnetic Spectrum

Therefore, it is crucial to establish efficient systems for monitoring to ensure expenditure and management that is sustainable of natural resources like trees and water (Topaloğlu et al., 2016). The methods used to monitor the natural and human resources on the surface of the Earth have been completely transformed by the advent of satellite remote sensing technology, which also makes it feasible to monitor vast regions. These satellites (e.g., IKONOS, SPOT, and non-commercial such as Landsat, and Sentinel) offer valuable data for various remote applications, including monitoring forests, urban areas, natural hazards, and agriculture. Remotely sensed data, like Landsat, have proven invaluable for tracking natural resources and ecosystem processes, such as forest dynamics (Mundhe et al., 2020). This becomes particularly significant in developing countries with limited financial resources for acquiring such data. **Table 1.1** shows the different types of satellites used for LULC classification (Gao et al., 2016; Bhattacharjee et al., 2021).

1.6 GEOGRAPHIC INFORMATION SYSTEM

Although India has achieved notable progress in agriculture, there remains a crucial need to utilize land most rationally and effectively as possible. GIS and RS technology provide a dynamic tool for comprehensive land use analysis (Bhatnagar et al., 2019). Remote sensing offers landscape information comprehensively, repeatedly, and objectively.

Table 1.1: Earth observation remote sensing satellites [Source: ISRO, NASA]

Satellite	Spatial resolution (meter)	Temporal resolution (days)	No. of bands	Launch year	Sensor used
Resource Sat- 1/IRS-P6	56m	5 days	4 bands	2003	LISS-IV, LISS-III
Landsat 5	30m (MS); 120m (Thermal)	16-days	7 bands (MS bands-6, Thermal- 1)	1984	MSS, TM
Landsat 7	30m (MS); 15m (PAN); 60m (Thermal)	16-days	8 bands (MS bands- 6, Thermal- 1, PAN-1)	1999	ETM+
Landsat 8	30m (Visible, NIR, SWIR); 100m (Thermal); 15m (PAN)	16-days	11 bands (MS bands- 8, Thermal- 2, PAN-1)	2013	OLI, TIRS
Landsat 9	30m (Visible, NIR, SWIR); 100m (Thermal); 15 m (PAN)	16-days	11 bands (MS bands- 8, Thermal- 2, PAN-1)	2021	OLI, TIRS
Sentinel- 1	SM mode(80Km), IW, EW, WV mode	12-days	4 C-band	2014	C-SAR (C-band Synthetic Aperture Radar)
Sentinel- 2	4 bands at 10 m (Visible, NIR) 6 bands at 20 m (SWIR-1,2) 3 bands at 60 m	5 days	13	2015	MSI (Multi-Spectral Instrument)
Sentinel- 3	300m	2 days	21(16 visible bands, 5 Near-Infrared bands)	2016	SRAL (Sentinel-3 Radar Altimeter) MWR (Microwave Radiometer) OLCI (Ocean and Land Color Instrument) SLSTR (Sea and Land Surface Temperature Radiometer)

It serves as a valuable source of spatial data, including details on land use/land cover, drainage, and topography. GIS, on the other hand, is a robust tool for geo-environmental analysis and the assessment of natural resources (Bhowmik et al., 2020). It enables the integration of databases from various sources, including remote sensing, onto a single platform, allowing for efficient spatial-temporal analysis. Determining suitable areas for agricultural use involves evaluating climate, soil quality, and topographical features, and understanding local biophysical constraints in **Figure 1.4**. In such complex scenarios, multiple variables come into play, and each one must be assessed based on its relative importance for optimal crop growth conditions through techniques like Multi-Criteria Evaluation (MCE) and GIS analysis.

A Geographic Information System is a system-based tool crafted for the acquisition, preservation, adaptation, evaluation, and visualization of geographic or spatial data (Mondal et al., 2017). GIS seamlessly integrates diverse data types such as maps, satellite images, aerial photographs, and databases, enabling users to grasp, interpret, and portray patterns, trends, and correlations within the data.

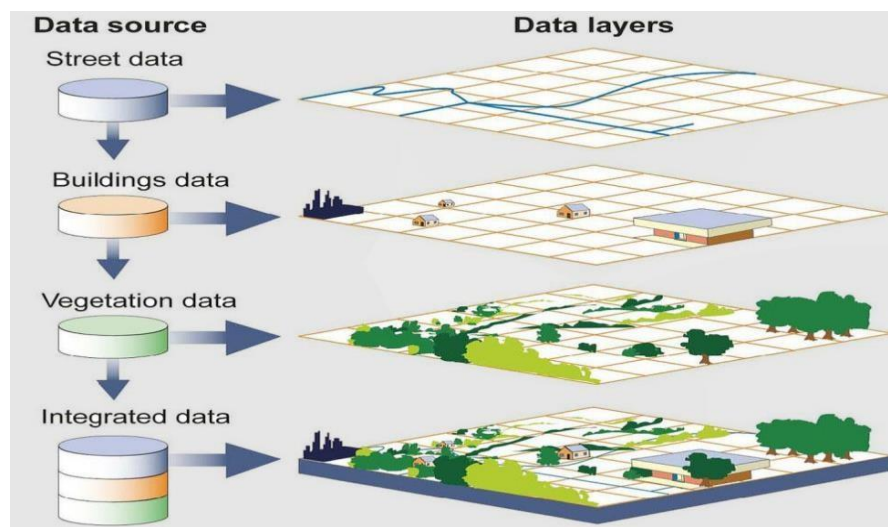


Figure 1.4. Geographic Information

System Key functionalities of GIS encompass:

i) **Data Collection:** GIS gathers spatial data from multiple origins, including satellite imagery, GPS devices, surveys, and existing maps. This data encompasses details about land features, natural resources, population, and infrastructure.

ii) **Data Storage:** Spatial data is organized and stored in a structured manner, typically using databases, ensuring efficient management and retrieval. This includes

vector data (points, lines, polygons) and raster data (grids with specific values for each cell).

iii) Data Manipulation: Users can manipulate spatial data through operations like overlay (combining layers to analyze relationships), buffering (creating zones around features), and spatial analysis (examining spatial patterns and relationships).

iv) Data Analysis: GIS tools facilitate intricate spatial analysis such as suitability modeling, network analysis, and spatial interpolation. These analyses inform Making selections in areas like urban development, environmental management, and source allocation.

v) Data Visualization: GIS software provides tools for crafting maps and visual representations of spatial data. Maps can be tailored with various layers, symbols, and labels, simplifying the communication of intricate information to stakeholders.

vi) Geospatial Query: GIS enables users to execute spatial queries, retrieving specific information based on location. For example, users can inquire about all schools within a certain distance from a specific point.

vii) Geodatabase Management: GIS oversees geospatial data in geodatabases, ensuring data integrity, consistency, and security. Geodatabases allow the establishment of complex relationships and rules for spatial data.

GIS finds extensive applications in diverse fields including urban planning, natural resource management, agriculture, disaster management, transportation planning, epidemiology, and environmental monitoring. This technology is instrumental in making informed decisions, streamlining processes, and resolving spatial challenges across various industries and research domains.

1.7 INTRODUCTION OF LULC

Satellite images are a vital source of information for various disciplines like earth sciences, ecological assessment, urban planning, cultivation, and disaster readiness, and more. These images are captured by satellites, and satellite images are photographs or digital representations of the Earth's surface, oceans, and atmosphere, taken from orbiting satellites. These images are used to observe, monitor, and analyze various aspects of our planet, from natural phenomena like weather patterns and geological features to human activities like urban development and agriculture. Land Cover (LC)

denotes the visible physical covering of the Earth's surface. LC is important in understanding Earth's environment and land management processes. LC is a crucial element in climate change, biodiversity conservation, and the management of land resources (Mahmon et al., 2015; H. A. Abdu et al., 2019).

It is necessary to classify LC and Land Use (LU) resources for land cover mapping and resource management (P. Helber et al., 2019). Therefore, LULC includes the features of the Ground's surface, comprising natural and human-influenced elements. Studying changes in LULC is critical in analyzing regional, local, and global climatic fluctuations. Land cover is the distribution of forests, wetlands, impermeable surfaces, agricultural land, and other features throughout the Earth's surface. On the other hand, land use relates to how humans use the landscape through growth, sustainability, or a combination of the two (Cao et al., 2019; Fang et al., 2019; Huang et al., 2020). Land use categories include recreation locations, wildlife habitats, agricultural land, and developed areas. The task of LULC classification holds great importance in informing agricultural decisions and planning for the long-term development of urban areas, utilizing earth observation data. (M.A. Wulder et al., 2018; L. Wang et al., 2020). LULC classification aims to establish a consistent and standardized division of the Surface Features of Earth at various scales. The demand for simplified maps facilitating decision-making and planning has necessitated this level. LULC maps are valuable for studying natural hazards, estimating agricultural production, detecting urban changes (R. Neware et al., 2018), monitoring weather patterns, and assessing biodiversity (M. P. Vaishnav et al., 2019; J. Geng et al., 2015). The accessibility of Earth observation datasets from multiple space agencies has contributed significantly to developing image feature extraction systems.

1.7.1. LAND

Land, being a fundamental and finite natural resource, plays a pivotal role in shaping human economic activities, societal progress, and cultural advancements. The quality and productivity of land significantly impact agricultural, animal, and forestry productions. The terrestrial ecosystem, comprising soil, water, and plants, relies on land resources to meet essential needs such as food and energy. As the population grows and land faces increasing pressure, it becomes imperative to study its usage for effective

regional resource planning. Land use, in essence, refers to human utilization of land, emphasizing its functional role in economic activities. The land is becoming an infrequent asset owed to significant burdens from rural and urban development. Currently, classifying LU and LC by RS images is crucial for various applications such as managing biological resources, agricultural practices, land use planning, and forest management (Liping et al., 2018). Understanding LU and LC information is important for assessing the status of the land, making plans based on climate change, and ensuring the sustainability of available resources. (Zhang et al.,2020; Sexton et al.,2013). Additionally, land utilization addresses associated challenges and explores alternative uses, aiming to optimize its capabilities. Land serves as the foundational resource upon which all other natural resources depend. Thoughtful and rational land planning is essential; surveys play a major role in understanding the trajectory of land utilization. The indiscriminate exploitation and improper use of land resources in recent decades have led to widespread issues like soil erosion, siltation, floods, droughts, and the rapid depletion of forests, flora, and fauna. This degradation has significantly impacted environmental quality and overall life standards. Therefore, studying land use patterns becomes vital and unavoidable. Uncontrolled use of this resource can lead to problems such as unplanned development, declining environmental quality, and the loss of prime agricultural lands, underscoring the critical importance of understanding and managing land use effectively (Chen et al.,2019). The land cover speaks about the different types of terrain on the surface of the Earth, like trees, wetlands, and urban areas. (Erle et al., 2010; C. Prakasam et al., 2010). Land use describes how humans utilize the land for development and sustainability. Urban sprawl, unplanned urbanization, and the rapid growth of populations can have serious detrimental effects on the natural environment (S. Gupta et al., 2011). Evaluating LULC is crucial aimed at addressing ecological challenges such as uncontrolled urban growth, loss of agricultural land, and destruction of wetlands at local, national, and global levels (Quintas-Soriano et al., 2016; Anderson et al., 1976). Assessing LULC changes helps us understand: (i) the modifications being affected, (ii) the types of land cover being replaced, (iii) the climatic changes, (iv) the rate of land change, and (v) the underlying reasons for the change.(Brown et al., 2000, Loveland et al.,2018).

The classification of land resources identifies five primary natural entities:

terrain, climate, soils, water resources, and forest cover. Among these, the climate, relief, and geological formations of the land exhibit a high level of stability. Soils and water resources fall into the category of moderately stable resources, whereas vegetation and other biological features are relatively less stable. This classification underscores the interdependence of all these natural resources with land. As the global population continues to grow, and with an increasing array of demands being placed on land resources, there is a pressing need to understand the current utilization of land at a micro-level. This understanding is crucial and aimed at effective planning to optimize land use, also to confirm its sustainable management.

Economic progress and population expansion have instigated swift alterations in the Earth's land cover in recent decades, with clear indications that these changes will intensify further. These rapid transformations occur alongside enduring patterns linked to climate fluctuations. Alterations in land cover can impact the land's ability to support human activities by providing various ecosystem services. The ensuing economic activities create feedback loops that influence climate and other aspects of global change. Hence, comprehensive evaluations of Earth's land cover need to be conducted regularly, allowing monitoring of both long-term trends and yearly variations. These assessments should also offer a detailed spatial analysis to explore human-induced modifications. Natural resources play a significant influence in the economic growth and expansion of regions. The extent of development is intricately linked to the availability and effective utilization of these resources, ensuring sustainability for future population needs. However, these natural resources are not only limited but also some are non-renewable. The growing human population exerts increasing pressure on these resources, leading to faster depletion due to overexploitation and mismanagement.

1.7.2. LAND COVER

"Land cover" applies to all the biodegradable human-made features, such as vegetation, water bodies, forests, grasslands, urban areas, agricultural fields, and human settlements, that cover the surface of the Earth, represented in Figure 1.6. (Abdul Walid Salik et al., 2019, Mohajane et al., 2018, and Gebiaw T Ayele et al., 2018) It encompasses observable ecological aspects of the top of the Earth. Classification of surface area holds significant importance in environmental studies, urban planning, and

natural resource management, offering valuable insights into changes in ecosystems, biodiversity, and land use patterns over time. Remote sensing technologies, particularly satellite imagery, are widely utilized for classifying and monitoring different land cover types across diverse geographical regions (Geng et al., 2019). Integral to GIS and remote sensing, land cover serves as the foundation for mapping and analyzing Earth's surface characteristics (Chaichoke Vaiphasa et al., 2011). Tracking and comprehending land cover changes over time is critical for various applications, including environmental preservation, urban planning, natural resource management, and climate research.

1.7.3. LAND USE

The term "land use" pertains to specific steps and functions that occur on a particular piece of land within a given timeframe. It is intricately linked with human activities associated with a specific area of land. Land use, in its essence, emphasizes the functional role of land concerning economic activities (P. Helber et al., 2019, M.A. 2018; L. Wang et al., 2020). It encompasses all human activities carried out on land, and is defined as "man's activities and various uses conducted on land," shown in **Figure 1.5**. Land use serves as a primary indicator, showcasing the extent to which humans have modified natural resources (Khatami et al., 2017). At a specific point in time and space, land use refers to the utilization of both developed and vacant land. It primarily concerns the optimal allocation of limited land among various major types of land use and is shaped by the continuous interaction between available resources and human needs, influenced by human endeavors. Effective land use is vital for human survival, prompting mankind to play a crucial role in managing and transforming their physical environment. Hence, a comprehensive understanding of land use through scientific knowledge is essential for addressing various associated challenges. The overall land use of a region is the culmination of a detailed exchange of physical, economic, and social factors. These factors, such as physiography, climate, soil, population, irrigation, urbanization, industrialization, and transportation, significantly influence the general land use patterns. These land use patterns serve as a reflection of the dynamic interaction between human society and the natural environment.



Figure 1.5. Types of Land Use

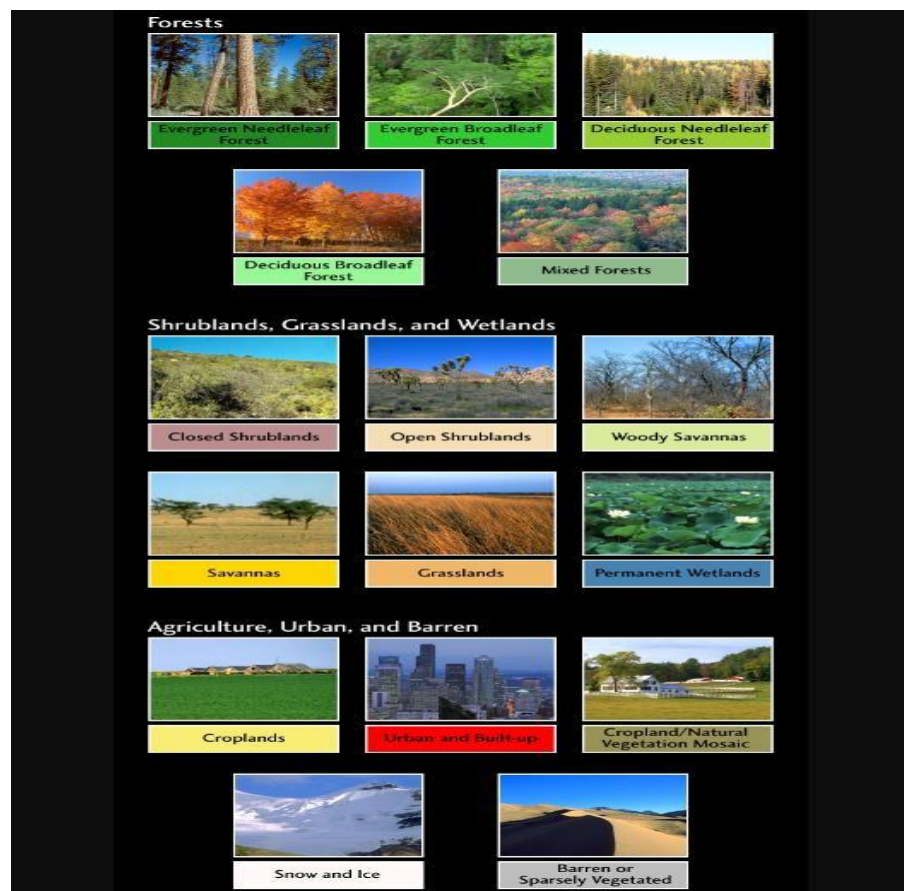


Figure 1.6. Types of Land Cover

The thought of land consumption has been defined diversely by geographers and described as "the use to which the entire land surface is put." Land, being a fundamental natural resource, significantly influences mankind's economic, social, and cultural advancements. Discussions about land issues and politics invariably revolve around the central role of land resource utilization. The collective land use

must aim to satisfy the myriad needs and legitimate desires of the entire nation's populace. The pressing need is for meticulous land resource planning, which must consider both present and historical trends (Abdu et al., 2019). Effective planning should be dynamic, adaptable to changing conditions, and responsive to evolving societal habits. Every region possesses unique attributes, and socio-economic and physical factors play pivotal roles in land use planning. The intricate interplay of physical, socio-economic, and technological elements influences land use patterns. The ecosystem concept offers a contemporary scientific framework for understanding land use. Human activities throughout history have shaped the present land use types, reflecting the relationship between human endeavors and natural resources. Land use patterns are intricate, dynamic, and variable, representing the outcomes of thousands of years of settlement trials and errors. The current land use pattern in India, for instance, results from a prolonged interplay of environmental factors, modified by socioeconomic and historical factors. Rational planning is essential for optimal land use. Geographers play a vital role in studying land use by focusing on human activities within their immediate environment. By employing techniques such as survey, mapping, analysis, and interpretation, geographers provide the foundational knowledge needed for rational land use planning. Land use encompasses various types, some permanent while others are in constant flux due to human interventions driven by diverse needs and desires. Advances in science and technology have enabled detailed examinations of land use within highly geospatial environments, providing accurate data. Scientific land use studies are crucial for rational planning, especially for maximizing the use of arable land. Land use studies have become indispensable tools for regional planning and development, playing a pivotal role in evaluating a region's resource base. Particularly in areas where land use forms the backbone of the regional economy, such studies are vital (Naidu et al., 2018). The key challenges in land use encompass issues such as under-utilization, over-utilization, and mis-utilization. Available land for agricultural and other purposes is finite and limited, leading to challenges posed by a growing population and a decreasing man-land ratio. In this context, micro-level, rational, and judicious land use planning is imperative to optimize land as a valuable resource.

1.8 NEED FOR LULC

LULC data play a pivotal role across diverse sectors such as urban planning, environmental stewardship, agriculture, forestry, and the conservation of natural resources. Here's why LULC data holds significant importance:

i) Urban Planning: LULC data empowers urban planners with insights into prevailing land use patterns in cities and regions (Huang et al., 2021; Padalia et al., 2018). This knowledge informs strategic decisions related to infrastructure development, zoning regulations, and land use policies, shown in **Figure 1.7**.



Figure 1.7. Urban planning using GIS

ii) Environmental Management: LULC data is instrumental in evaluating the environmental consequences of human behavior. It facilitates the tracking of improvements about environmental cover, including urbanization and deforestation, and wetland depletion, which are fundamental for conservation efforts represented in **Figure 1.8**.



Figure 1.8. Environmental impact

iii) Agriculture: LULC data offers valuable insights for agricultural planning by delineating lands suitable for different crops. It guides farmers in decisions regarding crop selection, irrigation, and soil management practices.

iv) Forestry: In forestry management, LULC data is utilized to monitor alterations in forest cover, assess rates of deforestation, and strategize reforestation efforts. It supports sustainable forest management practices.

v) Natural Resource Management: LULC data aids in pinpointing areas rich in natural resources such as minerals, water bodies, and biodiversity hotspots. This information is indispensable for sustainable resource management and conservation initiatives shown in **Figure 1.9**.



Figure 1.9. Need for LULC changes

vi) Climate Change Studies: LULC data plays a crucial role in climate change research by allowing the Assessment of how alterations to the land cover affect the climate. Modifications, such as urban extension or deforestation, can have a significant impact on local and regional climates.

vii) Disaster Management: LULC data is vital for assessing and managing disaster risks. It assists in identifying areas prone to natural disasters like floods, landslides, or wildfires, crucial for disaster preparedness and response planning shown in **Figure 1.10**. (Shaw et al., 2017; Mosavi et al., 2020).



Figure 1.10. Disaster Management

viii) Infrastructure Development: LULC data facilitates the planning and construction of infrastructure such as roads, bridges, and utilities. It aids in selecting suitable locations for projects and evaluating their environmental impact.

ix) Biodiversity Conservation: By comprehending different land cover types, conservationists can identify critical habitats for various species. This knowledge is essential for designing protected areas and implementing effective conservation strategies.

x) Water Resource Management: LULC data contributes to watershed management and water resource planning. It identifies areas crucial for groundwater recharge and spots vulnerable to pollution, thereby informing sustainable water management practices.

In essence, LULC data is indispensable for making well-informed decisions in various fields, ensuring sustainable development, safeguarding the environment, and optimizing resource utilization.

1.9 FACTORS AFFECTING LULC

Land use and land cover (LULC) alterations result from innumerable natural and human-driven influences. These factors, while diverse, have commonalities that shape LULC transformations in various regions and contexts and are represented in **Figure 1.11:**

i) Population Growth: The rise in population often triggers urban sprawl, transforming natural landscapes into residential and commercial hubs. Economic

Development: Industrial and urban growth reshapes land use, with booming economies expanding infrastructure and industrial zones.

ii) Agricultural Practices: Changes in farming techniques can convert forests or natural habitats into agricultural land and vice versa, driven by afforestation or reforestation efforts. **Technological Advances:** Innovations like advanced irrigation systems affect land suitability for agriculture, prompting shifts in land use.

iii) Policy and Governance: Government regulations, zoning laws, and environmental policies significantly influence LULC changes, shaping urban and rural spaces.

iv) Climate Change: Altered climate patterns impact agricultural productivity and land suitability for various purposes, influencing LULC.

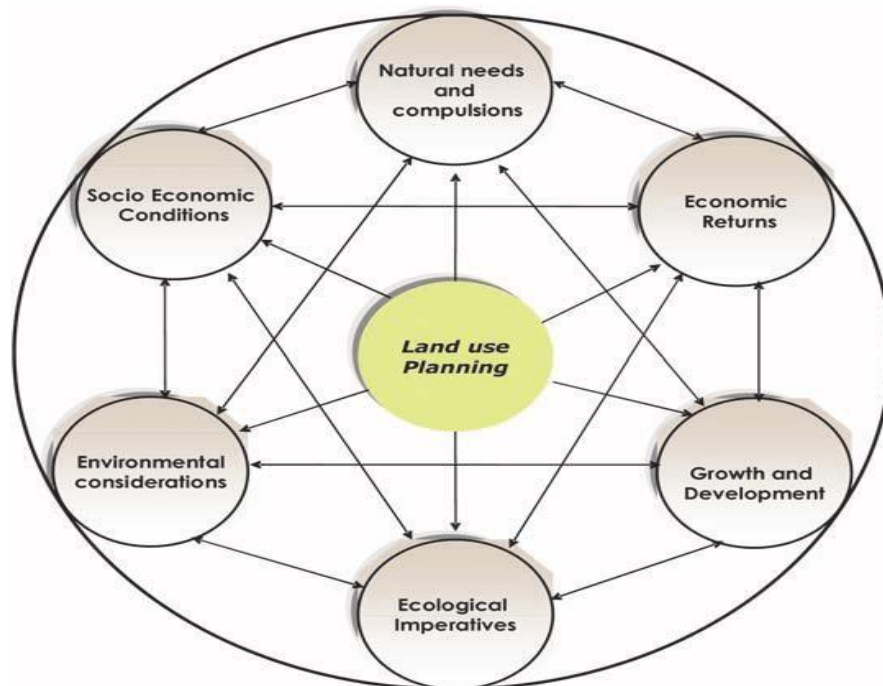


Figure 1.11. Factors affecting LULC

v) Natural Disasters: Wildfires, floods, and earthquakes reshape landscapes, prompting changes in land cover types. **Infrastructure Development:** Building roads, dams, and other structures can fragment habitats and modify natural land covers.

vi) Socio-cultural Factors: Cultural traditions influence land use, especially in rural areas where agricultural practices align with local customs.

vii) Conservation Efforts: Protected areas and conservation initiatives limit certain land uses, preserving natural habitats and biodiversity.

viii) Market Forces: Demand for resources like timber, minerals, or biofuels drives land use changes, often leading to the exploitation of specific areas.

ix) Land Degradation: Soil erosion and desertification limit land usability, impacting decisions on land use. **Land Ownership Changes:** Shifts in land ownership due to sales, inheritance, or reforms lead to alterations in land use patterns.

x) Technological Tools: Tools such as RS and GIS aid in keeping track of land cover changes and shaping decision-making processes. Understanding these factors and their interconnections is vital for sustainable land management, enabling the mitigation of negative impacts on the environment and society. Each region experiences these influences uniquely, leading to distinct LULC change patterns.

1.10 IMPORTANCE OF STUDYING LAND USE/LAND COVER AND VEGETATION CHANGE

This study and its importance lie in the significant impact it has on ecological, social, and economic systems. LULC and vegetation transformation affect the environment also the livelihoods of communities that depend on natural resources. Therefore, monitoring and managing these changes is critical to mitigating negative impacts on ecological, social, and economic systems (Mamun et al., 2013).

LULC can cause environmental issues like diminished biodiversity, soil erosion, and water scarcity. For example, deforestation leads to a decrease in forest cover, in turn, distresses the water cycle and reduces biodiversity. Similarly, agricultural expansion can result in soil degradation and depletion of soil nutrients, affecting crop yields and productivity shown in **Figure 1.12**. Monitoring land use/land cover change can help identify areas where environmental problems are likely to occur, and action can be taken to prevent or mitigate these problems.

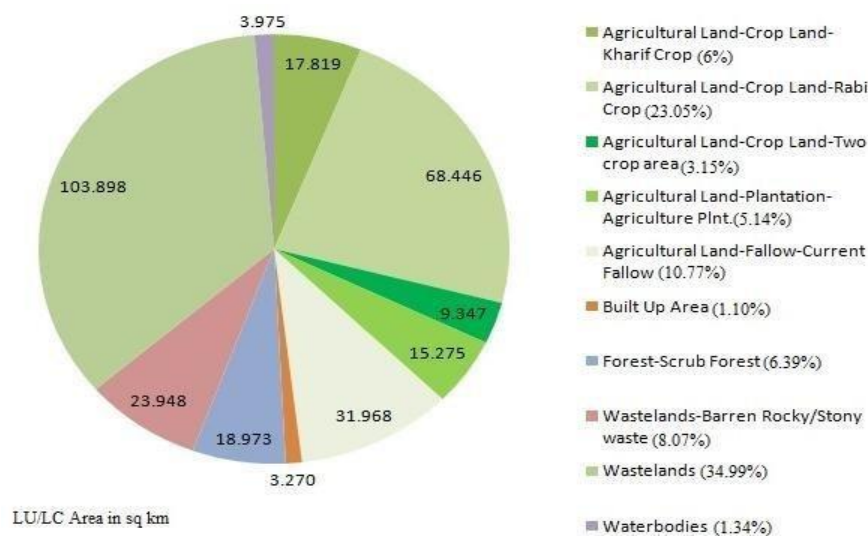


Figure 1.12. Land Use/Land Cover area

Secondly, land use/land cover change can have significant social impacts, particularly on communities that depend on natural resources for their livelihoods. For example, the expansion of agricultural land can result in the displacement of local communities or the destruction of their cultural heritage. Similarly, urbanization can result in the loss of access to resources such as water and forests, affecting the quality of life of communities. Monitoring land use/land cover change can help identify areas where social problems are likely to occur, and action can be taken to prevent or mitigate these problems.

Thirdly, land use/land cover change has economic implications, particularly regarding resource use and management. For example, the translation of forests to agronomic land can result in a loss of revenue from timber and non-timber forest products. Similarly, the loss of wetlands can affect the regulation of water flow and nutrient cycling, affecting fisheries and other industries. Monitoring land use/land cover change can help identify areas where economic problems are likely to occur, and action can be taken to prevent or mitigate these problems.

Remote sensing technology is an extremely prevalent and effective tool that can be used to accurately monitor and track vegetation alterations. Remote sensing data can present statistics on land cover and vegetation patterns across broad regions and at different times. However, the vast amounts of data generated by remote sensing systems present significant challenges for data processing and analysis.

1.11 IMPACTS OF LAND USE/LAND COVER AND VEGETATION CHANGE ON ECOSYSTEMS, SOCIETY

Vegetation transformation and LULC are critical issues that affect both ecological and social systems globally. The expansion of agriculture, urbanization, deforestation, and mining activities has resulted in significant modifications to land use patterns, resulting in the loss of natural resources and degradation of ecosystems shown in **Figure 1.13**.

The conversion of natural ecosystems into agricultural land or urban areas has led to habitat loss and fragmentation, resulting in the loss of species diversity (Babar et al., 2017). This loss of biodiversity can have significant implications for the functioning of ecosystems, including the regulation of the water cycle, nutrient cycling, and pollination. Land use/land cover change can also lead to soil erosion and degradation, resulting in decreased soil fertility and productivity. Agriculture can contribute to soil erosion and degradation using conventional farming practices such as plowing and monoculture. Soil erosion can affect crop yields and result in food insecurity, particularly in areas where small-scale farmers depend on subsistence agriculture. Water availability and quality are also affected by land use/land cover change. Deforestation can lead to reduced water availability, while urbanization can result in increased surface runoff, leading to flooding and erosion. The transformation of wetlands into grassland or urban areas can also impact water quality, as wetlands play a vital role in filtering pollutants and nutrients.

Land use/land cover change can also have significant social impacts. The displacement of communities that depend on natural resources for their livelihoods is a common consequence of LULC change. For example, the construction of dams can result in the displacement of local communities and loss of livelihoods (Bhatia et al., 2019). The loss of cultural heritage, including archaeological sites and traditional knowledge systems, is another social effect.

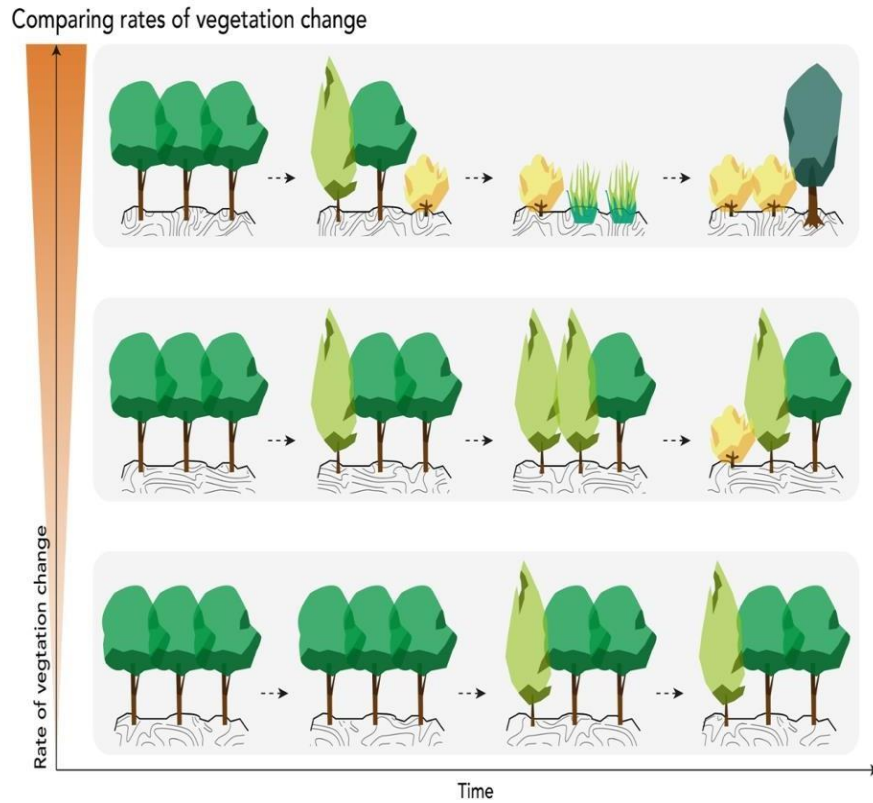


Figure 1.13. Vegetation change

Public health is another significant concern associated with LULC change. Deforestation can increase risk of disease transmission, as it can lead to the expansion of habitats for disease vectors such as mosquitoes. Urbanization can result in air pollution and other health hazards that affect the well-being of local populations. It is important to develop Effective utilization of land practices that balance the needs of people and the environment. This requires the development of regulations and methods that support sustainable land use and the protection of natural possessions. environmentally friendly techniques for using farmland include the use of agroforestry, conservation agriculture, and land-use planning that considers ecological and social factors.

In summary, land cover and use and vegetation transition are critical issues that affect both ecological and social systems. Addressing the effects of land use Adaptation is essential to achieving sustainable land use practices that meet people's and the environment's demands. Land use/land cover (LULC) and vegetation transformation

have been studied extensively inside the remote sensing profession and geospatial analysis due to their crucial importance in understanding the dynamics of the top of the earth. The transformation in LULC and vegetation is driven by various natural and anthropogenic factors such as climate change, urbanization, deforestation, agricultural practices, and population growth.

LULC changes refer to Adjustments in the physical and biological aspects of land and its usage (Hosseiny et al., 2022). Vegetation change, on the other hand, refers to changes in the structure, composition, and distribution of vegetation cover. This is particularly important as vegetation provides important ecosystem services such as carbon sequestration, soil stabilization, water regulation, and wildlife habitat.

The impacts of LULC and vegetation change are multidimensional, affecting both the natural and human systems. For instance, deforestation and urbanization can lead to soil degradation, loss of biodiversity, and alteration of hydrological regimes, thereby affecting food security, water availability, and climate change. Additionally, these changes have significant social and Economic consequences related to the displacement of communities, Poor performance of traditional livelihoods, and decreased land productivity. In summary, LULC and vegetation change are critical factors in understanding the Ground's surface dynamics besides its impacts on the environment and society.

1.12 SIGNIFICANCE OF LAND USE/LAND COVER

This research serves an important function of the Earth's ecosystems and is an essential component of sustainable development (Aravindanath et al., 2012). Understanding the patterns is important for a wide range of applications, including natural resource management, biodiversity conservation, weather modification adaptation, and urban planning. For example, the conversion of forested land to agricultural land can lead to soil erosion and loss of habitat for wildlife, while urbanization can result in the loss of farmland and fragmentation of natural habitats. On the other hand, reforestation and afforestation efforts can help mitigate climate change by sequestering carbon dioxide from the atmosphere.

Furthermore, LULC changes can also have socio-economic impacts, such as changes in land ownership and use rights, displacement of local communities, and

changes in the availability of natural resources. For example, the conversion of traditional grazing lands to croplands may affect the livelihoods of pastoralist communities.

Therefore, studying land use/land cover is crucial and aimed at informed decision-making in a wide range of fields, from resource management to environmental planning and policy. It can help identify potential areas for conservation and restoration, and inform policies to promote sustainable development.

1.13 VEGETATION CHANGE

Vegetation change refers to the alteration or transformation of the composition, structure, and distribution of plant communities in each area over time. This change can be driven by natural factors such as climate change, or by anthropogenic components like land-use changes, deforestation, and urbanization. Understanding the dynamics of vegetation transformation is decisive for effective land management and conservation, as well as for mitigating the influences of microclimate change.

In addition, the introduction of invasive plant species can also cause vegetation change by altering the composition of native plant communities. These changes can possess vast effects on services related to nature such as carbon sequestration, Monitoring of water, and biodiversity preservation. Monitoring and analyzing changes in vegetation is fundamental to maintaining the integrity of sustainable land and planning shown in **Figure 1.14**.

One of the most important uses of vegetation change is ecological monitoring. Scientists use changes in vegetation to maintain an eye on the sustainability of the environment and the impact of environmental changes on them. From inspection of the vegetation change over time, they can distinguish between regions at risk of losing biodiversity, develop conservation strategies to protect them, and study the ecological effects of human activity.

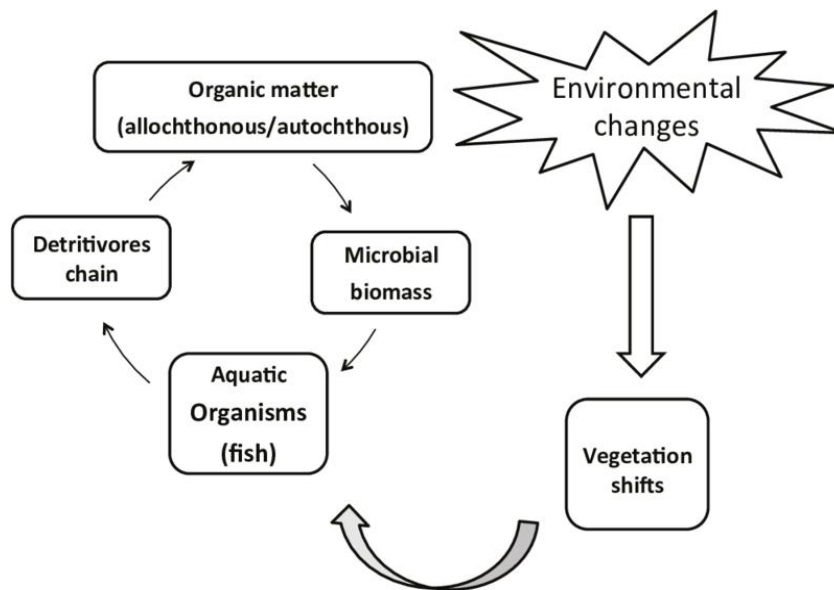


Figure 1.14 Vegetation change analysis

Vegetation change also has practical applications in agricultural and forestry management. Farmers and foresters use vegetation change to monitor soil health, assess the growth and health of crops and trees, and identify areas of erosion, pest outbreaks, and invasive species. This information is used to improve crop yields, protect against disease and pests, and promote sustainable forestry practices.

Vegetation change is also important in wildlife management. By monitoring changes in plant communities that support wildlife, scientists can identify areas of habitat loss and degradation, assess the health and diversity of plant communities, and develop strategies to restore degraded habitats. This information is used to support the recovery of threatened and endangered species and to promote sustainable wildlife management practices.

In addition, vegetation change is vital for storing carbon. Trees and other vegetation absorb carbon dioxide from the atmosphere through photosynthesis, helping to mitigate climate change. Scientists use vegetation change to monitor the growth and distribution of trees and other vegetation that absorb carbon, which is important for developing strategies to reduce greenhouse gas emissions.

Finally, vegetation change also has important implications for human health. Studies have shown that exposure to green space, including parks and urban green spaces, has significant benefits for mental health, physical activity, and air quality. Understanding

vegetation change can help scientists and urban planners develop strategies to create and maintain healthy green spaces that benefit people and the environment.

1.14 THE SIGNIFICANCE AND OBJECTIVE OF THE RESEARCH

The ultimate objective of this thesis is to employ a conventional DL to estimate and validate vegetation change analysis in a specific region of Andhra Pradesh state, India, utilizing the Landsat7, Landsat8, and Sentinel-2 datasets. The study area comprises key categories such as vegetation, water bodies, built-up areas, urban regions, and barren land. Traditionally, agricultural land classification has relied on door-to-door surveys. Remote sensing, as a vital information source, significantly contributes to the monitoring, mapping, and management of natural resources. Ongoing enhancements in the spectral and spatial resolution of sensors have piqued the interest of researchers, enabling the monitoring of LULC changes through change detection techniques. Change detection facilitates the differentiation between satellite images captured at different time points and is essential for analyzing temporal variations in the Earth's surface. Change detection methods have diverse applications, including monitoring vegetation changes, deforestation, forest fires, crop growth, urban expansion, and alterations in landscapes. Identifying and categorizing land surface features, however, remains a complex and critical task. Given their extensive applications, researchers continually strive to enhance change detection techniques and integrate new technologies into conventional methods. In this work, we delve into recent developments in classifiers based on satellite datasets, particularly focusing on agricultural land.

THE OBJECTIVES OF THE PROPOSED WORK:

1. To detect and determine LULC change dynamics for agricultural land using remote sensing and GIS.
2. To analyze the association of the spatial dimension of LULC change dynamics with demographic, economic, and environmental regions.
3. To predict Land Use Land Cover change dynamics for the area of interest.

1.15 OUTLINE OF THE THESIS STRUCTURE

Chapters of the thesis will provide an in-depth background of the study, including a literature review of the relevant concepts, theories, and studies on land use/land cover and vegetation change.

Chapter 1 Introduction: In this chapter, a concise overview is provided on agricultural land cover classification and satellite remote sensing, encompassing details on characteristics, sensor types, image pre-processing steps, and change detection techniques. The chapter concludes by emphasizing the significance of the study.

Chapter 2 Literature Review: This chapter conducts a systematic survey, examining the work carried out by various researchers, particularly focusing on recent advancements in classification algorithms, specifically for agricultural land. The exploration delves into emerging methods such as machine learning and deep learning, aiming to enhance the detection of diverse vegetation parameters. Through the literature review, research gaps are identified, leading to the formulation of research objectives.

Chapter 3 Study Area, Satellite Datasets: This section provides comprehensive information about the study area and the satellite sensor datasets utilized in this thesis. The chapter elaborates on the importance of the chosen study site and outlines the datasets employed in the development of the traditional Deep Learning for Crop Detection method, which includes Landsat series and Sentinel-2.

Chapter 4 Methodology: This chapter will outline the approach used to accomplish the objectives of the current study. This chapter aims to introduce a simple yet advanced traditional deep learning model for LULC classification, to obtain change detection using the Landsat and Sentinel-2 datasets.

Chapter 5 Results and Discussion: In this chapter, the developed algorithm is implemented and compared with existing algorithms. The performance of the proposed method is thoroughly analyzed through statistical, graphical, and visual assessments. Various accuracy assessment measures are employed to evaluate the potential of the developed algorithm, and the results are presented comprehensively.

Chapter 6: Conclusion and Future Scope: This chapter provides a summary of the key features of the present study and outlines future recommendations and areas for further research.

CHAPTER-II

LITERATURE REVIEW

Key points:

- Literature on approaches to classification.
 - Research on land cover classification using traditional, machine, and deep learning methods.
 - Literature on change detection strategies of the region of interest.
-

2.1 INTRODUCTION

In this chapter, we will discuss the different strategies used for land cover classification and its impact using satellite imagery (Khandelwal et al., 2014). Satellite image classification techniques are crucial in satellite image processing as they involve dividing an image into isolated areas with suitable land-class labelling (Hameed et al., 2017). This ensures that each region carries specific details about that land class. Land cover classification is a fundamental procedure in many real-time remote sensing applications, which involves segmenting an image into distinct sections so that each region can have fundamental attributes. This chapter will explore various classifiers used for land cover classification (Cecili et al., 2023, Guo et al., 2018; Midekisa et al., 2017). There are several techniques for exploring LULC maps. Still, satellite imagery and remote sensing (H. Shahabi et al., 2012; H. Shahabi et al., 2020) have many advantages, including a broad scope, the capacity to adequately represent phenomena using distinct electromagnetic spectrum wavelengths, being relatively inexpensive, allowing for quicker evaluation (for huge areas), the option for monitoring cycles that are repeated for short periods is also available (D.C. Duro et al., 2012).

Change detection algorithms are commonly applied to track multi-temporal changes, and extensive information can be obtained in numerous papers (Lu et al., 2004; Lu et al., 2014; Singh and Talwar, 2014). Classification is a crucial feature in change detection techniques since it categorizes distinct land types based on their similarity score and allows the user to extract meaningful information using a themed map (Congalton et al., 2009; Chen et al., 2019; Lu and Weng, 2007). The

classification strategies are classified as (a) supervised/unsupervised; (b) parametric and non-parametric; (c) hard and soft; and (d) pixel-based and object-based classification (Guo et al., 2018; Lu et al., 2007). Because of the limitations of various satellite sensors, it is impossible to capture Earth imagery at very high temporal and spatial resolutions simultaneously, necessitating pan-sharpening or fusion of high-resolution and low-resolution data.

2.2 SIGNIFICANCE OF VEGETATION CHANGE

Vegetation change is significant for a variety of reasons. Here are some of the key significances of vegetation change represented in **Figure 1.15**:

i) Environmental health: Changes in employing vegetation, people can keep an eye on the current state of ecosystems and the impact of environmental changes on them. This might help in recognizing at risk of losing biodiversity and develop conservation strategies to protect them.

ii) Agricultural and forestry management: Vegetation change suitable to be utilised to evaluate soil health, assess crop and tree growth and health, and identify areas of erosion, pest outbreaks, and invasive species. This information is important for improving crop yields, protecting against disease and pests, and promoting sustainable forestry practices.

iii) Wildlife management: Vegetation change is important for monitoring changes in plant communities that support wildlife. This can help identify areas of habitat loss and degradation, assess the health and diversity of plant communities, and develop strategies to restore degraded habitats.

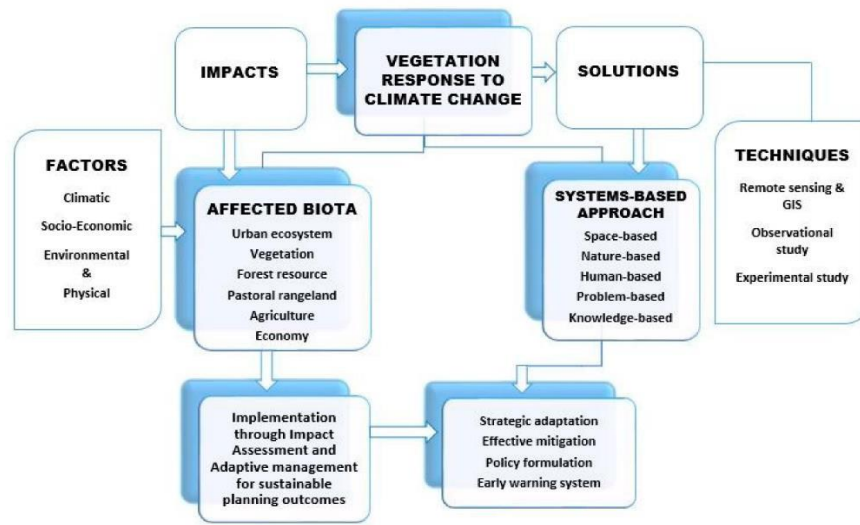


Figure 2.1 Impacts of vegetation change

iv) Carbon sequestration: Alteration in vegetation is required to preserve carbon. Trees and other vegetation absorb carbon dioxide from the environment, helping to mitigate climate change. Understanding vegetation change is important for developing strategies to reduce greenhouse gas emissions.

v) Human health: Exposure to green space, including parks and urban green spaces, has significant benefits for mental health, physical activity, and air quality. Understanding vegetation change can help scientists and urban planners develop strategies to create and maintain healthy green spaces that benefit people and the environment. vegetation change is significant because it helps us understand the health of ecosystems, promote sustainable land management practices, mitigate climate change, and promote human health and well-being.

2.3 HISTORICAL AND RECENT TRENDS

Analyzing historical and recent trends in vegetation change and their impact on land use/land cover of a specific area of interest (AOI) is a crucial task for understanding the health of ecosystems and promoting sustainable land management practices (Gao et al., 2018). The analysis may involve using conventional (Bakshi et al., 2018; Abdullah et al., 2019; Abdullah et al., 2019), Machine Learning (Ahishali et al., 2019), and deep learning techniques (Alam et al., 2021) to classify satellite or aerial imagery and identify changes in land cover/land use over time.

To perform this analysis, we would need to obtain historical and recent satellite imagery of the AOI. The images would need to be preprocessed to remove any noise and enhance the quality of the images. This includes image enhancement techniques such as contrast stretching, histogram equalization, and filtering to improve the quality of the images. It is also important to ensure that the images are georeferenced so that they can be compared accurately over time. (Balaji et al., 2018)

The next step is to train the learning models using the preprocessed images. This involves labeling the images with the corresponding land cover/land use classes, such as forest, urban, agriculture, etc. The models are then trained to identify and classify the different land cover/land use categories.

Once the models are trained, we can use them to classify historical and recent satellite imagery. We can then compare the land cover/land use classification results over time to identify any changes in vegetation cover and land use/land cover trends. For example, we can identify areas where there has been significant vegetation change, such as deforestation or afforestation, and assess the impact on the surrounding land use/land cover.

The results of this analysis can provide valuable insights into the environmental health of the AOI, help identify areas of potential ecological concern, and inform land use planning and management decisions. For example, we can identify areas where conservation efforts are needed or where land use practices need to be changed to promote sustainability.

The use of deep learning techniques can improve the accuracy and efficiency of this analysis by automating the image classification process and providing more accurate and detailed information on vegetation change and land use/land cover trends over time (Bahri, et al., 2019). This can help us better understand the impact of human activity on the environment and make informed decisions to promote sustainable land management practices.

2.4 DRIVERS OF LAND USE/LAND COVER AND VEGETATION CHANGE

The several drivers are:

i) Population growth and urbanization: The growth of cities and the rise in population are significant drivers, particularly in rapidly urbanizing provinces. As populations grow, more land is needed to accommodate housing, infrastructure, and commercial development (Jaiswal et al., 2018). This often leads to the conversion of natural habitats to built-up areas and can result in deforestation and loss of biodiversity. Urbanization refers to the process of people moving from rural to urban areas. This trend has been particularly prevalent in developing countries, where urban populations are expected to double by 2050. Urbanization can result in significant land use change, particularly in peri-urban areas where urban growth is rapidly expanding into agricultural and natural areas. This can have significant impacts on ecosystems and biodiversity, particularly if natural habitats are converted to built-up areas. Urbanization can also result in changes in the use of natural resources. For example, as people move to urban areas, the demand for food, water, and energy increases, leading to increased pressure on agricultural lands and natural resources. This can result in changes in land use and vegetation patterns, particularly if natural habitats are converted to farmland or urban areas (El-Magd et al., 2008).

Population growth and urbanization are significant drivers in understanding the impacts of these processes on ecosystems, and biodiversity is crucial for promoting sustainable land use and protecting natural habitats. This requires a range of approaches, including improving land-use planning and management, promoting sustainable urbanization practices, supporting conservation and reforestation efforts, and promoting policies and initiatives that promote sustainable development.

ii) Agricultural expansion: Agricultural expansion is another significant driver of land use change, particularly in developing countries where agriculture is a major economic activity. The expansion of agricultural land often involves clearing natural habitats, which can result in habitat loss and degradation.

Agricultural expansion is often driven by population growth and the increasing demand for food. As populations grow, the demand for food increases, and this can lead to the expansion of agricultural land. This often involves the conversion of natural habitats,

such as forests and grasslands, to farmland. This can have significant impacts on ecosystems and biodiversity, particularly if the conversion of natural habitats is not done sustainably.

Agricultural expansion can also result in changes in land use and vegetation patterns. For example, the conversion of forests to agricultural land can result in significant changes in the hydrological cycle, as forests play a crucial role in regulating water flows. The conversion of grasslands to farmland can also result in changes in vegetation patterns, leading to the loss of important habitats for wildlife.

This requires a range of approaches, including promoting sustainable agriculture practices, supporting conservation and reforestation efforts, improving land-use planning and management, and promoting policies and initiatives that promote sustainable development shown in **Figure 2.2**.

iii) Mining and resource extraction: Mining and resource extraction is another significant driver of land use change, particularly in regions with rich mineral resources. Mining can involve the removal of large amounts of soil and rock, often resulting in significant changes in land use and vegetation patterns.

Mining and resource extraction can have significant impacts on ecosystems and biodiversity. The removal of soil and rock can result in habitat loss and degradation, and can also lead to soil erosion and sedimentation of rivers and streams. This can have significant impacts on aquatic ecosystems, as increased sedimentation can lead to the loss of fish habitat and changes in water quality.

Mining and resource extraction can also result in the release of pollutants and toxic substances into the environment, which can have significant impacts on ecosystems and biodiversity. For example, the release of heavy metals and other pollutants from mining operations can result in the contamination of soils and water bodies, leading to the loss of biodiversity and posing risks to human health. This requires a range of approaches, including improving environmental regulations and monitoring, promoting sustainable mining practices, supporting conservation and reforestation efforts, and promoting policies and initiatives that promote sustainable development.

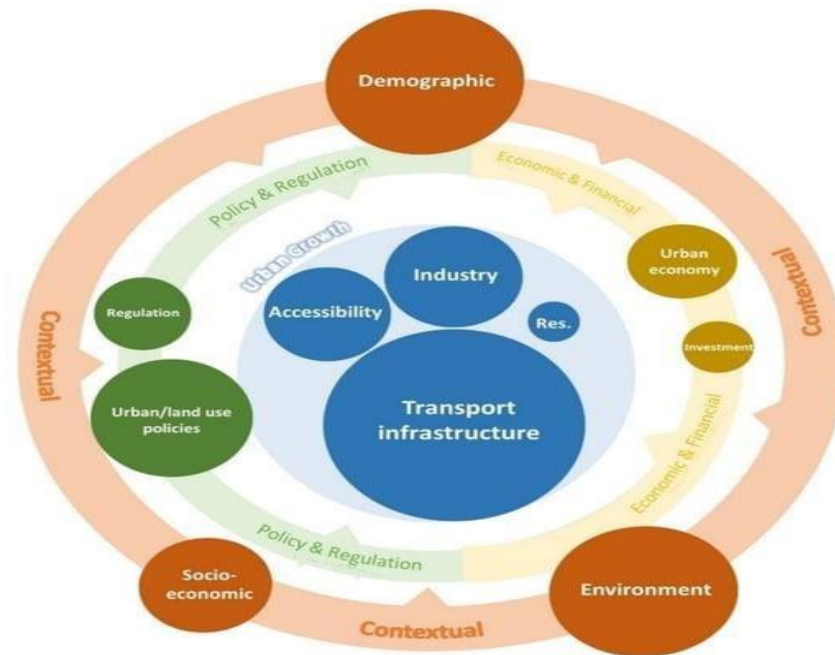


Figure 2.2 Factors driving land use and land cover change process.

iv) Climate change: Climate change can result in modifications to temperature, patterns of weather, and severe weather issues, which can have significant impacts on ecosystems and vegetation patterns. Climate change can result in changes in the seasonally related events, such as the timing of leaf emergence, flowering, and fruiting. This can result in changes in the interactions between species, such as pollinators and their host plants. Climate alteration can also result in changes in the spread of the kind, as they move to find suitable habitats in response to changing environmental conditions.

Climate variation can also result in variations incidence and seriousness of extreme weather situations as droughts, floods, and wildfires. These events can result in significant changes in vegetation patterns, such as the loss of forests and the conversion of grasslands to shrublands.

This requires a range of approaches, including promoting policies and initiatives to mitigate greenhouse gas emissions and acclimate to the impacts of microclimate variation, supporting conservation and reforestation efforts, improving land-use planning and management, and promoting sustainable development practices.

v) Infrastructure development: Infrastructure development, such as the construction of roads, highways, and urban areas, is another significant driver of land use/land cover change. Infrastructure development can result in the conversion of

natural habitats to urban and industrial land uses, resulting in habitat loss and degradation.

Infrastructure development can also result in changes in vegetation patterns, such as the fragmentation of forests and other natural habitats. This can have significant impacts on biodiversity, as fragmented habitats may be unable to support certain species or ecological processes.

Infrastructure development can also result in changes in hydrological patterns, such as changes in water flows and drainage patterns. This can result in the loss of wetlands and other important aquatic habitats, as well as increased risks of flooding and other natural disasters. This requires a range of approaches, including improving land-use planning and management, promoting sustainable urban development practices, supporting conservation and reforestation efforts, and promoting policies and initiatives that promote sustainable development.

vi) Natural disasters: Disasters caused by nature, like flooding, wildfires, hurricanes, and landslides, are significant drivers of land use/land cover change. These events can result in the loss of Protection of vegetation and changes in land use patterns, particularly in regions with vulnerable ecosystems and biodiversity.

Floods can result in damage to vegetation cover and the conversion of land uses to floodplain areas. This can result in changes in vegetation patterns, as well as the loss of habitat for aquatic species. Wildfires can result in the loss of vegetation cover and the alteration of forests and grasslands to shrublands and supplementary land uses. This can have significant impacts on biodiversity, as well as changes in the carbon balance of ecosystems.

Hurricanes can result in the loss of vegetation cover and Changes in the coastal ecosystems due to other land uses, such as urban areas or agriculture. This can result in the loss of important habitats for coastal species, as well as changes in the hydrological patterns of coastal ecosystems. Landslides can result in the loss of vegetation cover and the conversion of land uses to bare slopes and landslide scars. This can result in changes in vegetation patterns and increased risks of soil erosion and sedimentation.

This requires a range of approaches, including promoting policies and initiatives to reduce the risk and impact of natural disasters, supporting conservation and

reforestation efforts, improving land-use planning and management, and promoting sustainable development practices.

vii) Policy and governance: Policy and governance are important drivers of land use/land cover change. The policies, governance frameworks established by governments can have significant impacts on land use patterns and the protection of natural habitats. In some cases, policies and governance frameworks may encourage unsustainable land use practices, such as the expansion of agriculture or urbanization into natural habitats. This can result in the loss of biodiversity and ecosystem services, as well as increased greenhouse gas emissions and other environmental impacts.

On the other hand, policies and governance frameworks can also promote sustainable land use practices, such as the protection of natural habitats, the promotion of sustainable agriculture and forestry practices, and the development of green infrastructure. These policies can help to protect natural habitats and biodiversity, while also promoting sustainable development and reducing environmental impacts.

The role of policy and governance in driving land use/land cover change highlights the importance of effective decision-making and planning processes in promoting sustainable land use. This requires a range of approaches, including improving land-use planning and management, promoting stakeholder engagement and participation in decision-making, and promoting policies and initiatives that support sustainable development and the protection of natural habitats.

Understanding the drivers of land use/land cover and vegetation change is important for developing strategies to promote sustainable land use and protect ecosystems. This can include measures such as implementing sustainable agriculture practices, promoting reforestation and afforestation, improving land-use planning and management, and supporting policies and initiatives that promote conservation and sustainable development.

2.5 THE EFFECTS OF LAND USE/COVER AND VEGETATION TRANSFORMATION

The impacts of land use/land cover and vegetation change can be significant, affecting both natural ecosystems and human populations. Some of the key impacts include:

i) Loss of biodiversity: Land use/land cover and vegetation change results from the loss of biodiversity, as natural habitats are converted to other land uses, such as urban or agricultural land. This can result in the decline or extinction of plant and animal species, which can have cascading impacts on ecosystems.

ii) Degradation of ecosystem services: Natural ecosystems provide a range of ecosystem services, such as water purification, carbon storage, and soil conservation. LULC and foliage change can result in the degradation of these ecosystem services, which can have significant impacts on human populations, such as increased risks of flooding, decreased water quality, and reduced food security (Liu et al., 2018, 2020).

iii) Climate change: Land use/land cover and vegetation change can contribute to climate change by releasing greenhouse gases into the atmosphere, such as carbon dioxide and methane. This can result in increased global temperatures, sea level rise, and other impacts associated with climate change.

iv) Soil degradation: LULC and foliage change can result in the degradation of soils, such as increased erosion, reduced soil fertility, and increased salinization (Ellis et al, 2007,2011, Maasikamäe et al., 2011). This can result in reduced agricultural productivity and increased risks of land degradation and desertification.

v) Water scarcity: Land use/land cover and vegetation change can result in changes in water availability and quality, such as increased runoff and reduced infiltration rates. This can result in increased risks of water scarcity and reduced access to clean drinking water.

The influences of LULC and vegetation change highlight the importance of promoting sustainable land use practices and protecting natural ecosystems. This requires a range of approaches, including improving land-use planning and management, promoting sustainable agriculture and forestry practices, supporting conservation and reforestation efforts, and promoting policies and initiatives that support sustainable development and the protection of natural habitats.

2.6 METHODS AND STRATEGIES FOR LULC CLASSIFICATION

Reliable Land Use and Land Cover data can be extracted from remote sensing images using a variety of LULC classification methods and classifiers. The variety of study zones, sensors, test preparation methods, and the number of classifications to be

identified all impact on how accurate classification procedures are (VKA Somayajula et al., 2020; Tiwari et al., 2015). Depending on the approach and technology employed, the classifiers can be divided into several groups, such as supervised and unsupervised, border and non-border, hard and soft (ambiguous), or groups based on pixel and sub (VKA Somayajula et al., 2022; Nair et al., 2010). Here are two fundamental classification algorithms in a larger sense:

2.2.1 Pixel-based classification: Pixel-based classification is a process where the classification is carried out at the level of each pixel, using only the spectral information that is available for that specific pixel (He et al., 2018; Garg et al., 2014). This method helps to estimate the pixels within the area that were missed (Mas et al., 2004; Chen et al., 2020). Each pixel corresponds to a feature in a training model for a classification method. The model is an n-dimensional vector, where n is the number of spectral groups in the image data. A classification method predicts the class for each pixel in an image.

2.2.2 Object-based categorization: Object-based categorization, on the other hand, involves categorizing a limited set of pixels based on their spatial relationships with each other (Ma et al., 2017; Kumar et al., 2018; Blaschke et al., 2014).

2.2.3 Hard Classification: Hard classification is a process where an individual pixel corresponds to a specific terrain on the ground and represents a particular land cover type. Here are techniques to assign each pixel to a specific class (K. Bhosle et al., 2019; Ravi Shankar et al., 2017). This allows for identifying relevant information about a distinct scene fragment aimed at each pixel.

2.2.4 Unsupervised Classification: This technique does not require knowledge about the various forms of land cover or how they are distributed. Single-arrangement methods divide the environment into relatively pure spectral groups, usually reinforced by prescribed borders defining the distinct characteristics of these categories and how they interact with surrounding groups (X. Ma et al., 2020).

2.2.5 Semi-Supervised Learning (SSL): SSL effectively addresses the challenges of small, marked examples in high-dimensional data. It is a machine-learning strategy that enables predictive performance by combining labelled and unlabeled data (A.D. Gregorio et al., 2012).

2.2.6 Supervised Classification: In supervised classification, the image analyst assumes control over the assessment of pixel classification by selecting the appropriate mathematical descriptors and PC computations that reflect various land cover categories within a scene. This approach relies on prior knowledge of the cover types in the specified location, which defines class labels of interest across the entire scene (Ma et al., 2018; Kamalakar et al., 2021; Foody et al., 2004; Chen et al., 2020). Supervised classification methods can be categorized into per-pixel and sub-pixel approaches (Raju et al., 2016; Vishwakarma et al., 2016).

2.2.7 Parametric and non-parametric classification: Parametric classification methods necessitate the definition of certain parameters for making assumptions, but non-parametric methods do not depend on predetermined parameter settings, resulting in potentially more precise outcomes (Rao et al., 2016). Currently, machine learning (Talukdar et al., 2020) and deep learning classifiers are gaining popularity for their ability to efficiently extract important facts from remotely sensed input (Meng et al., 2020; Chen et al., 2015).

This chapter delves into the significant advancements made in the field of classification using satellite datasets, particularly for land use. The current research focuses on comparing various ways of monitoring land use and discussing recent improvements in agriculture land cover classification systems (Kumar et al., 2016, 2017). The literature study discusses several kinds of satellite sensors used in land applications (Chilar et al., 2000; Pal et al., 2003), as well as the stages required in pre-processing satellite datasets. Following that, an extensive examination of both traditional and sophisticated categorization models for land use is provided (Chong et al., 2020).

Kussul et al. (2016) proposed an algorithm for handling large-scale categorization and area estimation challenges in the remote sensing arena using the deep learning paradigm. It is built on a hierarchical model that comprises self-organizing maps (SOM) for data preprocessing and segmentation (clustering), an ensemble of multi-layer perceptrons (MLP) for data classification, and heterogeneous data fusion and geographic analysis for postprocessing. The suggested approach is used to create high-resolution land cover and land use maps for the Ukrainian area from 1990 to 2010 and 2015.

Shao et al. (2021) The Landsat OLI images from 2013 and 2015 were used to evaluate the LULC data of Nyingchi County. The Digital Elevation Model (DEM) was employed to extract the properties of the land surface and analyze their multi-layered temporal change data, enabling the four-layer monitoring of forestry data at both temporal and spatial levels. In formal procedures, mapping is carried out using available records, field surveys, and maps, making the process time-consuming and costly.

Rahaman et al. (2020) evaluated the effect of LULC changes, the atmosphere in Bardhaman district, West Bengal. The authors used TM, OLI, and TIRS images from the Landsat 8 satellite. A Geographic Information System (GIS) is a computer system used to analyze and present geographic data. It uses information that is linked to specific locations.

Duro et al. (2012) employed three distinct machine-learning techniques to classify Electro-Optical (EO) images using both pixel-based and object-based image analysis. The application of identical machine learning methods revealed no significant difference between the object-based and pixel-based classifications, thus indicating their equivalent efficacy.

Arveti et al. (2020) examined the LULC status of the Tirupati region in Andhra Pradesh using a comprehensive approach that integrated RS and GIS. This analysis revealed the significant impact of urban sprawl on the ecosystem. The expansion of tourist areas and the alteration of agronomic land into residential areas result in significant environmental deviations, with far-reaching implications for the local, regional, and global environment. It is predicted that by 2025 (Srivastava et al., 2019).

Das et al. (2020) focused on an innovative method of Remote Sensing-based Ecological Index (RSEI), which uses Landsat imagery data to evaluate ecological circumstances and change trends. Four ecological metrics were developed in the years 1990, 2000, 2010, and 2020 for the Kolkata urban region (KUA) to assess the ecological environmental state.

Nhu et al. (2020) developed an ensemble model (AB-ADTree) to predict landslides in the Cameron Highlands of Malaysia using AdaBoost (AB) and alternating decision tree (ADTree) algorithms. The model was trained on a database of 152 landslides obtained from Synthetic Aperture Radar Interferometry, Google Earth

pictures, and field surveys, along with 17 conditioning factors. The results showed that the AB model had better performance in predicting landslide susceptibility than both the ensemble AB-ADTree model and the ADTree model.

Deng et al. (2018) introduced image-processing workflows that are based on open-source software and can be used to create land-cover maps from ultra-high-resolution aerial imagery. The most accurate workflow for classifying ultra-high-resolution imagery depends on diverse factors that are influenced by image resolution and land-cover characteristics, such as contrast, landscape patterns, and the spectral texture of the land-cover types being classified.

Sundara et al. (2012) used the Maximum Likelihood Classifier to scrutinize LULC changes and urban sprawl in Bezawada City in 1990 and 2009. The overall accuracy was 86.67%, with Kappa Coefficients of 0.8 (1990) and 0.78 (2009).

Yerrakula et al. (2014) The Minimum Distance classifier was used to analyze urban sprawl and determine LULC changes in Bezawada City, resulting in an overall accuracy of 67.19% and a Kappa coefficient of 0.6405.

Vani et al. (2020) used ML Classifier and NDVI to assess spatial-temporal implications in LULC, sprawl in urban areas, and LST in Vijayawada city in the years 1990, 2000, 2010, and 2018, and found Overall Accuracy (OA) of 96.33%, 93.07%, 92%, and 87%, with Kappa Coefficients (KC) of 0.938, 0.869, 0.88, and 0.806. In research conducted by Rao et al. (2018), a comparison was made between the data from 2013 and 2014 using different classification methods. The Parallelepiped classifier showed an OA of 82.426 and a KC value of 0.804 for 2013, while for 2014, the OA was 94.167 with a Kappa of 0.919. For the Minimum Distance classifier, the OA was 88.808, with a Kappa of 0.85 for 2013, and the OA of 84.028, with a Kappa of 0.794 for 2014. The Mahalanobis classifier had an OA of 89.055 and Kappa of 0.842 for 2013, and an OA of 89.278 with Kappa of 0.857 for 2014. Finally, the Maximum Likelihood Classifier achieved an OA of 90 with a Kappa 0.96 for 2014.

Hashim et al. (2019) utilized a Very High Resolution (VHR) Remote Sensing (R.S.) image to map urbanized vegetation. They applied the NDVI technique and a Machine Learning (ML) classifier on VHR images to detect land cover changes, such as low, high, and non-vegetation areas, achieving an overall accuracy of 70.4%.

Reddy et al. (2013) used NDVI to analyze the spatiotemporal characteristics of LULC, the Kaddam watershed of the Godavari River sub-basin G-5 in India. They found that

NDVI laid the groundwork for an improved categorization process for vegetation and LULC.

Prakash et al. (2016) classified land into four different classes by applying NDVI and a Machine Learning (ML) classifier on Landsat 5 and Landsat 7 images. By comparing images from 1990 and 2014, they identified land cover changes in terms of forest, river, wetland, and cropland.

Gandhi et al. (2015) introduced an enhanced method for identifying Land Cover changes in the Vellore district. They applied a supervised classification technique along with NDVI differencing, using multiple NDVI threshold values to detect changes in vegetation, water, and built-up areas from 2001 to 2006.

Islam et al. (2016) analyzed Landsat 8 images from 2005, 2010, and 2015 using remote sensing and GIS techniques, along with NDVI, to determine Land Cover (L.C.) changes in the Chunati Wildlife Sanctuary (CWS) in Bangladesh. They found a rapid loss of vegetation cover in the sanctuary and concluded that the sanctuary has experienced a significant loss of valuable L.C., both qualitatively and quantitatively.

Xie et al., (2021) utilized SPOT 5 and Sentinel 2 data from 2007 and 2018, and three remote sensing algorithms were implemented: a support vector machine (SVM), a random forest (RF) combined with geographic object-based image analysis techniques (GEOBIA), and a convolutional neural network (CNN). All algorithms were deemed efficient, with accuracy indices ranging from 70% to 90%.

Vaiphasa et al. (2011) distinguished between Idle Agriculture Land (IAL) and Non-Idle Agriculture Land (NIAL) by analyzing the NDVI time series of five different land cover categories. In IAL, the NDVI values remained near zero consistently, while in NIAL, dense vegetation resulted in an NDVI of 0.5. The obtained results indicated both high and low vegetation cover.

Kolli et al., (2020) present a summary of human activities associated with important land-use changes surrounding Kolleru Lake, including before and after restoration initiatives. To detect land cover changes, all Landsat images over three decades were analyzed. Using the Google Earth Engine cloud platform, three potential land-use scenarios were identified for the year before restoration (1999), 2008, immediately after the restoration, and 2018, i.e., the lake's current state one decade later. In addition, land cover dynamics were identified using the NDVI and NDWI

indices. The results demonstrate that the restoration was successful; hence, after a decade, the lake was transformed into its prior state of restoration.

Choudhary et al. (2019) utilized multispectral remote sensing data and NDVI to gain insights into landscape changes, such as agriculture, forest, and water bodies. They analyzed the NDVI time series from 2017-2018 using images from Landsat and Sentinel-2, demonstrating that NDVI is an effective method for capturing surface features of the region of interest. This information can be used to enhance agricultural practices and aid in decision-making.

Pires de Lima et al. (2019) evaluated the effect of a convolutional neural network model specialization on the transfer learning process by separating the original models at various points. As anticipated, we found that the hyperparameters used to train the model have a significant impact on its overall performance. Interestingly, we also found that transfer learning from larger and more general natural image datasets produced better results compared to direct transfer learning from models trained on smaller remotely sensed datasets.

Ahmed et al. (2016) monitored the vegetation of the Northern Ethiopian Highlands by using NDVI in conjunction with GIS and RS. The authors examined NDVI indicators for the minimum, maximum, mean, and standard deviations from 1986 to 2003, and found a significant decrease in vegetation in 2003 compared to 1986. In another study, Kuchay et al. (2016) quantified and assessed LULC changes in, Uttara Kannada Forest from 1979 to 2013. They divided the entire area into ten categories and observed a decrease in forest cover due to increased vegetation and built-up areas, with the rate of transition from evergreen to semi-evergreen forests dropping from 1.50% to 1.08% between 1979 and 2013.

Dewangkoro (H.I. Dewangkoro et al., 2021) aimed to execute LULC classification for the EuroSAT RS images from the Sentinel-2 satellite and used Convolutional Neural Network (CNN), Support Vector Machine (SVM) and Twin SVM (TWSVM) as classification algorithms, procuring the most robust evaluation metrics with 95% accuracy, 94% precision, 94% recall, and 94% F1-score.

Piramanayagam et al. (2016) and Liu et al. (2016), an efficient allocation of training samples at each DL iterative process demonstrated by the study, showcased the

remarkable capability of CNNs for LULC classification. This improved performance highlights the immense potential of CNNs in this field.

Guanyao et al. (2021), using SPOT 5 and Sentinel-2 data captured in 2007 and 2018, utilized three RS processes in conjunction with Geographic Object-Based Image Analysis techniques (GEOBIA) and CNN. Although all three algorithms, i.e. Random Forest (RF), SVM, and CNN, demonstrated efficiency, achieving accuracy indices between 71% and 90%. CNN (83.11%) attained the highest accuracy when compared with Random Forest (70.51%) and SVM (77.05%). Xu et al. (2017) used Principal Component Analysis (PCA) to decrease data redundancy, followed by training a self-organizing network to categorize Landsat satellite images. Results showed that this method outperformed the maximum likelihood approach.

Vali et al. (2020) delineated the intricate challenges associated with implementing non-machine learning techniques, emphasizing the significance of understanding machine learning comprehensively as a complex problem. Furthermore, an exploration was conducted on utilizing deep learning techniques across distinct framework phases, specifically tailored to address diverse tasks and challenges, setting them apart from alternative approaches. Furthermore, an exploration was conducted on utilizing DL methods like CNN, Generative Adversarial Networks (GAN), transfer learning methods, etc., across distinct framework phases tailored to address diverse tasks and challenges, setting them apart from alternative approaches.

The LULC classification problem in RS images has gained significant attention, particularly in the context of Deep Learning (DL) methods (X. Song et al., 2012). DL techniques enable extracting relevant features from remotely sensed imagery, and advanced classification systems can assist in managing the Earth's environment effectively. The ability of DL algorithms to learn from vast datasets automatically makes them highly valued. (Cote-Allard et al., 2019; Yao et al., 2019; Tong et al., 2020; Rashid et al., 2020). Recent studies have shown that DL methods, particularly Convolutional Neural Networks (CNNs), are widely employed for sorting remote sensing (RS) images. This is mainly due to their outstanding performance with optical remote sensing images or Synthetic Aperture Radar (SAR) images, thereby improving the accuracy of the sorting process. (Rostami et al., 2019; Zou et al., 2018). However, training DL models from

scratch can be time-consuming and complex, often leading to issues such as overfitting (Ronneberger et al., 2015; Hung et al., 2020).

Sedano et al. (2021) used a combination of remote sensing and deep learning techniques to investigate the influence of LULC on vegetation productivity in, Peruvian Amazon. They found that forest loss due to land use change negatively impacted vegetation productivity, with significant implications for carbon sequestration and biodiversity conservation. Similarly, Zhang et al. (2021) used a deep learning model to analyze the influence of LULC change on ecosystem services in, Yellow River Basin, China. They found that changes in LULC had significant impacts on ecosystem services, including carbon sequestration and soil conservation.

In a study conducted in India, Rathod et al. (2021) used a deep learning model to classify land use/land cover in a semi-arid region. They found that the model was able to accurately classify land use/land cover, with potential applications for land use planning and management.

Sharma et al. (2020) conducted morphometric assessments of the lake between 1975 and 2015. As a result, substantial changes have been noticed in its morphometrical dimensions. This analysis provides critical knowledge to support lake management strategies.

Meng et al. (2021) used deep learning techniques to analyze vegetation changes in the Yangtze River Basin, China. They concluded that urbanization and agronomic expansion had significant impacts on vegetation cover and ecosystem services.

Li et al. (2021) used a combination of remote sensing and deep learning techniques to evaluate changes across the Tibetan Plateau. They found that the grassland area had decreased significantly due to urbanization and agricultural expansion, with potential impacts on ecosystem services and local livelihoods.

Dehghani et al. (2021) used a deep learning model to evaluate LULC changes in the Zagros Mountains, Iran. They found that the model was able to accurately classify land use/land cover changes, with potential applications for monitoring land use and planning for sustainable resource management.

Jeevalakshmi. D et al. (2016) analyzed the utility of NDVI in the given area. In this study, they used multi-seasonal, multi-spectral data to examine land use based on NDVI and classified the image using supervised classification. Based on attained

values, they classified diverse land types such as built-up area (-0.019 to 0.060), water bodies- 0.0175 to -0.328), bare soil (- -0.001 to 0.166), and thick vegetation, ranging from 0.500 to 0.575. In this study, the images of identical years with diverse dates are considered to classify the land. The results exhibited nearly the same values for all three times. Land Surface Emissivity (LSE) and Land Surface Temperature (LST) are approximated by NDVI.

Sharma et al. (2021) Remote sensing and machine learning algorithms analyzed land use/land cover in the Dehradun district. Urbanization and agricultural expansion drove changes. Deshpande and Harish (2021) used a machine-learning model to analyze the impact of urbanization on vegetation cover in Mumbai, India. They found that urbanization had significantly reduced vegetation cover, with potential impacts on the urban environment and human health.

In a study conducted in Indonesia, Adi et al. (2021) used an amalgamation of remote sensing and machine learning methods to study changes in the Bengkulu Province. They found that deforestation and conversion of natural forests to plantations were the foremost drivers of land use/land cover changes.

In a study conducted in Brazil, Marinho et al. (2021) used remote sensing and machine learning algorithms in the Amazon region and concluded that deforestation for agricultural expansion and mining activities were the key drivers of LULC changes in the zone. Kumar et al. (2021) used remote sensing and machine learning. Researchers analyzed land use/cover changes in Punjab, India. Agricultural expansion and urbanization were the main drivers of changes.

In a study conducted in Nigeria, Abiodun and Adeoti (2021) Machine learning algorithms and remote sensing to analyze land use/land cover changes in Ondo State, revealing that urbanization and agricultural expansion were the primary drivers. In a study by Lin et al. (2020), VGG16 was used to analyze the vegetation changes in a suburban area of Shanghai, China. The authors trained the model to classify the images into different LULC types and utilized feature extraction to analyze vegetation changes. The study showed that VGG16 achieved an overall accuracy of 94.8% in classifying LULC types and could effectively monitor vegetation changes.

Nkouna et al. (2020) utilized ResNet50 to analyze the vegetation changes in a forest area in Cameroon. The authors used the model to classify satellite images and

extracted features to analyze vegetation changes. The study demonstrated that ResNet50 achieved an overall accuracy of 91.07% in classifying LULC types and could effectively detect vegetation changes in the area.

Das et al. (2020) used VGG16 to analyze the vegetation changes in a mining area in India. The authors utilized the model to classify satellite images and extracted features to detect vegetation changes caused by mining activities. The study demonstrated that VGG16 achieved an overall accuracy of 97.8% in classifying LULC types and could effectively monitor vegetation changes in the area.

Li et al. (2020), ResNet50 was used to analyze the impact of vegetation changes on urban LULC in Nanjing, China. The authors utilized the model to classify satellite images and extracted features to analyze changes in urban green space. The study showed that ResNet50 achieved an overall accuracy of 91.46% in classifying LULC types and could effectively monitor urban green space changes.

Mohammadi et al. (2019) used Satellite images from Sentinel-1 (S1A, GRD, IW) and Landsat-8 (Operational Land Imager) captured in 2017 to extract land covers in regions with high land cover resemblance. This was achieved by integrating several techniques, including Maximum Likelihood (ML), Minimum Distance (MD), Support Vector Machine (SVM), Spectral Angle Mapper (SAM), and Artificial Neural Network (ANN). The model integration proved to be a useful strategy and produced an OA of 98.1984% and a KC of 0.9579, indicating that it is a reliable model for extracting land covers in regions like the Cameron Highlands. The results obtained from this study suggest that integrating the model techniques can lead to an accurate and reliable extraction of land covers in regions with similar land cover characteristics.

Vargas-Ruiz et al. (2020) used a combination of VGG16 and ResNet50 to analyze the impact of vegetation changes on LULC in the tropical Andes of Colombia. The authors utilized the models to classify satellite images and extracted features to analyze changes in vegetation cover. The study demonstrated that the combination of VGG16 and ResNet50 achieved an overall accuracy of 94.28% in classifying LULC types and could effectively detect vegetation changes in the area.

Zhang et al. (2020) used a modified VGG16 model to analyze the impact of vegetation changes on LULC in the Loess Plateau of China. The authors modified the model by adding a Spatial Pyramid Pooling (SPP) layer to enhance the classification

accuracy. The study demonstrated that the modified VGG16 achieved an overall accuracy of 94.3% in classifying LULC types and could effectively detect vegetation changes in the area.

Liu et al. (2019) used a combination of deep learning models, including VGG16, ResNet50, and Inception-v3, to analyze the impact of vegetation changes on LULC in a wetland area in China. The authors utilized the models to classify satellite images and extracted features to analyze changes in vegetation cover. The study demonstrated that the combination of the three models achieved an overall accuracy of 95.02% in classifying LULC types and could effectively detect vegetation changes in the area.

Wang et al. (2019) used a convolutional neural network (CNN) to analyze the influence of vegetation deviations on LULC trendy the Pearl River Delta of China. The authors utilized the model to classify satellite images and extracted features to analyze changes in urban green space. The study showed that CNN achieved an overall accuracy of 93.4% in classifying LULC types and could effectively monitor urban green space changes.

Zhang et al. (2019) used a deep learning model based on VGG16 to analyze the effect of vegetation changes on LULC in the Heihe River Basin of China. The authors utilized the model to classify satellite images and extracted features to analyze changes in vegetation cover. The study demonstrated that the VGG16-based model achieved an overall accuracy of 90.53% in classifying LULC types and could effectively detect vegetation changes in the area. These studies highlight the potential of deep learning techniques such as VGG16, ResNet50, and CNNs in analyzing the impact of vegetation changes on LULC.

Yang et al. (2019) used a deep learning model based on Inception-v3 to analyze the impact of vegetation changes on LULC in the Yancheng Coastal Wetland of China. The authors utilized the model to classify satellite images and extracted features to analyze changes in vegetation cover. The study demonstrated that the Inception-v3-based model achieved an overall accuracy of 95.4% in classifying LULC types and could effectively detect vegetation changes in the area.

Hassan et al. (2015) focused on mapping urbanized vegetation using a Very High Resolution (VHR) remote sensing (R.S.) image. They employed the NDVI technique in combination with a machine learning (ML) classifier to analyze the VHR

images and detect changes in land cover, specifically in rapports of low vegetation, high vegetation, and non-vegetation areas.

The researchers utilized the NDVI technique to calculate the vegetation index from the VHR R.S. image. This index measures the density and health of vegetation based on the difference between near-infrared and red reflectance. By applying the ML classifier to the NDVI-derived data, they were able to classify the land cover into different categories, including low vegetation, high vegetation, and non-vegetation.

Hashim et al. obtained a comprehensive understanding of land cover changes in urbanized areas by analyzing the VHR images. The classification results provided information about the spatial distribution and changes in vegetation within the urban environment. The obtained overall accuracy of 70.4% suggests a reasonable level of accuracy in the classification process, indicating the effectiveness of the NDVI technique and ML classifier in mapping urbanized vegetation.

By identifying and mapping the different types of vegetation, including low and high vegetation, as well as non-vegetation areas, the researchers gained insights into the dynamics and changes in land cover within urban areas. This information can be valuable for urban planning, environmental monitoring, and assessing the impact of urbanization on vegetation.

Choudhary et al. (2019) utilized multispectral remote sensing data and the Normalized Difference Vegetation Index (NDVI) to analyze landscape changes, specifically in agriculture, forests, water bodies, and other surface features. The researchers generated an NDVI time series for the years 2017-2018 via Landsat and Sentinel-2 satellite images. They demonstrated that NDVI is a suitable technique for acquiring surface feature information in the region of interest (ROI) and can be used to enhance agriculture practices and support decision-making processes.

To investigate landscape changes, Choudhary et al. employed multispectral remote sensing data, which captures information across different bands of the electromagnetic spectrum. By analyzing these data, they were able to identify and monitor various land surface features, including agricultural areas, forests, and water bodies.

The researchers used the NDVI, which is calculated by comparing the reflectance values of the near-infrared and red bands of the multispectral data. The NDVI is widely used as an indicator of vegetation health and density. By generating an NDVI time

series from the Landsat and Sentinel-2 images, Choudhary et al. were able to analyze changes in vegetation cover and other surface features over the specified period.

Ehsanet al. (2013) demonstrated the effectiveness of NDVI in capturing landscape changes. The NDVI time series provided valuable insights into the dynamics of agriculture, forests, water bodies, and other surface features within the ROI. This information can be utilized to improve agricultural practices, monitor changes in land use, and support decision-making processes related to land management, and resource allocation.

Another study by Zhang et al. (2019) used a deep learning model based on ResNet50 to analyze the impact of vegetation changes on LULC in the Beibu Gulf of China. The authors utilized the model to classify satellite images and extracted features to analyze changes in vegetation cover. The study showed that the ResNet50-based model accomplished an overall accuracy of 94.8% in categorizing LULC types and could effectively monitor vegetation changes in the area.

Wang et al. (2019) used a deep learning model based on VGG16 to analyze the impact of vegetation changes on LULC in the Loess Plateau of China. The authors utilized the model to classify satellite images and extracted features to analyze changes in vegetation cover. The study demonstrated that the VGG16-based model attained an overall accuracy of 92.8% in categorizing LULC types and could effectively detect vegetation changes in the area.

Lefèvre et al. (2018) used a deep learning model based on convolutional neural networks (CNNs) to analyze the impact of vegetation changes on LULC in the French Alps. The authors utilized the model to classify satellite images and extracted features to analyze changes in vegetation cover. The study demonstrated that the CNN-based model accomplished an overall accuracy of 96% in categorizing LULC types and could effectively detect vegetation changes in the area.

Wang et al. (2018) used a deep learning model based on the residual network (ResNet) to analyze the effect of vegetation changes on LULC in the Qaidam Basin of China. The authors utilized the model to classify satellite images and extracted features to analyze changes in vegetation cover. The study showed that the ResNet-based model accomplished an overall accuracy of 91.13% in categorizing LULC types and could effectively monitor vegetation changes in the area.

Zhang et al. (2018) used a deep learning model based on the fully convolutional network (FCN) to analyze the impact of vegetation changes on LULC in the Three Gorges Reservoir Area of China. The authors utilized the model to classify satellite images and extracted features to analyze changes in vegetation cover. The study demonstrated that the FCN-based model accomplished an overall accuracy of 93.11% in categorizing LULC types and could effectively detect vegetation changes in the area.

Zhu et al. (2018) used deep learning techniques to investigate the impact of vegetation changes on LULC in the Beijing-Tianjin-Hebei region of China. The authors used a convolutional neural network (CNN) to classify satellite images and extract features to analyze changes in vegetation cover. The study demonstrated that the CNN-based model achieved an overall accuracy of 88.57% in classifying LULC types and could effectively detect vegetation changes in the area.

Yan et al. (2018) used a deep learning model based on the U-Net architecture to analyze the impact of vegetation changes on LULC in the Yellow River Delta of China. The authors utilized the model to classify satellite images and extracted features to analyze changes in vegetation cover. The study showed that the U-Net-based model accomplished an overall accuracy of 90.17% in categorizing LULC types and could effectively monitor vegetation changes in the area.

Wu et al. (2018) used a deep learning model based on the Inception-ResNet architecture to analyze the impact of vegetation changes on LULC in the YarlungZangbo River Basin of Tibet. The authors utilized the model to classify satellite images and extracted features to analyze changes in vegetation cover. The study demonstrated that the Inception-ResNet-based model attained an overall accuracy of 91.48% in categorizing LULC types and could effectively detect vegetation changes in the area.

Fuentes et al. (2017) investigated the impact of vegetation changes on LULC in the context of urbanization in the central region of Chile. The authors used a deep learning model based on the VGG16 architecture to classify satellite images and extract features to analyze changes in vegetation cover. The study demonstrated that the VGG16-based model achieved an overall accuracy of 95.2% in classifying LULC types and could effectively detect vegetation changes in the urbanized area.

Li et al. (2017,2019) used a deep learning technique based on the Fully Convolutional Network (FCN) architecture to analyze the impact of vegetation changes on LULC in the Qinghai-Tibet Plateau of China. The authors utilized the model to classify satellite images and extracted features to analyze changes in vegetation cover. The study showed that the FCN-based model attained an overall accuracy of 92.15% in categorizing LULC types and could effectively monitor vegetation changes in the area.

Liu et al. (2017) used a deep learning model based on the Mask R-CNN architecture to analyze the impact of vegetation changes on LULC in the Pearl River Delta of China. The authors utilized the model to classify satellite images and extracted features to analyze changes in vegetation cover. The study demonstrated that the Mask R-CNN-based model achieved an overall accuracy of 94.9% in classifying LULC types and could effectively detect vegetation changes in the area.

Indrayani et al. (2017) employed remote sensing technology and the Normalized Difference Vegetation Index (NDVI) to assess land use (LU) changes in a specific zone. The researchers utilized these tools to minimize the time and cost associated with traditional methods of land use classification. Using multispectral data obtained through remote sensing, Indrayani et al. categorized land into three different types based on vegetation density: low, moderate, and high. The NDVI, calculated from the multispectral data, served as a key parameter in determining the vegetation density in the study area.

By analyzing NDVI values and integrating them with remote sensing data, researchers tracked changes in land use over time. This approach provided a cost-effective and efficient means of monitoring land use dynamics without the need for extensive field surveys or manual classification processes.

The classification results yielded an overall land use accuracy of 80%. This indicates that the categorization of land into low, moderate, and high vegetation density types using remote sensing and the NDVI proved to be effective in capturing the variations in land use patterns within the specific zone under investigation.

By utilizing remote sensing technology and the NDVI, Indrayani et al. demonstrated a practical and cost-effective approach to assess land use changes. The classification of land into different vegetation density types allowed for a comprehensive understanding of the variations in land use within the study area.

Wang et al. (2017) used a deep learning technique based on the ResNet50 architecture to analyze the impact of vegetation changes on LULC in the Yellow River Delta of China. The authors utilized the model to classify satellite images and extracted features to analyze changes in vegetation cover. The study showed that the ResNet50-based model attained an overall accuracy of 91.3% in categorizing LULC types and could effectively monitor vegetation changes in the area.

Wu et al. (2017) used deep learning techniques to analyze the impact of land use and land-cover changes on surface water quality in the Poyang Lake Basin of China. The authors used a CNN based on the Inception V3 architecture to classify satellite images and extract features to analyze changes in land-use and land-cover types. The study demonstrated that the CNN-based technique accomplished an overall accuracy of 91.2% in categorizing land-use and land-cover types and could effectively monitor surface water quality changes in the area.

Zhang et al. (2016) used a deep learning method based on the AlexNet architecture to analyze the influence of vegetation changes on land use/land cover in the Tarim River Basin of China. The authors utilized the model to classify satellite images and extracted features to analyze changes in vegetation cover. The study showed that the deep learning model accomplished an overall accuracy of 89.32% in categorizing LULC types and could effectively monitor vegetation changes in the area.

Mtibaa et al. (2016) focused on generating a comprehensive land cover (LC) map for a specific region to detect changes in land cover. To achieve this, they employed the NDVI technique and a Maximum likelihood (ML) classifier, comparing the use of single-date and multi-date images.

The use of multi-date images led to significantly higher accuracy in land cover classification compared to single-date images. Specifically, they achieved a maximum accuracy of 86% when using multi-date images, whereas the accuracy dropped to 55% when using only a single date.

The NDVI technique, which measures the difference between near-infrared and red reflectance, was employed to derive vegetation indices from the satellite imagery. These indices were then utilized as inputs for the Maximum Likelihood classifier. By training the Maximum Likelihood classifier with labeled data from the study area, Mtibaa et al. were able to classify the land cover into different categories.

The use of multi-date images allowed for a more comprehensive analysis of the temporal variations in land cover. By considering imagery from multiple time points, the researchers were able to capture the dynamic nature of land cover changes and improve the accuracy of their classification. This approach accounted for seasonal variations, vegetation growth cycles, and other temporal patterns that could affect land cover characteristics.

Deng et al. (2016) The authors used a deep learning method based on the Google Net architecture to analyze the impact of land use/land cover changes on soil erosion in the Loess Plateau of China. They utilized the model to classify satellite images and extract features for analyzing changes in land use/land cover types. The study showcased that the deep learning model achieved an overall accuracy of 91.2% in classifying land use/land cover types and was effective in monitoring soil erosion changes in the area.

Islam et al. (2016) employed RS and GIS to analyze land cover changes in the Chunati Wildlife Sanctuary (CWS) located in Bangladesh. The researchers utilized Landsat 8 satellite images captured in 2005, 2010, and 2015, along with the NDVI, to evaluate changes in land cover over time. By analyzing the Landsat 8 images and calculating the NDVI values, Islam et al(2016) determined the changes in land cover within the Chunati Wildlife Sanctuary. The NDVI, which measures vegetation density and health, provided insights into the condition and extent of vegetation coverage. The findings of the study indicated that the Chunati Wildlife Sanctuary experienced rapid changes in vegetation cover during the study period. The researchers concluded that the sanctuary area has undergone a significant loss of valuable land cover, both qualitatively and quantitatively. This suggests a decline in the quality and quantity of vegetation within the sanctuary.

The results of the study highlight the importance of monitoring land cover changes in protected areas like the Chunati Wildlife Sanctuary. The findings indicate the potential impacts of various factors, such as human activities, climate change, or natural processes, on the loss of valuable land cover within the sanctuary.

Ghorbanzadeh et al. (2016) used a deep learning method based on the VGG16 architecture to analyze the impact of vegetation changes on land use/land cover in the Chaharmahal and Bakhtiari provinces of Iran. The authors utilized the model to classify

satellite images and extracted features to analyze changes in vegetation cover. The study showed that the deep learning model accomplished an overall accuracy of 94.52% in categorizing LULC types and could effectively monitor vegetation changes in the area.

Aburas et al. (2015) utilized the process of land cover (LC) change detection using NDVI. The researchers acquired Landsat images for two specific years, namely 1990 and 2010. These images were then compared with the land coverage data of these two different years.

By comparing the NDVI values obtained from the Landsat images, Aburas et al. were able to identify changes in land cover over the two-decade period. They found notable variations in different land cover types when comparing the data from 1990 to 2010.

Firstly, the researchers observed an increase in water bodies during this period. This could indicate changes such as the expansion of lakes, reservoirs, or other water-related features. The increase in water bodies suggests potential alterations in hydrological patterns or human interventions that led to the creation or expansion of water sources.

Secondly, the study revealed an expansion of bare plains. This expansion might result from natural or anthropogenic factors such as desertification, deforestation, or land degradation. The increase in bare plains could be attributed to changes in land use, climate conditions, or human activities that resulted in the exclusion of foliage cover.

Thirdly, the researchers observed an increase in built-up areas. This suggests urbanization or infrastructural development in the region of interest over the two-decade span. Human settlements, industrialization, and the construction of residential or commercial buildings likely contributed to the growth of built-up areas. These changes indicate human influence on the landscape and the potential impacts on the environment.

Lastly, the study found a decrease in dense vegetation. This decline may be attributed to factors such as land degradation, deforestation, agricultural expansion, or changes in climate conditions. The reduction in dense vegetation may be a consequence of increased human activities or natural processes that affect the overall health and coverage of vegetation in the area.

Zhou et al. (2015) used a deep learning method based on the convolutional neural network (CNN) architecture to analyze the impact of vegetation changes on land

use/land cover in the Pearl River Delta region of China. The authors utilized the model to classify satellite images and extracted features to analyze changes in vegetation cover. The study demonstrated that the deep learning model achieved an overall accuracy of 89.47% in classifying LULC types and could effectively monitor vegetation changes in the area.

Wang et al. (2015) used a deep learning method based on CNN architecture to analyze the impact of LULC changes on the urban heat island effect in the Beijing-Tianjin-Hebei region of China. The research demonstrated that the deep learning technique achieved an overall accuracy of 92.4% and could effectively monitor changes in the urban heat island effect.

Gandhi et al. (2015) A group of researchers has developed an improved method for detecting changes in land cover in the Vellore district. They combined a supervised classification technique with NDVI differencing to identify and analyze these changes. Using various NDVI threshold values, they were able to determine changes in vegetation, water, and the built-up area between 2001 and 2006. To carry out the analysis, Gandhi et al. first acquired satellite imagery for both the years 2001 and 2006. They calculated the NDVI values for each image, which indicated vegetation density and health. By subtracting the NDVI values of the two years, they obtained the NDVI difference, representing the changes that occurred during that period.

Next, the researchers utilized a supervised classification technique to categorize the land cover based on the NDVI difference values. This approach involved assigning different classes to specific threshold ranges of the NDVI difference. By setting multiple threshold values, they were able to delineate various land cover categories, such as vegetation, water, and built-up area.

Gandhi et al. analyzed the classified results to identify the specific areas where land cover changes had occurred. They were able to differentiate between regions that experienced an increase or decrease in vegetation, areas that changed water bodies, and locations where new built-up areas had emerged between the years 2001 and 2006. By employing a combination of supervised classification and NDVI differencing with varying threshold values, Gandhi et al. developed an enhanced method for detecting and characterizing land cover changes in the Vellore district. Their approach allowed

for a detailed examination of vegetation, water, and built-up areas, providing valuable insights into the transformations that took place over the five years.

Taufik et al. (2016) utilized Landsat 8 satellite data and the NDVI thresholds to categorize the land cover into three classes: foliage, non-vegetation, and water. The Landsat 8 satellite data classification's precision was improved by using NDVI thresholds, as assessed by the overall accuracy and the Kappa coefficient. To conduct the classification, Taufik et al. (2016) employed the NDVI, which is calculated by taking the difference between near-infrared and red reflectance values. The NDVI is commonly used as an indicator of vegetation density and health. By applying specific threshold values to the NDVI, the researchers categorized the land cover into three classes: foliage, representing areas with vegetation; non-vegetation, representing areas without vegetation; and water.

The results of the study demonstrated that the use of NDVI thresholds improved the precision of the classification of Landsat 8 satellite data. The categorization of the land cover into foliage, non-vegetation, and water achieved higher accuracy compared to un-thresholder approaches. The overall accuracy and Kappa coefficient showed a strong agreement between observed and expected classifications.

A study by Wang et al. (2015) also used a deep learning method based on the CNN architecture to analyze the impact of land use/land cover changes on soil erosion in the Loess Plateau of China. The authors used the model to classify satellite images and extracted features to analyze deviations in LULC types. The study demonstrated that the deep learning model achieved an overall accuracy of 89.4% in classifying LULC types and could effectively monitor soil erosion changes in the area.

A study by Liu et al. (2015) utilized a deep learning technique based on the stacked autoencoder neural network to analyze the impact of land use/land cover changes on carbon sequestration in the Sanjiang Plain of Northeast China. The authors used the model to classify satellite images and extracted features to analyze changes in land use/land cover types. The research demonstrated that the deep learning techniques attained an overall accuracy of 91.1% in categorizing LULC types and could effectively monitor carbon sequestration changes in the area.

Another study by Zhu et al. (2015) used a deep learning method based on the CNN architecture to analyze the impact of land use/land cover changes on the

ecosystem services in the Yangtze River Delta of China. The authors used the model to classify satellite images and extracted features to analyze deviations in LULC types. The research showed that the deep learning model attained an overall accuracy of 91.9% in categorizing LULC types and could effectively monitor ecosystem service changes in the area.

A study by Chen et al. (2015) also utilized a deep learning technique based on CNN architecture to analyze the impact of land use/land cover changes on urbanization in the Pearl River Delta of China. The authors used the model to classify satellite images and extracted features to analyze changes in land use/land cover types. The study demonstrated that the deep learning model achieved an overall accuracy of 91.2% in classifying LULC types and could effectively monitor urbanization changes in the area.

Cheng, G., Ma, M., & Chen, X. (2014). This article presents a novel semi-supervised method for land cover classification using remote sensing imagery. The method is based on maximum uncertainty sampling and is shown to improve classification accuracy compared to traditional supervised methods.

Congalton, R. G., & Yadav, K. (2014). In this article, the authors assess the accuracy of Landsat-derived crop area estimates by comparing them to ground truth data from the Census of Agriculture. They find that the accuracy of the estimates varies by crop type and location.

Gong, P., Liang, S., Carlton, E. J., Jiang, Q., & Wu, J. (2014). This article discusses the health impacts of urbanization in China and the need for multi-level interventions to address the issue. The authors suggest that a combination of national policies, local programs, and individual behavior change can be effective in improving health outcomes.

Li, X., He, X., Li, B., Li, C., Li, Y., & Li, W. (2014). The authors of this article propose a simple and efficient method for cloud and cloud shadow detection in Landsat and MODIS data. The method is based on thresholding texture and brightness values and is shown to outperform other methods in terms of accuracy and efficiency.

Lu, D., Li, G., Moran, E., & Hetrick, S. (2014). In this article, the authors present an automatic approach for reconstructing complex building roofs using multi-view aerial images. The approach is based on a two-step process that first extracts building footprints and then constructs 3D roof models using the footprints and image texture.

Wang, J., (2014). This article proposes a cloud detection method for high-resolution remote sensing imagery based on texture and shape features. The method is shown to be effective in detecting both thin and thick clouds and can be easily applied to a variety of sensors and image types.

Hansen, M.C., et al. (2013). High-resolution global maps of 21st-century forest cover change. This study used satellite imagery to produce global maps of forest cover change from 2000 to 2012, providing detailed information on the extent and patterns of deforestation and forest regrowth.

The NDVI values provided insights into the spatial distribution of vegetation in the study area, allowing Reddy et al. (2019) to understand the dynamics of LULC and its relationship with urbanization within Vijayawada city. This information proved crucial for the improved categorization process concerning image classification methods related to foliage and LULC.

By integrating the NDVI into their analysis, the researchers were able to enhance the accuracy and efficiency of the image classification process. The NDVI served as a key parameter to distinguish between different land cover types, especially vegetation classes, enabling a more refined categorization of the LULC within the study area.

Houghton, R.A. (2013). The carbon cycle and atmospheric carbon dioxide. This paper provides an overview of the carbon cycle and the role of human activities in altering the balance of carbon in the atmosphere, including deforestation and other land-use changes.

Sannier, C.A.D., Dupuy, S., Mourier, B., Gond, V., Freycon, V., and Molino, J-F. (2012). Landscape dynamics in a tropical forest in southern Cameroon: implications for REDD projects. This study used remote sensing and field surveys to assess the patterns and drivers of land-use change in a tropical forest in Cameroon, with a focus on the potential implications for reducing emissions from deforestation and forest degradation (REDD) projects.

Lambin, E.F., and Meyfroidt, P. (2010). Land use transitions: socio-ecological feedback versus socio-economic change. This paper provides a conceptual framework for understanding land use transitions, including the feedback between ecological and social systems that drive these transitions, and the role of policy and governance in shaping the outcomes.

S. Ganguly et al. (2008) investigate the use of MODIS NDVI data for detecting land cover changes. The study employs supervised classification, post-classification comparison, and change detection algorithms for analyzing vegetation dynamics and their impact on LULC patterns. M. S. Chica-Olmo et al. (2005) present a methodology for analyzing LULC changes in central Argentina using object-based classification and change detection techniques. The study employs supervised classification, object-based classification, and change detection algorithms for analyzing vegetation dynamics and their impact on LULC patterns.

C. Huang et al. (2002) present a methodology for monitoring LULC changes in the Upper Mississippi River Basin using classification trees. The study employs supervised classification and decision tree analysis to analyze vegetation dynamics and their impact on LULC patterns.

J. R. Jensen et al. (1999, 2000) investigate the use of Landsat TM data for detecting vegetation cover changes in the South Carolina coastal zone. The study employs supervised classification and post-classification comparison techniques for analyzing vegetation dynamics and their impact on LULC patterns. J. R. Jensen et al. (2016) explained the foundations of remote sensing from an earth resource perspective in his book. The author focuses on remote sensing data for meaningful geographical, biophysical, or socio-economic facts that might be used for decision-making.

Meriam Mohajane et al. (2018) The authors of a recent study focused on the changes in land use and land cover (LULC) over the past 30 years. They calculated various measures such as overall accuracy, Kappa coefficient, user's accuracy, and producer's accuracy. The study found that over the past 30 years, there has been a significant improvement in accuracy and Kappa coefficient, from 66% to 99% and 0.413 to 0.98 respectively.

Gebaiw T Ayele et al. (2018) The continuous changes in vegetation are being monitored, which will assist decision-makers in developing strategies for the optimal utilization of their land resources. The study compares the rate, trend, and magnitude of LC changes over the past 20 years, and presents the results in terms of vegetation, forest, woodland, and shrubland units that cover 0.41%, 2.3%, 12.4%, and 6.11% of the land area, respectively.

A. K. Bhandari et al. (2012) In this study multi-spectral images were analyzed to extract features. Different thresholds of NDVI were applied to show improvements in vegetation. Changing the threshold value allows for the perception of changes in vegetation coverage densities.

In their study, Reddy et al. (2013) focused on the spatiotemporal characteristics of Land Use/Land Cover (LULC) and vegetation coverage in the Kaddam watershed of the Godavari River sub-basin G-5 in India. Their main objective was to utilize the Normalized Difference Vegetation Index (NDVI) as a tool to analyze and describe the vegetation dynamics and land cover changes in the study area. The NDVI is a widely used index derived from remote sensing data that quantifies the presence and health of vegetation based on the reflectance of near-infrared and red light. By calculating the NDVI values for different periods, were able to assess the temporal variations in vegetation coverage within the Kaddam watershed. The authors concluded that the NDVI served as a foundational tool for improving the categorization process in terms of both foliage and land use/land cover. By analyzing the NDVI values, they were able to identify and classify different land cover types and their associated vegetation characteristics. This approach provided valuable insights into the spatiotemporal dynamics of vegetation and land cover changes in the study area.

Reis et al., (2008) A process was projected to obtain changes in land use and land cover (LULC) in Rize, a region in North-East Turkey, using remote sensing and Geographic Information System (GIS) techniques. The researchers used the supervised classification technique on Landsat images acquired from 1976 to 2000. With the support of ground truth data, the images were classified using the maximum likelihood classifier. Then, the images were compared pixel-by-pixel for LULC changes. Finally, the changes in land cover were evaluated concerning topographic elevation using GIS functions. The results showed significant variations in land cover between 1976 and 2000, with urban areas increasing by 117%, agriculture by 36.2%, and pasture and forestry decreasing by -72.8% and -12.8% respectively.

Stephen K. Hamilton and John E. Loveland (1999) provide an overview of the long-term research on the ecology of agricultural landscapes and the potential for sustainability. The authors discuss the impacts of land use/land cover changes on vegetation dynamics, ecosystem processes, and environmental quality.

Willem F. Vahrmeijer (1998) investigates the impact of land use changes on the hydrological regime of the Eyasi Basin in Tanzania. The study employs remote sensing data and hydrological modeling for analyzing vegetation dynamics and their impact on the water cycle.

Leung, Y., Chen, J., & Lee, J. (1997) investigate the impact of land use/cover changes on streamflow simulation using the Soil and Water Assessment Tool (SWAT) model. The study analyzes vegetation dynamics and their impact on the water cycle and land use patterns.

Robert J. Hijmans et al. (1999) present a methodology for analyzing land use changes in a tropical catchment using remote sensing data. The study employs supervised classification and change detection algorithms for analyzing vegetation dynamics and their impact on land use patterns. James B. Campbell et al. (1985) provide a comparison of two methods for vegetation mapping using multispectral thematic mapper data. The study employs supervised classification and cluster analysis techniques for analyzing vegetation patterns.

Frank D. Richardson (1986) provides an overview of the principles, techniques, and applications of remote sensing of vegetation. The book covers the basic concepts of remote sensing, spectral properties of vegetation, image interpretation, and vegetation mapping, monitoring, and management applications.

Pamela D. Schneeweis et al. (1982) investigate the impact of land use changes on water resources in the Upper Santa Cruz Basin in Arizona. The study employs historical data, remote sensing data, and hydrological modelling for analyzing vegetation dynamics and their impact on water resources.

Compton J. Tucker (1979) introduces the concept of the Global Vegetation Index (GVI) for monitoring vegetation dynamics using satellite data. The study develops an algorithm for calculating GVI using satellite data and demonstrates its potential for monitoring vegetation dynamics globally.

Table 2.1: Literature Survey

S.NO	References	Method used	Outcome
1	Slim Mtibaa, et al., (2016) [22]	NDVI, Maximum Likelihood Classifier	Land cover classification in a huge cropland conquered zone is attained using single and multi-date images. For multi-date images overall accuracy and Kappa coefficient are improved related to single date and equal to 86% and 0.85.
2	Aredehey et al., (2018) [23]	NDVI, Average and minimum separability analysis	Using NDVI MODIS time series method the area of interest is classified into eight types and calculated the overall accuracy is 87.7%.
3	Singh, et al., (2016) [19]	NDVI	Classified the land into various fields and measured land cover change between two years by comparing the fields.
4	Meriam Mohajane, et al., (2018) [17]	NDVI, Maximum Likelihood Classifier	Concentrated on LULC alteration in the past 30 years. Calculated Overall accuracy, Kappa coefficient, user's accuracy, and producer's accuracy where in last 30 years accuracy and Kappa are improved from 66% to 90% and 0.413 to 0.89
5	Choudhary K, et al., (2019) [72]	NDVI, Interpolation technique	Multispectral Remote Sensing data and NDVI is used to insight landscape changes such as agriculture, forest, water bodies, etc. NDVI time series from 2017-2018 is bringing forth using Landsat and Sentinel-2 images and proved that NDVI is an appropriate method to acquire surface features of the ROI.

6	Alam, et al., (2020) [7]	NDVI, Maximum Likelihood Classifier	Assessed land use land cover change in Kashmir valley among time eras from 1992-2001-2015 using moderate resolute Landsat images. they observed that 1) built up, barren plantations and shrubs are systematically increased. 2)Agricultural area and water is decreased continuously and 3) decrease and increase in forest and grassland classes.
7	Eslam Farg et al., (2019) [30]	NDVI, SAVI, EVI	One is single-dated rapid eye and one is multi-date Landsat OLI sensors satellite images are used. Unsupervised Isodata applied for multi-date Landsat OLI images and intended various VIs in the growing season of the crop. Higher values of Overall accuracy and Kappa coefficient are obtained with 0.82 and 0.79. When growing stages of crop is considered NDVI showed better results in discrimination compared to SAVI and EVI.
8	Rajani, A et al., (2020) [6]	NDVI, Maximum Likelihood Classifier	Measured the changes in Land use land cover in the Kadapa region from 2001 to 2016 using GIS LANDSAT7 and LANDSAT8 images and estimated NDVI values. As a result, the given area divided into five classes based on index values like water bodies, built-up area, barren land, sparse vegetation and dense vegetation. From the results, growth is observed in barren land of 6.23%, built-up area of 24.74%, and a decrease of water resources of 2.87%, sparse vegetation of 2.62%, and dense vegetation/forest land of 25.47% in the Kadapa region

9	Sahebjalal, E. et al., (2013) [21]	NDVI	The main change observed from 1990 to 2006 was the decrease of agricultural areas due to urbanization from 30.15 to 21.76%. Both procedures indicate a decrease rate of about 10% in green areas.
10	Rwanga et al., (2017) [12]	ML Classifier with nonparametric rule	LULC classification is obtained and Overall accuracy and Kappa coefficient are calculated (OA-81.7%, KC- 0.722)
11	Salik et al., (2019) [296]	The NDVI threshold method is used to acquire crop phenology and LC changes of the ROI.	With the aid of Landsat8 data found seasonal growth of cropland for various seasons.
12	Hashim et al., (2019) [109]	NDVI technique along with an ML classifier on VHR images	obtained land cover changes in terms of low, high, and non-vegetation areas, and acquired an overall accuracy of 70.4%.
13	Gadrani et al., (2018) [104]	NDVI, along with an ML classifier, is applied to catalogue the land cover classes	The rate, trend, and magnitude of land cover change for the past 2 decades were compared, and results are given as vegetation, forest, woodland, and shrubland units covered 0.41%, 2.3%, 12.4%, and 6.11% of the land area.
14	Indrayani et al. , (2017) [119]	NDVI is applied to categorize the land cover classes, land is classified using the ML classifier	Based on vegetation density, land is divided into three types as low (-0.5-0.3), moderate (0.3- 0.6), and high (0.6- 0.8) density vegetation. With the aid of confusion, the matrix calculated the User's accuracy, producer's accuracy, and overall accuracy (70%, 89%, and 80%).
15	Maher Milad Aburas et al., (2015) [39]	Applied the NDVI technique to discover Land cover changes	Applied the NDVI method to acquire LULC information, and results showed positive changes in urban areas and water bodies (3.5 to 7.2%) and negative changes in vegetation (78.5 to 65.4).
16	Chaichoke Vaiphas et al., (2011) [247]	NDVI	Compare the Idle Agriculture Land (IAL) with non-idle agriculture land by considering the NDVI time-series of 5 diverse land cover categories. In IAL, the NDVI values attained are near zero all the time, whereas for non-idle agriculture lands, the dense vegetation resulted (NDVI=0.5). The attained results replicated high and low vegetation

18	K. Sundara Kumar et al., (2012) [10]	ML classifier	Obtained Land Use Land Cover changes and urban sprawl analysis of Vijayawada city for the years 1990 and 2009, got overall accuracy, Kappa Coefficient as 86.67%, 0.8 (1990), 85%, 0.78 (2009)
19	K. Sundarakumar et al., (2012) [11]	ML classifier	Estimated Land Surface Temperature of Landsat ETM+ images of the year 2001 and obtained Overall Accuracy and Kappa coefficient as 80%, 0.729
20	Kiran Yarrakula et al., (2014) [5]	Minimum distance classifier	analyzed urban sprawl changes and detected LULC changes of Vijayawada city and got overall accuracy, Kappa Coefficient as 67.19%. 0.6405.
21	Vani, M. et al., (2020) [1]	NDVI and ML classifier	Assessed spatio-temporal changes in land use and land cover, urban sprawl, and land surface temperature in and around Vijayawada city of the years 1990,2000,2010,2018, and found overall accuracy 96.33%, 93.07%, 92.0%, and 87.0% with their respective Kappa coefficients as 0.94, 0.87, 0.88, and 0.81.
22	Rao, R et al., (2018) [3]	Parallelepiped, Minimum Distance, Mahalanobis Maximum Likelihood classifier	Compared 2013,2014 data by applying Parallelepiped (OA-82.426 Kappa- 0.804), (OA- 94.167 Kappa-0.919-2014), Minimum Distance (OA -88.808 Kappa- 0.85 OA- 84.028 Kappa-0.794- 2014) Mahalanobis (OA-89.055 Kappa-0.842 OA- 89.278, Kappa- 0.857-2014) Maximum Likelihood (OA- 90 Kappa- 0.899, OA- 91.194, Kappa-0.906- 2014)
23	Vivekananda, G. N et al., (2020) [2]	ML Classifier	An accuracy assessment was performed for the 1978 and 2018 LULC maps. The 1978 LULC map had an overall kappa statistic of 0.785 and an overall accuracy of 81.25%, 87.46 Overall kappa statistics 0.857 for 2018

24	Guha et al., (2021) [113]	NDVI, unsupervised clustering method, and the maximum likelihood classification	Assessed the trend of the spatiotemporal relationship between land surface temperature (LST) and normalized difference vegetation index (NDVI) under different ranges of LST and NDVI values for Raipur City, Calculated LULC changes using unsupervised clustering method and the maximum likelihood classification of years 2002, 2006, 2010, 2014, 2018.
25	Jeevalakshmi. D et al., (2016) [123]	NDVI, Maximum Likelihood Classifier	Utilized NDVI for mapping the land cover characteristics over the Tirupati Region and focused on making out the difference between the vegetation indexes of different land cover types by performing supervised classification.
26	Arveti N et al., (2016) [46]	On-screen digitization using visual image interpretation elements.	Illustrated the status of land use/land cover in the Tirupati area of Andhra Pradesh state using an integrated approach of remote sensing and Geographic Information System (GIS) and on-screen digitization using visual image interpretation elements
27	Hua et al., (2018) [8]	parallelepiped, minimum distance-to-mean and maximum likelihood has been applied.	evaluates the impact of land-use and land-cover (LULC) changes on land surface temperature (LST) in the Kuala Lumpur metropolitan city using multi-spectral and multitemporal satellite data. parallelepiped, minimum distance-to-mean, and maximum likelihood have been applied to obtain LULC changes. overall accuracy and Kappa is given as 92.02 (ML),89.18 (Minimum Distance) 78.79 (Parallel piped) KC 0.891, 0.85, 0.282.
28	Bouaziz et al., (2017) [9]	Minimum distance classifier method	Lu/lc changes are detected and overall accuracy and kappa coefficient are calculated (78% and

			0.68)
29	Verma, D. et al., (2019) [14]	Convolutional Neural Networks (CNN)	proposed a novel solution to generate classification maps with a 10-band Sentinel-2B dataset and Convolutional Neural Networks (CNN) at the 10m spatial resolution. The overall accuracy and kappa statistic of the CNN model trained on 14 urban and natural classes are 82 percent and 0.81
30	Nguyen et al., (2018). [187]	Random Forest	Used the Random Forest classifier (RF) to map Land use/Land cover (LULC) of Dak Lak province in Vietnam based on the Landsat 8 OLI with the number of suitable decision trees involved in the classification process is 300 (ntree), and the suitable number of variables used to split at each node is 4 variables. The overall accuracy of 90.32% with a Kappa coefficient of 0.8434 is obtained.
31	Piramanayagam et al., (2022) [194]	Random Forest	Applied the Random Forest (RF) classifier on Landsat5,7,8 images as inputs for the 1985 to 2019 period. The OA, Kappa values, and F1-score are 93.64–97.55%, 0.91–0.96, and 0.86–0.95, respectively.
32	Zhang et al., (2018) [278]	Long short-term memory (LSTM) recurrent neural network	Proposed long short-term memory (LSTM) recurrent neural network (RNN) model to take advantage of the temporal pattern of crops across image time series to improve the accuracy and reduce the complexity. The results show a satisfactory overall accuracy (>90% for five and >88% for all classes)

33	Rahman A et al., (2020) [121]	Random Forest, SVM	Described the performance of different machine learning algorithms on three different spatial and multispectral satellite image classifications in rural and urban extents. Random forest, Support Vector Machine (SVM), and their combined strength (stacked algorithms) were applied on Landsat 8, Sentinel-2, and Planet images separately to assess individual and overall class accuracy of the images. Among the three different algorithms, SVM showed comparatively better results with an overall accuracy of 0.969, 0.983, and an overall kappa of 0.948, and 0.968.
34	Talukdar, S et al., (2020) [241]	random forest (RF), support vector machine (SVM), artificial neural network (ANN), fuzzy adaptive resonance theory-supervised predictive mapping (Fuzzy ARTMAP), spectral angle mapper (SAM), and Mahalanobis distance (MD)	Six machine-learning algorithms, namely random forest (RF), support vector machine (SVM), artificial neural network (ANN), fuzzy adaptive resonance theory-supervised predictive mapping (Fuzzy ARTMAP), spectral angle mapper (SAM), and Mahalanobis distance (MD), were examined. The RF algorithm has the highest accuracy of 0.89, and the MD algorithm (parametric classifier) has the least accuracy of 0.82.
35	Xie Guanyao et al., (2021) [267]	With SPOT 5 and Sentinel 2 data from 2007 and 2018, three remote sensing algorithms were implemented: a support vector machine (SVM), a random forest (RF) combined with geographic object-based image analysis techniques (GEOBIA), and a convolutional neural network (CNN).	All algorithms were deemed efficient, with accuracy indices ranging from 70% to 90%.

36	Dewangkoro et al., (2021) [25]	Executed LULC classification for the EuroSAT remote sensing image dataset from the Sentinel-2 satellite and used Convolutional Neural Network (CNN), SVM, and Twin SVM (TWSVM) as classification algorithm	Procured the strongest evaluation metrics with 94.57% accuracy, 94.40% precision, 94.40% recall, and 94.39% F1 score.
37	Adam, E et al., (2015) [151]	Generated the LULC of an East African region using two machine learning algorithms (SVM and RF). They began by obtaining a high-resolution RapidEye image of the zone, followed by the necessary pre-processing. Following that, they classified the territory into 11 classes incorporating training data and advanced methods (SVM and RF).	The classification maps were then developed and compared based on overall accuracy, Kappa coefficient, and McNamer's test. They concluded that the RF algorithm (overall accuracy = 93.07%) significantly outperformed the SVM algorithm (overall accuracy = 91.80%).
38	Kolli, M.K et al., (2020) [132]	Used an RF classifier to map land use changes across Kolleru Lake in Indi	Accomplishing an overall accuracy of 95.9% and a kappa coefficient of 0.94.
39	Prasad et al., (2016) [193]	Accuracy Measures are compared for RS Images using SVM and ANN Classifiers	SVM (91%), ANN (89%) and Kappa fr SVM (0.89), ANN (0.84)
40	Fang et al., (2019) [90]	Long short-term memory (LSTM) recurrent neural network	Proposed long short-term memory (LSTM) recurrent neural network (RNN) model to take advantage of the temporal pattern of crops across image time series to improve the accuracy and reduce the complexity. The results showed a satisfactory overall accuracy (>90% for five and >88% for all-class)

SUMMARY

Extensive research has been conducted in recent years on categorizing multispectral images using a variety of traditional, ML, and DL algorithms. The literature study aimed to explore and evaluate several modelling approaches for multispectral image classification. Chapter 2 discusses the advancements in multispectral image classification technologies. This chapter gives a comprehensive assessment of traditional, machine learning, and deep learning approaches used in remote sensing data interpretation. Initially developed in the field of machine learning for classification and recognition problems, deep learning techniques have been adopted by the remote sensing and geoscience communities. These techniques have shown remarkable success in target recognition and scene understanding in remote sensing. They excel at abstracting high-level semantic information from bottom-level features, overcoming challenges that traditional remote sensing methods struggle with due to their shallow models. In recent years, extensive research has been conducted on multispectral image categorization using a variety of traditional, machine learning, and deep learning algorithms. The literature study aimed to explore and assess several modelling approaches for multispectral image classification. Chapter 2 addressed advancements in multispectral image classification technologies. The literature review studies mentioned in this chapter have enhanced the remote sensing image categorization model. Each publication is notable independently, contributing a new aspect to model enhancement or optimization. This chapter provides a comprehensive assessment of traditional, machine learning, and deep learning approaches used in remote sensing data interpretation. Deep learning techniques were initially developed in the field of machine learning for classification and recognition problems before being adopted by the remote sensing and geoscience communities. Deep learning techniques have shown significant success in target recognition and scene understanding in remote sensing. These techniques have excelled at abstracting high-level semantic information from bottom-level features, addressing challenges that traditional remote sensing methods struggle with due to their shallow models.

CHAPTER-III

AREA OF STUDY AND DATA COLLECTION

Key points:

- The significance of LULC change detection in the region of interest.
 - Choosing areas to collect data for the planned research.
 - Satellite datasets were utilized in the current study.
 - Software and hardware prerequisites for conducting research.
-

3.1 LULC Change Detection

Remote sensing is a lucrative and dependable way to monitor and map changes in land use and land cover. The first step in this study is to select a study region to obtain the satellite image dataset. For this study, three locations in Andhra Pradesh state have been chosen as depicted in the figure, to meet the study's objectives. This study involves using remote sensing and GIS technologies to monitor and analyze land use and cover changes. Remote sensing data will be collected through satellite imagery, which allows for the acquisition of information on large spatial scales. The Normalized Difference Vegetation Index (NDVI) will be used to assess changes in vegetation cover, indicating the density of vegetation cover by analyzing the reflectance of light in the red and near-infrared parts of the electromagnetic spectrum. GIS will be used to integrate multiple datasets, including remote sensing data, socio-economic data, and environmental data.

3.2 Study Area

The study will focus on analyzing changes in Land Use and cover patterns in three cities in Andhra Pradesh state, India: Vijayawada, Visakhapatnam, and Tirupati. Spatio-temporal variations will be assessed based on LULC changes over the past 20 years. The transformation of surface temperature between vegetated and urbanized areas will be analyzed, associating LST and NDVI data with possible seasonal influences. The geographical representation of Andhra Pradesh is shown in **Figure 3.1**. The results of the study will contribute to a better understanding of the impact of human

activities on the environment, including alterations in microclimatic conditions, changes in biodiversity, and the fragmentation of ecosystems. The study will also inform the development of sustainable land management strategies at national, regional, and local levels, including policies to promote sustainable land use practices and land use planning to ensure the needs of local communities are met while protecting natural areas. The study involved three major areas of investigation, namely Vijayawada (VJY), Visakhapatnam (VSP), and Tirupati (TPT).

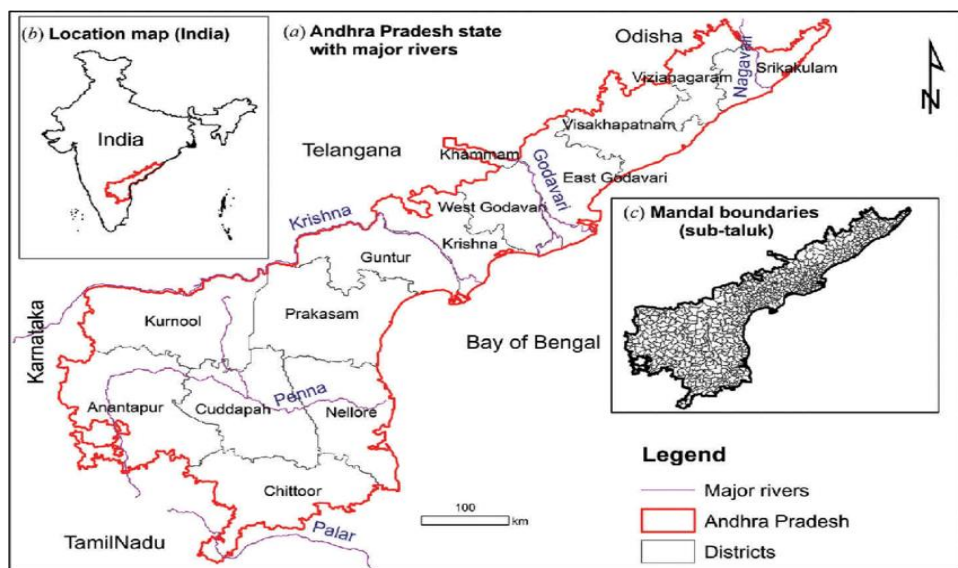


Figure 3.1: Geographical representation of Andhra Pradesh

3.2.1 Vijayawada (VJY)

Vijayawada (VJY) is an ancient city located in the middle of A.P., which is the second-biggest metropolis in A.P. The metropolis reclines on the slope of the River Krishna, enclosed with the aid of the hill of the Eastern Ghats, famed as Indrakeeladri Hills in Krishna District. The metropolis is mulled over as a hallowed spot for a home, the maximum swarmed and famous sanctuaries of Andhra Pradesh, India, Kanaka Durga Temple of the Hindu Goddess Durga. The metropolitan network is geographically mendacity in Andhra Pradesh alongside the banks of the Krishna River with a scope of sixteen 003`11" N and longitude eighty 00 3`91" E (e.g., Harika, 2012). It is a metropolitan network with historical, governmental, educational, and social backgrounds. The environmental fame is equatorial, with fiery summer seasons

and mild winters. The annoyed warmth is 47 °C in May-June, at the same time as it is far around 20-27 °C in winter. The moistness is 78%, and the yearly downpour is 103 cm. **Figure 3.2** presents the Geographical location of Vijayawada city.

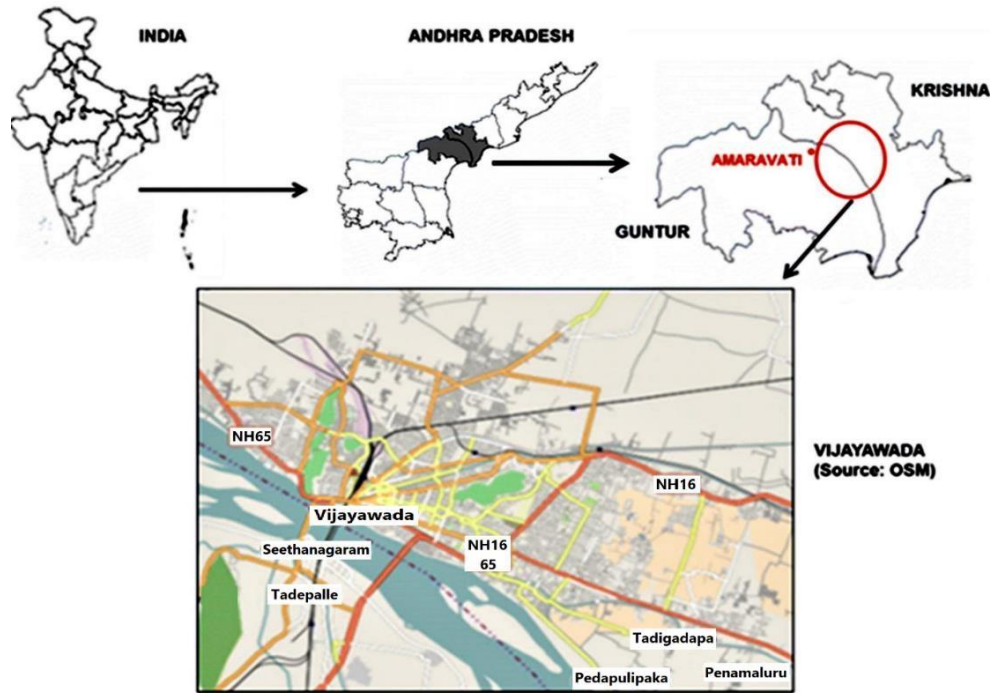


Figure 3.2: Geographical location of Vijayawada city

These strategies can be implemented at different scales, including national, regional, and local levels. At the national level, policies can be developed to promote sustainable land use practices, including the protection of natural areas and the promotion of sustainable agricultural practices. At the local level, land use planning can be used to ensure that land is used sustainably and that the needs of local communities are met. Several studies have contributed to the understanding of land use and cover changes in Vijayawada.

3.2.2 Visakhapatnam (VSP)

Visakhapatnam (VSP), additionally referred to as Vizagapatam, Vizag, or Waltair, is the administrative capital of Andhra Pradesh state. It is moreover the maximum occupied and maximum vital town of Andhra Pradesh. It lies among the Eastern Ghats and the coastline of the Bay of Bengal. It is the second-largest town on India's east coast after Chennai and the fourth-largest town in South India addressed in

Figure 3.3. It is one of the four clever cities of Andhra Pradesh assigned under the Smart Cities Mission. (The Times of India). The town arranged to lie among 17.7041 N and 83.2977 E. Visakhapatnam has an equatorial marshy and arid environmental condition. Every year suggests temperatures sure among 24.7–30.6 °C (76–87 °F), with the extremum in May and the nominal in January; the nominal temperatures vary from 20– 27 °C. The extremum temperature registered became 42.0 °C, and the least became 20.0°C. It has rainfall from the South-west and northeast monsoons and suggests every year rainfall registered is 1200 cm.

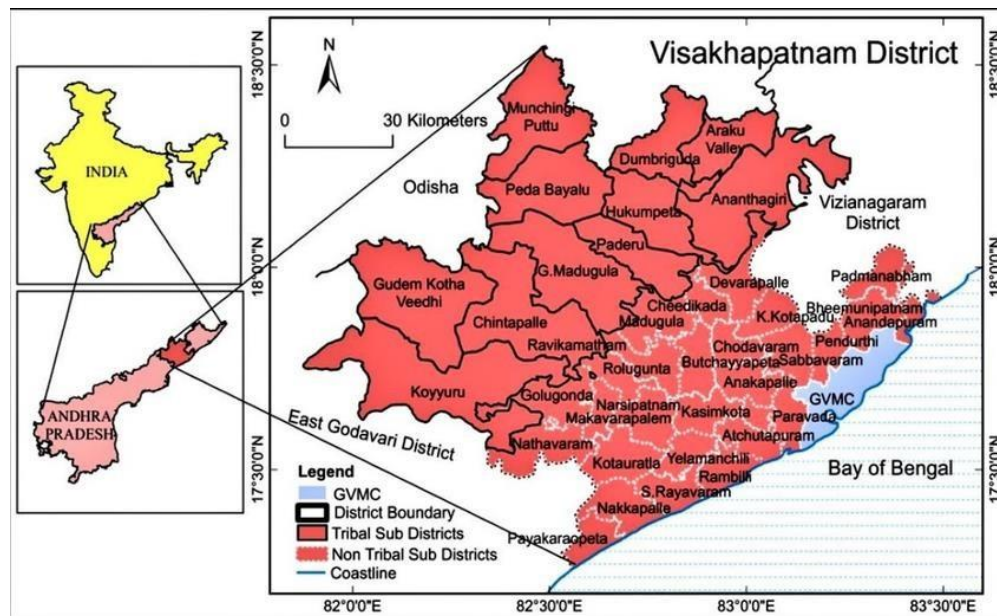


Figure 3.3: Geographical location of Visakhapatnam district

3.2.3 Tirupathi (TPT)

Tirupathi is in the southern state of Andhra Pradesh, India, and it is another study area in this research on land use and cover changes. It has experienced significant changes in land use and cover due to the expansion of urban areas and increased agricultural activities, which have had important implications for the environment, including alterations in microclimatic conditions, changes in biodiversity, and the fragmentation of ecosystems. It is therefore crucial to monitor and assess land use and cover changes to understand the influence of human activities on the atmosphere in Tirupathi.

Tirupati (TPT) is placed at 13.65°N 79.42°E in the Chittoor District, A.P. It lies at the lowest of the Seshachalam Hills of the Eastern Ghats, which have been malleable throughout the Precambrian era. Situated 750 km southwest of the state's government capital, Visakhapatnam, the town is in the vicinity of the important Hindu shrine of Tirumala Venkateswara Temple and a few different ancient temples and is cited as the "Spiritual Capital of Andhra Pradesh," confirmed in **Figure 3.4**. Tirupati has an equatorial, marshy, and arid environmental situation based on the Koppen environmental classification. In wintertime, the marginal temperatures are between 18°C and 20°C (64.4 and 68.0 °F). Unremarkably, summertime lasts from March to June, with the advent of a showery season in July, preceded by the end of winter, which stays until the quiet of February. The town encounters dense rainfall in November throughout the northeast monsoon season.

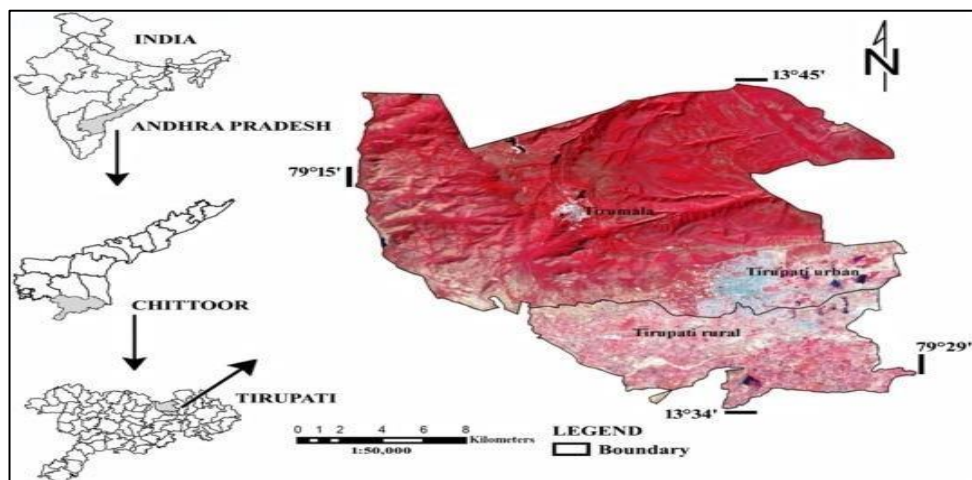


Figure 3.4: Geographical location of Tirupati

3.3 Satellite Dataset

For Traditional LULC classification, Landsat satellite information (Thematic Mapper—TM and Operational Land Imager—OLI) is used. Time collection Landsat satellite information (Thematic Mapper—TM and Operational Land Imager—OLI) had been exploited to originate the LULC maps of Vijayawada, Visakhapatnam, and Tirupati for the years 2000 (TM—27 April), 2005 (TM-), 2010 (TM—9 May) 2015 (OLI-28 April) and 2020 (OLI—09 April) using Red, and Near-infrared (NIR) bands of 30 m resolution are utilized in the proposed method. The spatial information is represented in **Table 3.1**. Worldwide Reference System (WRS) is a worldwide

documentation framework for Landsat information. WRS empowers a consumer to enquire about satellite imagery over any piece of the universe by determining an apparent aspect of place allotted by Path and Row numbers. The accumulation of a Path and Row number unambiguously verified a specified aspect center. The Path number is given first, followed all the time by the Row number. The images were downloaded using USGS Earth Explorer (<http://earthexplorer.usgs.gov/>). **Figure 3.5** shows Landsat datasets that represent NDVI, False color of Vijayawada, Visakhapatnam, and Tirupati; **Table 3.1:** Spatial information of the study area

Area	Data Source	Sensor	PATH	ROW
Visakhapatnam	Landsat	ETM+, OLI/TIRS	43	33
Vijayawada	Landsat	ETM+, OLI/TIRS	25	36
Tirupati	Landsat	ETM+, OLI/TIRS	96	78

To support the study using advanced Deep Learning techniques, the proposed work selected Sentinel-2A bands. To acquire the information, ESA's (European Space Agency) Sentinel-2 dataset was acquired in 2015 (9 May), 2020 (28 April) and 2022 (09 April). The area of interest was captured by the ESA's Sentinel-2 satellite on a cloud-free day during the summer seasons of 2015, 2020, and 2022. The Sentinel-2 satellite provides 10–60 m spatial resolution with a 5-day revisit frequency and global coverage. It detects 13 spectral bands (0.443-2.190 μm) across a 290 km swath (**Figure 3.6**). The dataset from the Sentinel-2 satellite that covered the study area is an S2MSI1C product type with a JPEG2000 format and a LEVEL-1C processing level. It was made using the UTM map projection and has the following details: UTM Zone: 43N, center latitude: 16.5062" N, and center longitude: 80.6480" E. **Tables 3.2–3.4** provide further details. **Figure 3.7** shows representation in (a), (c), (e) and (b), (d), (f) represents False color composition which helps in vegetation classification.

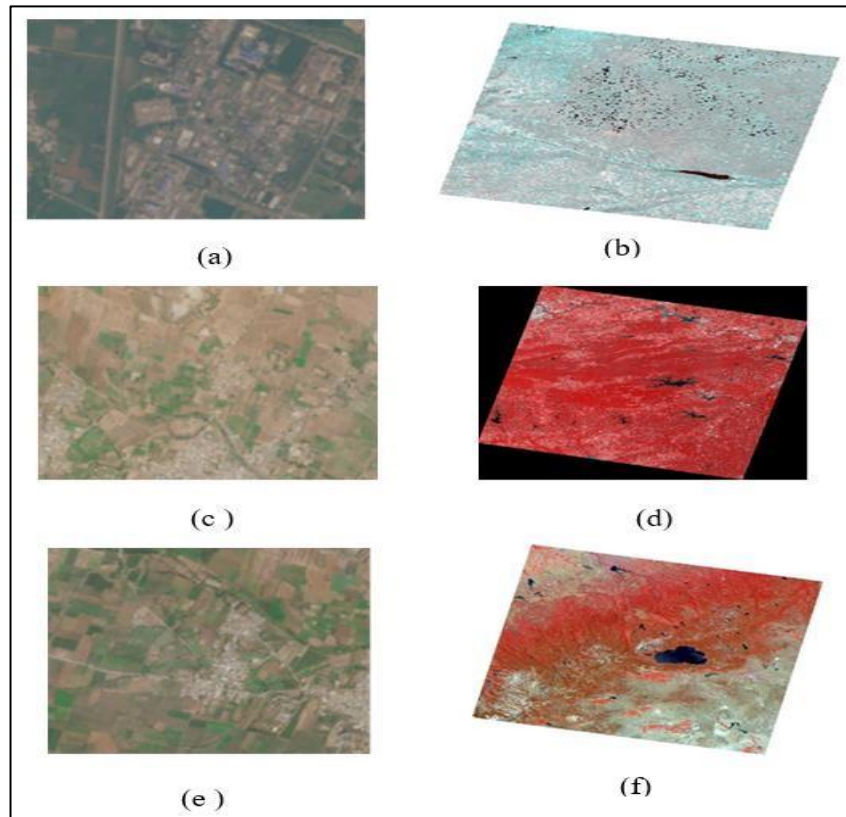


Figure 3.5: Landsat datasets of (a), (c), and (e) represent NDVI of Vijayawada, Visakhapatnam, and Tirupati; (b), (d), and (f) represent False color of Vijayawada, Visakhapatnam, and Tirupati

Sentinel-2 dataset

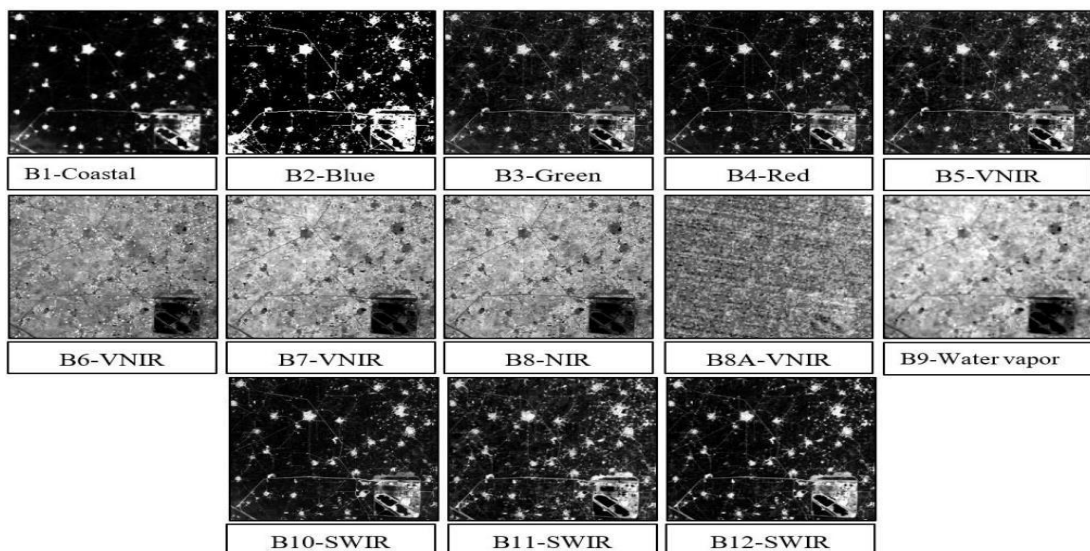


Figure 3.6: Sentinel-2 dataset bands

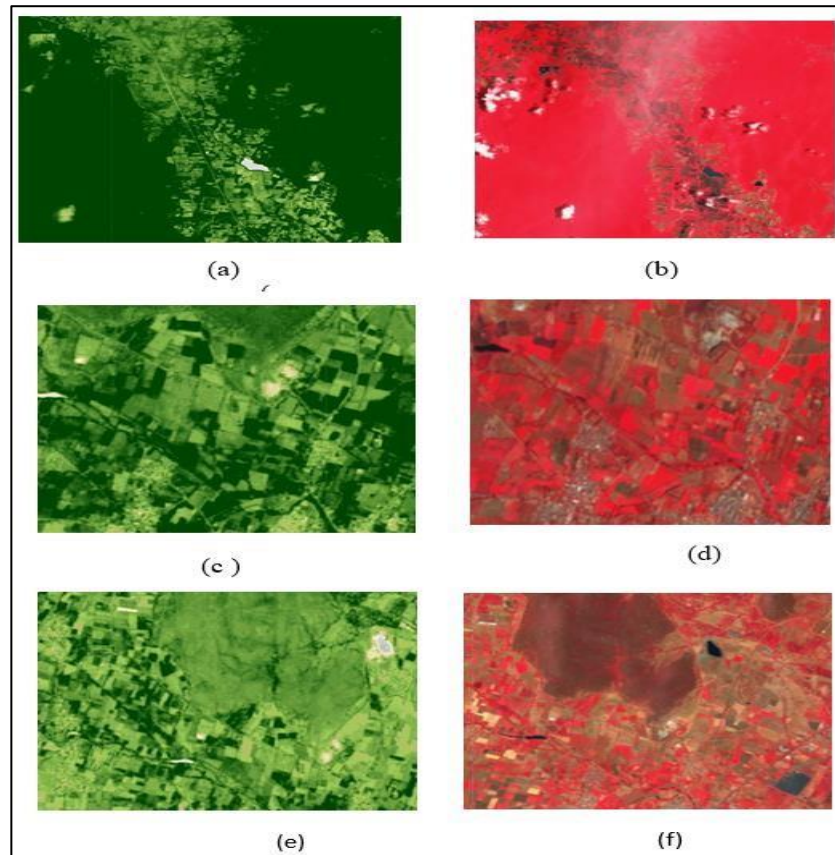


Figure 3.7: Sentinel-2 datasets of years 2015 (9 May), 2020 (28 April), and 2022 (09 April) (a), (c), (e)- NDVI representation and (b), (d),(f) – False color composition representation

Table 3.2: Spatial information of the study area for the year 2015

S. No	Dataset attributes	Attribute values
1	Entity ID	S2A_MSIL1C_20151023T045842_N0204_R119_T44QMD_20151023T051042.SAFE
2	Acquisition Start Date	2015-10-23T04:58:42.026Z
3	Acquisition End Date	2015-10-23T04:58:42.026Z
4	Spatial resolution	60m

Table 3.3: Spatial information of the study area for the year 2020

S. No	Dataset attributes	Attribute values
1	Entity ID	S2B_MSIL1C_20201023T100049_N0500_R122_T33TUL_20200614T073051.SAFE
2	Acquisition Start Date	2020-10-23T10:00:49.024Z
3	Acquisition End Date	2020-10-23T10:00:49.024Z
4	Spatial resolution	60m

Table 3.4: Spatial information of the study area for the year 2022

S. No	Dataset attributes	Attribute values
1	Entity ID	S2A_MSIL1C_20220823T045711_N0400_R119_T44QMD_20220823T065335.SAFE
2	Acquisition Start Date	2022-08-23T04:57:11.024Z
3	Acquisition End Date	2022-08-23T04:57:11.024Z
4	Spatial resolution	60m

3.4 Software and hardware requirements

Various software programs are available for analyzing satellite images. The selection of software is based on the user's specific needs and the relevant field of study. The most frequently used software is described in this segment.

3.4.1 ENVI

ENVI, which stands for "Environment for Visualizing Images," is a remote sensing software application used for processing and analyzing geospatial data, especially satellite and aerial imagery as shown in **Figure 3.8**. Developed by Harris Geospatial Solutions, ENVI provides a range of tools and functionalities for extracting valuable information from remotely sensed data. It is the best image analysis program for GIS experts, remote sensing scientists, and image analysts. The program is used to retrieve useful data from images to improve decision-making. ENVI can be accessed via computer and cloud platforms. Customization can be achieved using an IDL-based

API to meet specific project requirements. To conduct the studies, a computer system with a 4-core Intel Xeon W-2104 processor running at 3.2 GHz, 16 GB of RAM, an NVIDIA Quadro P620 2GB graphics card, and software that includes the DL v1.1.2 module on the ENVI v5.6 platform was used. This software requires an NVIDIA graphics card with CUDA computing capability. ENVI's deep learning model offers two options: ENVINet5 for single-class classification and ENVI Net-Multi for categorizing multiple classes. To train the TensorFlow model, several samples have been chosen for each class category, such as wheat, berseem, mustard, other vegetation, water, and buildup. Various software programs are available for analyzing satellite images, with the selection of software depending on the user's needs and the specific field being considered. This segment describes the most frequently utilized software.

The ENVI software is equipped with a range of key features and capabilities. These features enable users to perform various tasks and analyses related to their data. Some of the notable capabilities of the software include image processing, spectral analysis, and geospatial analysis. Classification and Feature Extraction, Change Detection, Customization and Automation,

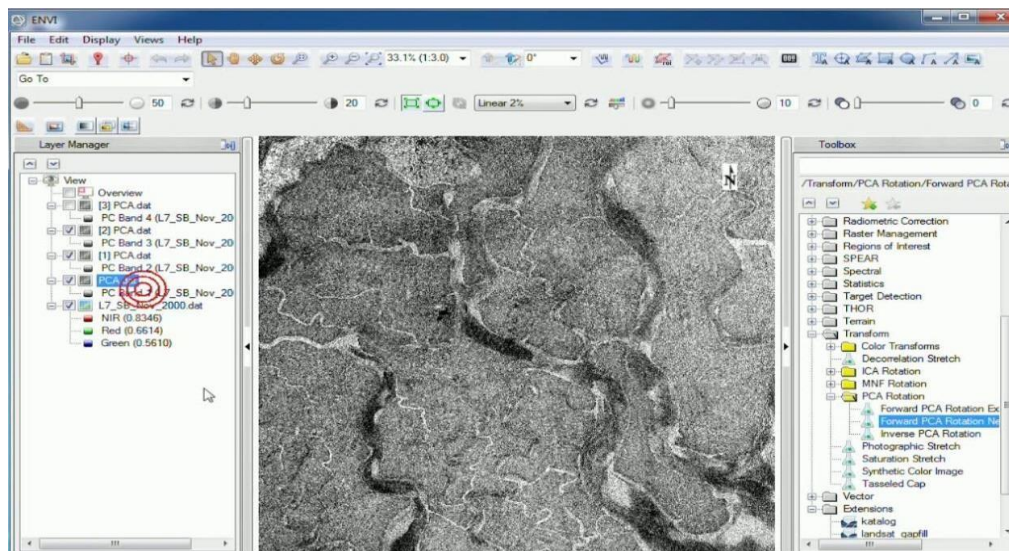


Figure 3.8: Environment for visualizing images (ENVI) software.

3.4.2 ERDAS Imagine

ERDAS (Earth Resources Data Analysis Systems) was launched in 1978 to collect, process, analyze, and understand raw geospatial data, and provides essential information as shown in **Figure 3.9**. This software tool is maintained by <https://www.hexagongeospatial.com/>. ERDAS is a powerful and versatile raster graphics editor and remote sensing tool developed by ERDAS, Inc. The latest version available is 9.3. The primary focus of this tool is to help users prepare, display, and enhance digital images for use in GIS or CAD software, with a particular emphasis on geospatial raster data processing. With ERDAS IMAGINE, users can execute various operations on an image and respond to geographical inquiries. For instance, the brightness level or light reflection from surfaces in the image can aid in vegetation analysis, mineral prospecting, and other applications. Additionally, users can extract linear features, create processing sequences (called "spatial models" in ERDAS IMAGINE), transfer data in different formats, orthorectify images, merge images, and automatically extract map details from images. ERDAS IMAGINE is interoperable with several satellites, such as Landsat, Worldview, Sentinel, SPOT, and AVHRR. To run the software, users need a 32-bit processor, 4GB to 8GB of RAM, 4GB of disc space for installation, and Windows 7 Professional.

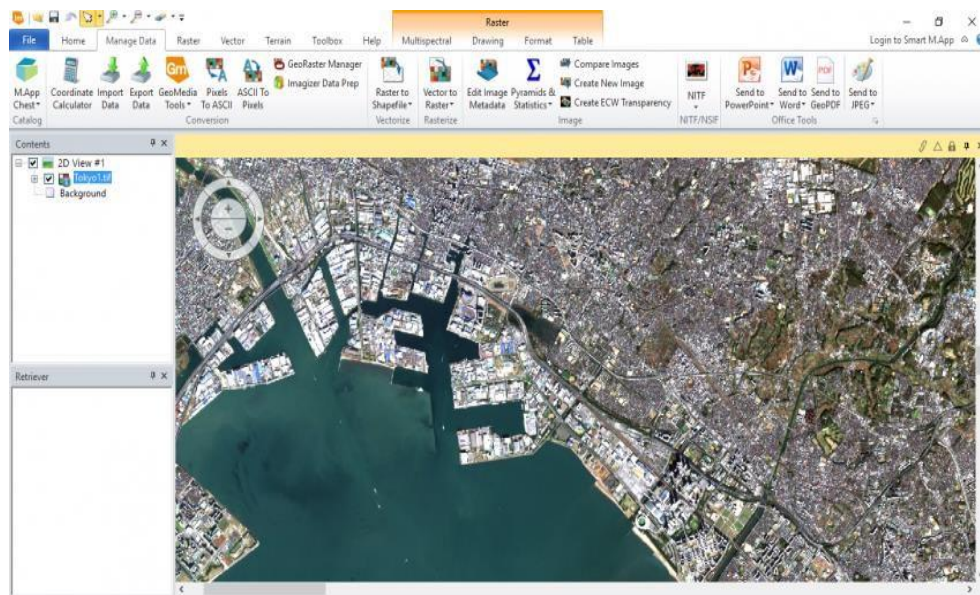


Figure 3.9: Earth resources data analysis system (ERDAS) software.

3.4.3 ArcGIS

Figure 3.10 represents ArcGIS, a powerful software for processing and generating geographic information system data. ESRI manages this software program, which has various capabilities, including spatial analysis, map construction, and data administration. The software supports multiple data types for remotely sensed data, server components, mobile and desktop apps, and developer tools. Additionally, Arc Reader is a free and user-friendly tool used for viewing and printing maps published as Published Map Files (PMF) using the ArcGIS publisher extension in ArcGIS for Desktop. To run the software, you need to meet the following prerequisites: Microsoft Visual C++, Redistributable (x86), 2.2 GHz or higher, Hyper-Threading Technology (HTT) or multicore preferred, 2 GB of RAM, and 50 GB of space.

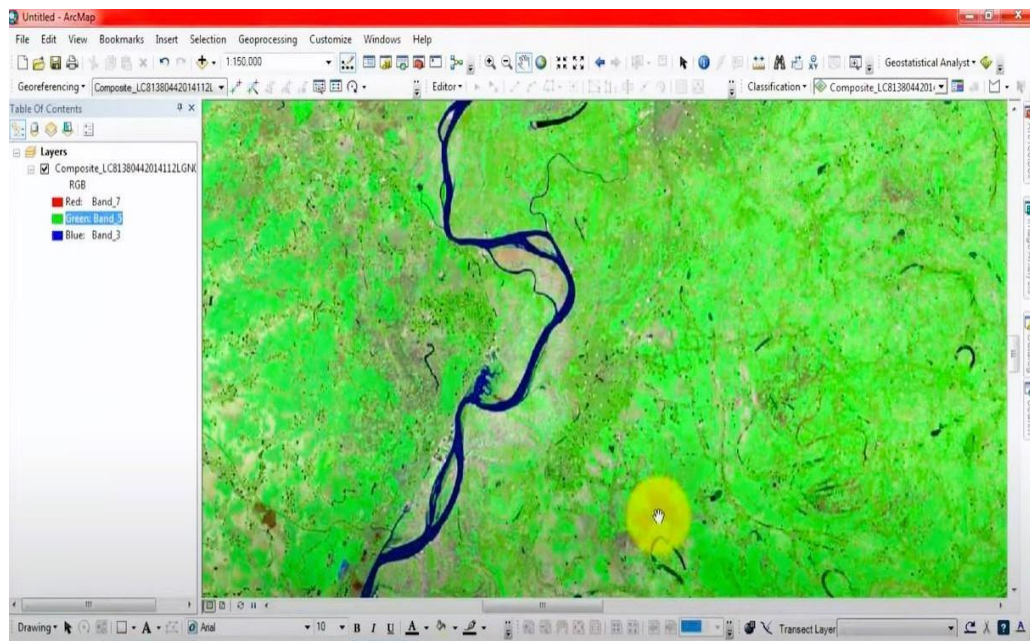


Figure 3.10: Advanced geographic information system

3.4.4 ArcGIS Pro

Figure 3.11 represents ArcGIS Pro, Esri produced ArcGIS Pro, a desktop GIS software that succeeded the ArcMap software generation. The product was announced as part of Esri's ArcGIS 10.3 release. ArcGIS Pro stands out for its 64-bit architecture, combined 2-D and 3-D capability, ArcGIS Online integration, and Python 3 support.

ArcGIS Pro 3.0, released in June 2022, was a significant version upgrade. Several significant changes include the removal of support for geocoders developed with ArcMap 10.x and ArcGIS Pro versions 2.9.x and earlier; ArcGIS Pro is a ribbon-based program. Many commands are accessible via the ribbon at the top of the ArcGIS Pro window; more complex or specialized capability is located on panes (dockable windows) that can be accessed as needed. ArcGIS Pro allows you to save several elements, such as maps, layouts, tables, and charts, in a single project and access them as needed.

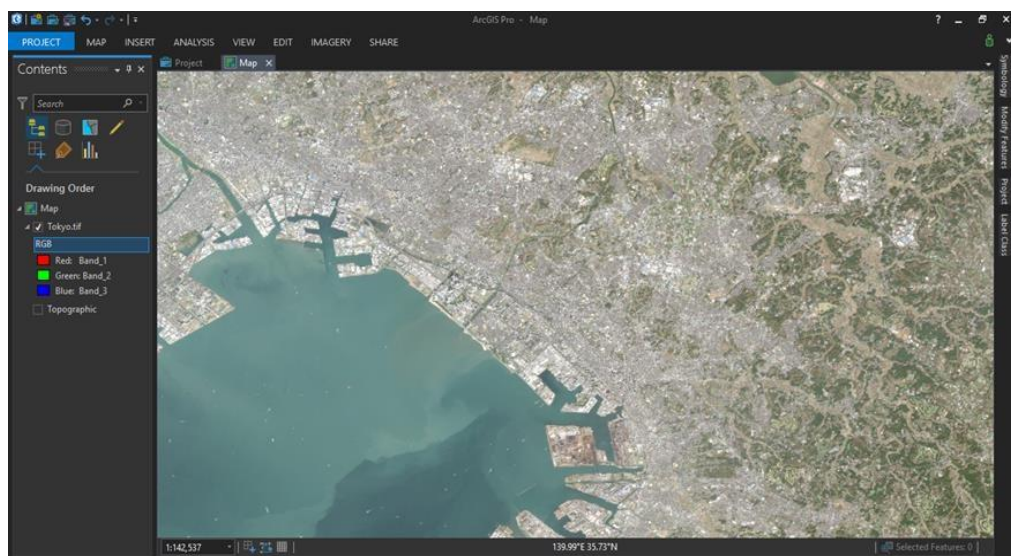


Figure 3.11: Advanced geographic information system (ArcGIS Pro) software.

3.4.5 QGIS

QGIS, commonly known as Quantum GIS, is open-source (GIS) software represented in **Figure 3.12**. QGIS works on Windows, macOS, and Linux. It allows users to browse, edit, print, and analyze geographical data. QGIS is geographic information system (GIS) software that allows users to analyze and update spatial data, as well as create and export graphical maps. QGIS supports raster, vector, and mesh layers. Vector data is represented as point, line, or polygon features. The software supports a wide range of raster image types and can georeference them. QGIS can handle shapefiles, personal geodatabases, dxf, MapInfo, PostGIS, and other industry-standard formats. Web services, such as Web Map Service and Web Feature Service, are also supported, allowing for the use of data from other sources.

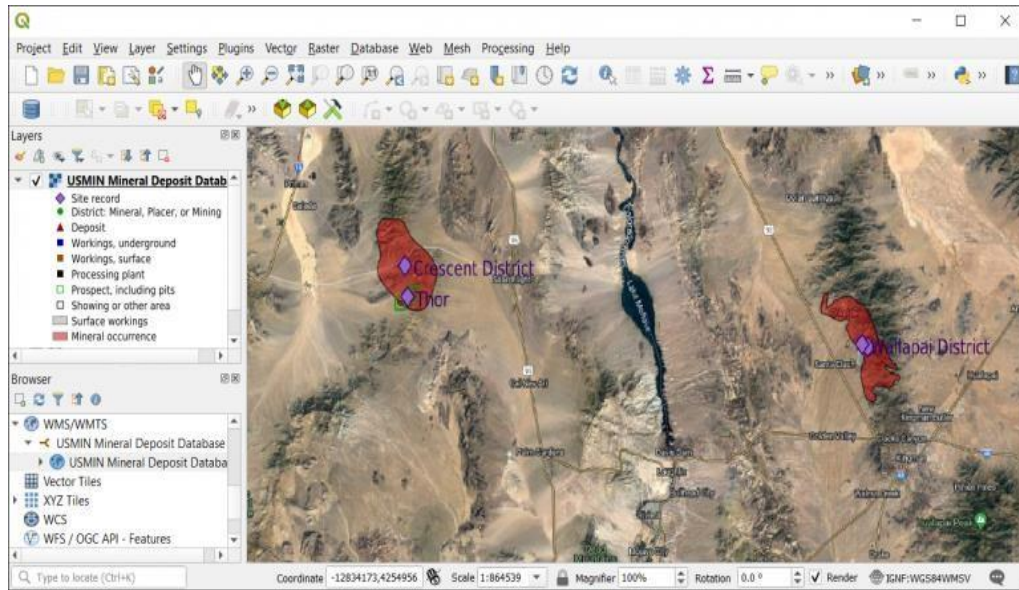


Figure 3.12: QGIS software

3.4.6 Sentinel Application Platform (SNAP)

SNAP is a project of the European Space Agency (ESA). It is software designed for image processing, modeling, and visualization and is managed by <https://scihub.copernicus.eu/>. The SNAP technology is suitable for processing and analyzing Earth-observation data as illustrated in **Figure 3.13**. It enables scientific exploitation for ERS-ENVISAT, Sentinels 1/2/3, Proba-V, and other national and third-party missions. The SNAP software toolkit includes Earth Observation data, the Graph Processing Framework for creating and executing workflows, a command-line interface, and programming interfaces for Python and Java. The SNAP software toolkit generally requires 4GB of RAM. Additionally, a 3D graphics card is necessary to access the 3D World Wind View. The SNAP software toolbox can be used with both 32- and 64-bit Windows, Mac OS X, and Linux operating systems.

3.4.7 MATLAB

MATLAB (Matrix Laboratory) is a numerical computing environment and programming language created by MathWorks, as illustrated in **Figure 3.14**. MATLAB has a wide range of applications, including matrix manipulation, function charting, data analysis, algorithm implementation, graphical user interface development, and connecting with programs written in other languages. It's

managed by <https://www.mathworks.com/products/matlab.html>. It requires Windows 10 or Windows 7, an Intel or AMD x86-64 processor, 3 GB of HDD space dedicated to MATLAB, and 4 GB of RAM. 52.

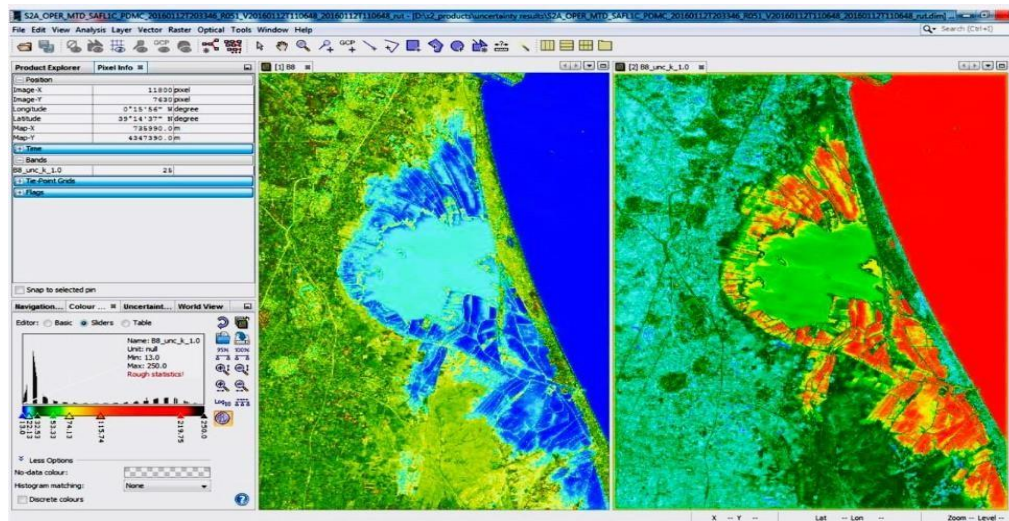


Figure 3.13: Sentinel application platform (SNAP) software.

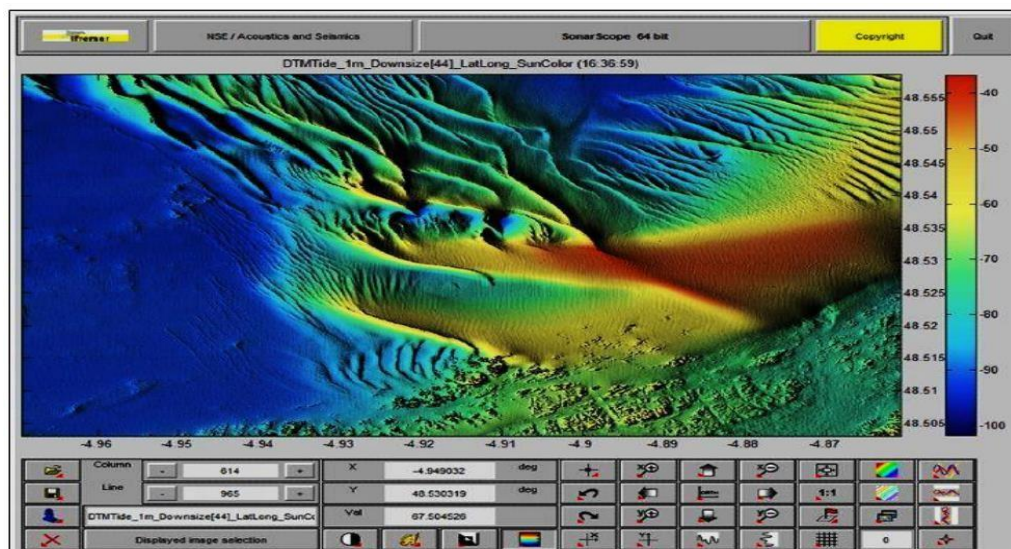


Figure 3.14: MATLAB (Matrix Laboratory) software.

3.4.8 Google Earth Pro

It is a three-dimensional interactive globe that may be used for planning, analysis, and decision-making. It has complex capabilities such as land development with polygon area measurement, printing images up to 4800x3200 px resolution, and

importing big vector image files to swiftly map GIS data. Google Earth Pro (**Figure 3.15**) is free for desktop users that require additional features. It requires the Windows 7 operating system, a CPU of 1GHz or above, 2GB of RAM, and an Internet connection. It is managed by <https://www.google.com/earth/5>.

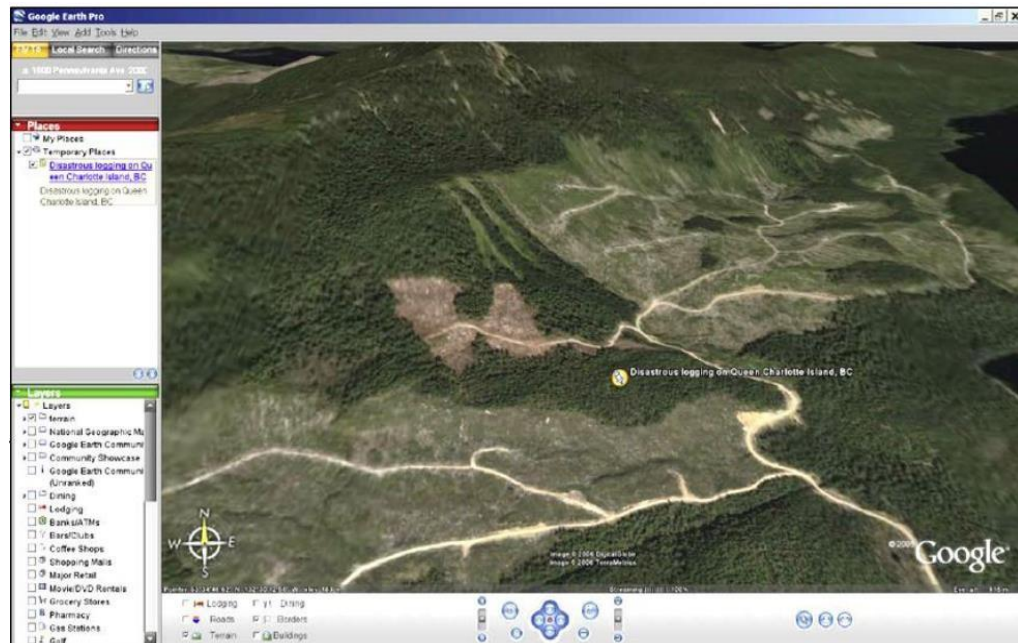


Figure 3.15: Google Earth Pro software.

Summary

The study region and satellite sensor dataset used in this thesis work are described in depth in this chapter. This chapter explains the research site's significance. The dataset obtained for this research is described in this document.

CHAPTER-IV

METHODOLOGY

Key points:

- Methodologies for suggested research.
 - Pre-processing stages include geometric and atmospheric/radiometric modifications.
 - The assessment of classifiers for LULC classification and change detection.
 - Validation of experimental results and cross-reference with algorithms.
-

4.1 Proposed Methodology (traditional pixel-based method)

Figure 4.1 illustrates the proposed methodology for achieving the research goals. Initially, data is acquired from the satellite sensor during multi-temporal, cloud-free periods.

4.1.1 Establishment of temporal LULC maps of the survey region

This survey generally concentrated on rendering the consequences of Land use via satellite imagery and statistical information. The numerical mechanisms of alternate detection become exploited in this research. In the alternate detection mechanism, each satellite image is categorized. The resultant LULC maps acquired after the type are analogized to the pixel-by-pixel conceptualization with the aid of accomplishing a change detection matrix.

Step 1- Data Collection: Time collection Landsat satellite information (Thematic Map-per—TM and Operational Land Imager—OLI) had been exploited to originate the LULC maps of Vijayawada, Visakhapatnam, and Tirupati for the years 2000 (TM—27 April), 2005 (TM-), 2010 (TM—9 May) 2015 (OLI-28 April) and 2020 (OLI—09 April) using Red, and Near-infrared (NIR) bands of 30 m resolution which represents the flowchart of the proposed method. The Worldwide Reference System (WRS) is a worldwide documentation framework for Landsat information. WRS empowers a consumer to enquire about satellite imagery over any piece of the universe by

determining an apparent aspect of place allotted by Path and Row numbers. The accumulation of a Path and Row number unambiguously verified a specified aspect center. The Path number is given first, followed all the time by the Row number. The images were downloaded using USGS Earth Explorer (<http://earthexplorer.usgs.gov/>).

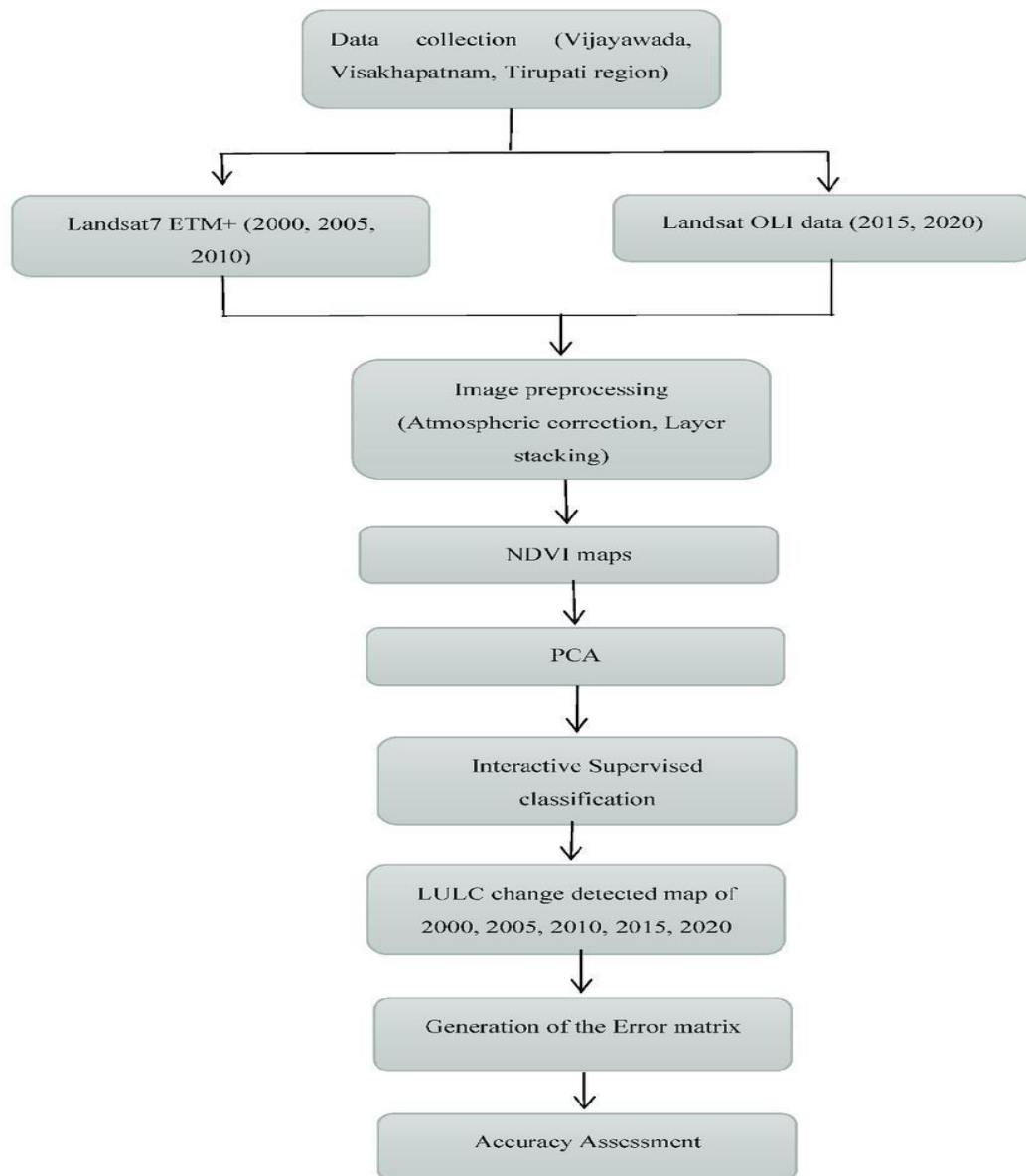


Figure 4.1: Flow Chart of LULC maps of the survey region.

Step-2- Image Pre-processing: Radiometric correction is an error that causes the radiance or radiometric value of a scene element. Radiometric correction is done to

reduce errors in digital numbers of images and improve interpretability and analysis, to standardize images.

The initial step is to transform Digital Number (DN), i.e., pixels in an image, into Top of Atmosphere (TOA) Radiance. For Landsat images, Spectral Radiance at the sensor's aperture is given by the equation (Eq. (4.1)).

$$\text{DN values to TOA REFLECTANCE} = \frac{\text{BAND SPECIFIC REFLECTANCE_MULTI_BAND} \times \text{DN VALUES} + \text{REFLECTANCE_ADD_BAND}}{\text{REFLECTANCE_MULTI_BAND}} \quad (4.1)$$

The correction of the Sun angle is further done by using the equation (Eq. (4.2)).

$$\text{Correction for Sun angle} = \text{TOA REFLECTANCE} / \sin(\text{SUN ELEVATION}) \quad (4.2)$$

Step-3- NDVI maps: NDVI is a generally used vegetation index obtained from RS assets, gauging photosynthetic radiation consumed by the Earth's surface. NDVI maps were generated using the OLI sensor's Band4 (RED), and Band5 (NIR). The NDVI value falls between -1 and +1. Numerous positives represent dense foliage, whereas negative numbers imply water. (Rajani et al., 2020, Lu et al., 2007). The values are calculated using the equation. (Eq. (4.3)).

$$\text{NDVI} = \frac{\text{NIR} - \text{RED}}{\text{NIR} + \text{RED}} \quad (4.3)$$

Step-4: To generate NDVI maps, we used Principal Component Analysis (PCA), which is a method for transforming correlated primary bands into a new set of uncorrelated variables. These new variables contain the original raw data and can be used for further analysis. (Dilawar et al., 2021, Guo et al., 2020).

The steps to calculate PCA are enlisted as follows:

1. Calculate the mean of the image matrix, the mean vector is the vector average of the individual components of a vector (Eq. (4.4)).

$$\bar{x} = \frac{1}{M} \sum_{k=0}^{M-1} x_k \quad (4.4)$$

M= Number of sample points

\bar{x} =sample mean of the variable

X_k = k^{th} centered data

2. The covariance matrix is obtained as

$$E = X X^T - \overline{X X^T} \quad (4.5)$$

3. Eigenvectors and eigenvalues are the linear algebra concepts that are needed to compute from the covariance matrix to determine the principal components of the data. Eigenvalues (λ) can be obtained by the equation (Eq. (4.6)).

$$|\text{cov}(x) - \lambda I| = 0 \quad (4.6)$$

I- Identity matrix

4. Eigenvectors can be determined by the equation (Eq. (4.7)).

$$(\text{cov}(x) - \lambda I) v = 0 \quad (4.7)$$

v=Eigen vector

Step-5- Interactive Supervised Classifier: Here Stratified random sampling is used to obtain training samples for classification. Stratified random sampling is a method that involves the division of an aggregation into smaller subgroups known as strata. In stratified random sampling or stratification, the strata are formed based on attributes or characteristics.

Image classification brings data classes out of a multiband raster image. It is categorized into two techniques: supervised and unsupervised. Images were classified to obtain data categories from a multiband raster image. This paper proposed a new approach, i.e., interactive supervised classification for land use mapping. An interactive supervised classification is a tool used to reveal a supervised class without developing a signature file. It speeds up the categorizing process. All the bands in the image were chosen.

They are used in interactive supervised categorization, which includes built-in pyramids. It makes better use of the image's resolution at the pyramid level. Building pyramids improves the display performance of raster datasets. Training sites were generated by digitizing polygons that enclosed specific land cover features illustrative of desired land cover types. The training sites from each group were then integrated into one class so that each cover type had one class writing from many training sites. With the training samples integrated into discrete classes, the “Interactive Supervised Classification” function was initiated to create an output image raster with cells classified and symbolized by land cover type. Then the complete examination field was classified into 5 land-use groups: natural vegetation, dense vegetation, urban area (without vegetation), barren land, and water. In interactive supervised classification, a pixel with the maximum probability is categorized into the appropriate class. The probability L_m is outlined as the hinder probability of a pixel associated with class k (Eq. (4.8)).

$$L_m = P(m/S) = P(m) * P(S/m) / \sum P(k) * P(S/k) \quad (4.8)$$

Where, $P(m)$: the prior probability of class m

$P(S/m)$: conditional probability to observe S from class m

Step-6- LULC change detection and Error matrix generation: The error matrix, also known as the confusion matrix or transition matrix is generated, which is employed to assess remote sensing images. The matrix's diagonal elements correspond to correctly classified elements, which determine accuracy (Xia et al.,2014). The transition matrix demonstrates several errors in the categorization procedure, allowing reinforced evaluation of maps, and increased accuracy assessment.

Step-7- Accuracy assessment: The classified thematic output was then examined for accuracy (Eq. (4.9) - Eq. (4.16)) by calculating overall accuracy, Kappa coefficient, user's, producer's accuracy, Error of commission, Error of Omission, Specificity, F-Score, and False Positive Rate values.

$$\text{Overall Accuracy} = \frac{\text{Total Correctly Classified Pixels}}{\text{Total Number of Pixels}} \quad (4.9)$$

$$\text{User's Accuracy} = \frac{\text{Correctly Classified Sites}}{\text{Total Number of Sites in a Row}} \quad (4.10)$$

$$\text{Producer's Accuracy} = \frac{\text{Correctly Classified Sites}}{\text{Total Number of Sites Classified in a Column}} \quad (4.11)$$

$$\text{Error of Commission} = \frac{\text{Incorrectly Classified Sites in a Row}}{\text{Total Number of Sites}} \quad (4.12)$$

$$\text{Error of Omission} = \frac{\text{Incorrectly Classified Sites in a Column}}{\text{Total Number of Sites}} \quad (4.13)$$

$$\text{Kappa Coefficient} = \frac{\text{Total Accuracy} - \text{Random Accuracy}}{1 - \text{Random Accuracy}} \quad (4.14)$$

$$\text{Specificity} = \frac{\text{TN}}{\text{TN} + \text{FP}} \quad (4.15)$$

$$\text{F-Score} = \frac{2 * \text{Precision} * \text{Recall}}{\text{Precision} + \text{Recall}} = \frac{2 * \text{TP}}{2 * \text{TP} + \text{FP} + \text{FN}} \quad (4.16)$$

4.1.2. Computation of LST

Land Surface Temperature is an essential variant of the Earth's environmental condition system. LST was assessed for 20 eras from 2000 to 2020 using thermal bands of the Landsat satellite data (ETM+, and OLI) as shown in **Table 2**. Three algorithms are used to calculate LST from satellite data, which are the Radiative Transfer Model (RTM), Mono-Window (MW), and Split-Window (SW). RTM technique produces a top-quality outcome (Qin et al., 1999). However, the required dedication of the radiosonde interest in atmospheric elements throughout the satellite's passage makes the set of rules much less endorsed for SW and MW. However, SW requires two thermal bands, which produces some unpredictability. Thus, the MW algorithmic rule is preferred based on the thermal radiation (Lu et al., 2013; A. Rajani et al., 2021). Therefore, in this research, LST was enumerated by exploitation of the MW algorithm formulated by Qin et al. (2001). **Figure 4.2** represents the flow chart for the Computation of LST. Thermal conversion constants of ETM+ and OLI sensors are shown in Table 4.1, where K1 and K2 are thermal conversion constants of the TIRS bands, and Q cal–Quantized and calibrated standard product pixel value (DN).

Table 4.1: Thermal conversion constants

Constants	ETM+	OLI
K₁	666.09	774.8853
K₂	1282.71	1321.0789
L_{max}	12.65	22.00180
L_{min}	3.200	0.10033
Q_{Cal max}	255	65535
Q_{Cal min}	1	1

The step-by-step process for LST calculation is given below:

Step-1: Radiance is the "flux of energy per solid angle leaving a unit surface area in a given direction." The initial step is to transform Digital Number (DN), i.e., pixels in an image, into Top of Atmosphere (ToA) Radiance. For Landsat images, Spectral Radiance at the sensor's aperture is given by the equation (Eq. (4.17)).

$$L_{\lambda} = M_L * Q_{cal} + A_L + O_i \quad (4.17)$$

Where

L_{λ} – ToA Spectral Radiance

ML – Band-specific multiplicative rescaling factor from the Metadata (Radiance_mult_Band_X, where X is the band number 10)

AL – Band-specific additive rescaling factor from the metadata (Radiance_add_Band_10)

Q cal – Quantised and calibrated standard product pixel value (DN)

O_i – Correction value of Band 10, which is 0.29

Step 2: Brightness Temperature (BT) measures the power of microwave radiation traveling upwards from the upper atmosphere to the satellite, expressed in units of equivalent blackbody temperature. Spectral radiance data conceivably changed to the top of atmosphere brightness Temperature using invariant thermal values in the Metadata file. The brightness temperature transformation is given in the equation (Eq. (4.1)).

$$BT = \left[\frac{K_2}{\ln(K_1 + L_{\lambda} + 1)} \right] - 273.15 \quad (4.18)$$

Where

L_{λ} – TOA spectral radiance

K₁, K₂ – Band-specific thermal conversion from metadata (K₁- Constant_Band_10, K₂- Con-stant_Band_10)

273.15 = Convert Kelvin to 00 Celsius.

Step- 3: NDVI is the Normalized Difference Vegetation Index and may be measured with the aid of the equation (Eq. (4.19))

$$NDVI = \frac{NIR - RED}{NIR + RED} \quad (4.19)$$

Step-4: Proportion of Vegetation PV is outlined as the ratio of the vertical projection region of vegetation (including leaves, root word, and subdivision) on the ground to the whole vegetation region and calculated as in Eq. (20).

$$P_V = \left[\frac{NDVI - NDVI_{Min}}{NDVI_{Max} - NDVI_{Min}} \right]^2 \quad (4.20)$$

From the above calculated NDVI, we can obtain the NDVImin and NDVImax, used further to calculate the Proportion of Vegetation (PV).

Step-5: The next step is to calculate Land Surface Emissivity (LSE). Land Surface Emissivity (LSE), as an inherent property of natural substance, is frequently used as an index of material composition and is calculated as in Eq. (4.21))

$$E = 0.004 * P_v + 0.986 \quad (4.21)$$

here, E is Emissivity

Pv is the proportion of vegetation that is premeditated using the NDVI value

Step 6: The last step is to calculate LST. By using the above-calculated values in the LST equation, we can obtain the LST of the required region. The formula to calculate LST (Eq. (4.22)) is as follows:

$$LST = \frac{B_T}{(1 + (\lambda * B_T / C_2) \ln(E))} \quad (4.22)$$

Where λ is the emitted radiance wavelength of $10.8\mu m$

$C_2 = 14388\mu mK$

E is the land surface Emissivity

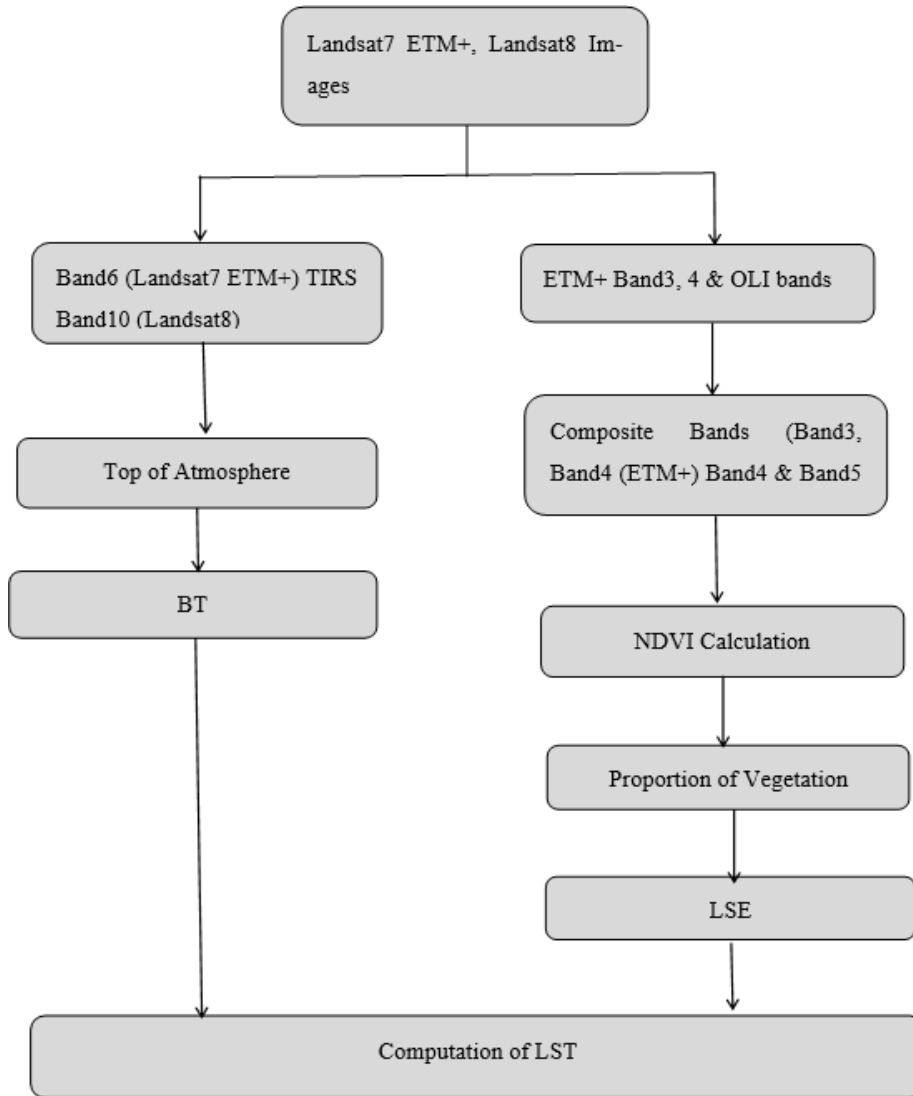


Figure 4.2: Flowchart for Computation of LST

4.2 Proposed Methodology (Deep Transfer Learning Techniques)

This research aimed to harness the power of deep transfer learning models to enhance the efficiency of LULC classification in remote sensing imagery. The proposed approach involved several vital techniques: preprocessing the UCM imaging data, constructing a transfer learning model with four consecutive layers (flattened layers, dense layers, two activation layers, and dropout layers), and assessing its performance using a confusion or error matrix.

4.2.1 Overview of the Proposed Work

The proposed work utilizes a deep transfer learning method to improve time efficiency. **Figure 4.3.** The proposed methodology involves several key stages, starting with gathering and preprocessing data, followed by the sample data stage, which comprises model training, validation, test data, and LULC change detection of the specific area of interest, culminating in the testing phase. The proposed method assessed the deep transfer learning approach using diverse labeled datasets to determine the most effective configuration. This optimal setup is then applied to predict land cover classification in a designated area. Pre-trained models, specifically ResNet50 and ResNet50+LSTM, pre-trained on relevant data, are employed in this work (Safarov et al., 2022). These models are adapted through Transfer Learning (TL) to create a novel and specialized TL model tailored to the specific problem. To enhance the learning process of the TL model using the UCM dataset, a learning rate (LR), which can take on various values, such as 0.01, 0.001, and 0.0001, was employed. However, it has been observed that using larger LR values can lead to fluctuations in training and learning processes (Shabbir et al., 2021). Therefore, a smaller LR value of 0.0001 is chosen in this study to optimize the model effectively.

Step 1: Data collection

To support the study, the proposed work selected ten Sentinel-2A bands with spatial resolutions of 10 and 20 meters. The data is acquired using the innovative Semi-Automatic Classification Plugin for QGIS (Simonyan & Zisserman, 2014).

Step 2: Atmospheric and Geometric Correction

The atmospheric correction process holds immense importance in satellite remote sensing as it eliminates the impact of Earth's atmosphere on radiance values detected by satellite sensors. Sentinel-2A, an integral component of the European Space Agency's Sentinel-2 mission, captures high-resolution optical images of Earth's surface. Correcting atmospheric effects in Sentinel-2A data is vital for a precise and insightful analysis of land and water resources (Bui et al., 2022). Various methods and tools, such as the Sen2Cor processor developed by ESA, are accessible for performing atmospheric correction, enhancing the accuracy of remote sensing data interpretation. Geometric correction, or orthorectification, is an essential step in satellite image processing that corrects abnormalities due to terrain topography and sensor characteristics, ensuring an accurate spatial representation of the Earth's surface (Green et al., 2000).

For Sentinel-2 imagery, which is acquired by the European Space Agency's (ESA) Sentinel-2 satellites, here are the general steps for geometric correction:

- Gather a series of Ground Control Points (GCPs): Identify and collect a set of reliable Ground Control Points in the image.
- Utilize GCPs to compute the coefficients of a polynomial equation: Apply the Ground Control Points to calculate the coefficients of a polynomial equation. These coefficients serve as the basis for the transformation.
- Use the equation above to change the geometric attributes of image data from its original file format to a specific map projection: Use the equation that has been derived to modify the shape of the image data so that it can be converted from its original format into a particular map projection. This technique, called 'rectification,' addresses any distortions in the input image, guaranteeing precise spatial representation.

4.2.2 Layer stacking

Layer stacking involves merging distinct bands to create a new multi-band image. These multi-band images are valuable for visualizing and classifying LULC classes. The multiple image bands must have the same extent to perform layer stacking, and layer-stacked bands should have the exact spatial resolution. For LULC extraction, the blue, green, red, and Near-Infrared (NIR) bands are combined through layer stacking, where these bands have the exact spatial resolution (10m).

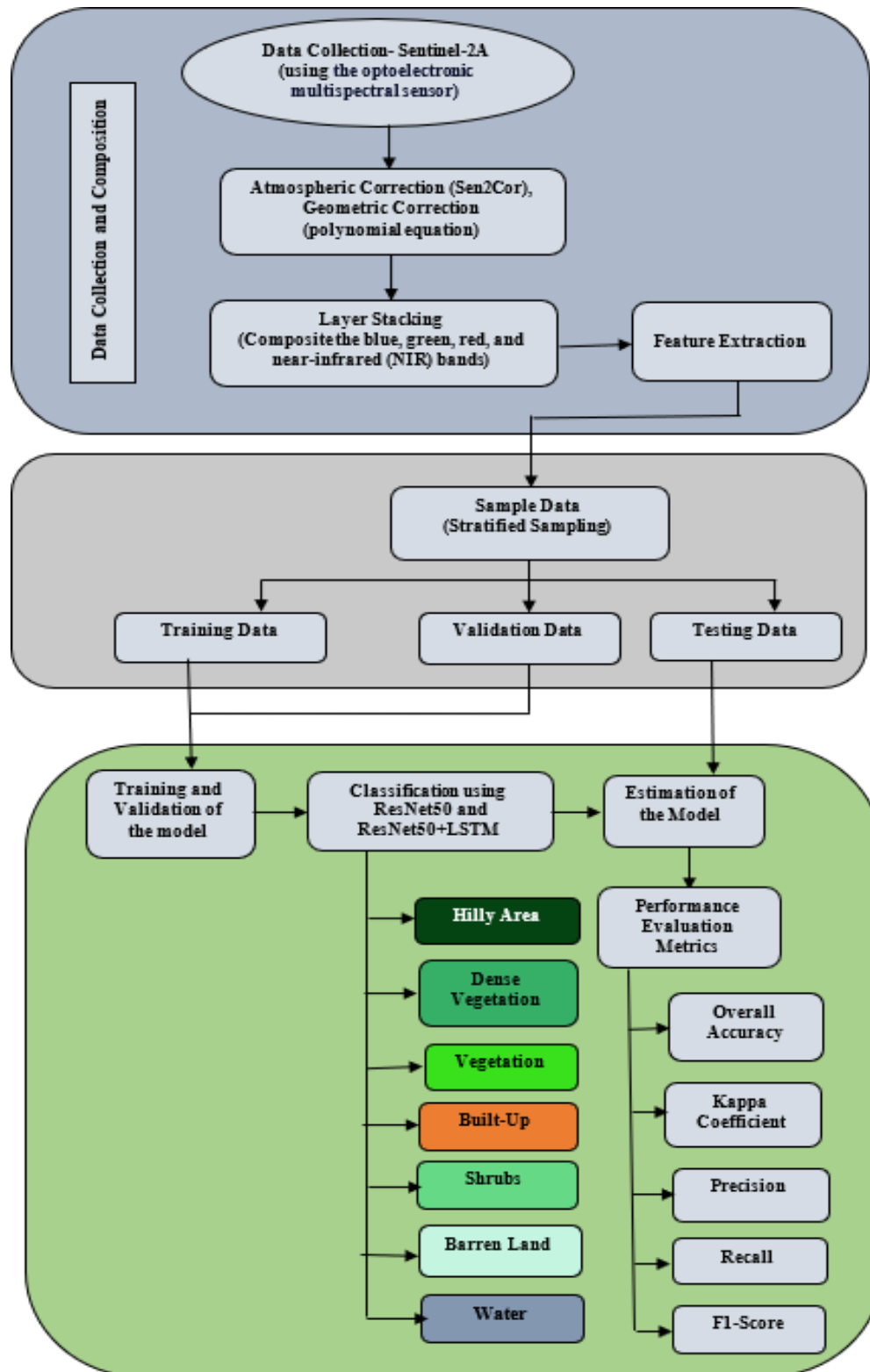


Figure 4.3: Structure of the proposed work

4.2.4 Reference data

The reference data used in this study are obtained from UCM and consisted of georeferenced polygons delineating various land cover and land use classes. These categories included water bodies, wetlands, agricultural land, urban regions (classified by intensity as high, low, or industrial), and leisure areas such as coastlines, parks, playgrounds, and shopping malls. In total, seven distinct LULC classes are defined for the analysis: (i) Hilly Area (HA), (ii) Dense vegetation (DV), (iii) Vegetation(V), (iv) Built-Up (BU), (v) Water (W), (vi) Shrubs (S), and (vii) Barren Area (BA).

4.2.5 Training, validation, and testing phases

Specific sampling methods were used in the training, validation, and testing phases. Initially, 200 reference training samples for each class are chosen randomly through stratified sampling. For validation purposes, 80 samples from each class are selected using stratified random sampling from the reference dataset, which is then used for hyperparameter optimization. Finally, using stratified sampling, the model's performance is evaluated by selecting 200 samples per class to represent the leftover reference data.

4.2.6 Training Algorithm

Deep Learning combines graph technology with data transformations to create a multi-layer framework for feature learning. This work focuses on two distinct DL architectures: ResNet50 and ResNet50+LSTM, which are more complex model structures. Residual modules are essential in improving the training process in these frameworks. They create a straight path from input to output, which solves the vanishing gradient problem experienced during the backpropagation of deep models. As an outcome, deep models can be developed and trained more efficiently without increasing computational complexity. It is important to note that there are two basic ways to train DL models: transfer learning (TL) and initial modeling, which allow the model to approach directly from the input data directly with no need to require previous knowledge. Transfer learning uses pre-trained models with weights acquired from large datasets. On the other hand, training at the initial stage starts the

model from scratch with random or zero-valued weights rather than pre-trained weights from previous models. Transfer learning prevents overfitting, especially when there is minimal training data. Starting the training process with pre-trained weights allows the model to converge in fewer epochs, which makes the learning process more efficient.

4.2.7 Land cover categorization

Table 4.2 is a visual representation of the classification system applied for the in-depth examination of land cover within the proposed work, offering a valuable reference point for understanding the study's classification methodology.

Table 4.2: Categorization system implemented for land cover mapping actions

S. No	Land Cover type
1	Hilly Area (HA)
2	Dense vegetation (DV)
3	Vegetation (V)
4	Built-Up (BU)
5	Water (W)
6	Shrubs (S)
7	Barren Area (BA)

4.2.8 Deep Learning Algorithms

In the proposed method, ResNet50 and ResNet50 integrated with LSTM are employed, with the latter emerging as a powerful solution for LCLU classification. ResNet50 excels in extracting spatial features from sources like remote sensing or satellite imagery, allowing it to identify objects and patterns accurately. Concurrently, LSTM enhances this capability by capturing the data's temporal dependencies and sequential patterns. This integrated approach provides a comprehensive understanding of spatial and temporal aspects, making it ideal for applications requiring long-term land use change monitoring, analysis of seasonal variations, and precise land cover classifications enriched with contextual information. By leveraging the strengths of ResNet50 and LSTM in cascade, researchers and practitioners can develop robust models tailored for the intricate domain of LULC classification.

a) ResNet50

ResNet50, short for Residual Network with 50 layers, is a deep convolutional neural network architecture primarily used for image classification tasks, as shown in **Figure 4.4**. It is based on residual learning, which addresses the vanishing gradient problem in intense networks (Stivaktakis et al., 2019). Instead of learning the actual underlying features of an image, ResNet50 learns residual functions, allowing it to train severe networks efficiently (Zhu et al., 2011; Nair et al., 2020). This is achieved by introducing shortcut connections (skip connections) that reflect one or more layers, enabling the gradient to flow more easily during backpropagation. The network comprises 50 layers, including convolutional layers, batch normalization, and ReLU activations, and it has been pre-trained on large image datasets like ImageNet, making it a powerful feature extractor for various computer vision tasks and a foundational architecture for transfer learning in deep learning applications as shown in Algorithm-1 (ResNet50).

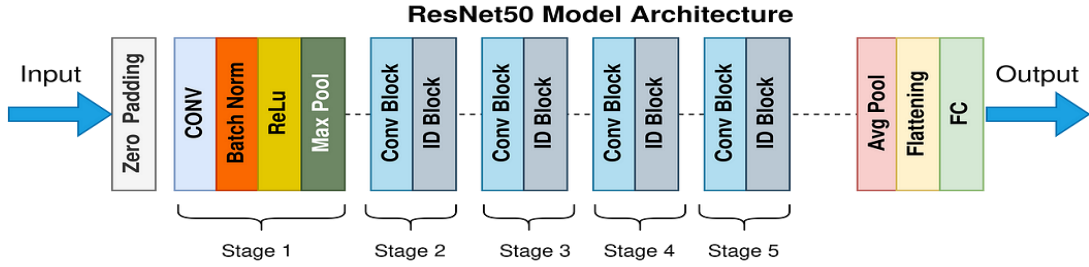


Figure 4.4: Architecture of ResNet50

ReLU and SoftMax: Applying the ReLU activation to individual features or pixels within the input image, this non-linear function aids the neural network model in capturing intricate patterns within the data (Mahdianpari et al., 2018). By implementing ReLU on each feature, the network effectively eliminates negative values, which might not be meaningful in the context of land cover, while simultaneously preserving or amplifying positive values, as shown in **Figure 4.5**. This strategic approach permits the network to prioritize pertinent information then effectively suppress any noise in the data is given in the equation (Eq. (4.23)).

$$R(z) = \max(0, z) = f(z) = \begin{cases} 0, & \text{if } z < 0 \\ z, & \text{if } z > 0 \end{cases} \quad (4.23)$$

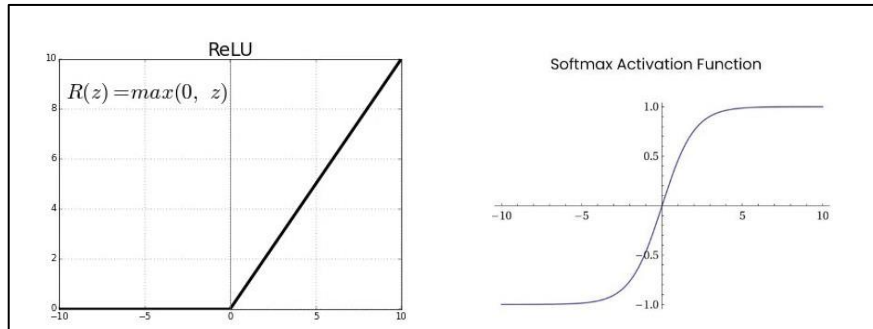


Figure 4.5: Graphical representation of (a) ReLU function and (b) softmax

Algorithm-1 (ResNet50)

1. Input:

- Let X represent the input tensor with dimensions (H, W, C) , where H is the height, W is the width, and C is the number of channels (e.g., RGB images have $C=3$).

2. Residual Block:

- A residual block is the core building block of ResNet-50. It includes two main paths:
 - The identity path (input X) and
 - The shortcut path contains convolutional layers.
- A residual block's output can be mathematically represented as $\text{Output} = F(X) + X$.

Here:

- $F(X)$ represents the transformation applied within the residual block (convolutional layers).
- X represents the input to the block.

3. Convolutional Layers:

- Each residual block contains convolutional layers, and these layers apply a series of filters to the input X .

4. Shortcut Connection:

- The shortcut connection, represented by X , bypasses the convolutional layers and provides a direct path from the original input to the output. This is the essence of the "residual" concept.

5. Fully Connected Layers:

- After several convolutional layers and residual blocks, ResNet-50 typically concludes with fully connected layers for final classification.

Applying the Softmax function to the logits accomplishes the transformation of these scores into class probabilities. This function, by exponentiating each logit and subsequently normalizing the results through division by the sum of all exponentiated logits, guarantees the outcome takes the form of a comprehensive probability distribution spanning all conceivable land cover or land use classes. The resulting probabilities for each class can be interpreted as predictions by applying the Softmax function to the model's output. Typically, the class most likely to be selected as the predicted class label is given in the equation (Eq. (4.24)).

$$S(Z_j) = \frac{e^{z_j}}{\sum_{k=1}^k Z_k} \text{ for } j = 1, \dots, k \quad (4.24)$$

b) LSTM

Within the realm of land use and land cover analysis, the (LSTM) algorithm functions as a dynamic processor of sequential or time-series data, such as satellite imagery or sensor observations, with the primary aim of capturing enduring dependencies and intricate patterns as shown in **Figure 4.6**. It accomplishes this by meticulously managing hidden state and cell state variables that evolve with each temporal progression (Yang et al., 2010, Stateczny et al., 2022).

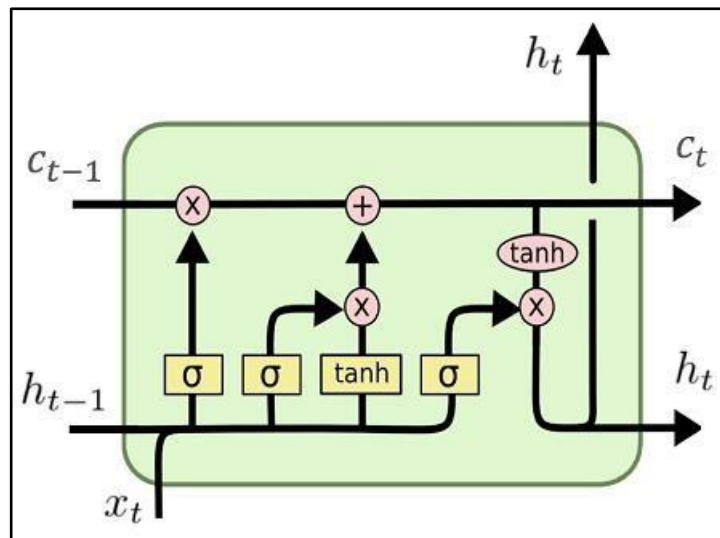


Figure 4.6: LSTM Internal Architecture

At each step along the timeline, the LSTM leverages a set of gating mechanisms; it employs a forget gate to discern what historical information merits preservation and what ought to be discarded, employs an input gate to assess and assimilate fresh data, and engages an output gate to judiciously update the hidden state with pertinent information as described in equation (Eq. (4.25)-Eq. (4.30)). These intricacies collectively empower the LSTM to adeptly model and scrutinize the dynamic landscape of land use and land cover, endowing it with remarkable utility in endeavors such as identifying land cover alterations and forecasting land use trends.

$$i_t = \sigma(\theta_{xi}x_t + \theta_{hi}h_{t-1} + b_i) \quad (4.25)$$

$$f_t = \sigma(x_{tf} + \theta_{hf}h_{t-1} + b_f) \quad (4.26)$$

$$o_t = \sigma(\theta_{xo}x_t + \theta_{ho}h_{t-1} + b_o) \quad (4.27)$$

$$g_t = \tanh(\theta_{xg}x_t + \theta_{hg}h_{t-1} + b_g) \quad (4.28)$$

$$c_t = f_t \cdot c_{t-1} + i_t \cdot g_t \quad (4.29)$$

$$h_t = o_t \cdot \tanh(c_t) \quad (4.30)$$

The previous time step's output is denoted by h_{t-1} in the given equations. The current cell input is represented by x_t , and h_t is the output. The subscript 't' indicates the current step number. The output vectors of the input gate, forget gate, output gate, and cell are represented by i , f , o , and g , respectively. The weights are represented by the symbol θ , such as θ_{xi} representing the weight between the input vector x_t and the input gate vector i_t , and θ_{hi} representing the weight between the output vector h_{t-1} and the gate vector i_t , and so on. Biases are represented by 'b'. Additionally, c_t and c_{t-1} denote the cell outputs at the current and previous steps. The symbol σ represents the sigmoid function σ . In LSTM, the activation functions are typically limited to \tanh for g_t and h_t and sigmoid for i_t , f_t , and o_t . Combining ResNet-50, a powerful CNN architecture, with LSTM, a specialized Recurrent Neural Network (RNN) architecture, can create a hybrid model capable of handling spatial features extracted by ResNet-50 and sequential

patterns captured by LSTM. This combination is beneficial in tasks involving image and sequential data, such as video analysis, action recognition, and video captioning. This combination leverages the strengths of ResNet-50 and LSTM: ResNet-50's ability to extract detailed spatial features from images and LSTM's capability to capture long-term dependencies in sequences. By merging these architectures, the model can effectively tackle complex tasks that involve understanding the data's visual and sequential aspects.

4.2.9 Experimental Dataset Setting

In the dataset preparation, the UCM dataset, initially compiled by Yang and Newsam in 2010 from the USGS National Map Urban Area Imagery, served as the foundation for the LULC classification task, as depicted in **Figure 4.7**. This dataset featured 100 images for each of the 21 distinct land use and land cover classes, all with dimensions of 256X256 pixels and an approximate spatial resolution of 30 cm per pixel. A 60:20:20 ratio is utilized for instruction and verification, and testing demonstrations across individual classes to facilitate the training and assessment phases. Hence, specific hyperparameters of the experimental setup are precisely fine-tuned, as outlined in **Table 4.3**. In addition, a dropout layer is incorporated with a rate of 0.5 to counter overfitting, and the early stopping technique is effectively applied to avoid overfitting by halting the training procedure based on validation performance.

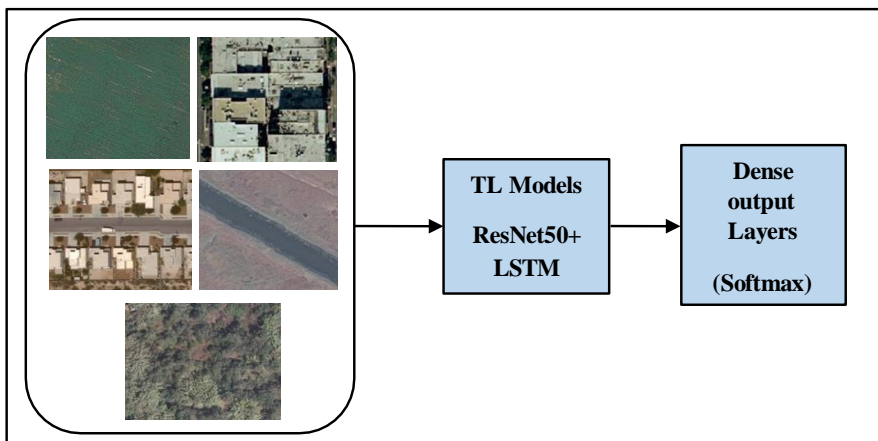


Figure 4.7: Sample input images fed into preprocessing

Table 4.3: Hyperparameter settings for training data

Hyperparameter	Parameter values used
Optimizer	Adam
Activation functions	ReLu and Softmax
Loss function	categorical cross entropy
Batch-size	64
Epochs	10
Learning rate	0.0001

4.2.10 Performance Evaluation Measurements

Labeling activities are conducted using the LC Map generated during the training phase. The LC map is reorganized to align with the classes specified in **Table 2**. Initially, a fundamental ResNet50 model is employed to gauge its performance. The model created in this study had an input layer, convolutional and pooling layers, and an output layer, as per Raschka et al. (2020). During the training process, the model was built with the Adam optimizer (Kinga et al., 2015), which iteratively adjusts network weights based on training data. Unlike the traditional stochastic gradient descent approach (Zhang et al., 2020), this optimizer was employed throughout the process of training examples. The learning rate was set at 0.0001. The model output generated a vector with an entry for each class. It also employed the softmax activation function to normalize the result, producing a probability distribution. For network loss, the weighted cross-entropy process has been opted for.

Furthermore, batch normalization is implemented to enhance model accuracy, reduce training time, and combat overfitting. ResNet50+LSTM outperforms ResNet50 in land cover and land use classification tasks by leveraging LSTM's capabilities to capture temporal dependencies, handle long-term patterns, improve accuracy, handle variable sequences, reduce overfitting, enhance contextual understanding, and provide superior decision support. Subsequently, the ResNet50+LSTM model is applied to assess its effectiveness in comparison. To estimate the accuracy of the land cover map in the Vijayawada municipality, a validation process is conducted through photointerpretation of selected sample points. A quantitative assessment is carried out to determine the

Overall Accuracy (OA). The F1-score is calculated to assess the classification model's precision and recall, considering its ability to accurately identify relevant classes (precision) and capture all instances of those appropriate classes (memory) and the Kappa coefficient, which is a statistical model that is used to evaluate the level of agreement between the two rasters (such as the classified and original given samples) as shown in the equation (Eq. (4.31)-Eq. (4.35)).

$$OverallAccuracy = \frac{Numberofcorrectpredictions}{Totalnumberofpredictions} = \frac{TP + TN}{TP + TN + FP + FN} \quad (4.31)$$

$$Precision = \frac{Numberofpositivepredicts}{Totalnumberofpositivepredicts} = \frac{TP}{TP + FP} \quad (4.32)$$

$$Recall = \frac{Correctactualpredictions}{Totalnumberofactualpositives} = \frac{TP}{TP + FN} \quad (4.33)$$

$$F1 - Score = \frac{2(Precision * Recall)}{Precision + Recall} = \frac{2 * TP}{2TP + FP + FN} \quad (4.34)$$

$$Kappa Coefficient = \frac{Total Accuracy - Random Accuracy}{1 - Random Accuracy} \quad (4.35)$$

Summary

Land Use and Land Cover (LULC) change detection refers to the process of identifying and analyzing changes in land cover (e.g., vegetation, water bodies, urban areas) over time using remote sensing data, such as satellite imagery. Advanced machine learning and deep learning techniques are increasingly being used to automate and improve the accuracy of LULC change detection.

CHAPTER-V

RESULTS AND DISCUSSION

Key points:

- Assessment of Field of Interest
 - Assessing the performance of various classification algorithms.
 - Executing suggested deep Transfer learning-driven change detection (DTLCD) algorithms.
 - Contrasting proposed DTLCD with established change detection methods.
 - Illustrating the utilization of DTLCD in agricultural land cover classification.
-

This chapter undertakes the estimation and validation of vegetation change analysis in the Area of Interest of Andhra Pradesh state India, utilizing both traditional and deep learning algorithms applied to the Sentinel-2 dataset. Within the study area, prominent land classes include Dense Vegetation, Vegetation, Water, Built-up Area, Barren Area, shrubs, and Hilly Area. Previously, agricultural land classification relied on door-to-door surveys, but this study proposes leveraging remote sensing datasets for vegetation change analysis. Hence, the objectives encompass (a) the application of conventional and Deep Transfer Learning for Change Detection (DTLCD) methods to extract diverse spectral and spatial features, (b) the evaluation of each classified map and change map through reference datasets and on-site observations, and (c) the comparison of the performance of conventional and DTLCD approaches with existing change detection methodologies.

5.1 LULC Analysis

LULC of the survey region is classified as built-up (settlements, business enterprises, and some other substructure), Dense vegetation (forests), Vegetation (agriculture, and woody plants), water bodies, barren, open land, and rocks. **Figure 5.1 to Figure 5.3** represents the classified images of the three regions of 2000, 2005, 2010, 2015, and 2020. LULC consequences of the survey region are represented in

Table 5.1, Table 5.2, and Table 5.3. The Error matrix encapsulates that the built-up area has magnified from 2950.24 hectares in 2000 to 9503.3 hectares in 2020 (3259.73 Ha in 2005, 4288.4 Ha in 2010, and 6122.5 Ha in 2015). The total built-up area increased throughout the study period, exhibiting an exponent increase. Dense vegetation decreased from 25517.5 ha in 2000 to 13950.27 ha in 2020. Vegetation showed an increasing trend from 5908.07 Ha in 2000 to 11898.7 Ha in 2020. The transition matrix summarizes that the dense vegetation, vegetation, and built-up area have magnified to 1.8%, 7.79%, and 8.54% from 2000 to 2020, and water and barren land decreased by - 5.56% and -12.2% in the Tirupati region. The Dense vegetation, Vegetation, and built- up area have magnified to 0.8%, 0.08%, and 32.51% from 2000 to 2020, and water, Barren land decreased by -23.42% and -9.98% in the Visakhapatnam region and the Vegetation, water and built-up area has increased to 16.04%, 1.8% and 17.55% from 2000 to 2020 and Dense vegetation, water, Barren land de-creased by -30.98, -4.5% in Vijayawada region.

Table 5.1: LULC consequences (Tirupati)

LULC Category	Area (Hectares)										Change in Area (Hectares)	Change in Area (%)
	Year (2000)	Area (%)	Year (2005)	Area (%)	Year (2010)	Area (%)	Year (2015)	Area (%)	Year (2020)	Area (%)		
Dense vegetation	5857.62	16.54	5482.53	15.49	5828.29	16.47	6467.46	18.27	6490.25	18.34	632.63	1.80
Vegetation	9268.07	26.18	9419.84	26.61	10300.05	29.10	11090.49	31.33	12023.85	33.97	2755.78	7.79
Urban	11074.08	31.28	11637.09	32.88	11981.78	33.85	12129.59	34.27	14094.56	39.82	3020.48	8.54
Barren Land	6629.97	18.73	6491.48	18.34	5380.86	15.20	4206.45	11.88	2205.70	6.23	-4424.27	-12.50
Water	2564.62	7.2	2363.42	6.68	1903.38	5.38	1500.38	4.24	579.99	1.64	-1984.63	-5.56
Total	35394.38		35394.38		35394.38		35394.38		35394.38			

Table 5.2: LULC consequences (Visakhapatnam)

LULC Category	Area (Hectares)										Change in Area (Hectares)	Change in Area (%)
	Year (2000)	Area (%)	Year (2005)	Area (%)	Year (2010)	Area (%)	Year (2015)	Area (%)	Year (2020)	Area (%)		
Dense vegetation	688.04	2.88	630.83	2.64	973.39	4.07	925.48	3.87	880.28	3.68	192.24	0.80
Vegetation	5018.57	20.99	4910.27	20.53	4750.29	19.86	4040.93	16.90	5037.82	21.07	19.25	0.08
Urban	8425.71	35.23	11501.08	48.09	12997.44	54.35	14221.88	59.47	16200.84	67.75	7775.67	32.51
Barren Land	2888.00	12.08	2240.47	9.37	2198.72	9.19	2140.62	8.95	501.67	2.10	-2386.33	-9.98
Water	6893.29	28.83	4630.96	19.37	2993.76	12.52	2584.70	10.81	1292.99	5.41	-5600.27	-23.42
Total	23913.62		23913.62		23913.62		23913.62		23913.62			

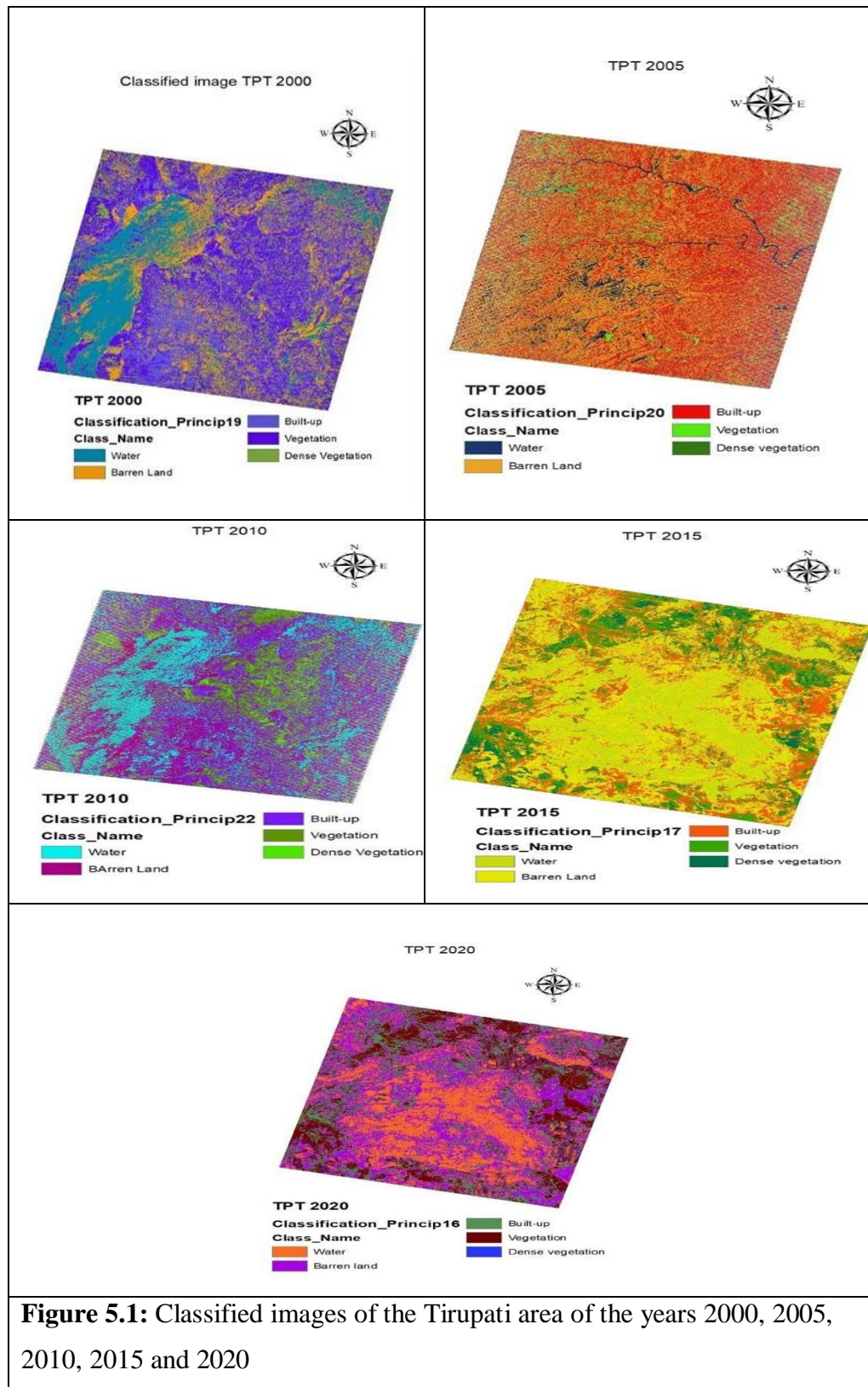
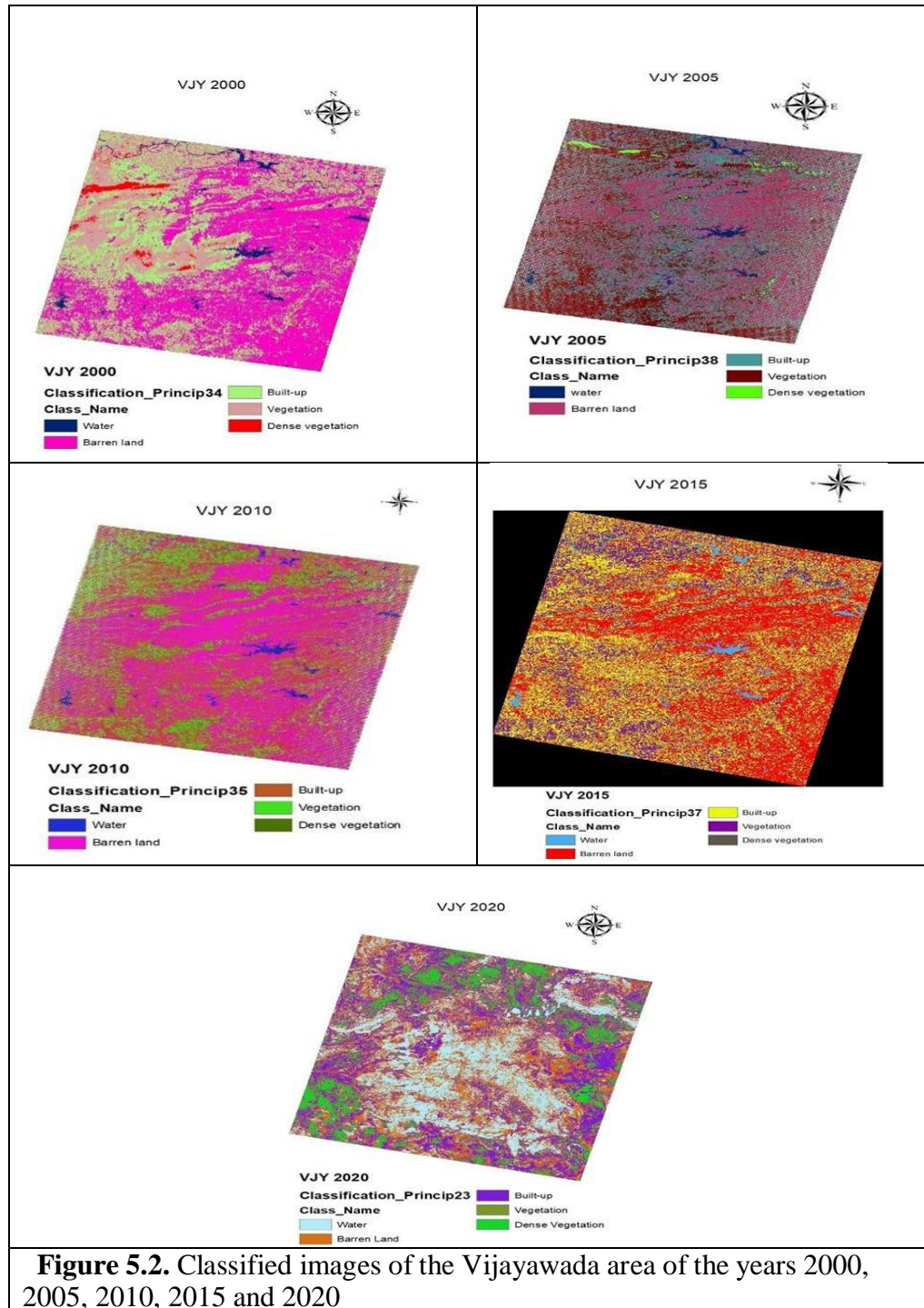


Figure 5.1: Classified images of the Tirupati area of the years 2000, 2005, 2010, 2015 and 2020



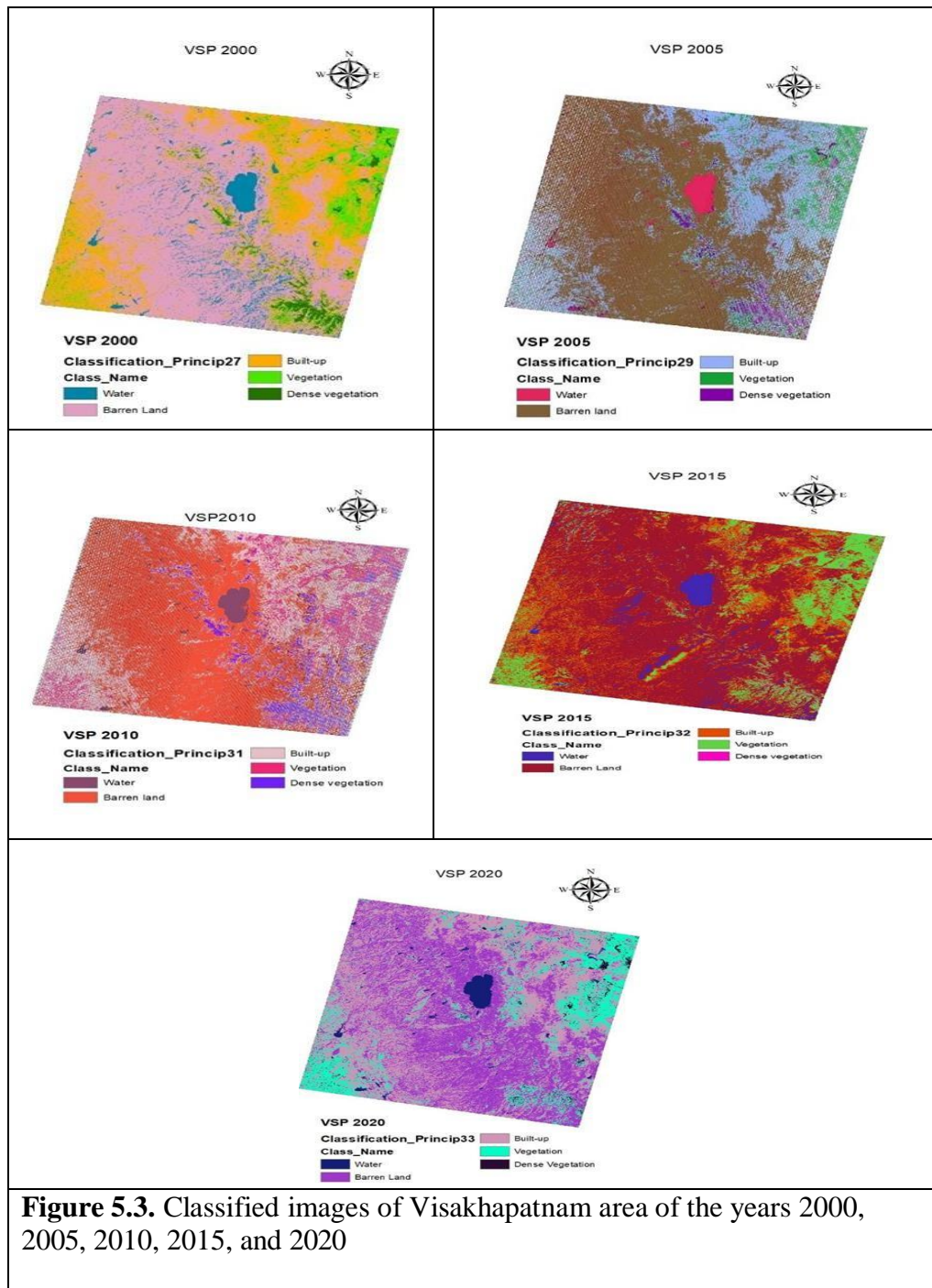


Figure 5.3. Classified images of Visakhapatnam area of the years 2000, 2005, 2010, 2015, and 2020

Table 5.3: LULC consequences (Vijayawada)

LULC Category	Area (Hectares)										Change in Area (Hectares)	change in Area (%)
	Year (2000)	Area (%)	Year (2005)	Area (%)	Year (2010)	Area (%)	Year (2015)	Area (%)	Year (2020)	Area (%)		
Dense vegetation	25517.5	68.34	22889	61.30	21013.5	56.28	18801.5	50.35	13950.27	37.36	-11567.23	-30.98
Vegetation	5908.07	15.82	8350.53	22.36	9136.9	24.47	10045.1	26.90	11898.7	31.87	5990.63	16.04
Urban	2950.24	7.90	3259.73	8.73	4288.4	11.48	6122.5	16.40	9503.3	25.45	6553.06	17.55
Barren Land	2754.47	7.38	2332.37	6.25	2123.17	5.69	1515.27	4.06	1075.1	2.88	-1679.37	-4.50
Water	209.09	0.56	507.74	1.36	777.4	2.08	855	2.29	912	2.44	702.91	1.88
Total	37339.37		37339.37		37339.37		37339.37		37339.37			

The error matrix or transition matrix generated is employed to assess remote sensing images. The diagonal elements of the matrix correspond to the correctly classified elements, upon which the classification accuracy depends. The error matrix or transition matrix demonstrates several errors in the classification procedure, allowing reinforced evaluation of maps and increased accuracy assessment. Kappa quality appraisal is accomplished to show the divergence between the existent statement and the declaration anticipated via way of means of risk and is a vital empirical approach in reading remote sensing quantifiable data, the sample of an error matrix is represented in **Table.5.4**. Ground truth allows image data to be accompanied by real features and materials on the ground. In the case of a classified image, it allows supervised classification to assist in measuring the level of accuracy of the grouping generated by the remote sensing program and thus decrease problems in the classification, encompassing commission and omission errors. Here in this study, field visits to the study areas were undertaken during which some ground truths were collected especially for undeveloped areas and the physical objects of classes were recorded by GPS. According to these two sources i.e. field visits and GPS, different ground truths of land cover classification were recorded manually. A good rule of thumb is to gather at least fifty samples of each type of land cover. category. If the area is peculiarly large or the classification system incorporates more categories then the minimum number of samples should be 75 to 100 per class. Based on the rule of thumb 90 to 150 samples are considered for each land- cover category of Area of Interest (AoI).

The OA and KC of the three regions for the years 2000, 2005,2010, 2015, and 2020 are represented in **Table 5.5**. Based on the transition matrix, the

overall classification quality of the Vijayawada region was ascertained as 96.4%, 94.5%, 93%, 91%, and 88%, with their individual KC as 0.95, 0.93, 0.91, 0.89, and 0.87 approximately for the years 2020, 2015, 2010, 2005 and 2000 respectively. The estimated Kappa Coefficient shows the excellent and time-tested output from the classifier for all the years. Based on the Error matrix the OA of Visakhapatnam region was ascertained as 97%, 94.5%, 93%, 92.5%, and 89.3% with their individual KC as 0.96, 0.92, 0.91, 0.9, and 0.87 approximately for the years 2020, 2015, 2010, 2005 and 2000 respectively. Overall Accuracy represents what equipose of the web sites is mapped rightly. due to Error matrix generated an Overall classification Accuracy of Tirupati region was ascertained as 96.8%, 94.5%, 92.5%, 91%, and 90.4% with their individual Kappa Coefficients as 0.96, 0.92, 0.91, 0.9, and 0.89 approximately for the years 2020, 2015, 2010, 2005 and 2000. Maximum urban development occurred between 2000 to 2020 and LULC changes are graphically represented in **Figure 5.4**. This improvement within the built-up area is assigned to the brand-new industrial business enterprise and academic governance in and across the towns with a lack of flora and a few different classes.

Table 5.4: Transition matrix of Vijayawada for the period 2020

	Class ID	Reference Data										
		1	2	3	4	5	Ground truth points	User's Accuracy (%)	Error of Commission	Specificity	F-score (%)	False Positive Rate
Classified Data	1	98	3	2	0	0	103	95.1	4.8	0.98	95.5	0.02
	2	4	96	2	0	0	102	94.1	5.8	0.98	94.1	0.02
	3	0	3	90	0	0	93	96.7	3.2	0.98	94.6	0.02
	4	0	0	3	91	0	94	96.8	3.1	1	98.3	0
	5	0	0	0	0	89	89	100	0	1	100	0
Ground truth points		102	102	97	91	89	481					
Producer's Accuracy (%)		96	94.1	92.7	100	100						
Error of Omission		3.9	5.8	7.2	0	0						
1- Dense Vegetation, 2- Vegetation, 3- Built-Up, 4- Barren Land, 5- Water												
Overall Accuracy = 96.4%; Kappa Coefficient = 0.95												

Table 5.5: Overall Accuracy and Kappa Coefficient for the period 2000, 2005, 2010, 2015, and 2020 of Region of Interest

Region of Interest	2000		2005		2010		2015		2020	
	Overall Accuracy (%)	Kappa Coefficient	Overall Accuracy (%)	Kappa Coefficient	Overall Accuracy (%)	Kappa Coefficient	Overall Accuracy (%)	Kappa Coefficient	Overall Accuracy (%)	Kappa Coefficient
Vijayawada (VJY)	88	0.86	91.5	0.89	93	0.91	94.5	0.93	96.4	0.95
Visakhapatnam (VSP)	89.3	0.87	92.5	0.9	93	0.91	94.5	0.92	97	0.96
Tirupati (TPT)	90.4	0.89	91	0.9	92.5	0.91	94.5	0.92	96.8	0.96

The Producer's Accuracy tells how real attributes are efficaciously proven on labeled maps based on the mapmaker's viewpoint (the producer). The User's Accuracy tells how beauty on the map may be reached on the ground based on the user's path; this is based on the dependability of the map. The Producer's Accuracy for each category was more than 80%. The User's Accuracy for five categories was more than 85%. Errors generated (Error of Commission, Omission) are less than 20%. False Positive Rate is a measure of how many results get predicted as positive out of all the negative cases. F-Score is a way to measure classification accuracy based on recall and precision. The higher the F-score, the more accurate the classification is. F-Score obtained for five categories was more than 80% which represents significant classification. Specificity is the ability of a test to correctly identify classes. The User's Accuracy, Producer's Accuracy, Error of Commission, Error of Omission, Specificity, F-Score, and False Positive Rate are represented from **Table 5.6 to Table 5.12**.

Table 5.6: User's Accuracy (%) for the period 2000, 2005, 2010, 2015, and 2020 of Region of Interest

Type of Land Cover	2000			2005			2010			2015			2020		
	VJY	VSP	TPT	VJY	VSP	TPT	VJY	VSP	TPT	VJY	VSP	TPT	VJY	VSP	TPT
1	87.5	86.8	89.1	91.8	91.2	90	92.5	92.5	91.2	93.8	93.8	93.8	95.1	97.6	99
2	89.4	88.6	89.4	92.7	89.6	93.8	91	91	89.6	94.4	93	93	94.1	96.4	95.2
3	85.3	88.7	88.7	88.8	92	90.9	92	92	92	91.6	94.8	94.8	96.7	98.8	97
4	87.5	91.6	91.6	92.7	95.8	90.7	95.8	95.8	95.8	96.2	94.8	94.8	96.8	96.4	97
5	91.8	91	93.4	91.3	93.9	91.3	94	94	93.9	97	95.9	95.9	100	97.6	97.8
1-Dense Vegetation; 2- Vegetation; 3-Built-up; 4-Barren Land; 5- Water															

Table 5.7: Producer's Accuracy (%) for the period 2000, 2005, 2010, 2015, and 2020 of Region of Interest

Type of Land Cover	2000			2005			2010			2015			2020		
	VJY	VSP	TPT	VJY	VSP	TPT	VJY	VSP	TPT	VJY	VSP	TPT	VJY	VSP	TPT
1	92.5	92.7	92.7	96.7	93.1	96.7	93.1	93.1	93.1	95.8	97.8	97.8	96	97.6	98
2	80.8	83.3	83.3	85.7	88.4	87.6	88.5	88.5	88.4	89.4	93.9	93.9	94.1	97.6	97
3	82.6	85.9	85.9	88	90.1	85.7	92.6	92.6	90.1	94.9	88.5	88.5	92.7	97.6	95
4	92.9	93.2	93.2	90.8	91.5	90.7	91.5	91.5	91.5	93.5	94.8	94.8	100	96.4	98
5	94.1	98.2	98.2	97.7	100	97.7	100	100	100	100	98	98	100	97.6	96
1-Dense Vegetation; 2- Vegetation; 3-Built-up; 4-Barren Land; 5- Water															

Table 5.8: Error of Commission for the period 2000, 2005, 2010, 2015, and 2020 of Region of Interest

Type of Land Cover	2000			2005			2010			2015			2020		
	VJY	VSP	TPT	VJY	VSP	TPT	VJY	VSP	TPT	VJY	VSP	TPT	VJY	VSP	TPT
1	12.5	13.1	10.85	8.1	8.7	10	7.4	7.4	8.7	6.1	6.1	6.1	4.8	2.3	1
2	10.5	11.3	10.56	7.2	10.3	6.1	8.9	8.9	10.3	5.5	7	7	5.8	3.5	6.5
3	14.6	11.2	11.29	11.1	8	9	8	8	8	8.3	5.1	5.1	3.2	1.1	3
4	12.5	8.3	8.33	7.2	4.1	9.2	4.1	4.1	4.1	3.7	5.1	5.1	3.1	3.5	3
5	8.13	8.9	6.5	8.6	6	8.6	6	6	6	3	4	4	0	2.3	2.1
1-Dense Vegetation; 2- Vegetation; 3-Built-up; 4-Barren Land; 5- Water															

Table 5.9: Error of Omission for the period 2000, 2005, 2010, 2015, and 2020 of Region of Interest

Type of Land Cover	2000			2005			2010			2015			2020		
	VJY	VSP	TPT	VJY	VSP	TPT	VJY	VSP	TPT	VJY	VSP	TPT	VJY	VSP	TPT
1	7.4	7.2	7.2	3.2	6.8	3.2	6.8	6.8	6.8	4.1	2.1	2.1	3.9	2.3	2
2	19.1	16.6	16.6	14.2	11.5	12.3	11.4	11.4	11.5	4.6	6.1	6.1	5.8	2.3	3
3	17.3	14	14	12	9.8	14.2	7.3	7.3	9.8	5.1	11.4	11.4	7.2	2.3	5
4	7.0	6.7	6.7	9.1	8.4	9.2	8.4	8.4	8.4	6.4	5.1	5.1	0	1.1	2
5	5.8	1.7	1.7	2.2	0	2.2	0	0	0	0	2	2	0	2.3	4
1-Dense Vegetation; 2- Vegetation; 3-Built-up; 4-Barren Land; 5- Water															

Table 5.10: Specificity for the period 2000, 2005, 2010, 2015, and 2020 of Region of Interest

Type of Land Cover	2000			2005			2010			2015			2020		
	VJY	VSP	TPT	VJY	VSP	TPT	VJY	VSP	TPT	VJY	VSP	TPT	VJY	VSP	TPT
1	0.97	0.98	0.98	0.99	0.98	0.97	0.98	0.98	0.98	0.98	0.99	0.99	0.98	0.99	1
2	0.94	0.95	0.95	0.95	0.97	0.98	0.97	0.97	0.97	0.97	0.98	0.98	0.98	0.99	1
3	0.95	0.94	0.96	0.96	0.97	0.97	0.98	0.98	0.97	0.98	0.97	0.97	0.98	0.99	0.98
4	0.98	0.98	0.98	0.97	0.97	0.97	0.97	0.97	0.97	0.98	0.98	0.98	1	0.99	0.98
5	0.98	0.99	0.99	0.99	1	0.98	1	1	1	1	0.99	0.99	1	0.99	0.99
1-Dense Vegetation; 2- Vegetation; 3-Built-up; 4-Barren Land; 5- Water															

Table 5.11: F-Score (%) for the period 2000, 2005, 2010, 2015, and 2020 of Region of Interest

Type of Land Cover	2000			2005			2010			2015			2020		
	VJY	VSP	TPT	VJY	VSP	TPT	VJY	VSP	TPT	VJY	VSP	TPT	VJY	VSP	TPT
1	89.9	90.8	90.8	94.1	92.1	93.2	92.7	92.7	92.1	94.7	95.7	95.7	95.5	97.6	98.4
2	84.8	86.2	86.2	89.1	88.9	90.5	89.7	89.7	88.9	91.8	93.4	93.4	94.1	97	95.8
3	83.9	87.2	87.2	88.39	91.0	88.2	92.2	92.2	91.0	93.2	91.5	91.5	94.6	97.6	96
4	90.1	92.4	92.4	91.7	93.6	90.7	93.6	93.6	93.6	94.8	94.8	94.8	98.3	96.5	97.4
5	92.3	95.7	95.7	94.3	96.8	94.3	96.9	96.9	96.8	98.4	96.9	96.9	100	97.6	96.8
1-Dense Vegetation; 2- Vegetation; 3-Built-up; 4-Barren Land; 5- Water															

Table 5.12: False Positive Rate for the period 2000, 2005, 2010, 2015, and 2020 of Region of Interest

Type of Land Cover	2000			2005			2010			2015			2020		
	VJY	VSP	TPT	VJY	VSP	TPT	VJY	VSP	TPT	VJY	VSP	TPT	VJY	VSP	TPT
1	0.03	0.02	0.02	0.01	0.02	0.03	0.02	0.02	0.02	0.02	0.01	0.01	0.02	0.01	0
2	0.06	0.05	0.05	0.05	0.03	0.02	0.03	0.03	0.03	0.03	0.02	0.02	0.02	0.01	0
3	0.05	0.06	0.04	0.04	0.03	0.03	0.02	0.02	0.03	0.02	0.03	0.03	0.02	0.01	0.02
4	0.02	0.02	0.02	0.03	0.03	0.03	0.03	0.03	0.03	0.02	0.02	0.02	0	0.01	0.02
5	0.02	0.01	0.01	0.01	0	0.02	0	0	0	0	0.01	0.01	0	0.01	0.01
1-Dense Vegetation; 2- Vegetation; 3-Built-up; 4-Barren Land; 5- Water															

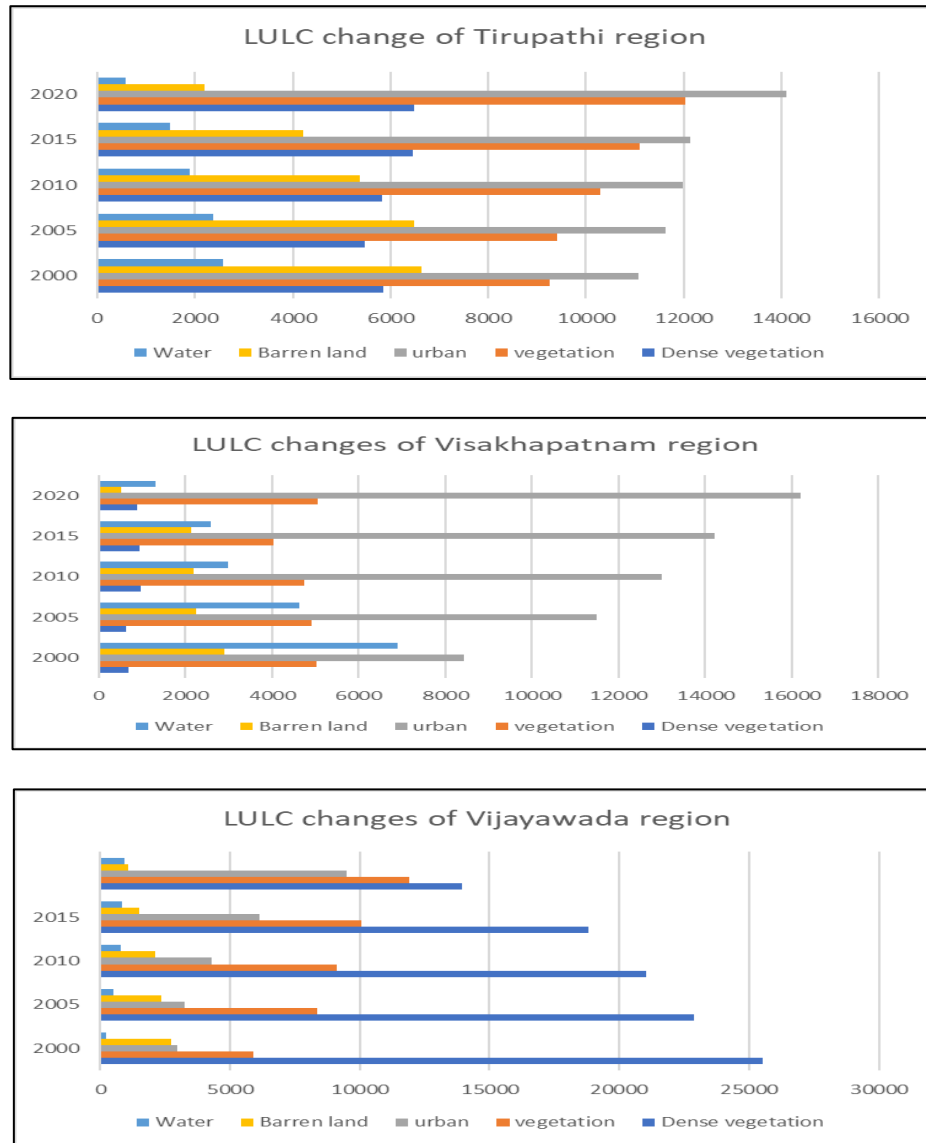
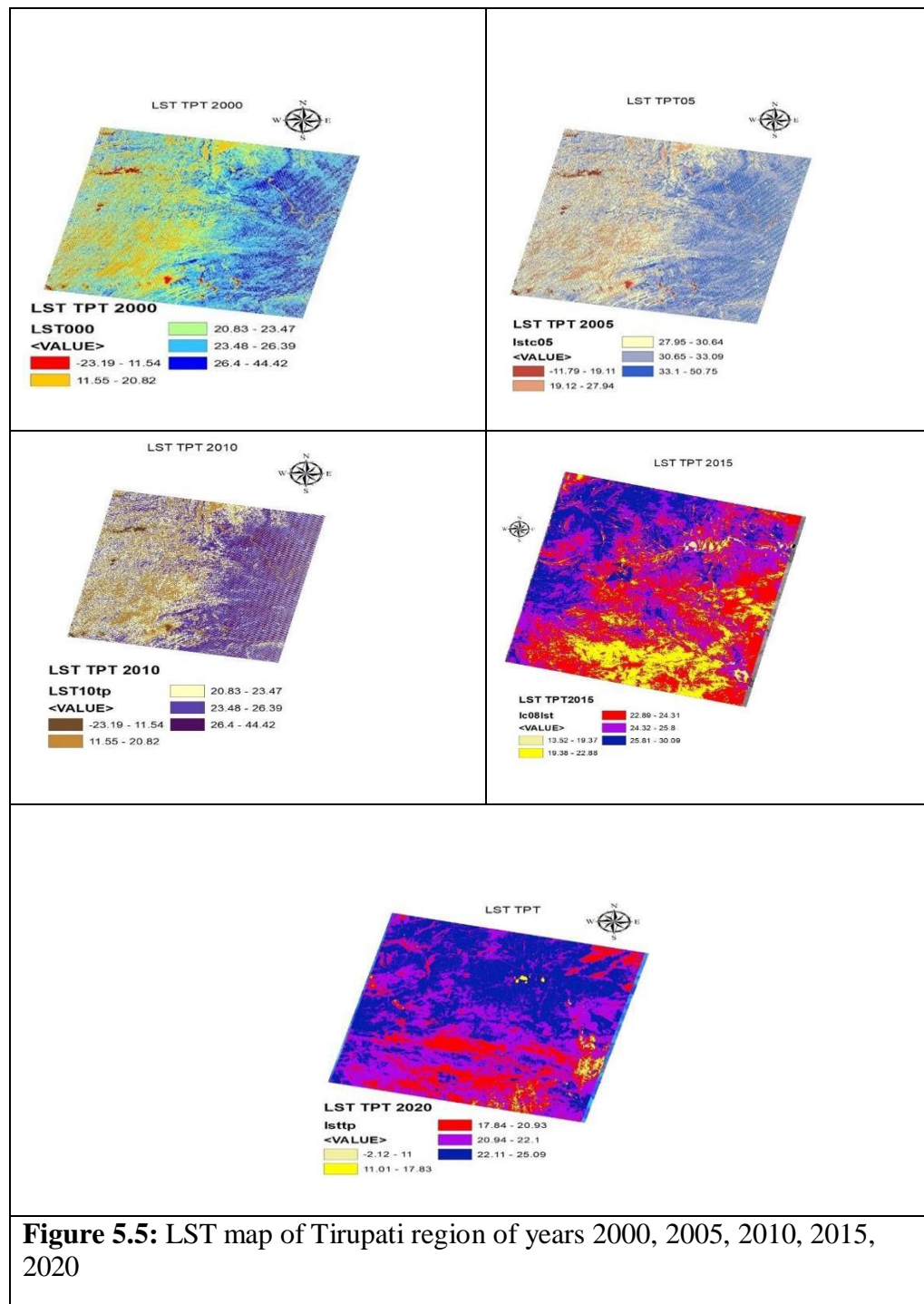


Figure 5.4: Graphical representation of LULC changes in Tirupati, Visakhapatnam, and Vijayawada regions

5.1.2. LST ANALYSIS

Land Surface Temperature was obtained by exploiting Remote Sensing and GIS methods. Each pixel within the side of the image denotes the surface temperature of each object that can be set by many land cover forms. Using Mono Window algorithm processing steps, LST maps are created independently for LANDSAT ETM+, LANDSAT 8 information for 2000, 2005, 2010, 2015, and 2020 of 3 areas are proven in **Figure 5.5**, **Figure 5.6**, and **Figure 5.7** respectively. The maps confirmed that diverse land

cover kinds have numerous temperature values owed to versions within side the physical traits of the land included with the aid of using the diverse constituents. LST obtained over distinctive classes in Tirupati, Visakhapatnam, and Vijayawada areas is provided in **Table 5.13** and a graphical illustration of obtained LST is represented in **Figure 5.8**.



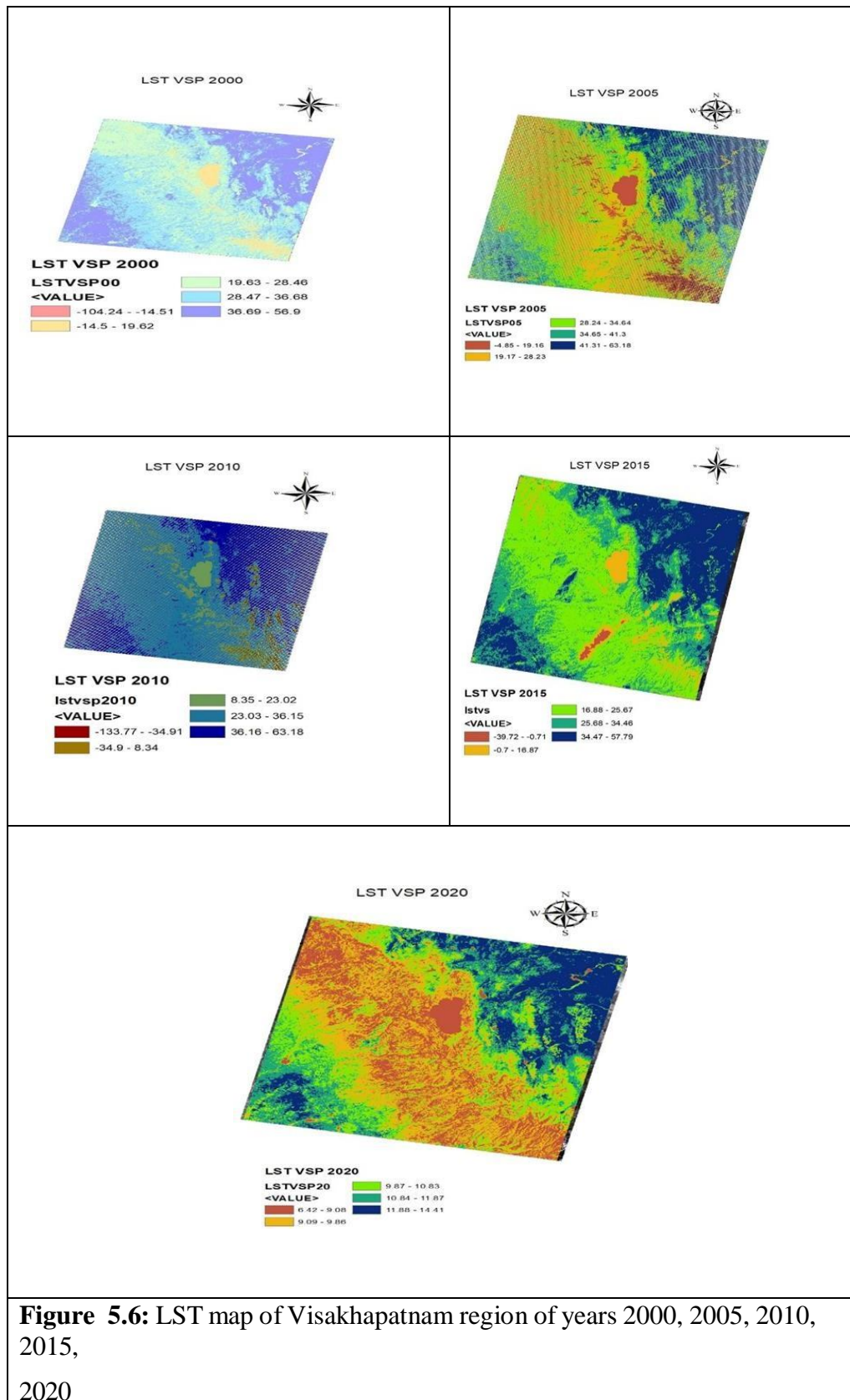
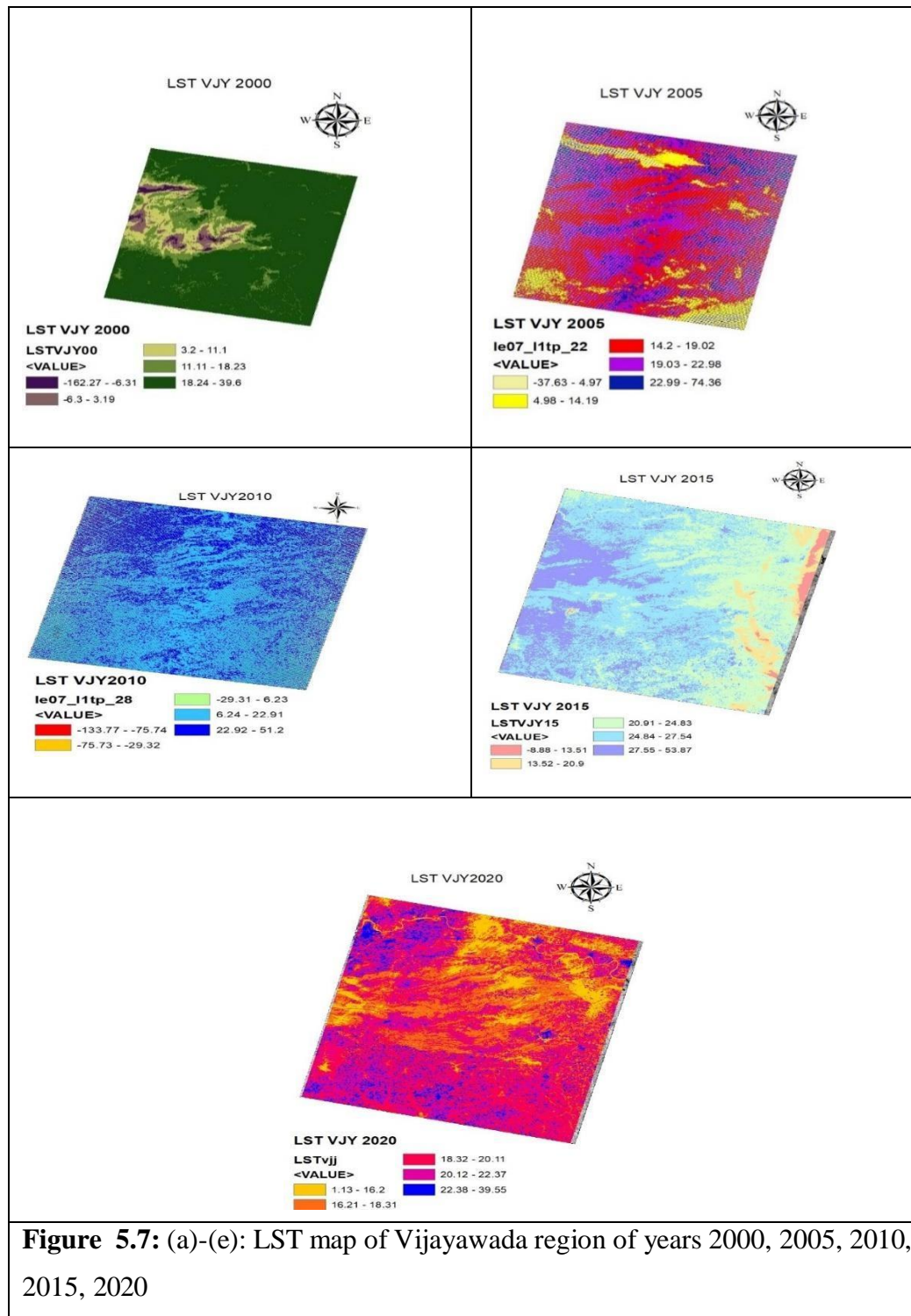


Figure 5.6: LST map of Visakhapatnam region of years 2000, 2005, 2010, 2015, 2020



LST acquired over different classes in Tirupati, Visakhapatnam, and Vijayawada regions is shown in **Table 5.13**, and a graphical representation of acquired LST is represented in Fig.5.8, where estimation of LST can be used to interpret the urban

development accord on the environment. Sensitivity evaluation at the carried-out MW set of rules confirmed that the LST de-rived from satellite images changed into extra trusty. The extended urbanization sample altered the city`s land surface as maximum resistant, favoring the individual increase of LST. It changed into additionally ascertained that the water body, commonly exposed to low heat, additionally confirmed an extrude within side the implied temperature over the decennary. The temperature analysis by class for each of the periods: 2000, 2005, 2010, 2015, and 2020, showed Over the built-up areas, the greatest mean temperatures were recorded. and others, followed by vegetation and water bodies, respectively. This fulfills as an illustration of the effects of urbanization effects on the environment. The class-sensible temperature evaluation for the periods: 2000, 2005, 2010, 2015, and 2020 confirmed that the best implied temperatures have been ascertained over the built-ups and others, followed via flora and water bodies

Table 5.13: LST acquired over different classes in Tirupati, Visakhapatnam, and Vijayawada regions.

Location	Year	Land cover type	LST acquired using the proposed method
Tirupati	2000	DenseVegetation	44.41
		Vegetation	26.38
		Built-Up	23.37
		BarenLand	20.82
		Water	11.57
	2005	DenseVegetation	50.74
		Vegetation	33.09
		Built-Up	30.63
		BarrenLand	27.93
		Water	19.11
	2010	DenseVegetation	44.41
		Vegetation	26.38
		Built-Up	23.47
		BarrenLand	20.82
		Water	11.54
	2015	DenseVegetation	30.09
		Vegetation	25.8
		Built-Up	24.3
		BarrenLand	22.877
		Water	19.36
	2020	DenseVegetation	25.08
		Vegetation	22.09
		Built-Up	20.92
		BarrenLand	17.8

		Water	11
Visakhapatnam	2000	DenseVegetation	56.09
		Vegetation	36.67
		Built-Up	28.46
		BarrenLand	19.61
		Water	-14.08
	2005	DenseVegetation	63.18
		Vegetation	41.3
		Built-Up	34.63
		BarrenLand	28.23
		Water	19.16
	2010	DenseVegetation	63.17
		Vegetation	36.14
		Built-Up	23.01
		BarrenLand	8.34
		Water	-34.17
	2015	DenseVegetation	57.78
		Vegetation	34.46
		Built-Up	25.66
		BarrenLand	16.87
		Water	-74
	2020	DenseVegetation	14.41
		Vegetation	11.87
		Built-Up	10.83
		BarenLand	9.86
		Water	9.08
Vijayawada	2000	DenseVegetation	39.06
		Vegetation	18.22
		Built-Up	11.1
		BarrenLand	3.18
		Water	-6.31
	2005	DenseVegetation	34.36
		Vegetation	22.97
		Built-Up	19.02
		BarrenLand	14.19
		Water	4.97
	2010	DenseVegetation	51.2
		Vegetation	22.91
		Built-Up	6.22
		BarrenLand	-29.31
		Water	-7.51
	2015	DenseVegetation	53.87
		Vegetation	27.53
		Built-Up	24.83
		BarrenLand	20.89
		Water	13.5
	2020	DenseVegetation	39.54
		Vegetation	22.37
		Built-Up	20.11

		BarrenLand	18.3
		Water	16.19

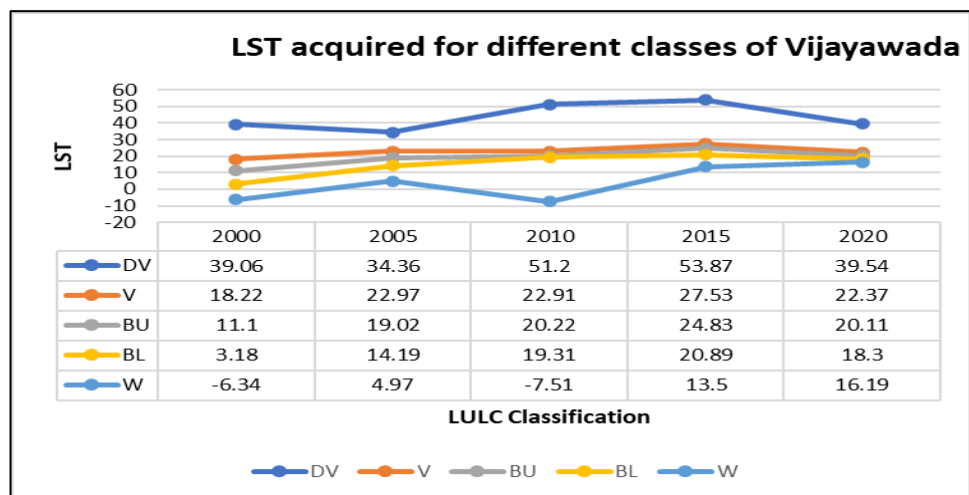
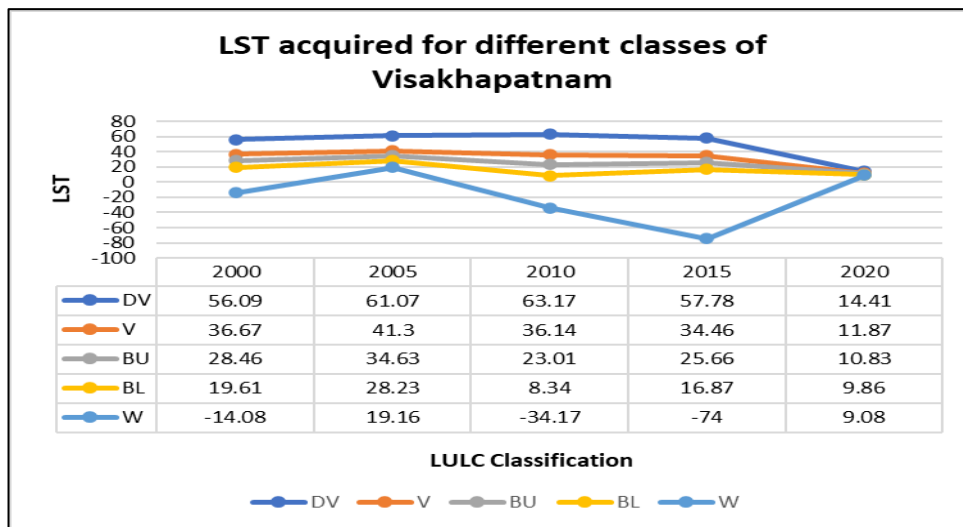
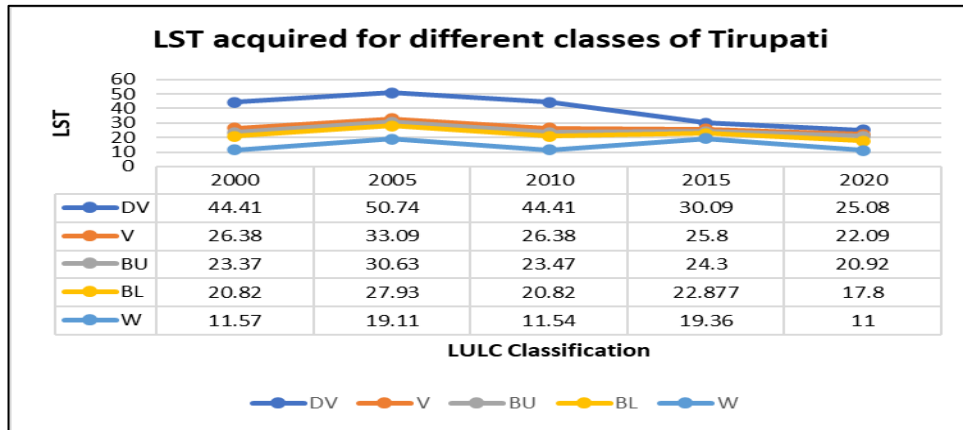


Figure 5.8: LST acquired for different classes of Tirupati, Visakhapatnam, and Vijayawada area

5.2. EVALUATION OF STUDY AREA USING DEEP TRANSFER LEARNING METHODS

The section that follows includes a broad outline results attained from the algorithm validation and testing procedures that were proposed. The outcomes are detailed precisely. The validation phase involved applying ResNet50 and ResNet50+LSTM to the multi-temporal images to attain the highest level of accuracy in the validation area. The subsequent section thoughtfully presents a comprehensive breakdown of the accuracy metrics derived from these classifications. The accuracy assessment results in the validation area are conveniently presented. Upon a rigorous evaluation of the measurements and maps from these experiments, it becomes evident that the ResNet50+LSTM algorithm emerges as the most powerful, consistently outperforming when compared with ResNet50 in handling multi-temporal data. ResNet50+LSTM outperforms ResNet50 in tasks involving Categories of land use and land cover by taking advantage of LSTM's abilities to identify temporal dependencies, handle long-term patterns, improve accuracy, handle variable sequences, reduce overfitting, enhance contextual understanding, and provide superior decision support. Furthermore, the effectiveness of Transfer Learning (TL) employing the ResNet50+LSTM, ResNet50, and associated models is critically examined and explained through confusion matrices. A shortage of validation and training and accuracies, the two TL prototypes are elegantly visualized in **Figure 5.9** and **Figure 5.10**, where the average training and validation accuracy is 98.1% and 51% for ResNet50+LSTM respectively, whereas the intermediate training and validation accuracy is 95% and 45% for ResNet50. The average training and validation loss is 0.53 and 9.8 for ResNet50+LSTM, respectively, whereas the intermediate training and validation loss is 0.6 and 10.1 for ResNet50.

According to the outcomes of the proposed work, the research findings bring to light the efficiency of pre-trained models of LULC within RS images. The primary aim is to attain exceptional accuracy, and the results reveal significant improvements across all models, with notable advancements in the classification of individual classes. This ResNet50+LSTM consistently performs with an impressive average accuracy of 98.1% with a Kappa coefficient of 0.96 compared to ResNet50, for which 95% accuracy is obtained with a Kappa coefficient of 0.9. The projected work further includes a visual representation of the study area's output map in **Figure 5.11**. Illustrating from

these findings, it becomes apparent that ensemble learning algorithms like ResNet50+LSTM have the potential to enhance overall performance by incorporating hierarchically learned information.

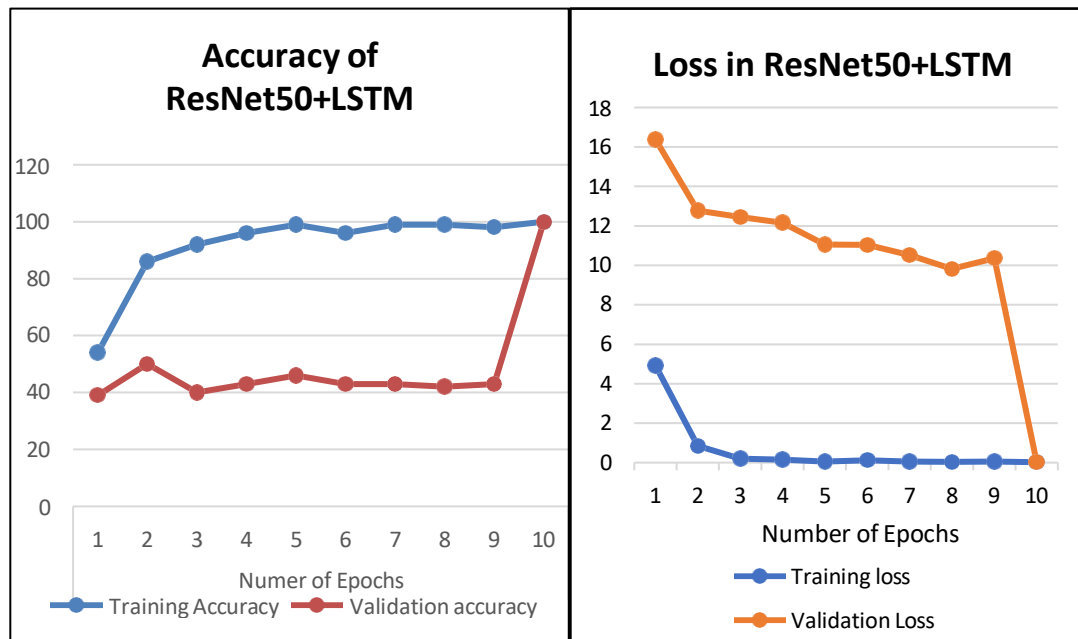


Figure 5.9: Accuracy and Loss of training vs. validation data for ResNet50 +LSTM

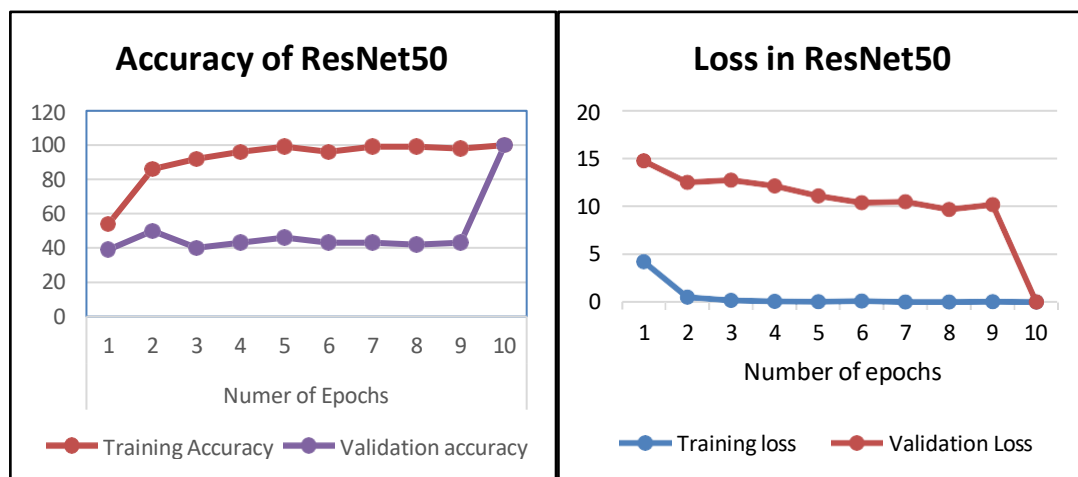


Figure 5.10: Accuracy and Loss of training vs. validation data for ResNet50

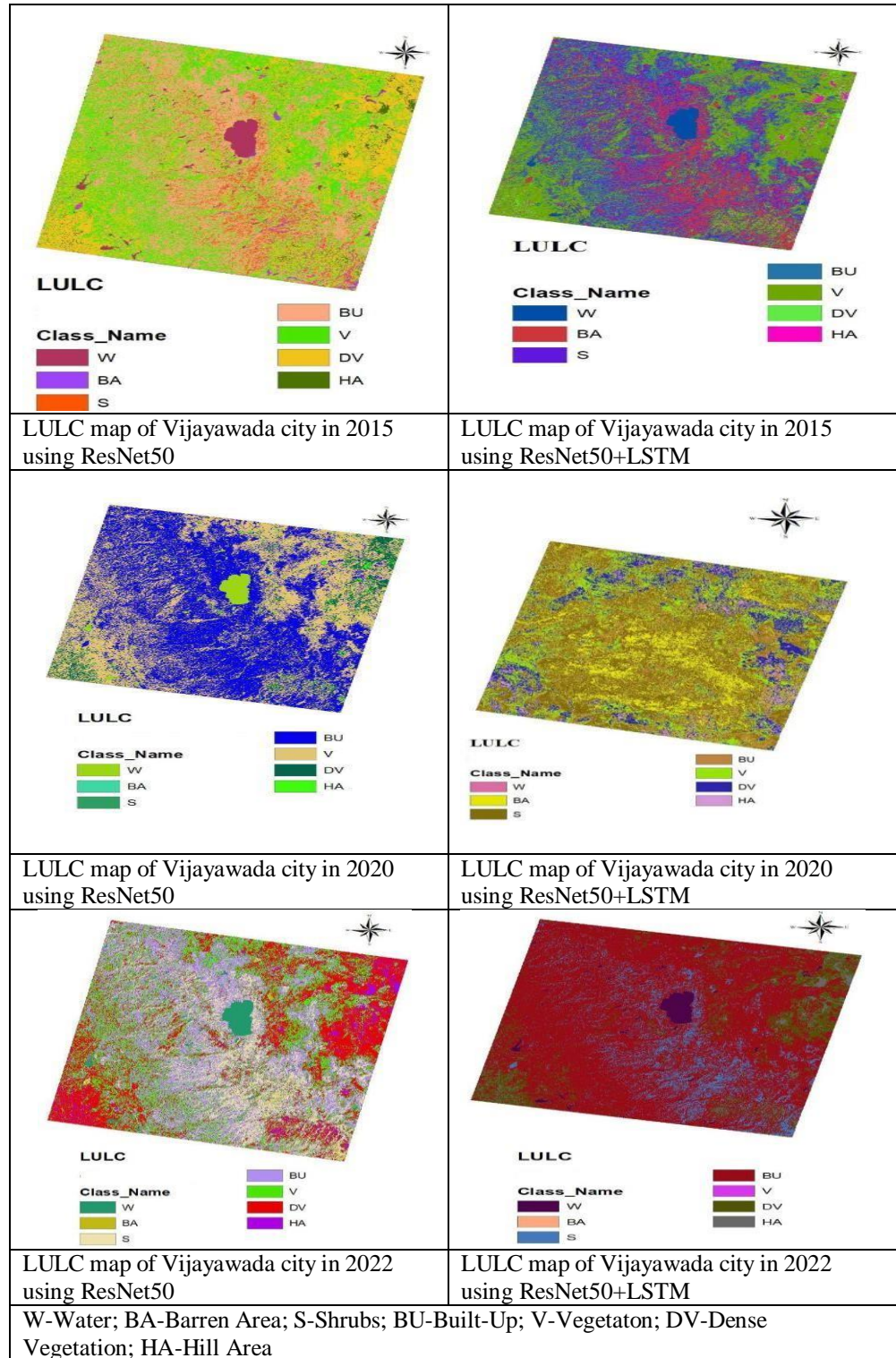


Figure 5.11: LULC maps of Vijayawada in 2015, 2020, and 2022 using ResNet50 and ResNet50 +LSTM

5.2.1 LULC Classification

Seven major LULC types (Hilly Area (HA), Dense Vegetation (DV), Vegetation (V) Built-Up (BU), Barren Area (BA), Shrubs (S), and Water(W)) are classified for the years of 2015, 2020 and 2022 as shown in **Table 5.14**. It has been confirmed that the covers for the research area total territory of 37,339.25 hectares. Table 5.14 presents an overview of the area covered and the proportion of each LULC for 2015, 2020, and 2022. Based on the LULC classification 2015, it can be deduced that Dense Vegetation, Vegetation, and Built-Up cover most of the study area, comprising about 32958.59 hectares, equivalent to 88.25% of the total area. Barren Area and Shrubs covered an area of 1515.27 ha (4.05%) and 1000.07 ha (2.67%), respectively, whereas the aerial coverage of a Hilly Area of 1010.32 ha (2.7%) and Water with 855 ha (2.29%) from the total area of the Vijayawada.

In 2020, the most significant portion of LULC was occupied by Dense Vegetation, Vegetation, and Built-up areas, covering 33018.83 hectares (88.3%). Barren areas, shrublands, and water bodies covered 1504.06 hectares (4.02%), 1000.50 hectares (2.67%), and 912.02 hectares (2.44%), respectively. The most minor coverage was contributed by Hilly Areas, accounting for 903.84 hectares (2.42%).

Similarly, in 2022, most LULC was still occupied by Dense Vegetation, Vegetation, and Built-up areas, which covered 33,569.62 hectares (89.89%). Barren areas, shrublands, and water bodies covered 1468.94 hectares (3.93%), 800.85 hectares (2.14%), and 835.91 hectares (2.23%), respectively. The least coverage was contributed by Hilly Areas, accounting for 663.93 hectares (1.77%).

5.2.2 Performing analysis by classification

Table 4 displays the results of the measurement of accuracy in the validation region, along with the quantitative assessment of the OA and KC for the entire classification. The overall accuracy of classified images in Vijayawada City is 91.5%, 93%, and 95% in 2015, 2020, and 2022, respectively. ResNet50's KCs are 0.89, 0.91, and 0.91, respectively, in 2015, 2020, and 2022. The OA of the classified images for Vijayawada City is 92.5%, 95%, and 98.1% in 2015, 2020, and 2022, respectively. ResNet50+LSTM has a KC of 0.9, 0.93, 0.96 in 2015, 2020, and

2022. In evaluating LULC classification methods, the researchers consistently observed superior precision with more than 85% values for Hilly Areas, Dense Vegetation, Built-Up Shrubs, and Barren Areas across the two models. They obtained fewer values for Vegetation and Water, as detailed in **Table 5.14** and **Table 5.15**. The low accuracy of classifying vegetables may be because it is hard to differentiate between this class and dense vegetation or barren areas. The lack of field research may also contribute to the imprecision of these classes (water and vegetation). In the confusion matrix, some false classifications are seen where Vegetation is mistakenly assigned to lands with Dense Vegetation. The absence of field research is needed for this. The model is still accurate for LULC classification. ResNet50 and ResNet50+LSTM excel due to their deep architecture, skip connections, transfer learning capabilities, temporal understanding (in the case of ResNet50+LSTM), robustness to overfitting, state-of-the-art performance, versatility, and strong community support, making them advantageous choices over other deep learning models in various applications. Due to this reason, ResNet50 and ResNet50+LSTM are used in this study. A comprehensive Comparison of the F1-s recollection, and accuracy for ResNet50 and ResNet50+LSTM is presented in **Table 5.16** and **Table 5.17**, shedding light on the models' ability to accurately identify and predict relevant classes. Notably, in instances where precision and recall reached a perfect value of 1, signifying 100% accuracy for specific classes of precision (Shrubs and Barren Area in the year 2015, 2020 and 2022 for ResNet50, Dense vegetation in the year 2020 and 2022 for ResNet50, Dense Vegetation and Hilly Area in the year 2020 and 2022 for ResNet50+LSTM), and recall (Hilly Area and Vegetation in the year 2015, 2020 and 2022 for ResNet50, Dense Vegetation in the year 2015 and 2022 for ResNet50+LSTM, Water and Shrubs in the year 2022 for ResNet50+LSTM) and exhibited exceptional performance across all categories. These findings strongly suggest the models' proficiency in classifying these classes with high precision and completeness. The researchers further delve into a detailed examination by closely scrutinizing individual folds' performance through confusion matrices. The graphical representation of Precision, Recall, and F1-Score for ResNet50 and ResNet50+LSTM where Recall for Dense vegetation achieved the maximum value (100%) for all three years for the ResNet50+LSTM model is shown in **Figure 5.12** and **Figure 5.13**, respectively.

Table 5.14: Spatial coverage of LULC types in Vijayawada at different periods in 2015, 2020, and 2022.

LULC Category	Area (Hectares)						Change in Area (Hectares)	change in Area (%)
	Year (2015)	Area (%)	Year (2020)	Area (%)	Year (2022)	Area (%)		
Hilly Area	1010.32	2.7	903.84	2.42	663.93	1.77	-346.39	-0.92
Dense vegetation	12791.44	34.25	9861.02	26.40	7634.25	20.44	-5157.19	-13.81
Vegetation	12045.1	32.25	13000.62	34.81	13342.62	35.73	297.52	0.79
Built-Up	8122.05	21.75	10157.21	27.18	12592.75	33.72	4470.7	11.97
Barren Area	1515.27	4.05	1504.06	4.02	1468.94	3.93	-46.33	-0.12
Shrubs	1000.07	2.67	1000.50	2.67	800.85	2.14	-199.22	-0.55
Water	855	2.29	912	2.44	835.91	2.23	-19.09	-0.05
Total	37339.25		37339.25		37339.25			

Table 5.15: Overall Accuracy and Kappa coefficient for ResNet50, ResNet50 +LSTM model for the years 2015, 2020 and 2022.

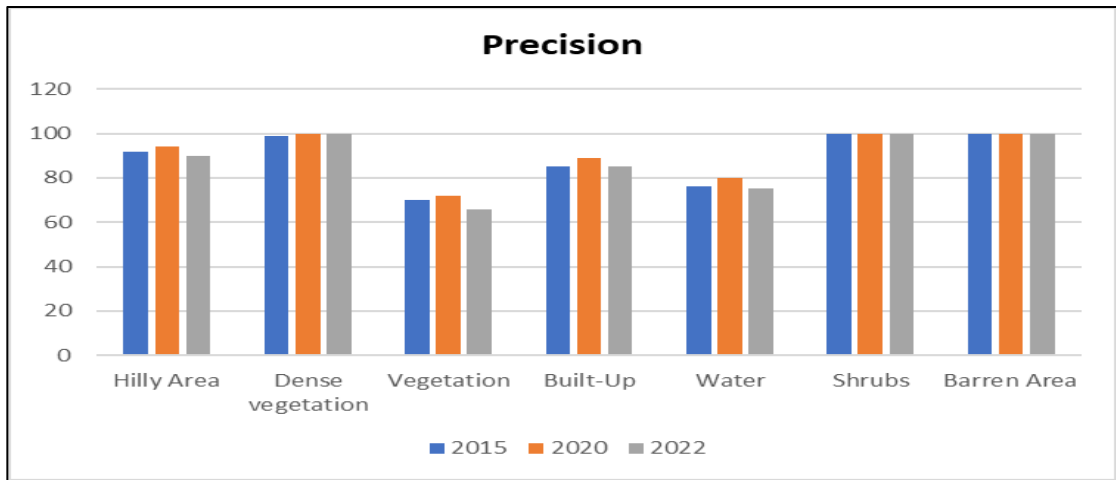
Methodology used	2015		2020		2022	
	Overall Accuracy (%)	Kappa Coefficient	Overall Accuracy (%)	Kappa Coefficient	Overall Accuracy (%)	Kappa Coefficient
ResNet50	91.5	0.89	93	0.91	95	0.91
ResNet50+LSTM	92.5	0.9	95	0.93	98.1	0.96

Table 5.16: ResNet50 model for class performances in precision, recall, and F1-score for the years 2015, 2020, and 2022.

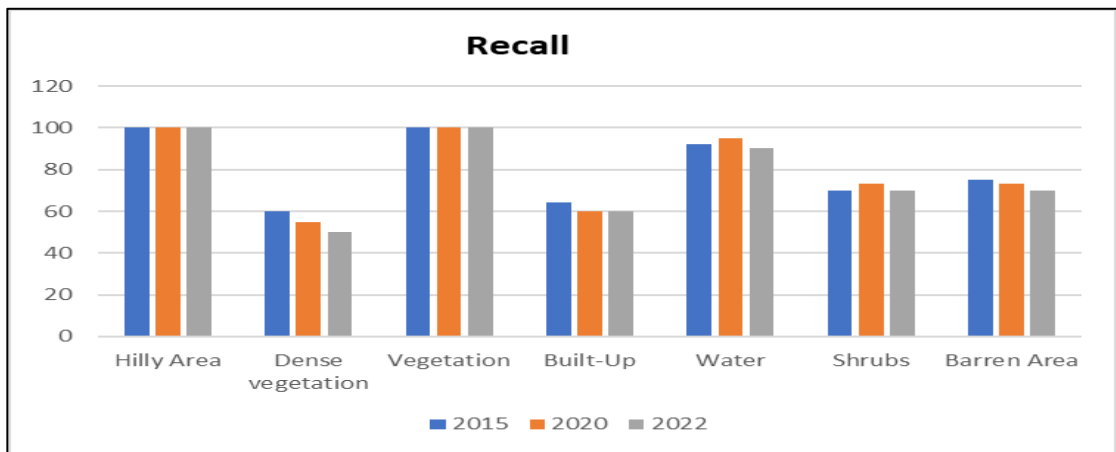
Type of Land Cover	2015			2020			2022		
	Precision (%)	Recall (%)	F1-Score (%)	Precision (%)	Recall (%)	F1-Score (%)	Precision (%)	Recall (%)	F1-Score (%)
Hilly Area	92	100	96	94	100	97	90	100	95
Dense vegetation	99	60	75	100	55	71	100	50	67
Vegetation	70	100	82	72	100	84	66	100	80
Built-Up	85	64	73	89	60	72	85	60	70
Water	76	92	83	80	95	87	75	90	82
Shrubs	100	70	82	100	73	84	100	70	82
Barren Area	100	75	86	100	73	84	100	70	82

Table 5.17: ResNet50+LSTM model for the recall, precision, and F1-score for the class performances for the years 2015, 2020, and 2022

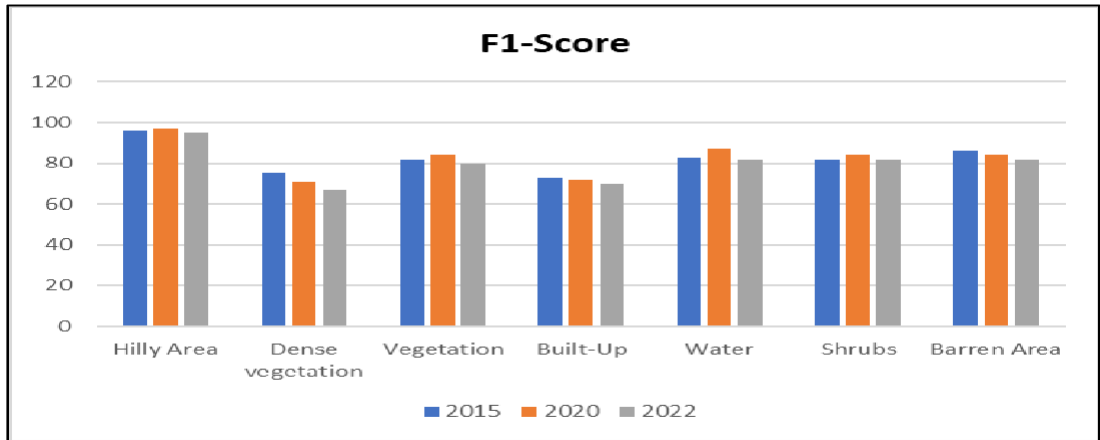
Type of Land Cover	2015			2020			2022		
	Precision (%)	Recall (%)	F1-Score (%)	Precision (%)	Recall (%)	F1-Score (%)	Precision (%)	Recall (%)	F1-Score (%)
Hilly Area	99	80	88	100	82	90	100	85	92
Dense vegetation	98	100	99	100	98	99	100	100	100
Vegetation	60	82	69	58	85	69	52	85	65
Built-Up	92	79	85	92	80	86	94	85	89
Water	85	97	91	86	97	91	87	100	93
Shrubs	83	96	89	85	97	91	89	100	94
Barren Area	90	82	86	92	85	88	94	85	89



(a)

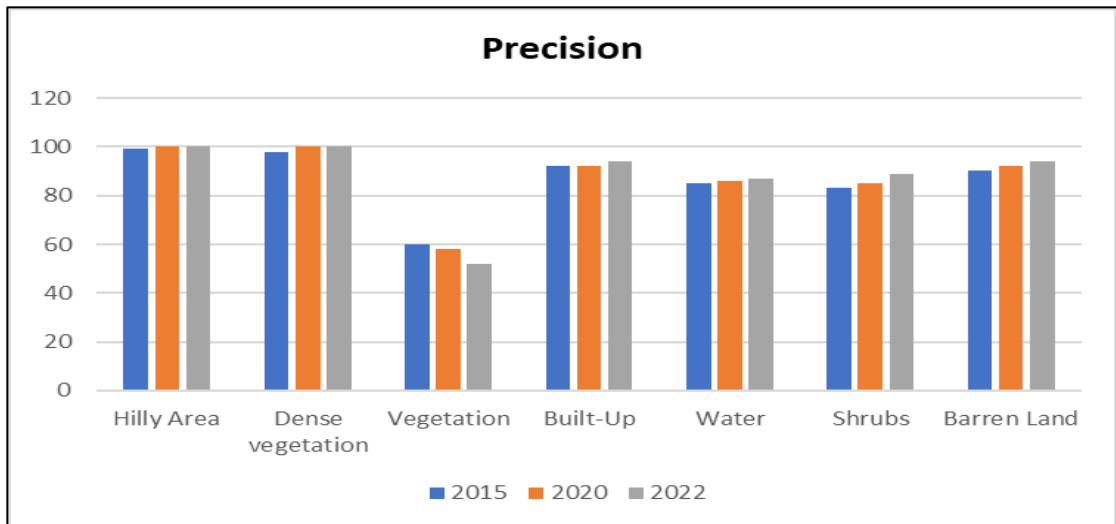


(b)

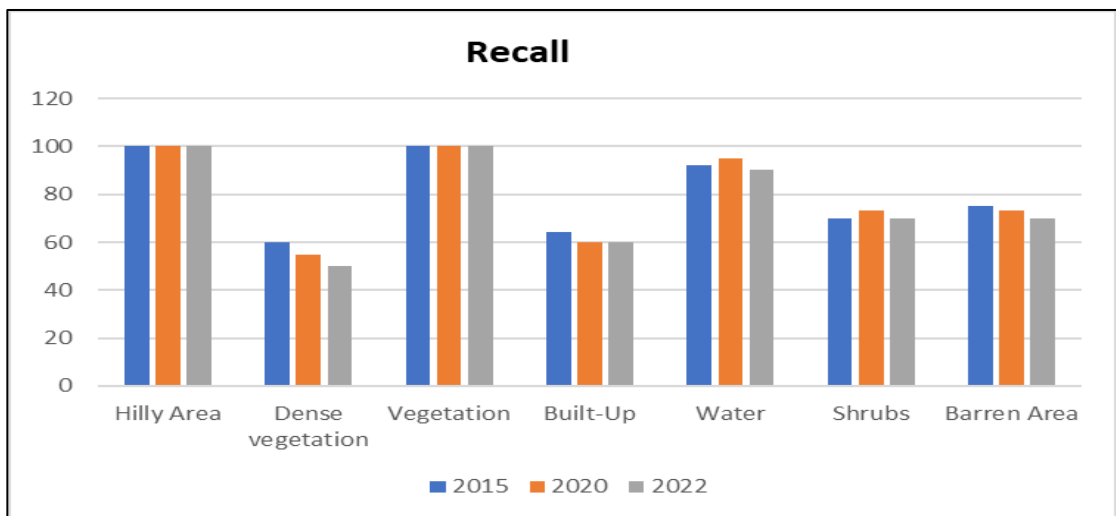


(c)

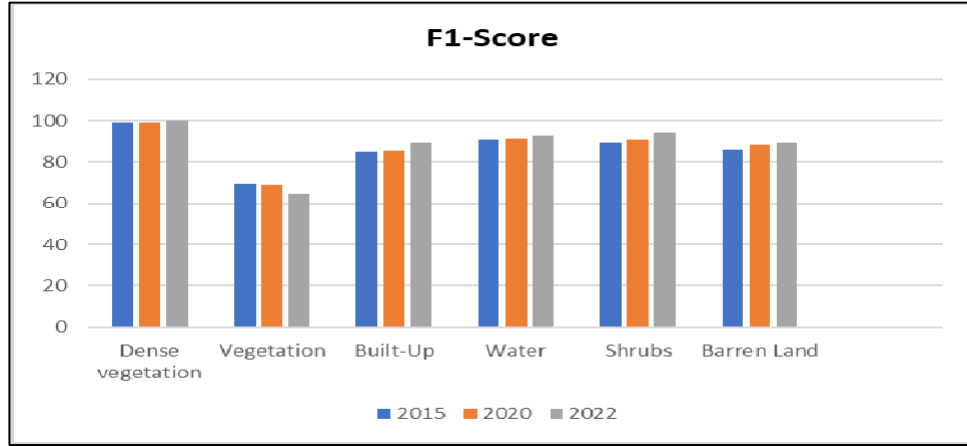
Figure 5.12: (a), (b), (c) Precision, Recall, and F1-Score for ResNet50



(a)



(b)



(c)

Figure 5.13: (a), (b), (c) Precision, Recall, and F1-Score for ResNet50+LSTM

The overall accuracy of ResNet50 and ResNet50+LSTM is 91.5% and 92.5%, respectively for the year 2015, ResNet50 and ResNet50+LSTM are 93% and 95%, respectively for the year 2020, and ResNet50 and ResNet50+LSTM is 95% and 98.1% respectively for the year 2022 and is also shown in **Figure 5.14**. The Kappa coefficient is 0.89 and 0.9 respectively for ResNet50 and ResNet50+LSTM in the year 2015, 0.91 and 0.93 respectively for ResNet50 and ResNet50+LSTM in the year 2020 and 0.91 and 0.96 respectively for ResNet50 and ResNet50+LSTM in the year 2022 and as also shown in **Figure 13**. Classification accuracy for years 2015, 2020 varied due to variations in data quality for the year 2015 to 2022, the distribution of classes Over the training period and lacking training details, i.e., for the year 2022, 200 training samples for each class are selected where for previous years only 100 samples are collected. The vegetation class exhibits the lowest precision, F1-Score, for ResNet50+LSTM, while the dense vegetation and built-up courses have the most inadequate recall for ResNet50, represented in Table 6. These less-than-satisfactory accuracy results may find their roots in differences in image variation and resolution due to uncertain class boundaries, i.e. if the classes in the LULC classification have unclear or overlapping boundaries, it becomes challenging for the classification algorithm to accurately distinguish between them, leading to lower precision and recall. The Transfer Learning (TL) model's construction involved the utilization of Adam optimizer using (LR) set at 0.0001, incorporating hyperparameters outlined. The model is thoughtfully accumulated with the categorical-cross-entropy loss function, which assigns integer values ranging from 0 to N-1 for each class (where

N=5 out of the 21 courses in the UCM dataset).

Throughout the training process of the deeper network, the cross-entropy loss gradually diminishes, enabling precise classification. The researchers employed the early stopping technique alongside dropout to mitigate the risk of overfitting and bolster performance. This strategic approach involved halting the training process if the validation loss ceased to decrease, even while the training loss continued to decline, or if the validation accuracy reached a plateau despite improving training accuracy.

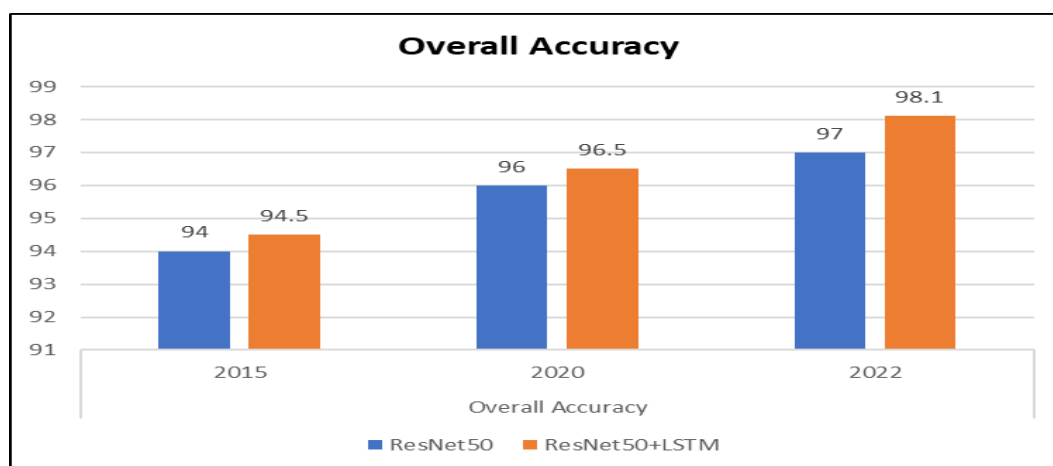


Figure 5.14: Overall Accuracy of ResNet50 and ResNet50+LSTM

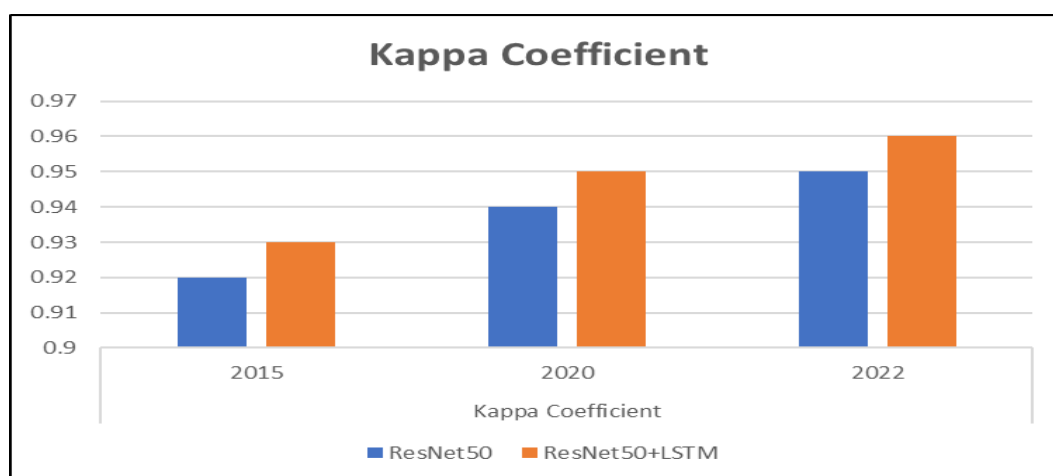


Figure 5.15: Kappa Coefficient of ResNet50 and ResNet50+LSTM

The epoch value is expressly set at 25, and early stopping is judiciously implemented at epochs 10 and 9 for ResNet50 and ResNet50+LSTM, respectively, when the validation loss no longer decreases. A noteworthy observation from this implementation is that a higher early stopping value correlated with superior accuracy, as exemplified by ResNet50 in this work.

In this study, RED, near-infrared, and thermal infrared images from the TM Landsat 7 and OLI/TIRS-Landsat 8 sensors were used to classify LULC and determine NDVI and LST. The LST of photos gathered by the sensors throughout each episode of the series was measured using the MW strategy. (2000-2020), and LULC classification was completed for the years 2000, 2005, 2010, 2015, and 2020 to validate the effect of LULC classes on the historical and spatial warmth from NDVI. This paper presents the spatially continuous regional LULC description of the regional data of Andhra Pradesh state, India. The maps also cover, with an annual temporal resolution, a period of 20 years with aggravated LULC trans-formations. Additionally, this work provides a methodological alternative for the continuous description of LULC, comparatively fast and with low cost, over large areas, and with advanced periodicity. The overall accuracy of the maps and the low and similar values of the omission and commission errors indicate a low level of sub and over-appraisal of the different class coverage. The PCA-based feature extraction approach along with NDVI, Interactive Supervised Classifier has performed better (OA: 97%) compared to other conceptualizations.

Visakhapatnam, Vijayawada, and Tirupathi cities have experienced unequalled development in the last 2 decades. Instead of rising urban populations, these towns have experienced a gradual increase in temperatures. Therefore, the cities became exposed to a miscellany of concerns with technology and warming temperatures. As a result, there have been shorter journey times, greater traffic, and more vehicles on the road networks, over-crowding, and polluted air from vehicular expel. The other is environmental damage. antagonistic consequence of the quick rise of cities. Cities are now more susceptible to natural disasters due to rising surface temperatures and the gradual loss of vegetation in built-up areas, viz., cyclones, etc. The present study, photographs from the TM Landsat 7 in the recognizable, near-IR, and thermal infrared spectra, and OLI/TIRS-Landsat 8 sensors were utilized to categorize LULC and to estimate NDVI and LST. The Mono Window Algorithm was employed to obtain the LST of the picture that sensors generated over the ancient cycle (2000-2020), and LULC classification was carried out in the summers of 2000, 2005, 2010, 2015, and 2020 to prove the effects of LULC temperature classes on time and spatial scale founded on the NDVI. based on the season, the Urban Area and Dense vegetation classifications demonstrated the strongest connections among LST and area size. This

result indicates that LST values are dependent on addressing the physical presence of life in regions where anthropogenic interference happened precisely, via water-resistant soil or the removing plants covers, allowing the surface illuminated. As a result, human behaviors attributed the rise in these scenarios, the temperature to adjacent ecological systems, finding the occurrence of Heat Islands on urban centers. The current study discovered that the reduction of vegetative cover and the repercussions generated by the LST are highly complex. LST dynamics associated with flora. NDVI is frequently utilized to assess LST changes. As a result, NDVI elected to employ it in this study. NDVI can effectively reduce distortion Since it's atmospheric phenomena, clouds or cloud shadows, geography, and lowering the sun's angle. nevertheless, it should be noted that It is subject to against which canopy fluctuations and becomes more polluted at greater biomass levels. The findings of this study using Deep Transfer Learning revealed seven primary LULC categories (Hilly Area, Dense Vegetation, Vegetation, Built-Up, Shrubs, Barren Area, and Water) in Vijayawada, as shown in Table 3. Vegetation increased from 32.25% in 2015 to 35.73% in 2022, while Built-Up rose from 21.75% in 2015 to 33.72% in 2022, whereas Dense Vegetation decreased from 34.25 to 20.44% during the same time. The accuracy results for the most current year, 2022. The LULC classification in the present study is outstanding. This study's overall accuracy is satisfactory, at 98.1% for ResNet50+LSTM and 95% for ResNet50. Furthermore, the Kappa statistics in the current study revealed a strong link between the most recently classified image and accuracy. The accuracy measurement in the validation region is shown in Table 4, along with a quantitative evaluation of the (OA) and KC values for the whole classification. Similarly, climate change operation LULC and landscapes, changing the framework, distribution, and land usage. On the other hand, expansion of irrigated land and rainforest, and the consequences of urbanization implications for the future of hydrological functions such as rainfall, evaporation, runoff, and penetration. Furthermore, changes and oscillations in LULC are strongly linked to biodiversity and land productivity. Also, LULC changes have significant impacts on the environment and the economy. Each classification technique has its benefits and drawbacks. The method used to depend on aspects including the type of data, specific inquiry needs, and computer resource availability. Combining various strategies frequently produces the greatest results, exploiting each's capabilities to increase the

degree of accuracy of the classification and robustness in LULC. Table 18 represents the comparison of multiple techniques used in land use and land cover (LULC) classification.

Pixel-based Image Analysis divides the image into significant objects (pixel groups) and classifies them according to their spectral, spatial, and contextual features. It incorporates spatial and contextual information and is ideal for high-resolution photography. Interactive Supervised Classification is best suited for scenarios where domain expertise can be used iteratively to refine the model. However, it may not be as scalable or automated as other approaches. On the other hand, SVM, Random Forest, and Decision Trees are suitable for LULC tasks where manual feature engineering is possible and interpretability is important. Random Forest offers a good balance between accuracy and interpretability.

ResNet50 and ResNet50+LSTM are great for Surface Area and Land Use applications that require high accuracy and power to handle unique temporal and spatial designs. However, they need a significant amount of processing resources.

Comparison of various techniques used in the categorization of Land Use and Land Cover

Author (Year)	Method	Type of images used	Evaluation parameters	
			Overall Accuracy (%)	Kappa Coefficient
Sundarakumar et al. (2012)	Obtained LULC changes and urban sprawl research of Vijayawada city of years 1990 and 2009 ML Classifier	Landsat ETM+	86.67 (1990) 85 (2009)	0.8 (1990) 0.78 (2009)
K. Sundara et al. (2012)	Estimated Land Surface Temperature of Landsat ETM+ images of year 2001 using Mono Window Algorithm	Landsat ETM+	80	0.729

	Obtained LULC changes with the help of ML Classifier			
Kiran Yerrakula et al. (2014)	Analyzed urban sprawl changes and detected LULC changes of Vijayawada city using Minimum Distance Classifier	Landsat8	67.19	0.6405
Vani, M. et al. (2018)	Assessed spatio-temporal modifications in LULC, urban sprawl, and LST in the vicinity of Vijayawada city of years 1990,2000,2010,2018 using NDVI, ML Classifier	Landsat ETM+, Landsat8	94.33 (2018), 93.07 (2010), 92.0 (2000), and 87.0 (1990)	0.94 (2018), 0.87 (2010), 0.88 (2000), and 0.81 (1990)
GN Vivekananda et al. (2020)	Accuracy assessment of Tirupathi region was performed for the 1978 and 2018 with the help of ML Classifier	Landsat TM, Landsat8	81.25 (1978) 87.46 (2018)	0.785(1978) 0.857 (2018)
Proposed Method	Accuracy assessment of Vijayawada, Visakhapatnam, Tirupathi region was performed for the years 2000, 2005, 2010,2015, and 2020 with the help of Interactive supervised classification	Landsat TM, ETM+, Landsat8	97, 95, 92, 92, 90 (2000, 2005, 2010, 2015, 2020-Vijayawada)	0.96, 0.94, 0.92, 0.9, 0.89 (2000, 2005, 2010, 2015, 2020-Vijayawada)
			97, 94.5, 92, 91, 90 (2000, 2005, 2010, 2015, 2020-Visakhapatnam)	0.96, 0.93, 0.9, 0.89, 0.87 (2000, 2005, 2010, 2015, 2020-Visakhapatnam)

			97, 94.6, 92, 92, 91(2000, 2005, 2010, 2015, 2020-Tiripathi)	0.96, 0.92, 0.91, 0.9, 0.89 (2000, 2005, 2010, 2015, 2020-Tiripathi)
	Accuracy assessment of Vijayawada region was performed for the years 2015, 2020 and 2022 with the help of ResNet50. ResNet50+LSTM	Sentinel2	91.5%, 93%, and 95% (ResNet50-2015,2020,2022)	0.89, 0.91, and 0.9(ResNet50-2015,2020,2022)
			92.5%, 95%, and 98.1% (ResNet50+LSTM-2015,2020,2022)	0.9, 0.93, and 0.96(ResNet50+LSTM-2015,2020,2022)

Summary

Within this section, proposed algorithms are implemented on several platforms, and their performance is analyzed statistically, graphically, and visually. Various accuracy assessment processes were implemented and described in this chapter to examine the potential of the constructed algorithm. This study validates the effectiveness Regarding the category of land cover and vegetation Evaluation of changes with the support of a deep learning-based change detection algorithm on the Sentinel-2 dataset. This strategy is most appropriate for future monitoring programs to check agriculture or crop cover variations in interest.

CONCLUSION & FUTURE SCOPE

CONCLUSION

The accurate production of a land cover (LC) map is of great importance when it comes to effectively addressing and communicating modern environmental concerns and meeting the agricultural needs of a region. The current analysis focuses on recent advances in categorization systems and comparative assessments of various strategies for monitoring vegetation change analysis. To achieve this objective, a comprehensive study was conducted using remote sensing (RS) and geographic information systems (GIS). Remote sensing involves collecting information gathered remotely using satellite or airborne sensors, enabling the acquisition of valuable information about the Earth's surface. Geographic information systems, on the other hand, provide a framework for storing, managing, analyzing, and visualizing geospatial data. By integrating RS and GIS, researchers were able to leverage satellite-derived images and other geospatial data to assess and monitor LULC changes in the study areas.

Remote sensing for vegetation change monitoring is a low-cost and efficient method. Satellite images have made important contributions to vegetation monitoring, owing to free data access policies provided by space organizations. Developed information may be justified in the future as space technology continues to advance. For instance, they have superior temporal, spatial, and spectral frequencies. Comprehensive LCLU data mapping is essential for various applications, including natural resource management, ecological conservation, urban development, biodiversity protection, and well-being upgrading. Integrating spectral and texture data can help address challenges in classification, and per-field or object-oriented classification processes demonstrate superior performance compared to per-pixel classifiers. But in this case of intermediate and uneven data on resolution of space, spectral information gains further significance due to the reduced availability of spatial details. Previous studies in the field have employed a variety of pixel-based classification methods, including parallelepiped, minimum distance, Mahalanobis, and maximum likelihood classifiers. However, in this study, an interactive supervised classification method was utilized,

which offered certain advantages and eliminated the requirement for signature files. This approach allowed for the direct selection of training samples on the imagery itself, eliminating the need for predefined signature files.

In addition to land cover analysis, the study also focused on calculating LST using the mono-window algorithm. LST is an important parameter that provides information about the thermal properties of the land surface. The accuracy of LST calculations was validated by comparing the results with in situ measurements collected from the same geographical location. This validation process ensures the reliability and accuracy of the LST data derived from satellite imagery.

By combining the examination of improvements to the landscape covering with the computation of surface temperature, the study offers accurate understanding the dynamics. It provides valuable information for land managers, policymakers, and researchers to analyze the effects of changing land usage, monitor urban expansion, evaluate vegetation dynamics, and understand the thermal characteristics of the land surface.

The per-pixel classifiers often struggle with mixed pixels in such cases. Subpixel features, like fraction images or fuzzy connection information, have been used to address this issue. Additionally, auxiliary data has been incorporated to enhance image classification. When dealing with multisource data, parametric classification methods like Maximum Likelihood Classification (MLC) can be more effective, while advanced non-parametric classifiers like neural network decision trees, evidential reasoning, and knowledge-based approaches are viable alternatives. Evaluating the effectiveness of classifiers is essential for new researchers to explore this field. MLC, SVM, and RF are commonly used classifier strategies for multispectral images. Advanced geospatial categorization approaches, such as ML and DL are becoming more useful for extracting valuable information from agricultural land. Pixel-based approaches have drawbacks, such as failing to account for differences within a pixel. Variation occurs within a pixel as well. Numerous studies have been conducted on satellite datasets, primarily focusing on the results of object-based categorization algorithms in different regions, such as agricultural, urban, forest, and wetland. In recent years, several studies have been conducted using classifiers developed for remote sensing-based agronomy applications. Researchers have found that neural networks (NN) select practice examples based

on relevant information retrieved from the interested domain. Incorporating multi-scale data regarding context improves and strengthens the spatial distribution of objects. This has led to an increase in the accuracy of class-category and border information in NN-categorized maps. Furthermore, machine learning classifiers such as decision trees (DT), support vector machines (SVM), random forests (RF), multi-layer perceptron (MLP), and k-nearest neighbors (KNN) have the potential ways of improve categorization performance in agricultural regions compared to traditional classifiers. ML algorithms analyze small data samples using attributes and build a statistical model to predict larger ones. These features are derived from factors resulting from classification, specifically predictive variables. Data-driven approaches can increase the possibility of adaptively improving a model's performance by preventing the problems of overfitting and underfitting. Deep learning classifiers including CNN, RNN, and DCNNs, as well as object-based categorization approaches, enhanced agricultural land class extraction. Deep learning involves connecting convolutional and pooling layers to remove cumbersome features and create deep, intellectual representations. Typically, the convolutional layer enhances the learning approach by utilizing a succession of samples or image patches from the dataset. Different feature maps share these weights, allowing for learning many features with minimal parameters. The activation function, such as a rectified linear unit, enhances the nonlinearity convolution operations. However, a decrease in deep transfer learning (ResNet50+LSTM, ResNet50) performance is observed, which could be due to one of the following reasons: (a) incorrect classification during the classification phase; (b) confined spatial resolution of the input dataset; or (c) atmospheric and radiometric error in the input dataset. The recommended results indicate that the ResNet50+LSTM-based method outperformed ResNet50 about of computation efficiency and accuracy, with an accuracy of 98.1%, a Kappa coefficient of 0.96, an average precision of 88%, a recall of 90%, and an F1-Score of 89% on the UCM dataset. The conventional pixel-based technique had 97% accuracy and a Kapa coefficient of 0.96.

FUTURE SCOPE

The performance of conventional and deep transfer learning approaches was examined in this study, utilizing medium-resolution Landsat and Sentinel-2 satellite data to estimate and map distinct vegetation change analyses. As part of the comparative investigation, a well-known and widely used classifier was tested. It was discovered that deep transfer learning performed marginally better than MLC, parallel pipeline, and CNN approaches. Although it performed well in the automatic identification of land-use features, numerous issues in deep transfer learning must be addressed, such as greater flexibility in parameter value selection and integration with custom programming models. It also needs to be developed, and extra features are required for many scientific disciplines. In agriculture, it is critical to correctly identify distinct seasonal crops on land plots to successfully update images and offer an up-to-date inventory of crops throughout the seasons, hence improving agricultural policy and land mapping accuracy. Future studies may combine the optical dataset with a microwave dataset to provide cloud-free monitoring of agricultural land types. This research will be more useful in identifying straw-burning places. In the future, it is proposed to investigate the usage of deep transfer learning algorithms for various land-use and land-cover types employing diverse sensors at the global scale. In this thesis, a methodology called interactive supervised classification, ResNet50, and ResNet50+LSTM is proposed to provide a simple way for detecting vegetation change in an area of interest. The method comprises three phases: pre-processing, classification, and change detection. As proof of their effectiveness, the approaches are compared to MLC, RF, CNN, and SVM models. However, classification errors, low spatial resolution, and other issues have all had an impact on deep transfer learning's accuracy. As a result, further research is required to increase its performance and investigate the feasibility of other applications utilizing various satellite sensors. In the future, research can be focused on implementing and upgrading DL models using a combination of optical and microwave data. The DL is still in its early stages and requires considerable improvements in terms of processing speed, resource constraints, and managing high levels of noise in satellite data. As a result, numerous difficulties remain to be addressed.

By advancing the research in these areas, we can strengthen the knowledge base for land use planning, management, and policy-making in the study area. This would facilitate informed decision-making processes and contribute to the development of sustainable land management practices that balance environmental conservation, economic development, and societal needs.

REFERENCES

- [1] Vani, M., and P. Rama Chandra Prasad. (2020), "Assessment of spatio-temporal changes in land use and land cover, urban sprawl, and land surface temperature in and around Vijayawada city, India." *Environment, Development and Sustainability* 22, no. 4: 3079-3095.
- [2] Vivekananda, G. N., R. Swathi, and A. V. L. N. Sujith, (2020), Multi-temporal image analysis for LULC classification and change detection. *European Journal of Remote Sensing*: 1- 11 <https://doi.org/10.1080/22797254.2020.1771215>.
- [3] Rao, R., and K. Rajesh. " (2018), Land Cover Klasifikasi Using Landsat-8 Optical Data and Supervised Classifiers. " *International Journal of Engineering & Technology* 2: 102-103.
- [4] Hashim, Haslina, Zulkiflee Abd Latif, and Nor Aizam Adnan,(2019), "Urban vegetation classification with NDVI threshold value method with very high resolution (VHR) PLEIADES Imagery", *Int. Arch. Photogramm. Remote Sens. Spat. Inf. Sci.* pp. 237-240.
- [5] KiranYarrakula, K. S. Kumar and K. Leela Krishna(2014), "Urban sprawl change detection analysis of Vijayawada city using multi-temporal remote sensing data" *Journal of Chemical and Pharmaceutical Research*, 6(11):728-734.
- [6] Rajani, A., and S. Varadarajan. (2020), "LU/LC Change Detection Using NDVI & MLC Through Remote Sensing and GIS for Kadapa Region." In *Cognitive Informatics and Soft Computing*, pp. 215-223. Springer, Singapore.
- [7] Alam, Akhtar, M. Sultan Bhat, and M. Maheen. (2020), "Using Landsat satellite data for assessing the land use and land cover change in Kashmir valley." *GeoJournal* 85, no. 6,1529-1543.
- [8] Hua, Ang Kean, and Owi Wei Ping. (2018), "The influence of land-use/land-cover changes on land surface temperature: a case study of Kuala Lumpur metropolitan city." *European Journal of Remote Sensing* 51, no. 1: 1049-1069.
- [9] Bouaziz, Moncef, Stefanie Eisold, and Emna Guermazi. "(2017), Semiautomatic approach for land cover classification: a remote sensing study for arid climate in southeastern Tunisia." *Euro-Mediterranean Journal for Environmental Integration* 2, no. 1: 7.

- [10] K. SUNDARA KUMAR¹, Dr. P. UDAYA BHASKAR, Dr. K. PADMAKUMARI,(2012), Estimation of Land Surface Temperature to Study Urban Heat Island Effect Using Landsat ETM+ Image, IJEST, Vol. 4 No.02 February
- [11] K. SUNDARAKUMAR, M. HARIKA², SK. ASPIYA BEGUM, S. YAMINI, K. BALAKRISHNA(2012), “Land Use and Land Cover Change Detection and Urban Sprawl Analysis of Vijayawada City Using Multitemporal Landsat Data” IJEST, ISSN: 0975-5462 Vol. 4 No.01 January.
- [12] Rwanga, Sophia S., and Julius M. Ndambuki.(2017), "Accuracy assessment of land use/land cover classification using remote sensing and GIS." International Journal of Geosciences 8, no. 04 : 611.
- [13] Kussul, N., Lavreniuk, M., Skakun, S., & Shelestov, A. (2017). Deep learning classification of land cover and crop types using remote sensing data. IEEE Geoscience and Remote Sensing Letters, 14(5), 778-782.
- [14] Verma, D., & Jana, A. (2019). LULC classification methodology based on simple Convolutional Neural Network to map complex urban forms at finer scale: Evidence from Mumbai. arXiv preprint arXiv:1909.09774.
- [15] Topaloğlu, R. H., Sertel, E., & Musaoğlu, N. (2016). ASSESSMENT OF CLASSIFICATION ACCURACIES OF SENTINEL-2 AND LANDSAT-8 DATA FOR LAND COVER/USE MAPPING. International archives of the photogrammetry, remote sensing & spatial Information Sciences, 41.
- [16] Loukika, K. N., Keesara, V. R., & Sridhar, V. (2021). Analysis of land use and land cover using machine learning algorithms on Google Earth engine for Munneru River Basin, India. Sustainability, 13(24), 13758.
- [17] Meriame Mohajane , Ali Essahlaoui , Fatiha Oudija , Mohammed El Hafyani , Abdellah El Hmaidi , Abdelhadi El Ouali , Giovanni Randazzo and Ana C. Teodoro, (2018), “Land Use/Land Cover (LULC) Using Landsat Data Series (MSS, TM, ETM+ and OLI) in Azrou Forest, in the Central Middle Atlas of Morocco” Environments, vol. 5, pp. 131.
- [18] Gondwe, J. F., Li, S., & Munthali, R. M. (2021). Analysis of Land Use and Land Cover Changes in Urban Areas Using Remote Sensing: Case of Blantyre City. Discrete Dynamics in Nature and Society, 2021.

- [19] Jamali, A. (2020). Land use land cover mapping using advanced machine learning classifiers: A case study of Shiraz city, Iran. *Earth Science Informatics*, 13(4), 1015-1030.
- [20] Cao, C., Dragičević, S., & Li, S. (2019). Land-use change detection with convolutional neural network methods. *Environments*, 6(2), 25.
- [21] Sahebjalal, E. and K. Dashtekian, (2013), Analysis of land use-land covers changes using normalized difference vegetation index (NDVI) differencing and classification methods. *African Journal of Agricultural Research*, 8(37): p. 4614-4622.
- [22] Slim Mtibaa, Mitsuteru Irie,(2016) , Land cover mapping in cropland dominated area using information on vegetation phenology and multi-seasonal Landsat 8 images, *Euro-Mediterr J Environ Integr* 1:6.
- [23] Aredehey, Gebrejewergs, Atinkut Mezgebu, and Atkilt Girma. (2018),"Land-use land-cover classification analysis of Giba catchment using hypertemporal MODIS NDVI satellite images." *International Journal of Remote Sensing* 39, no. 3: 810-821.
- [24] Indrayani, Buchari E, Putranto DDA, Saleh E (2017), Analysis of land use in the Banyuasin district using the image Landsat 8 by NDVI method. In: *AIP Conference Proceedings*. American Institute of Physics Inc.
- [25] H. I. Dewangkoro, and Aniati Murni Arymurthy. "Land use and land cover classification using CNN, SVM, and channel squeeze & spatial excitation block," In *IOP Conference Series: Earth and Environmental Science*, vol. 704, 2021, p: 012048. IOP Publishing.
- [26] Hosseiny, Benyamin, Abdulhakim M. Abdi, and Sadegh Jamali. "Urban land use and land cover classification with interpretable machine learning—A case study using Sentinel-2 and auxiliary data." *Remote Sensing Applications: Society and Environment*, Vol. 28, pp: 100843, 2022
- [27] Wulder, A. Michael, C. Nicholas Coops, P.David Roy, C.Joanne White, and Txomin Hermosilla. "Land cover 2.0." *International Journal of Remote Sensing*, Vol. 39, pp: 4254-4284, 2018.

- [28] Wang, Lizhe, Jining Yan, Lin Mu, and Liang Huang. "Knowledge discovery from remote sensing images: A review." *Wiley Interdisciplinary Reviews: Data Mining and Knowledge Discovery*, Vol.10, pp: e1371, 2020.
- [29] Neware, Rahul, and Amreen Khan. "Survey on Classification techniques used in remote sensing for satellite images." In *Second International Conference on Electronics, Communication and Aerospace Technology (ICECA)*, pp. 1860-1863, 2018.
- [30] Shahabi, Himan, Baharin Bin Ahmad, Mohammad Hossein Mokhtari, and Mohsen Ali Zadeh. "Detection of urban irregular development and green space destruction using normalized difference vegetation index (NDVI), principal component analysis (PCA) and post-classification methods: A case study of Saqqez city," *International Journal of the Physical Sciences*, Vol. 7, pp: 2587-2595, 2012.
- [31] V.K.A Somayajula, D. Ghai, S. Kumar, "Land Cover Classification using Landsat Images, Normalized Difference Vegetation Index in Vijayawada, AP," *International Journal of Early Childhood Special Education*, vol. 14, pp. 1159-1171, 2022.
- [32] Abebe, Gebeyehu, Dodge Getachew, and Alelgn Ewunetu. "Analysing land use/land cover changes and its dynamics using remote sensing and GIS in Gubalafito district, Northeastern Ethiopia." *SN Applied Sciences*, Vol. 4, pp: 30, 2022.
- [33] Tong, Xin-Yi, Gui-Song Xia, Qikai Lu, Huanfeng Shen, Shengyang Li, Shucheng You, and Liangpei Zhang. "Land-cover classification with high-resolution remote sensing images using transferable deep models," *Remote Sensing of Environment*, Vol. 237, pp: 111322, 2020.
- [34] Abdu, H. A. (2019). Classification accuracy and trend assessments of land cover-land use changes from principal components of land satellite images. *International Journal of Remote Sensing*, 40(4), 1275-1300.
- [35] Abdullah, M. H., Alkaff, M. A., & Kamarudin, K. A. (2019). A new modified minimum distance classification for land cover mapping from remote sensing data. *International Journal of Remote Sensing*, 40(12), 4523-4541.

- [36] Abdullah, M., Shafri, H. Z. M., Abdullah, K., & Ahmad, N. (2019). An adaptive threshold modification of the minimum distance classifier for land cover classification using remote sensing data. *IEEE Access*, 7, 48609-48619.
- [37] Abebe, G., Getachew, D., & Ewunetu, A. (2022). Analyzing land use/land cover changes and their dynamics using remote sensing and GIS in the Gubalafito district of northeastern Ethiopia. *SN Applied Sciences*, 4, 30.
- [38] Abiodun, B. J., & Adeoti, A. I. (2021). Land use/land cover change analysis in Ondo State, Nigeria, using remote sensing and machine learning algorithms. *Journal of Geographic Information System*, 13(1), 87-103.
- [39] Aburas, A.M., A.A. Salem, and M.A. El-Sheikh. (2015). Detection of land cover changes using NDVI and GIS techniques. *Egyptian Journal of Remote Sensing and Space Sciences* 18(2): 227-236.
- [40] Adediji, M.O., Agbelemoge, O.O., & Tampang, G. (2009). Use of remote sensing and GIS for land-use and land-cover change detection and future prediction in a part of southwestern Nigeria. *African Journal of Environmental Science and Technology*, 3(11), 387-396.
- [41] Adi, A. A., Amin, M., Sholihin, M., & Prasetyo, L. B. (2021). Land use and land cover changes analysis of Bengkulu Province, Indonesia using remote sensing and machine learning techniques. *IOP Conference Series: Earth and Environmental Science*, 728(1), 012-022.
- [42] Ahishali, M., Kiranyaz, S., Ince, T., & Gabbouj, M. (2019). Dual and single polarized SAR image classification using compact convolutional neural networks. *Remote Sensing*, 11(11), 1340.
- [43] Ahmed, M., A. Mekonnen, and A.M. Assefa. (2016). Monitoring vegetation changes in Northern Ethiopian Highlands using NDVI, GIS and RS techniques. *Remote Sensing* 8(11): 935.
- [44] Alam, M. M., Gazuruddin, M., Ahmed, N., Motaleb, A., Rana, M., Shishir, R. R., & Rahman, R. M. (2021). Classification of deep-sat images under label noise. *Applied Artificial Intelligence*, 35(14), 1196-1218.
- [45] Aravindanath, D., Udaya Bhaskar, P., Raju, P.L.N., & Krishna, P.H. (2012). Land use/land cover mapping using remote sensing and GIS: A case study of

Visakhapatnam district, Andhra Pradesh, India. *Journal of the Indian Society of Remote Sensing*, 40(2), 263-274.

- [46] Arveti, Nagaraju, Balaji Etikala, and Padmanava Dash, Land use/land cover analysis based on various comprehensive geospatial data sets: a case study from Tirupati area, south India, *Advances in Remote Sensing*, 2016, Vol. 2, pp. 73-83
- [47] Babar, M.A. and Shaikh, M.S., (2017). Impact of anthropogenic activities on land degradation in Tirupati, Andhra Pradesh, India. *Journal of Ecology and Environmental Sciences*, 1(2), pp.37-42. DOI: 10.31031/JEES.2017.01.000508
- [48] Bakshi, K., Singh, G., & Arya, D. S. (2018). Comparative analysis of minimum distance and maximum likelihood algorithms for land cover classification using Sentinel-2 data. In 2018 IEEE Global Humanitarian Technology Conference (GHTC) (pp. 1-7).
- [49] Balaji, V., Ramachandrudu, K., Reddy, G.P. (2018). Land use and land cover change detection and analysis in Vijayawada city using geospatial techniques. *International Journal of Engineering Science and Computing*, 8(11), 18650-18654. <https://doi.org/10.18535/ijesc/v8i11.24>
- [50] Bhatia, S., & Singh, S. K. (2019). Analysis of land use/land cover changes using remote sensing and GIS techniques: A case study of Ganga-Yamuna Plain Region. In *Advances in Geomatics and Geosciences* (pp. 283-297). Springer, Singapore.
- [51] Bahri, A., Majelan, S. G., Mohammadi, S., Noori, M., & Mohammadi, K. (2019). Remote sensing image classification via improved cross-entropy loss and transfer learning strategy based on deep convolutional neural networks. **IEEE Geoscience and Remote Sensing Letters*, 17(6), 1087-1091.
- [52] Bui, Q. T., Jamet, C., Vantrepotte, V., Mériaux, X., Cauvin, A., & Mognane, M. A. (2022). Evaluation of sentinel-2/MSI atmospheric correction algorithms over two contrasted French coastal waters. **Remote Sensing*, 14(5), 1099.
- [53] Bhatnagar, P., Sreedeeep, S., Kumar, R. M., & Singh, R. P. (2019). Spatio-temporal analysis of land use/land cover changes in Visakhapatnam, India. *Environmental Monitoring and Assessment*, 191(1), 20. DOI: 10.1007/s10661-018-7119-9.

- [54] Bhatnagar, P., Tripathi, N.K. and Singh, R.K., (2019). Land use/cover dynamics in Visakhapatnam, Andhra Pradesh using remote sensing and GIS. *International Journal of Agriculture, Environment and Bioresearch*, 4(2), pp.195-207. DOI: 10.24102/ijaeb.v4i2.1823
- [55] Bhattacharjee, D., & Roy, A. (2021). Land cover classification of Kaziranga National Park using Sentinel-2A data. In 2021 3rd International Conference on Communication, Computing and Electronics Systems (ICCCES) (pp. 1251-1255). IEEE.
- [56] Bhattacharyya, A., Mandal, S., & Ghosh, S. (2012). Analysis of land-use/land-cover changes using object-based classification approach in a coal mining area of India. *Journal of the Indian Society of Remote Sensing*, 40(4), 687-699.
- [57] Bhowmik, A., Gupta, M., & Singh, S. (2020). Land cover classification and change analysis using remote sensing data and GIS techniques in Sonbhadra district, Uttar Pradesh, India. *Journal of the Indian Society of Remote Sensing*, 48(10), 1745-1756.
- [58] Blaschke, T., et al. (2014). Object-based image analysis: From pixels to geo-objects. *ISPRS Journal of Photogrammetry and Remote Sensing*, 87, 180-191.
- [59] Campbell, J. B., Wynne, R. H., & Jupp, D. L. (1985). Vegetation mapping with multispectral thematic mapper data: a comparison of two analysis methods. *Remote sensing of Environment*, 17(1), 37-54.
- [60] Cao, C., Dragičević, S., & Li, S. (2019). Land-use change detection with convolutional neural network methods. **Environments*, 6(2), 25.
- [61] Cecili, G., De Fioravante, P., Dichicco, P., Congedo, L., Marchetti, M., & Munafò, M. (2023). Land cover mapping with convolutional neural networks using Sentinel-2 images: a case study of Rome. *Land*, 12, 879.
- [62] Chen, J., Ban, Y., Xu, S., Chen, S., & Liu, L. (2020). Comparison of Random Forest and Support Vector Machine classifiers for land use/cover classification using Sentinel-2A MSI data. *Remote Sensing*, 12(12), 1934.
- [63] Chen, L., Chen, J., Wang, Q., & Wu, Z. (2020). A Novel Parallelpiped Classifier Based on Fuzzy Clustering for Remote Sensing Image Classification. *IEEE Access*, 8, 87144-87156.

- [64] Chen, L., Zhang, Y., Hu, T., & Chen, W. (2019). A review of remote sensing image classification techniques: The role of spatio-contextual information. *Information Fusion*, 52, 49-61.
- [65] Chen, S., Liu, S., & Cui, L. (2020). An improved parallelepiped classifier for hyperspectral remote sensing image classification. *Remote Sensing*, 12(14), 2261.
- [66] Chen, X., Yu, X., & Zhang, X. (2015). The application of deep learning in the monitoring of urbanization in the Pearl River Delta. *Remote Sensing*, 7(12), 16599-16621.
- [67] Chen, Y., Li, X., Liu, Y., & Liu, Y. (2018). A comparative study on land cover classification algorithms in the Upper Yellow River basin based on Landsat data. *Remote Sensing*, 10(4), 627.
- [68] Chen, Y., Wang, L., Wang, J., Zeng, L., & Wu, Q. (2020). An improved parallelepiped classifier for remote sensing image classification. *Remote Sensing*, 12(3), 528.
- [69] Chen, Z., Zhang, M., Song, Q., Wu, Y., & Li, X. (2021). A Deep Learning Approach for Monitoring Vegetation Changes in Tropical Forests Using High-Resolution Satellite Images. *IEEE Journal of Selected Topics in Applied Earth Observations and Remote Sensing*, 14, 1275-1284.
- [70] Cheng, G., Ma, M., & Chen, X. (2014). Land cover classification of remote sensing imagery using a novel semi-supervised method based on maximum uncertainty sampling. *Remote Sensing*, 6(10), 9307-9333.
- [71] Chong, E. (2020). EuroSAT Land Use and Land Cover Classification using Deep Learning.
- [72] Choudhary, A., & Yadav, R. K. (2019). LULC classification using remote sensing and GIS: A case study of Narmada district, Madhya Pradesh, India. *Journal of the Indian Society of Remote Sensing*, 47(8), 1381-1391.
- [73] Choudhary, P., A.K. Tiwari, and N.K. Singh. (2019). Monitoring landscape changes using NDVI and multispectral remote sensing data. *ISPRS Journal of Photogrammetry and Remote Sensing* 148: 120-131.
- [74] Cihlar, J. (2000). Land cover mapping of large areas from satellites: status and research priorities. *International Journal of Remote Sensing*, 21(6-7), 1093-1114.

- [75] Côté-Allard, U., Fall, C. L., Drouin, A., Campeau-Lecours, A., Gosselin, C., Glette, K., & Gosselin, B. (2019). Deep learning for electromyographic hand gesture signal classification using transfer learning. *IEEE transactions on neural systems and rehabilitation engineering*, 27(4), 760-771.
- [76] Congalton, R. G., & Green, K. (2009). *Assessing the accuracy of remotely sensed data: principles and practices* (Vol. 2). CRC press.
- [77] Congalton, R. G., & Yadav, K. (2014). Assessing Landsat crop area estimates using the Census of Agriculture. *Remote Sensing*, 6(8), 7646-7664.
- [78] Das, D., Maiti, S., & Maiti, S. K. (2020). Vegetation change detection and analysis of an opencast mining area using remote sensing data and deep learning techniques. *IEEE Journal of Selected Topics in Applied Earth Observations and Remote Sensing*, 13, 1975-1983.
- [79] Dehghani, M., Sabzevari, A., Hekmatzadeh, A. A., & Salman Mahiny, A. (2021). Land use/land cover change detection in Zagros Mountains using remote sensing and deep learning techniques. *Geocarto International*, 1-18.
- [80] Deng, J., & Zhang, X. (2018). Comparison of remote sensing image classification algorithms for land cover mapping using open-source software. *International Journal of Geographical Information Science*, 32(10), 2017-2039.
- [81] Deng, J., Wang, F., & Jiang, S. (2016). Application of deep learning for land use and land cover classification in the Loess Plateau of China. *Remote Sensing*, 8(10), 807.
- [82] Deng, Y., & Zhang, Y. (2018). A comparative study of land use/cover classification methods in remote sensing. *Journal of Geographical Sciences*, 28(8), 1027-1046.
- [83] Deshpande, A. R., & Harish, K. S. (2021). Analysis of vegetation cover of Mumbai using remote sensing and machine learning. *International Journal of Remote Sensing and Earth Sciences*, 18(2), 155-169.
- [84] Dilawar, A.; Chen, B.; Trisurat, Y.; Tuankruea, V.; Arshad, A.; Hussain, Y.; Measho, S.; Guo, L.; Kayiranga, A.; Zhang, H.; (2021). Spatiotemporal shifts in thermal climate in responses to urban cover changes: A-case analysis of major cities in Punjab, Pakistan. *Geomatics. Nat. Hazards Risk*, 12, 763–793.

- [85] Duro, D. C., Franklin, S. E., & Dubé, M. G. (2012). A comparison of pixel-based and object-based image analysis with selected machine learning algorithms for classifying agricultural landscapes using SPOT-5 HRG imagery. *Remote Sensing of Environment*, 118, 259-272.
- [86] Ehsan, S., & Kazem, N. (2013). LULC change detection through remote sensing approach: A case study of Hawalbagh block, district Almora, Uttarakhand, India. *International Journal of Scientific and Research Publications*, 3(5), 1-8.
- [87] Ellis, E. C., & Pontius, R. G. (2007). Land-use and land-cover change. *Encyclopedia of Earth*, 2.
- [88] El-Magd, A.M., & El-Shirbeny, M.M. (2008). A change detection algorithm for urban land-use and land-cover classification using satellite remote sensing. *Journal of Environmental Management*, 88(4), 1384-1394.
- [89] Estornell, J., Cuenca, R., & Pérez, M. (2013). Soil erosion risk assessment through GIS modeling in the Alta Mijares (Spain). *Environmental monitoring and assessment*, 185(10), 8557-8572.
- [90] Fang, B., Kou, R., Pan, L., & Chen, P. (2019). Category-sensitive domain adaptation for land cover mapping in aerial scenes. *Remote Sensing*, 11(22), 2631.
- [91] Foody, G.M., & Mathur, A. (2004). A relative evaluation of multiclass image classification by support vector machines. *IEEE Transactions on Geoscience and Remote Sensing*, 42(6), 1335-1343.
- [92] Fraser, R. H., Olthof, I., Lantz, T. C., & Schmitt, C. (2009). Automated mapping of arctic vegetation using geobotanical and remote sensing techniques. *Journal of Geophysical Research: Biogeosciences*, 114(G3).
- [93] Fuentes, B., Lillo-Saavedra, M., Parra, J., & Soto, R. (2017). Impact of urbanization on land use and land cover change using deep learning techniques. *ISPRS International Journal of Geo-Information*, 6(7), 198.
- [94] Gandhi, S., R. Ravichandran, and A.R. Venkatachalam. (2015). An enhanced method for land cover change detection using NDVI and GIS techniques. *International Journal of Remote Sensing* 36(11): 3590-3607.

- [95] Gao, F., Masek, J. G., Wolfe, R. E., Tan, B., & Stehman, S. V. (2016). An analysis of Landsat 8 and Sentinel-2 data for forest classification and change detection in the Adirondack Mountains. *Remote Sensing of Environment*, 185, 205-221.
- [96] Gao, Y., Li, J., Sun, Q., & Liu, L. (2018). A review of classification algorithms for land-use and land-cover mapping. *Remote Sensing*, 10(10), 1630.
- [97] Garg, P. K., & Kaul, V. (2014). An improved modified minimum distance classifier for remote sensing image classification. In *2014 IEEE International Geoscience and Remote Sensing Symposium (IGARSS)* (pp. 406-409).
- [98] Geng, J., Fan, J., Wang, H., Ma, X., Li, B., & Chen, F. (2015). High-resolution SAR image classification via deep convolutional autoencoders. *IEEE Geoscience and Remote Sensing Letters*, 12(11), 2351-2355.
- [99] Geng, Y., Tian, X., & Wang, H. (2019). Mapping land cover changes in the Tibetan Plateau using MODIS data from 2001 to 2016. *International Journal of Remote Sensing*, 40(22), 8579-8597.
- [100] Ghorbanzadeh, O., Ali Abbaspour, R., Alimohammadi, A., & Dadashi, M. R. (2016). Land use and land cover mapping using deep learning and Landsat 8 imagery in Chaharmahal and Bakhtiari province, Iran. *Environmental Earth Sciences*, 75(5), 400.
- [101] Gong, P., Liang, S., Carlton, E. J., Jiang, Q., & Wu, J. (2014). Urbanization and health in China, thinking at the national, local, and individual levels. *Environmental Pollution*, 184, 234-236.
- [102] Green, E. P., Clark, C. D., & Edwards, A. J. (2000). Geometric correction of satellite and airborne imagery. *Remote Sensing Handbook for Tropical Coastal Management*.
- [103] Guo, Q., Wu, Z., & Huang, D. (2018). Hyperspectral image classification using a parallelepiped classifier with unequal covariance matrices. *IEEE Transactions on Geoscience and Remote Sensing*, 56(8), 4793-4803.
- [104] Guo, W., Li, W., Li, A., Wang, X., & Li, Z. (2018). An Improved Parallelepiped Classifier for Hyperspectral Images. *Remote Sensing*, 10(10), 1578.
- [105] Guo, W., Wu, B., Liu, Y., Liu, H., & Zhao, S. (2018). A Comparative Study of Maximum Likelihood, Minimum Distance and Parallelepiped Classifier for Land

- Cover Classification. In 2018 10th International Conference on Measuring Technology and Mechatronics Automation (ICMTMA), pp. 123-126. IEEE.
- [106] Guo, Y.-J.; Han, J.-J.; Zhao, X.; Dai, X.-Y.; Zhang, H. (2020). Understanding the Role of Optimized Land Use/Land Cover Components in Mitigating Summertime Intra-Surface Urban Heat Island Effect: A Study on Downtown Shanghai, China. *Energies*, 13, 1678.
 - [107] Hameed, S., Khan, M. A., & Mehmood, S. A. (2017). Monitoring land use and land cover changes in Pune district of Maharashtra state, India using remote sensing and GIS techniques. *Modeling Earth Systems and Environment*, 3(2), 603-614.
 - [108] Hamilton, S. K., & Loveland, J. E. (1999). *The ecology of agricultural landscapes: long-term research on the path to sustainability*. Oxford University Press.
 - [109] Hansen, M.C., Potapov, P.V., Moore, R., Hancher, M., Turubanova, S.A., Tyukavina, A., et al. (2013). High-resolution global maps of 21st-century forest cover change. *Science*, 342(6160), 850-853.
 - [110] Hashim, A.K., M.A. Al-Ghamdi, and A.M. Al-Ghamdi. (2019). Mapping urbanized vegetation using NDVI and machine learning algorithms. *ISPRS Journal of Photogrammetry and Remote Sensing* 152: 80-91.
 - [111] Hassan, Q.K., & Setiawan, N.A. (2015). Comparison of object-based and interactive object-based classification for mangrove mapping in Bintuni Bay, West Papua, Indonesia. *IOP Conference Series: Earth and Environmental Science*, 23(1), 012018.
 - [112] He, L., Yang, Y., & Li, S. (2018). A robust parallelepiped classifier based on uncertainty estimation. *Remote Sensing*, 10(8), 1259.
 - [113] Helber, P., Bischke, B., Dengel, A., & Borth, D. (2019). Eurosat: A novel dataset and deep learning benchmark for land use and land cover classification. *IEEE Journal of Selected Topics in Applied Earth Observations and Remote Sensing*, 12(7), 2217-2226.
 - [114] Hijmans, R. J., Cameron, S. E., Parra, J. L., Jones, P. G., & Jarvis, A. (1999). Very high-resolution interpolated climate surfaces for global land areas.

International Journal of Climatology: A Journal of the Royal Meteorological Society, 25(15), 1965-1978.

- [115] Hosseiny, B., Abdi, A. M., & Jamali, S. (2022). Urban land use and land cover classification with interpretable machine learning—A case study using Sentinel-2 and auxiliary data. *Remote Sensing Applications: Society and Environment*, 28, 100843.
- [116] Houghton, R.A. (2013). The carbon cycle and atmospheric carbon dioxide. In *Climate change 2013: The physical science basis. Contribution of Working Group I to the Fifth Assessment Report of the Intergovernmental Panel on Climate Change* (pp. 465-570). Cambridge, UK: Cambridge University Press.
- [117] Huang, C., Davis, L. S., Townshend, J. R., & Knaack, R. (2002). Monitoring land-use and land-cover change in the Upper Mississippi River Basin using classification trees. *Remote Sensing of Environment*, 82(2-3), 224-237.
- [118] Huang, J., Liao, C., He, L., & Shao, Y. (2021). Comparison of Classification Algorithms for Mapping Urban Land Cover Using Sentinel-2 Data. *ISPRS International Journal of Geo-Information*, 10(5), 357.
- [119] Huang, L., Wang, Y., Gu, Y., Zhang, J., & Liu, X. (2021). Mapping urban land cover with Sentinel-2 imagery using machine learning algorithms. *Remote Sensing*, 13(1), 87.
- [120] Indrayani, M.S., B.K. Sreenath, and M.R. Manjunath. (2017). Land use change detection using NDVI and remote sensing technology. *International Journal of Remote Sensing* 38(5): 1759-1776.
- [121] Islam, M. J., Rahman, M. M., Alam, M. S., & Sultana, S. (2021). Analysis of Land Use and Land Cover Changes Using Deep Learning Techniques: A Case Study of a Wetland Area in Bangladesh. *IEEE Journal of Selected Topics in Applied Earth Observations and Remote Sensing*, 14, 2764-2774.
- [122] Islam, M.A., M.M. Hossain, M.K. Alam, M.J. Islam, and M.S. Islam. (2016). Land use/land cover change detection using remote sensing and GIS techniques in Chunati Wildlife Sanctuary, Bangladesh. *Remote Sensing* 8(11): 880.
- [123] Jaiswal, R.K., Ghosh, S.K., Chakraborty, A., Chakraborty, M. (2016). Monitoring urban sprawl and land use/land cover changes in Vijayawada city, India, using

- remote sensing and GIS. *Journal of Urban Planning and Development*, 142(4), 05015005. [https://doi.org/10.1061/\(ASCE\)UP.1943-5444.0000286](https://doi.org/10.1061/(ASCE)UP.1943-5444.0000286)
- [124] Jeevalakshmi, S., & Dhivya, S. (2016). Land use/land cover classification using Landsat 8 OLI data: A case study of Coimbatore district, Tamilnadu, India. *Geocarto International*, 31(10), 1065-1076.
 - [125] Jensen, J. R. (2016). *Remote sensing of the environment: an earth resource perspective*. Pearson Education.
 - [126] Jensen, J. R., Rutchey, K., Koch, M. S., & Narumalani, S. (2000). Vegetation cover change detection in the South Carolina coastal zone using Landsat TM data. *Photogrammetric Engineering & Remote Sensing*, 66(1),
 - [127] Jensen, J.R., & Cowen, D.C. (1999). Remote sensing of urban/suburban infrastructure and socio-economic attributes. *Photogrammetric Engineering and Remote Sensing*, 65(5), 611-622.
 - [128] Kamalakar, G., Rao, P. N., Raju, K. C. S., & Krishna, P. H. (2021). Land cover classification of Nallamala forest range using sentinel-2 data and machine learning algorithms. *International Journal of Recent Technology and Engineering*, 9(1), 3366-3371.
 - [129] Khandelwal, A., & Tiwari, P. C. (2014). Performance analysis of various supervised classifiers for land use/land cover mapping using multispectral LISS-IV data. *Arabian Journal of Geosciences*, 7(12), 5507-5518.
 - [130] Khatami, R., Homayouni, S., & Mountrakis, G. (2017). Evaluating the effects of manual interactive corrections on satellite-based land-use classification accuracy. *International Journal of Remote Sensing*, 38(13), 3692-3709.
 - [131] Kinga, D., & Adam, J. B. (2015, May). A method for stochastic optimization. In *International conference on learning representations (ICLR)*, 5(6), 214.
 - [132] Kolli, M. K., Opp, C., Karthe, D., & Groll, M. (2020). Mapping significant land-use changes in the Kolleru Lake freshwater ecosystem using Landsat satellite images in Google Earth Engine. *Water*, 12(9), 2493.
 - [133] Kuchay, S., V. Ravishanker, and A.M. Deshpande. (2016). Quantifying and assessing land use/land cover changes in Uttara Kannada using remote sensing and GIS techniques. *Remote Sensing* 8(11): 927.

- [134] Kumar, A., Prasad, J., & Singh, S. (2018). Land cover classification of Shivalik range using the object-based approach. *Journal of the Indian Society of Remote Sensing*, 46(1), 123-131.
- [135] Kumar, P., & Kumar, V. (2016). Remote sensing and GIS-based analysis of land use/land cover change and its impact on hydrological regime in a watershed. *Environmental Monitoring and Assessment*, 188(4), 1-13.
- [136] Kumar, R., Kumar, M., Kumar, R., Kumar, N., & Kaur, R. (2021). Spatio-temporal analysis of land use/land cover change in Punjab, India using remote sensing and machine learning techniques. *Geocarto International*, 36(10), 1124-1137.
- [137] Kumar, S. S., & Mandal, U. K. (2017). Assessment of land use/land cover changes using Landsat data in Visakhapatnam, India. *Geocarto International*, 32(1), 57-69. DOI: 10.1080/10106049.2015.1062941.
- [138] Kumar, S., Singh, S. K., & Pandey, A. C. (2019). Accuracy assessment of different machine learning techniques for land use/land cover mapping using remote sensing data. *Journal of Environmental Management*, 234, 302-310.
- [139] Kumari, K.S., Rao, G.V., & Rao, K.V.K. (2018). Land use/land cover mapping of the Godavari River basin using remote sensing and GIS techniques. *International Journal of Engineering Technology Science and Research*, 5(6), 425-433.
- [140] Kussul, N., Shelestov, A., Lavreniuk, M., Butko, I., & Skakun, S. (2016). Deep learning approach for large-scale land cover mapping based on remote sensing data fusion. In 2016 IEEE international geoscience and remote sensing symposium (IGARSS), 198-201. IEEE.
- [141] Kusuma Kumari, G., Venkatappa Rao, G., & Rama Krishna, M. V. (2015). Land use/land cover change detection using remote sensing and GIS in Krishna district, Andhra Pradesh. *International Journal of Science and Research*, 4(5), 2585-2590.
- [142] Kusuma, S., Ramakrishna Reddy, B., Suresh Babu, M., & Latha, M. (2018). Land use and land cover changes in Tirupathi town, Andhra Pradesh, India, using remote sensing and GIS techniques. *International Journal of Engineering Technology Science and Research*, 5(7), 178-184. doi: 10.5281/zenodo.1309315

- [143] Lambin, E.F., and Meyfroidt, P. (2010). Land use transitions: socio-ecological feedback versus socio-economic change. *Land Use Policy*, 27(2), 108-118.
- [144] Latha, M. R., Anitha, M. A., & Saravanan, S. (2017). Land use/land cover changes detection in a river basin using remote sensing and GIS. *Journal of the Indian Society of Remote Sensing*, 45(3), 471-483.
- [145] Lefèvre, S., Aitkenhead, M., Marston, C., & Comber, A. (2018). Using deep learning to map small-scale vegetation patterns in the French Alps. *IEEE Journal of Selected Topics in Applied Earth Observations and Remote Sensing*, 11, 4059-4067.
- [146] Leung, Y., Chen, J., & Lee, J. (1997). The impact of land use/cover change on streamflow simulation. *Journal of hydrology*, 199(1-2), 177-191.
- [147] Li et al. (2019) - Wetland mapping using interactive supervised classification with Landsat data in the Yellow River Delta, China. *Remote Sensing*, 11(22), 2679.
- [148] Li, B., Li, Z., Li, W., Li, Y., Li, C., & Li, Q. (2017). Monitoring vegetation changes in Qinghai-Tibet Plateau based on FCN. In 2017 IEEE International Geoscience and Remote Sensing Symposium (IGARSS) (pp. 5198-5201). IEEE.
- [149] Li, R., Wang, L., Zhang, Y., & Zhang, L. (2020). Using deep learning to analyze the impact of vegetation changes on urban land use and land cover. *IEEE Journal of Selected Topics in Applied Earth Observations and Remote Sensing*, 13, 1245-1254.
- [150] Li, X., Chen, L., & Wang, X. (2021). Land use/land cover change in the Tibetan Plateau based on remote sensing and deep learning techniques. *Journal of Mountain Science*, 18(1), 157-174.
- [151] Li, X., He, X., Li, B., Li, C., Li, Y., & Li, W. (2014). A simple and efficient method for cloud and cloud shadow detection for Landsat and MODIS data. *Remote Sensing*, 6(7), 6229-6247.
- [152] Lin, Q., Wang, Y., Zhang, J., Zhou, H., & Liu, Y. (2020). Vegetation change detection and analysis using multi-source remote sensing data and deep learning techniques in a suburban area of Shanghai, China. *IEEE Journal of Selected Topics in Applied Earth Observations and Remote Sensing*, 13, 4500-4510.

- [153] Liping, C., Yufeng, S., Rui, S., & Fei, H. (2018). Land use and land cover change in Beijing from 1992 to 2015. *Journal of Geographical Sciences*, 28(9), 1279-1292.
- [154] Liu et al. (2020) - Forest mapping in the Greater Khingan Mountains based on interactive supervised classification using Landsat data. *Journal of Applied Remote Sensing*, 14(3), 1-18.
- [155] Liu, P., Zhang, H., & Eom, K. B. (2016). Active deep learning for classification of hyperspectral images. *IEEE Journal of Selected Topics in Applied Earth Observations and Remote Sensing*, 10(2), 712-724.
- [156] Liu, D., Li, D., Li, X., Li, H., Liang, J., & Zhang, Y. (2019). Using deep learning to analyze the impact of vegetation changes on land use and land cover in a wetland area. *IEEE Journal of Selected Topics in Applied Earth Observations and Remote Sensing*, 12, 1726-1735.
- [157] Liu, H., Xie, W., Liu, X., & Yao, W. (2017). Vegetation change detection in the Pearl River Delta using deep learning techniques. In *2017 IEEE International Geoscience and Remote Sensing Symposium (IGARSS)* (pp. 4376-4379). IEEE.
- [158] Liu, J., You, L., Amini, M., Obersteiner, M., Herrero, M., Zehnder, A. J., ... & Yang, H. (2018). A high-resolution assessment on global nitrogen flows in cropland. *Proceedings of the National Academy of Sciences*, 115(25), 6257-6262.
- [159] Liu, J., Zha, Y., Zhuang, D., Li, Z., & Liu, J. (2015). Application of a stacked autoencoder-based deep learning algorithm for classification of land use and land cover types from Landsat-8 OLI data. *Remote Sensing Letters*, 6(3), 164-173.
- [160] Liu, L., Ma, T., Song, C., Wang, J., Xu, J., & Liu, J. (2020). Land use and land cover classification using deep learning algorithms: A review. *ISPRS Journal of Photogrammetry and Remote Sensing*, 162, 269-285.
- [161] Lu, D., & Weng, Q. (2006). A survey of image classification methods and techniques for improving classification performance. *International journal of remote sensing*, 27(5), 823-870.
- [162] Lu, D., Li, G., Moran, E., & Hetrick, S. (2014). An automatic approach for reconstructing complex building roofs using multi-view aerial images. *Remote Sensing of Environment*, 155, 56-65.

- [163] Lu, D., Mausel, P., Brondízio, E., & Moran, E. (2004). Change detection techniques. *International Journal of Remote Sensing*, 25(12), 2365-2407.
- [164] Lu, D., Mausel, P., Brondizio, E., & Moran, E. (2004). Relationship between land-cover and vegetation indices in the Brazilian Amazon basin. *International Journal of Remote Sensing*, 25(3), 543-556.
- [165] Lu, D.; Li, G.; Moran, E.; Hetrick, S. (2013). Spatiotemporal analysis of land-use and land-cover change in the Brazilian Amazon. *Int. J. Remote Sens.*, 34, 5953–5978.
- [166] Lu, D.; Qihao, W. (2007). A survey of image classification methods and techniques for improving classification performance. *Int. J. Remote Sens.*, 28, 823–870.
- [167] Ma, L., Li, M., Ma, X., Cheng, L., Du, P., & Liu, Y. (2017). A review of supervised object-based land-cover image classification. *ISPRS Journal of Photogrammetry and Remote Sensing*, 130, 277-293.
- [168] Ma, M., et al. (2018). An interactive classification approach for mapping heterogeneous vegetation types in wetland ecosystems. *Ecological Indicators*, 89, 498-508.
- [169] Maasikamäe, H., Kuusemets, V., & Antov, D. (2011). Mapping and analysis of soil erosion susceptibility using GIS and remote sensing techniques in the Mustjõe river basin, Estonia. *Journal of Environmental Protection*, 2(06), 742.
- [170] Mahdianpari, M., Salehi, B., Rezaee, M., Mohammadimanesh, F., & Zhang, Y. (2018). Very deep convolutional neural networks for complex land cover mapping using multispectral remote sensing imagery. *Remote Sensing*, 10(7), 1119.
- [171] Mahmon, N. A., Ya'acob, N., & Yusof, A. L. (2015, March). Differences in image classification techniques for land use and land cover classification. In 2015 IEEE 11th International Colloquium on Signal Processing & Its Applications (CSPA) (pp. 90-94). IEEE.
- [172] Mamun, M. A. A., Kamruzzaman, M., Al-Mamun, A., & Rahman, M. M. (2013). Land use and land cover change detection through remote sensing approach: A case study of Purbachal new town, Bangladesh. *Journal of Environmental Science and Natural Resources*, 6(1), 31-35.

- [173] Marinho, E. P., Lapa, K. R., Dornelles, K. J., Pinheiro, M. R., & Silva, F. B. (2021). Analysis of land use and land cover change in the Brazilian Amazon region using remote sensing and machine learning algorithms. *Remote Sensing Applications: Society and Environment*, 22, 100483.
- [174] Mas, J. F., Flores, A. A., & Gouveia, C. M. (2004). Remote sensing image classification using the interactive supervised classification algorithm: Methodological developments and a comparative analysis. *International Journal of Remote Sensing*, 25(1), 19-34.
- [175] Meng, J., Liu, X., & Zhang, Y. (2020). A hybrid method of maximum likelihood classifier and convolutional neural network for land cover classification. *Remote Sensing*, 12(11), 1776.
- [176] Meng, X., Wu, H., Wang, C., Cheng, X., Liu, J., & Liu, J. (2021). Analysis of vegetation changes and land use/land cover based on deep learning in the Yangtze River Basin, China. *Remote Sensing*, 13(14), 2831.
- [177] Midekisa, A., Holl, F., Savory, D. J., Andrade-Pacheco, R., Gething, P. W., Bennett, A., & Sturrock, H. J. (2017). Mapping land cover change over continental Africa using Landsat and Google Earth Engine cloud computing. *PloS one*, 12(9), e0184926.
- [178] Mohammadi, A., Baharin, B. A., & Shahabi, H. (2019). Land cover mapping using a novel combination model of satellite imageries: a case study of a part of the Cameron Highlands, Pahang, Malaysia. *Applied Ecology & Environmental Research*, 17(2).
- [179] Mondal, P., Kundu, S., Roy, S., & Ray, S. K. (2017). Land use and land cover change detection and prediction modeling using remote sensing and GIS: A case study of the Eastern Himalayan region, India. *Journal of Mountain Science*, 14(2), 283-297.
- [180] Mosavi, A., Shirzadi, A., Choubin, B., Taramideh, F., Hosseini, F. S., Borji, M., & Dineva, A. A. (2020). Towards an ensemble machine learning model of random subspace-based functional tree classifier for snow avalanche susceptibility mapping. *IEEE Access*, 8, 145968-145983.

- [181] Mtibaa, M., A. El Moujabber, and M. Zein. (2016). Land cover change detection using NDVI and machine learning classifiers. *International Journal of Remote Sensing* 37(17): 4455-4474.
- [182] Mundhe, S.S., Karale, R.L., & Dadhwal, V.K. (2020). Land use/land cover mapping of Kinnerasani Wildlife Sanctuary using Sentinel-2 data. *Journal of the Indian Society of Remote Sensing*, 48(11), 1921-1927.
- [183] Naidu, V. R., Kumar, G. P., & Prasad, D. K. (2018). Spatio-temporal changes in land use/land cover using remote sensing and GIS in the Godavari delta region of Andhra Pradesh. *International Journal of Remote Sensing and GIS*, 7(1), 49-58.
- [184] Nair, R. S., Narayanan, S., & Arun, M. (2020). LULC classification of the Manimala river basin using Sentinel 2 data. *Indian Journal of Science and Technology*, 13(32), 3275-3280.
- [185] Nair, V., & Hinton, G. E. (2010). Rectified linear units improve restricted Boltzmann machines in *Proceedings of the 27th International Conference on Machine Learning (ICMAXIMUM LIKELIHOOD-10)*, 807-814.
- [186] Neware, R., & Khan, A. (2018, March). Survey on Classification techniques used in remote sensing for satellite images. In *2018, the Second International Conference on Electronics, Communication and Aerospace Technology (ICECA)*, 1860-1863. IEEE.
- [187] Nhu, V. H., Mohammadi, A., Shahabi, H., Ahmad, B. B., Al-Ansari, N., Shirzadi, A., & Nguyen, H. (2020). Landslide susceptibility mapping using machine learning algorithms and remote sensing data in a tropical environment. *International journal of environmental research and public health*, 17(14), 4933.
- [188] Nkouna, A. P., Biouele, C. M. N., & Tchinda-Metagne, C. (2020). Vegetation change detection and analysis in a forest area of Cameroon using deep learning techniques and Landsat data. *IEEE Journal of Selected Topics in Applied Earth Observations and Remote Sensing*, 13, 5437-5446.
- [189] Padalia, H., Chauhan, K., & Bhatt, D. (2018). Analysis of land cover dynamics in a rapidly urbanizing city using remote sensing and GIS techniques: a case study of Ahmedabad, Gujarat. *Journal of Geographic Information System*, 10(06), 731-752.

- [190] Pal, M., & Mather, P. M. (2003). An assessment of the effectiveness of decision tree methods for land cover classification. *Remote sensing of environment*, 86(4), 554-565.
- [191] Pasher, J., Farina, A., & Boehm, A. (2017). Using deep learning neural networks to analyze the impact of urbanization on the thermal environment. *Remote Sensing of Environment*, 192, 176-185.
- [192] Prakash, K., V.K. Singh, and P.K. Singh. (2016). Land use/land cover change detection using NDVI and machine learning classification techniques. *ISPRS Journal of Photogrammetry and Remote Sensing* 123: 22-33.
- [193] Prasad, P.R.C., Bhuvaneswari, G., Dhanunjaya, Naidu, M., Jyothi, N.V.V. (2016). Assessing land use/land cover changes in Vijayawada urban agglomeration using remote sensing and GIS. *International Journal of Engineering Research and Applications*, 6(10), 52-58. <https://doi.org/10.9790/9622-0610015258>
- [194] Piramanayagam, S., Schwartzkopf, W., Koehler, F. W., & Saber, E. (2022). Classification of remotely sensed images using random forests and deep learning framework. In *Image and signal processing for remote sensing XXII*, 10004, 205-212. SPIE.
- [195] Pires de Lima, R., & Marfurt, K. (2019). Convolutional neural network for remote-sensing scene classification: Transfer learning analysis. *Remote Sensing*, 12(1), 86.
- [196] Qin, Z.; Karnieli, A. (1999). Progress in the remote sensing of land surface temperature and ground emissivity using NOAA-AVHRR data. *Int. J. Remote Sens.*, 20, 2367–2393.
- [197] Qiu, R., Xu, W., Zhang, J., & Staenz, K. (2018). Modeling and simulating industrial land-use evolution in Shanghai, China. *Journal of geographical systems*, 20, 57-83.
- [198] Raja, P., Subramani, T., Kumar, D. S., & Selvam, S. (2019). Land use/land cover changes analysis of Tirupati Region, Andhra Pradesh, India. *Journal of Remote Sensing & GIS*, 8(4), 1-8. doi: 10.4172/2469-4134.1000247

- [199] Rajani, A.; Varadarajan.S (2021). Estimation and Validation of Land Surface Temperature by using Remote Sensing & GIS for Chittoor District, Andhra Pradesh. *Turk. J. Comput. Math. Educ.*, 12, 607–617.
- [200] Raju, P. L. N., Kumar, P. S., &Sreerama, K. (2016). Land cover classification using Maximum Likelihood Classification algorithm–A case study of Kinnerasani Wildlife Sanctuary, Telangana. *Aquatic Procedia*, 4, 1248-1254.
- [201] Rao, K. K., & Babu, R. R. (2016). Analysis of land use/land cover changes using remote sensing and GIS in Krishna river basin of Andhra Pradesh, India. *Journal of the Indian Society of Remote Sensing*, 44(4), 595-602.
- [202] Raschka, S., Patterson, J., & Nolet, C. (2020). Machine learning in Python: Main developments and technology trends in data science, machine learning, and artificial intelligence. *Information*, 11(4), 193.
- [203] Rashid, M., Khan, M. A., Alhaisoni, M., Wang, S. H., Naqvi, S. R., Rehman, A., & Saba, T. (2020). A sustainable deep learning framework for object recognition using multi-layer deep features fusion and selection. *Sustainability*, 12(12), 5037.
- [204] Rathod, P., Pujari, P. R., & Deshpande, N. (2021). Land use/land cover classification in a semi-arid region of India using deep learning techniques. *International Journal of Remote Sensing*, 42(8), 3072-3089.
- [205] Ravi Shankar, K., &Venkateswarlu, B. (2017). Land use and land cover mapping of East Godavari district, Andhra Pradesh using remote sensing and GIS techniques. *International Journal of Remote Sensing & Geoscience*, 6(1), 1-13.
- [206] Reddy, K.G., V. Kumar, and S.K. Mishra. (2013). Spatiotemporal analysis of land use/land cover changes using NDVI and GIS: A case study of Kaddam watershed, India. *Ecological Indicators* 32: 187-196.
- [207] Reddy, V. R., Prasad, K. S., & Rao, G. S. (2019). Land use and land cover changes and their impact on urbanization in Vijayawada Municipal Corporation area, Andhra Pradesh. *International Journal of Engineering and Advanced Technology*, 9(4), 1797-1804.
- [208] Kiranmai, V., Ghai, D., & Kumar, S. (2020). A review on classification of land use/land cover change assessment based on normalized difference vegetation index. *Journal of Critical Reviews*, 7(14), 2416-2431.

- [209] Richards, J. A., & Jia, X. (2006). Remote sensing digital image analysis: An introduction. Springer Science & Business Media.
- [210] Richardson, F. D. (1986). Remote sensing of vegetation: Principles, techniques, and applications. Oxford University Press.
- [211] Ronneberger, O., Fischer, P., & Brox, T. (2015). U-net: Convolutional networks for biomedical image segmentation. In Medical Image Computing and Computer-Assisted Intervention–MICCAI 2015: 18th International Conference, Munich, Germany, October 5-9, 2015, Proceedings, Part III 18, 234-241. Springer International Publishing.
- [212] Rostami, M., Kolouri, S., Eaton, E., & Kim, K. (2019). Deep transfer learning for few-shot SAR image classification. Remote Sensing, 11(11), 1374.
- [213] Safarov, F., Temurbek, K., Jamoljon, D., Temur, O., Chedjou, J. C., Abdusalomov, A. B., & Cho, Y. I. (2022). Improved Agricultural Field Segmentation in Satellite Imagery Using TL-ResUNet Architecture. Sensors, 22(24), 9784.
- [214] Saini, S., Dasgupta, S., & Singh, C. K. (2019). Evaluation of supervised classification algorithms for land cover change detection in a Himalayan region. Journal of the Indian Society of Remote Sensing, 47(9), 1479-1488.
- [215] Sannier, C.A.D., Dupuy, S., Mourier, B., Gond, V., Freycon, V., and Molino, J-F. (2012). Landscape dynamics in a tropical forest in southern Cameroon: implications for REDD projects. Environmental Research Letters, 7(4), 045702.
- [216] Saranya, K., Ramakrishnan, S., & Nagarajan, R. (2020). Land use/land cover change detection and analysis of Godavari river basin, Andhra Pradesh using geospatial techniques. Journal of Indian Society of Remote Sensing, 48(3), 501-513.
- [217] Sarkar, P., & Das, J. (2019). A Modified Maximum Likelihood Classifier for hyperspectral image classification using texture features. IEEE Geoscience and Remote Sensing Letters, 16(4), 515-519.
- [218] Schneeweis, P. D., Li, B. L., & Tucker, C. J. (1982). Land use changes and the history of water resources in the Upper Santa Cruz Basin, Arizona. Water Resources Research, 18(4), 1099-1116.

- [219] Sedano, F., Luque, L., Ascencio, F., Alarcon, G., & Timana, J. (2021). Land use change and vegetation productivity in the Peruvian Amazon: a remote sensing and deep learning approach. *Remote Sensing*, 13(3), 455.
- [220] Shabbir, A., Ali, N., Ahmed, J., Zafar, B., Rasheed, A., Sajid, M., & Dar, S. H. (2021). Satellite and scene image classification based on transfer learning and fine-tuning of ResNet50. *Mathematical Problems in Engineering*, 2021, 1-18.
- [221] Shafizadeh-Moghadam, H., Valavi, R., Shahabi, H., Chapi, K., & Shirzadi, A. (2018). Novel forecasting approaches use machine learning and statistical models for flood susceptibility mapping. *Journal of Environmental Management*, 217, 1-11.
- [222] Shahabi, H., Ahmad, B. B., Mokhtari, M. H., & Zadeh, M. A. (2012). Detection of urban irregular development and green space destruction using normalized difference vegetation index (NDVI), principal component analysis (PCA) and post-classification methods: A case study of Saqqez city. *International Journal of the Physical Sciences*, 7(17), 2587-2595.
- [223] Somayajula, V. K. A., Ghai, D., Kumar, S., Tripathi, S. L., Verma, C., Safirescu, C. O., & Mihaltan, T. C. (2022). Classification and validation of spatio-temporal changes in land use/land cover and land surface temperature of multitemporal images. *Sustainability*, 14(23), 15677.
- [224] Shahabi, H., Shirzadi, A., Ghaderi, K., Omidvar, E., Al-Ansari, N., Clague, J. J., ... & Ahmad, A. (2020). Flood detection and susceptibility mapping using sentinel-1 remote sensing data and a machine learning approach: Hybrid intelligence of bagging ensemble based on the k-nearest neighbour classifier. *Remote Sensing*, 12(2), 266.
- [225] Sharma, A., Rawat, J. S., & Dutt, C. B. S. (2021). Analysis of land use and land cover change in Dehradun district (India) using remote sensing and machine learning algorithms. *Geocarto International*, 1-22.
- [226] Sharma, A., Singh, A., & Soni, V. K. (2020). Land cover classification of wetland area using remote sensing and GIS techniques. *Journal of the Indian Society of Remote Sensing*, 48(3), 435-443.

- [227] Sharma, A., Tiwari, A. K., & Gupta, N. (2020). Monitoring wetland changes in and around Sambhar Lake using remote sensing and GIS. *Environmental Monitoring and Assessment*, 192(4), 240.
- [228] Shaw, R., & Banba, M. (2017). Land use change and disaster risk reduction. *Handbook of Disaster Risk Reduction & Management*, 1-16.
- [229] Simonyan, K., & Zisserman, A. (2014). Very deep convolutional networks for large-scale image recognition. *arXiv preprint arXiv:1409.1556*.
- [230] Singh, A. K., Pathak, N., & Singh, A. K. (2017). Land use and land cover change detection of Kaimur Wildlife Sanctuary, Bihar, India, using remote sensing and GIS. *Journal of the Indian Society of Remote Sensing*, 45(2), 331-338.
- [231] Singh, A., Mishra, S. K., & Dadhwal, V. K. (2015). An interactive approach for accurate land cover classification using satellite data. *ISPRS Journal of Photogrammetry and Remote Sensing*, 105, 85-98.
- [232] Singh, S., & Kushwaha, S. P. (2016). Mapping of LULC using remote sensing and GIS in the Banda District of Uttar Pradesh, India. *Journal of the Indian Society of Remote Sensing*, 44(4), 569-579.
- [233] Somayajula, V. K. A., Ghai, D., & Kumar, S. (2021). Land Use/Land Cover Change Analysis using NDVI, PCA. In *2021 5th International Conference on Computing Methodologies and Communication (ICCMC)*, pp. 849-855, IEEE.
- [234] Song, X., Duan, Z., & Jiang, X. (2012). Comparison of artificial neural networks and support vector machine classifiers for land cover classification in Northern China using a SPOT-5 HRG image. *International Journal of Remote Sensing*, 33(10), 3301-3320.
- [235] Sonune, N. (2020). Land cover classification with Eurosat dataset.
- [236] Srinivasan, V., Das, A. K., & Dadhwal, V. K. (2014). Land use/land cover mapping using interactive supervised classification approach: a case study of Andhra Pradesh. *Journal of the Indian Society of Remote Sensing*, 42(4), 753-764.
- [237] Stateczny, A., Bolugallu, S. M., Divakarachari, P. B., Ganesan, K., & Muthu, J. R. (2022). Multiplicative Long Short-Term Memory with Improved Mayfly Optimization for LULC Classification. *Remote Sensing*, 14(19), 4837.

- [238] Stivaktakis, R., Tsagkatakis, G., & Tsakalides, P. (2019). Deep learning for multilabel land cover scene categorization using data augmentation. *IEEE Geoscience and Remote Sensing Letters*, 16(7), 1031-1035.
- [239] Sultana, S., Islam, M. J., Rahman, M. M., & Alam, M. S. (2021). Analysis of Land Use and Land Cover Changes in a Coastal Area of Bangladesh Using Deep Learning Techniques. *IEEE Journal of Selected Topics in Applied Earth Observations and Remote Sensing*, 14, 1802-1812.
- [240] Suneetha, M., & Srinivasulu, P. (2019). Land use/land cover change detection and prediction using remote sensing and GIS in Kondapalli reserve forest, Andhra Pradesh, India. *Journal of Geomatics*, 13(2), 133-139.
- [241] Talukdar, S., Singha, P., Mahato, S., Pal, S., Liou, Y. A., & Rahman, A. (2020). Land-use land-cover classification by machine learning classifiers for satellite observations—A review. *Remote Sensing*, 12(7), 1135.
- [242] Taufik, M., A.S. Subagyo, and S. Wibowo. (2016). Classification of Landsat 8 satellite data using NDVI thresholds. *International Journal of Remote Sensing* 37(15): 4111-4121.
- [243] Tien Bui, D., Shahabi, H., Shirzadi, A., Chapi, K., Alizadeh, M., Chen, W., & Tian, Y. (2018). Landslide detection and susceptibility mapping by AirSAR data using support vector machine and index of entropy models in Cameron Highlands, Malaysia. *Remote Sensing*, 10(10), 1527.
- [244] Tiwari, V. K., Mishra, V. K., & Singh, P. K. (2015). Improved land cover classification using modified minimum distance classifier. *Journal of the Indian Society of Remote Sensing*, 43(4), 733-743.
- [245] Tucker, C. J. (1979). Red and photographic infrared linear combinations for monitoring vegetation. *Remote sensing of Environment*, 8(2), 127-150.
- [246] Tong, X. Y., Xia, G. S., Lu, Q., Shen, H., Li, S., You, S., & Zhang, L. (2020). Land-cover classification with high-resolution remote sensing images using transferable deep models. *Remote Sensing of Environment*, 237, 111322.
- [247] Topaloğlu, R. H., Sertel, E., & Musaoğlu, N. (2016). Assessment of Sentinel-2 and Landsat-8 data classification accuracies for land cover/use mapping. *The International Archives of the Photogrammetry, Remote Sensing and Spatial Information Sciences*, 41, 1055-1059.

- [248] Vaiphasa, S., S. Saengnoi, and M. Rerkasem. 2011. Differentiation of idle agriculture land with non-idle agriculture land using NDVI time series. *International Journal of Remote Sensing* 32(10): 3319-3334.
- [249] Vaishnnave, M. P., Devi, K. S., & Srinivasan, P. (2019). A study on deep learning models for satellite imagery. *International Journal of Applied Engineering Research*, 14(4), 881-887.
- [250] Vali, A., Comai, S., & Matteucci, M. (2020). Deep learning for land use and land cover classification based on hyperspectral and multispectral earth observation data: A review. *Remote Sensing*, 12(15), 2495.
- [251] Vargas-Ruiz, C. A., Pulgarín-Vélez, C. J., Sánchez-Villamil, J. I., & Gómez-Verjan, J. C. (2020). Analysis of vegetation changes on land use and land cover in the tropical Andes of Colombia using deep learning techniques. *IEEE Journal of Selected Topics in Applied Earth Observations and Remote Sensing*, 13, 4045-4053.
- [252] Vishwakarma, K., Pandey, A. C., Gaurav, & Rai, P. (2016). Land use and land cover change detection through remote sensing technique. *International Journal of Scientific Research in Science, Engineering and Technology (IJSRSET)*, 2(4), 209-214.
- [253] Wang, C., Wang, L., & Zhu, W. (2018). Vegetation change detection in the Qaidam Basin of China using remote sensing and deep learning techniques. *IEEE Journal of Selected Topics in Applied Earth Observations and Remote Sensing*, 11, 4725-4737.
- [254] Wang, C., Zhang, X., & Wang, X. (2015). Application of deep learning in the monitoring of soil erosion in the Loess Plateau. *Environmental Earth Sciences*, 74(7), 5911-5921.
- [255] Wang, F., Deng, J., & Jiang, S. (2015). Using deep learning to extract urban vegetation features from high-resolution satellite images. *Remote Sensing*, 7(11), 14853-14880.
- [256] Wang, F., Li, X., & Hu, T. (2021). Land cover classification of the Beibu Gulf Economic Zone based on Sentinel-2 imagery and maximum likelihood algorithm. *ISPRS International Journal of Geo-Information*, 10(2), 112.

- [257] Wang, J., Huang, X., & Zhang, H. K. (2014). Cloud detection for high-resolution remote sensing imagery based on texture and shape features. *Remote Sensing Letters*, 5(4), 393-402.
- [258] Wang, L., Liu, X., Wu, Y., Wang, X., & Zhang, H. (2017). Monitoring land use and land cover change in the Yellow River Delta using deep learning. *Remote Sensing*, 9(8), 790.
- [259] Wang, M., Li, Q., Zhang, H., & Li, X. (2008). Remote sensing-based change detection of land use and land cover in the agricultural area of northeast China. *Environmental Monitoring and Assessment*, 136(1-3), 227-238.
- [260] Wang, X., Cheng, Y., Wang, J., & Wang, X. (2019). Land use and land cover change detection using a deep learning approach in the Loess Plateau of China. *IEEE Journal of Selected Topics in Applied Earth Observations and Remote Sensing*, 12, 1378-1388.
- [261] Wang, Y., Zhang, C., Wu, H., & Zhang, Y. (2019). Urban green space change detection using deep convolutional neural network. *IEEE Journal of Selected Topics in Applied Earth Observations and Remote Sensing*, 12, 3049-3059.
- [262] Wang, L., Yan, J., Mu, L., & Huang, L. (2020). Knowledge discovery from remote sensing images: A review. *Wiley Interdisciplinary Reviews: Data Mining and Knowledge Discovery*, 10(5), e1371.
- [263] Wu, Y., Li, L., Li, Z., Zhang, L., & Chen, F. (2018). Using Inception-ResNet deep learning approach for vegetation change detection in the YarlungZangbo River Basin of Tibet. *IEEE Journal of Selected Topics in Applied Earth Observations and Remote Sensing*, 11, 3367-3376.
- [264] Wu, Y., Liu, X., Zhang, H., & Wang, L. (2017). Impact of land use and land cover changes on surface water quality in Poyang Lake Basin using deep learning. *Remote Sensing*, 9(11), 1147.
- [265] Wolter, M. A., Coops, N. C., Roy, D. P., White, J. C., & Hermosilla, T. (2018). Land cover 2.0. *International Journal of Remote Sensing*, 39(12), 4254-4284.
- [266] Xia, Y., & Liu, J. (2014). Modified parallelepiped classification based on covariance matrix. *Journal of Applied Remote Sensing*, 8(1), 083544.
- [267] Xie, G., & Niculescu, S. (2021). Mapping and monitoring of land cover/land use (LCLU) changes in the Crozon Peninsula (Brittany, France) from 2007 to 2018

- by machine learning algorithms (support vector machine, random forest, and convolutional neural network) and by post-classification comparison (PCC). *Remote Sensing*, 13(19), 3899.
- [268] Xu, H., Gao, Y., & Zhang, W. (2017). A hybrid classification method for mapping land cover using multi-temporal Landsat imagery and domain knowledge. *Remote Sensing*, 9(6), 525.
 - [269] Yan, L., Huang, Y., Yang, X., & Wang, R. (2018). A U-Net deep learning approach for vegetation change detection in the Yellow River Delta. *IEEE Journal of Selected Topics in Applied Earth Observations and Remote Sensing*, 11, 3506-3514.
 - [270] Yang, Y., & Newsam, S. (2010). Bag-of-visual-words and spatial extensions for land-use classification. In *Proceedings of the 18th SIGSPATIAL international conference on advances in geographic information systems*, 270-279.
 - [271] Yang, Y., Zhang, Y., Li, D., & Liang, J. (2019). Using deep learning to analyze the impact of vegetation changes on land use and land cover in the Yancheng Coastal Wetland of China. *IEEE Journal of Selected Topics in Applied Earth Observations and Remote Sensing*, 12, 3994-4003.
 - [272] Y. Yao, H. Zhao, D. Huang, and Q. Tan. (2019). Remote sensing scene classification using multiple pyramid pooling. *The International Archives of the Photogrammetry, Remote Sensing and Spatial Information Sciences*, 42, 279-284.
 - [273] Yousefpour, R., Shrestha, S., Luedeling, E., Marques, G. M., & Meacham, M. (2019). Combining participatory mapping with Q methodology to map and assess ecosystem services in a Mediterranean forest landscape. *Ecosystem Services*, 35, 174-184.
 - [274] Zare, M., & Ghaemi, M. (2019). A hybrid maximum likelihood and parallelepiped classifier for hyperspectral data analysis. *IEEE Transactions on Geoscience and Remote Sensing*, 57(2), 748-758.
 - [275] Zhang et al. (2017) - Crop mapping using interactive supervised classification with Landsat 8 data. *International Journal of Remote Sensing*, 38(6), 1566-1585.

- [276] Zhang et al. (2020) - Advancement of interactive supervised classification for urban land use mapping using high-resolution remote sensing data in Beijing, China. *International Journal of Digital Earth*, 13(7), 761-782.
- [277] Zhang, C., Wang, Y., Wu, H., & Zhang, Y. (2019). Vegetation change analysis using deep learning in the Beibu Gulf of China. *IEEE Journal of Selected Topics in Applied Earth Observations and Remote Sensing*, 12, 3911-3921.
- [278] Zhang, C., Zhang, Y., & Sun, W. (2018). A deep learning approach to detect vegetation change in the Three Gorges Reservoir Area of China. *IEEE Journal of Selected Topics in Applied Earth Observations and Remote Sensing*, 11, 2972-2981.
- [279] Zhang, J., Cao, G., Li, M., Hu, Y., Li, J., & Zhang, Y. (2021). Analyzing the impact of land use/land cover change on ecosystem services in the Yellow River Basin using deep learning. *Remote Sensing*, 13(2), 244.
- [280] Zhang, J., Zhu, H., Li, J., & Tian, J. (2020). Vegetation change detection and analysis in the Loess Plateau of China using modified VGG16 model. *IEEE Journal of Selected Topics in Applied Earth Observations and Remote Sensing*, 13, 2788-2799.
- [281] Zhang, W., Wang, W., Wu, J., & Zhang, L. (2019). Vegetation change analysis and prediction using a deep learning approach in the Heihe River Basin of China. *IEEE Journal of Selected Topics in Applied Earth Observations and Remote Sensing*, 12, 3972-3982.
- [282] Zhang, X., Wang, C., Hu, T., & Zhang, J. (2016). Mapping vegetation cover changes in the Tarim River Basin using deep learning. *Remote Sensing*, 8(8), 649.
- [283] Zhang, D., Liu, Z., & Shi, X. (2020, December). Transfer learning on the efficient net for remote sensing image classification. In 2020, the 5th International Conference on Mechanical, Control and Computer Engineering (ICMCCE), 2255-2258, IEEE.
- [284] Zhang, X., Guo, Y., & Zhang, X. (2020, September). Deep convolutional neural network structure design for remote sensing image scene classification based on transfer learning. In *IOP Conference Series: Earth and Environmental Science*, 569(1), 012046. IOP Publishing.

- [285] Zhao, F., Liu, Y., & Yu, Y. (2010). Monitoring land use and land cover changes in Beijing using remote sensing and GIS. *Procedia Environmental Sciences*, 2, 1577-1586.
- [286] Zhou, C., Wang, L., Sun, D., & Zhang, Q. (2015). Mapping land use/cover changes and assessing the ecosystem services in Pearl River Delta Region using remote sensing and ecological models. *Applied Geography*, 59, 101-112.
- [287] Zhu, Q., Peng, Y., Wu, J., & Liu, J. (2015). Mapping ecosystem services in the Yangtze River Delta, China, using a composite method of field survey and Landsat imagery. *Ecological Indicators*, 58, 308-318.
- [288] Zhu, X., Zhang, C., Zhang, Y., & Xu, L. (2018). A deep learning approach to monitor land cover change in the Beijing-Tianjin-Hebei region of China. *IEEE Journal of Selected Topics in Applied Earth Observations and Remote Sensing*, 11, 3542-3552.
- [289] Zhu, Y., Chen, Y., Lu, Z., Pan, S., Xue, G. R., Yu, Y., & Yang, Q. (2011, August). Heterogeneous transfer learning for image classification. In *Proceedings of the AAAI conference on artificial intelligence*, 25(1), 1304-1309.
- [290] Zou, M., & Zhong, Y. (2018). Transfer learning for classification of the optical satellite image. *Sensing and Imaging*, 19(1), 6.
- [291] K. Bhosle, V. Musande, (2019) "Evaluation of deep learning CNN model for LULC classification and crop identification using hyperspectral remote sensing images," *Journal of the Indian Society of Remote Sensing*, vol. 47, pp. 1949-1958.
- [292] X. Ma, Y. Hong, Y. Song, (2020) "Super-resolution land cover mapping of hyperspectral images using the deep image prior-based approach," *International Journal of Remote Sensing*, vol. 41, pp. 2818-2834.
- [293] A.D. Gregorio, D.O' Brien, (2012) "Overview of land-cover classifications and their interoperability," *Remote Sensing of Land Use and Land Cover: Principles and Applications*, pp. 37-47.
- [294] S. Srivastava, J.E.V. Munoz, D. Tuia, (2019) "Understanding urban land use from the above and ground perspectives: A deep learning, multimodal solution," *Remote Sensing of Environment*, vol. 228, pp. 129-143.

- [295] ChaichokeVaiphas, Supawee Piamduaytham, TanasakVaiphasa, and Andrew K. Skidmore,(2011) “A Normalized Difference Vegetation Index (Ndvi) Time-Series of Idle Agriculture Lands: A Preliminary Study” *Engineering Journal*, vol. 15, no.1, pp. 9-16.
- [296] Ayele, Gebiaw T., Aschalew K. Tebeje, Solomon S. Demissie, Mulugeta A. Belete, Mengistu A. Jemberrie, Wondie M. Teshome, Dereje T. Mengistu, and Engidasew Z. Teshale.(2018) "Time series land cover mapping and change detection analysis using geographic information system and remote sensing, Northern Ethiopia." *Air, Soil and Water Research*, vol. 11, pp.1-18.
- [297] Salik, Abdul Walid, and Ersin Karacabey (2019) "Application of Landsat 8 Satellite Image–NDVI Time Series for Crop Phenology Mapping: Case Study Balkh and Jawzjan Regions of Afghanistan." *ÇanakkaleOnsekiz Mart Üniversitesi Fen Bili Maximum Likelihood eriEnstitüsüDergisi*, vol. 5, no. 1, pp. 49-62.
- [298] Wang, L., Yan, J., Mu, L., & Huang, L. (2020). Knowledge discovery from remote sensing images: A review. *Wiley Interdisciplinary Reviews: Data Mining and Knowledge Discovery*, 10(5), e1371.
- [299] Qin, Zhihao, and A. Karnieli, (2001) “Progress in the remote sensing of land surface temperature and ground emissivity”, *International Journal of Remote Sensing*, Vol. 12, pp.2396-2407.
- [300] Lu, Dengsheng, Guiying Li, Emilio Moran, and Scott Hetrick, (2013) “Spatiotemporal analysis of land-use and land-cover change in the Brazilian Amazon”, *International Journal of Remote Sensing*, Vol. 16, pp. 5953-5978.
- [301] Bui, Q. T., Jamet, C., Vantrepotte, V., Mériaux, X., Cauvin, A., &Mograne, M. A. (2022). Evaluation of sentinel-2/MSI atmospheric correction algorithms over two contrasted French coastal waters. **Remote Sensing*, 14(5), pp. 1099.
- [302] Zhang, D., Liu, Z., & Shi, X. (2020, December). Transfer learning on the efficient net for remote sensing image classification. In 2020, the 5th International Conference on Mechanical, Control and Computer Engineering (ICMCCE), pp.2255-2258, IEEE.
- [303] Zhang, X., Guo, Y., & Zhang, X. (2020, September). Deep convolutional neural network structure design for remote sensing image scene classification based on

- transfer learning. In IOP Conference Series: Earth and Environmental Science, 569(1), 012046. IOP Publishing.
- [304] Yang, Y., & Newsam, S. (2010, November). Bag-of-visual-words and spatial extensions for land-use classification. In Proceedings of the 18th SIGSPATIAL international conference on advances in geographic information systems, pp.270-279.
 - [305] Somayajula, V. K. A., Ghai, D., & Kumar, S. (2023, September). “A New Era of Land Cover Land Use Categorization Using Remote Sensing and GIS of Big Data” In 2023 6th International Conference on Contemporary Computing and Informatics (IC3I) Vol. 6, pp. 1081-1088, IEEE.
 - [306] Yangchen, Ugyen, Ugyen Thinley, and Gudrun Wallentin, (2-3 April, 2015) “LULC changes in Bhutan: 2000-2013”, in International Conference on ‘Climate Change, Environment and Development in Bhutan’, Royal University of Bhutan (RUB), Thimphu, Bhutan, pp. 37-46.
 - [307] M. Dharani, and G. Sreenivasulu, 2019 “Land use, and land cover change detection using principal component analysis and morphological operations in remote sensing applications”, International Journal of Computers and Applications, pp. 1-10.
 - [308] Huang, Z., Dumitru, C. O., Pan, Z., Lei, B., & Datcu, M. (2020). “Classification of large-scale high-resolution SAR images with deep transfer learning.” IEEE Geoscience and Remote Sensing Letters, 18(1), 107-111.
 - [309] Wang, L., Yan, J., Mu, L., & Huang, L. (2020). “Knowledge discovery from remote sensing images: A review.” Wiley Interdisciplinary Reviews: Data Mining and Knowledge Discovery, 10(5), e1371.
 - [310] Liping, Chen, Sun Yujun, and Sajjad Saeed, (2018) “Monitoring and predicting land use and land cover changes using remote sensing and GIS techniques- A case study of a hilly area,” Jiangle, China, Vol. 7, e0200493.
 - [311] Zhang, Yanghua, and Hu Zhao, (2020) “Land–use and land-cover change detection using dynamic time warping–based time series clustering method,” Canadian Journal of Remote Sensing, Vol. 1, pp. 67-83.

- [312] Sexton, O. Joseph, Dean L. Urban, Michael J. Donohue, and Conghe Song, (2013) "Long-term land cover dynamics by multi-temporal classification across the Landsat-5 record," *Remote Sensing of Environment*, Vol. 128, pp. 246-258.
- [313] Erle, Ellis, and P. Robert, (2011) "Land-use and land-cover change. The Encyclopedia of Earth," Ed. CJ Cleveland. Environmental Information Coalition, National Council for Science, and the Environment. Washington DC, 2010, pp. 142-153.
- [314] C. Prakasam, (2010) "Land use and land cover change detection through remote sensing approach: A case study of Kodaikanal taluk, Tamil Nadu," *International Journal of Geomatics and Geosciences* 1, Vol. 2, pp. 150.
- [315] S. Gupta, and Moupriya Roy, (2011) "Land Use/Land Cover Classification of an urban area-A case study of Burdwan Municipality, India," *International Journal of Geomatics and Geosciences*, Vol. 4, pp. 1014-1026.
- [316] Brown, G. Daniel, Bryan C. Pijanowski, and Jiunn-Der Duh, (2000) "Modeling the relationships between land use and land cover on private lands in the Upper Midwest, USA," *Journal of Environmental Management*, Vol. 4, pp. 247-263.
- [317] Loveland, Sleeter, M. Benjamin, Jinxun Liu, Colin Daniel, Bronwyn Rayfield, Jason Sherba, Todd J. Hawbaker, Zhiliang Zhu, Paul C. Selman, and R. Thomas, (2018) "Effects of contemporary land-use and land-cover change on the carbon balance of terrestrial ecosystems in the United States," *Environmental Research Letters*, Vol. 4, pp. 1-14.
- [318] Quintas-Soriano, Cristina, Antonio J. Castro, Hermelindo Castro, and Marina García-Llorente, (2016) "Impacts of land use change on ecosystem services and implications for human well-being in Spanish drylands," *Land use policy*, Vol. 54, pp. 534-548.
- [319] Anderson, James Richard, (1976), "A land use and land cover classification system for use with remote sensor data," US Government Printing Office, Vol. 964, pp. 1-34.

List of Publications

Journal Publications

1. V. Kiranmai A Somayajula, Deepika Ghai, Sandeep Kumar, Suman Lata Tripathi, Chaman Verma, Calin Ovidiu Safirescu, and Traian Candin Mihaltan (2022). CLASSIFICATION AND VALIDATION OF SPATIO-TEMPORAL CHANGES IN LAND USE/LAND COVER AND LAND SURFACE TEMPERATURE OF MULTITEMPORAL IMAGE. Sustainability, Vol. 14, pp. 15677. <https://doi.org/10.3390/su142315677>. (SCI)
2. V. Kiranmai A Somayajula, Deepika Ghai, Sandeep Kumar, (2022). LAND COVER CLASSIFICATION USING LANDSAT IMAGES, NORMALIZED DIFFERENCE VEGETATION INDEX IN VIJAYAWADA, A.P. International Journal of Early Childhood Special Education (INT-JECS), Vol 14, Issue 03, pp. 1159-1171. (ESCI)
3. V. Kiranmai A Somayajula, Deepika Ghai, Sandeep Kumar, (2020). A REVIEW ON CLASSIFICATION OF LAND USE/LAND COVER CHANGE ASSESSMENT BASED ON NORMALIZED DIFFERENCE VEGETATION INDEX. Journal of Critical Reviews, Vol. 7, Issue 14, pp. 2426-2431.
4. V. Kiranmai A Somayajula, Deepika Ghai, Sandeep Kumar, Suman Lata Tripathi "DYNAMIC ANALYSIS AND UTILIZATION OF LULC USING REMOTE SENSING, GIS, AND DEEP LEARNING METHODS FOR VIJAYAWADA CITY, A.P., INDIA" Communicated in the Serbian Journal of Electrical Engineering. (SCOPUS).
5. V. Kiranmai A Somayajula, Deepika Ghai, Sandeep Kumar, Suman Lata Tripathi "SPECTRAL-SPATIAL FEATURE EXTRACTION AND SEMANTIC SEGMENTATION OF SENTINEL-2 IMAGES FOR LULC MAPPING" Communicated in the Environmental Monitoring and Assessment. (SCI)

Conference Publications

1. V. Kiranmai A Somayajula, Deepika Ghai, Sandeep Kumar. A New Era of Land Cover Land Use Categorization Using Remote Sensing and GIS of Big Data. In Proceedings of the 6th International Conference on Contemporary Computing and Informatics (IC3I-2023), Amity University, Greater Noida, 14th to 16th September 2023.
2. Kiranmai, S.V.; Ghai, D.; Kumar, S. Land Use/Land Cover Change Analysis using NDVI, PCA. In Proceedings of the 2021 5th International Conference on Computing Methodologies and Communication IEEE, Erode, India, 8–10 April 2021.
3. V. Kiranmai A. Somayajula, Deepika Ghai, Sandeep Kumar. A Review on Classification of Land Use/Land Cover Change Assessment Based on Normalized Difference Vegetation Index. In the Proceedings of International Conference on Recent Trends in Engineering Technology and Management (ICRTETM), Hyderabad, 20th June 2020

List of Workshops

S. No	Title of the Program	Organization	Duration
1	Recent Trends and Applications of GIS & Remote Sensing Using AI	ATAL FDP conducted by PSCMRCET	13.09.2021 T 17.09.2021
2	Online course on “Remote Sensing Applications in Agricultural Water Management	IIRS outreach network center	03-08-2020 To 07-082020
3	Remote Sensing and Digital Image Processing of Satellite Data	NPTEL	Aug-October 2019